UNIVERSITY OF
BIRMINGHAM

Multi-asset Option Pricing Problems: A Variational Approach

by

Chienmin Chuang

Supervisor: Dr Daniel Loghin

A thesis submitted to The University of Birmingham for the degree of Doctor of Philosophy

2

The School of Mathematics
College of Engineering and Physical Sciences
University of Birmingham
November 2012

This thesis is dedicated to my parents, Wen-ning Chuang and Yua-shung Yo, for their love, endless support and encouragement.

Acknowledgements

I am most grateful to my supervisors, Dr. Daniel Loghin and Professor Stephen Decent for their supportive instruction to my research during my time in the University of Birmingham. I also acknowledge Professor Paul Feehan of Rutgers University for helpful discussion via email communications.

Also, I would like to express my heartfelt thanks to Ms. Janette Lowe and Dr. Michael Finney for their kindly assistance over the years in the School of Mathematics.

Finally, I would like to thank Jung-chen for her invaluable love and support throughout the course of my research.

Abstract

Options are important and frequently traded products in the modern financial market. How to price them fairly and reasonably is always an interesting issue for academia and industry. This research is performed under the classical multi-asset Black-Scholes-Merton (BSM) model and can be extended to other exotic models.

We show how to reformulate the multi-asset Black-Scholes-Merton partial differential equation/inequality (BSM PDE/PDI) and provide theorems to justify the unique solution of reformulations. In terms of discretization, we adopt the finite element method (FEM) in space and finite difference method (FDM) in time. Moreover, we develop the closed-form formulas for the elemental matrices used in the finite element assembly process in a general high-dimensional framework.

The discrete systems of option pricing problems are presented in the form of linear system of equations (LSE) and linear complementary problems (LCP) for European and American/perpetual options respectively. Up to six different algorithms for the LCP are introduced and compared on the basis of computational efficiency and errors.

The option values of European, American and perpetual types are calibrated when given various payoffs and up to three assets. Particularly, their numerical free boundaries are identified and presented in the form of $(d-1)-$dimensional manifold in a $d-$asset framework. In the last chapter, we conclude our research with our contributions and potential extension.

Contents

Chapter 1

Introduction

1.1 Financial derivatives

Dating back to 1848, the Chicago Board of Trade (CBOT) was established to provide farmers and merchants a platform to trade agricultural products. A few years later, it started to offer standardized contracts for both buyers and sellers. Investors and speculators soon realized that trading such contracts was much more profitable than their underlying products. A *financial derivative* is a lawful contract underlaid with a valuable asset and endowing their owners with specific trading rights in the future. Since the Securities Exchange Act (SEA) was codified in the US in 1934, the trading volume of financial derivatives started to be boosted in the American market. Nowadays, trading of financial derivatives is thriving in global financial markets. The use of financial derivatives has a double-edged power. Sellers and buyers can buy options to lock their future transactional prices. Fund managers can buy corporate and national bonds to lock the return rates in specific periods. In this fashion, financial derivatives facilitate market participants to hedge the future uncertainty and enhance the market efficiency. On the other hand, they can be regarded as bets on the future for speculators. Due to the fact that financial derivatives are generally manipulated at high financial leverage/gear ratios, they may bring about the downfall of business giants overnight. The first and most recent examples are bankruptcies of Orange County (1994) and Lehman Brothers (2008). Pricing derivatives is a vital and practical issue because their use for hedging is highly demanded in the City. However, an enormous financial loss may be caused by their mispricing. Driven by these, both industry and academia are keen to discover the fair prices of financial derivatives by combining financial models with mathematical theories.

1.2 Terminology

Among all financial derivatives, *options* are the financial contracts giving their owners the one-time-use right, but not obligation, to buy or to sell a portfolio of shares for a pre-agreed price at a future time. The pre-agreed price is called *exercise/strike price*. The last valid time to exercise such a right is called *expiry/maturity time*.

1.2.1 Notation

We denote time by t and let $t = 0$ and $t = T > 0$ be the current and expiry times respectively. At time t, a share price, a portfolio price and an option's value are denoted by S_t, S_t^p, v_t individually. When the time can be omitted in the context, they are simply denoted by S, S^p, v. When a portfolio is composed of $d \in \mathbb{N}$ shares, $\mathbf{S}_t := \left(S_t^{(1)}, S_t^{(2)}, ..., S_t^{(d)}\right)' := \mathbf{S} := \left(S^{(1)}, S^{(2)}, ..., S^{(d)}\right)'$ are used to denote their values. The exercise price is denoted by E.

1.2.2 Exercise Restriction

The time to exercise the right is called *exercise/strike time*. If an option can be exercised only on expiry date, it is said to be a *European option*. If it can be exercised prior to or on expiry date, it is an *American option*. Such a flexibility to exercise at any time is called *early-exercise property*. In particular an option is called a *perpetual* option if it can be exercised at any time *without expiry restriction*. Naturally, perpetual options are the most expensive followed by their American and European counterparts.

1.2.3 Portfolio

Given a portfolio associated with d assets, we say a financial product is

- a *basket* option if $S^p := S_t^p := \sum_{i=1}^d w_i S_t^{(i)}$ where w_i are non-negative weights,
- a *maximum* option if $S^p := S_t^p := \max_{i=1\sim d}\{S_t^{(i)}\}$,
- a *minimum* option if $S^p := S_t^p := \min_{i=1\sim d}\{S_t^{(i)}\}$.

1.2.4 Payoff

Payoff refers to the monetary value gained from exercising an option which depends on its exercise price and the share/portfolio price at exercise time. Provided an exercise price E, a payoff linked to a portfolio composed of d assets is denoted by $g(S_t^p) := g(\mathbf{S})$. An

option is called a *call*, a *put* or a *straddle* if they give the right for buying, selling or both, individually. We hence define

- $[x]^+ := \max\{x, 0\}$,
- $1_{\{\mathbf{con}\}}$ as an indicator function which has the value one if condition **con** is satisfied and zero otherwise.
- payoff of a call by $g(\cdot) := [S^p - E]^+ \equiv (S^p - E) \cdot 1_{\{S^p \geq E\}}$,
- payoff of a put by $g(\cdot) := [E - S^p]^+ \equiv (E - S^p) \cdot 1_{\{E \geq S^p\}}$,
- payoff of a straddle by

$$\begin{aligned} g(\cdot) &:= [E - S^p]^+ + [S^p - E]^+ \\ &\equiv (S^p - E) \cdot 1_{\{S^p \geq E\}} + (E - S^p) \cdot 1_{\{E \geq S^p\}}. \end{aligned}$$

One-asset European call and put are also called vanilla options due to their simplicity. It is worth to mention that call, put and straddle options have continuous payoffs while those of the following two are generally discontinuous.

- Cash-or-nothing: $g(\cdot) := c \cdot 1_{\{\mathbf{S} \in A\}}$ for some $c > 0$ and $A \subset \mathbb{R}^d$,
- Asset-or-nothing: $g(\cdot) := S^p \cdot 1_{\{\mathbf{S} \in A\}}$ for some $A \subset \mathbb{R}^d$.

Most payoff functions are assumed to be non-negative convex functions (over a convex domain) depending on underlying asset prices. However, continuity is not one of the assumptions which implies Lipschitz continuity and may not be satisfied by some exotic payoffs.

1.3 How to Discover the Fair Price

1.3.1 Self-financing and No-arbitrage

We say a generalized portfolio, including shares, cash and options, is *self-financing* if it keeps adding new assets by selling existing ones. In other words, a self-financing portfolio keeps being adjusted without extra cash influx. A portfolio is called a *replication* if it can provide identical monetary value as another one in the future. We say there is *no arbitrage* if any portfolio has an equivalent monetary value as all its replications in a market.

1.3.2 Parities

There exist some parities showing the relations between different options against no arbitrage, cf. [50, p.208] and [54]. A trader without advanced mathematical techniques can easily establish a fair price by using different parities. Theoretically, an option disobeying the existing parties provides a risk-free arbitrage opportunity and its price will then be pushed toward an equilibrium by market power until no arbitrage is available in the market. Below are two famous ones in one-asset and two-asset cases.

$$\begin{aligned}
&\text{Put-call parity: } C(t,S) - P(t,S) = Se^{-q\tau} - Ee^{-r\tau} \\
&\text{Min-max parity: } C_{min}(t,S^{(1)},S^{(2)}) + C_{max}(t,S^{(1)},S^{(2)}) = C(t,S^{(1)}) + C(t,S^{(2)}) \\
&\qquad\qquad P_{min}(t,S^{(1)},S^{(2)}) + P_{max}(t,S^{(1)},S^{(2)}) = P(t,S^{(1)}) + P(t,S^{(2)})
\end{aligned}$$

where r is the interest rate, q is the dividend rate, C and P are the values of one-asset European vanilla call and put and those with subscripts are their two-asset minimum and maximum counterparts.

1.3.3 Model

We will look at the assumptions of different models in the next chapter. Once a rigorous model is provided, the fair price of an option is then discovered by creating a self-financing portfolio and using no-arbitrage argument. From the aspect of stochastic analysis, the fair price discovered by self financing and no arbitrage can be equivalently expressed as the expected option value against a risk-neutral (probability) measure, cf. [50, ch.5].

1.4 Research Objectives

There are a variety of models under different assumptions to formulate an option pricing problem. We would work under the classical Black-Scholes-Merton (BSM) model introduced in the next chapter, considered different exercise restrictions and included more than one asset in our problems.

We had two objectives to achieve in this research. The first goal was to find a common variational framework for different pricing problems including the European, American and perpetual options and extendable to multiple assets. Such different exercise restrictions and multi-dimensional consideration would request the common framework to be more generalized and consequently be more challenging for us. We wanted to reformulate the various problems from functional point of view and would achieve this in our selected Sobolev spaces. We further investigated the solvability of the reformulated problems under specific assumptions with the help of three powerful theorems introduced in chapter four. In terms of discretization of variational problems, we adopt finite difference method (FDM)

in time and finite element method (FEM) in space. The closed-form formulas of elemental matrices for the implementation of FEM were devised to speed up its assembly process and to avoid the error arising from numerical integration.

The second was to find applicable algorithms to solve the discrete problems and to compare them from different aspects. The discrete form of European pricing problem would be expressed in the form of a system of equalities, which can be solved numerically by a variety of well-known methods. However, the early-exercise property of American and perpetual options would turn the pricing problems to finite dimensional variational inequalities in discrete sense. We showed how these problems could be converted to equivalent linear complementarity problem (LCP) which were much more demanding for numerical solution than European cases. We investigated up to six algorithms for solving the LCPs and compared their performance in terms of numerical error, iteration number and computational time. By solving the problems numerically, we would calibrate their values on a computational domain and could visualize the evolution of the free boundary, the intersection of early-exercise and non-early-exercise regions over the domain, up to three dimensions.

1.5 Thesis Organization

Outlined below are the contents of the following chapters.

Chapter 2: Literature Survey. We begin with the classical Black-Scholes-Merton (BSM) model and show how to derive the celebrated BSM partial differential equation/inequality (BSM PDE/PDI). We then look at other variant models with relaxing assumptions. A variety of approaches for solving the problems are described in the latter part.

Chapter 3: Auxiliary Conditions. We look at boundary conditions, terminal conditions and complementarity conditions requested for different portfolios, expiry restrictions and dimensions. Such conditions will be used in following reformulation and numerical computation.

Chapter 4: Reformulation. We reformulate the pricing problems in variational approach. Relevant theories and analysis from a functional point of view are provided. The unique solution of reformulations are justified by proving sufficient conditions, in particular the Garding's inequality, are met in our framework.

Chapter 5: Discrete Systems and Solvability. The infinite-dimensional problems can be approximated by finite-dimensional counterparts and form discrete systems. The sequential system of equalities, the sequential system of linear complementarity problem and the steady system of linear complementarity problem will be summarized for European, American and perpetual options separately.

Chapter 6: Finite Element Matrices. We investigate how to compute the different elemental matrices arising from finite element approximation and their assembly to global matrices. Instead of using quadrature methods, we devised different closed-form formulas for our elemental matrices. The formulas can be applied to arbitrary dimensions/number of assets and produce exact integrals of the elemental entries, speed up the assembly process and avoid the numerical error of numerical integration.

Chapter 7: Algorithms. We describe various algorithms to solve the discrete problems, especially those for LCPs. The solvability and convergence of each algorithm for LCP depends on the class of coefficient matrix in the problem. However, there is no efficient way to identify the class of a matrix to the present.

Chapter 8: Numerical Experiments. We examine the robutness of LCP solvers for solving American and perpetual options in one, two and three assets. The European, American and perpetual options are then calibrated when given different payoffs and different number of assets. For European and American options, their free boundaries are calibrated in the form of a manifold. Truncation errors and discretization errors are investigated numerically in various circumstances.

Chapter 9: Conclusion. We summarize the points of this research and list our contributions, followed by possible extensions in the future, and make the final remark.

Chapter 2

Literature Survey

2.1 Models in Mathematical Finance

In mathematical finance, the pricing problems of financial derivatives generally start from modelling the dynamics of an underlying asset in terms of a discrete or continuous stochastic process. A comprehensive content of the stochastic theories can be found in [85] and [86]. A financial derivative can hence be investigated in a stochastic framework. It is possible to derive a necessary condition, generally in the form of an (integro-)differential equation, for no-arbitrage pricing and even to find the analytical solution to the no-arbitrage price. We recommend [50] and [98] for a general introduction to mathematical finance.

2.1.1 Black-Scholes-Merton Model

Of all models, the Black-Scholes-Merton (BSM) model, cf. [8] and [69], is the first and most well-known. Black and Scholes invented their model but its use was proposed and extended to include continuous dividend rate by Merton. Two years after Black's departing, the 1997 Nobel Prize in Economics was awarded to Scholes and Merton along with Black's contribution honored. Its resultant BSM formulas introduced later are applied for pricing one-asset European call and put. However, the account that the BSM model earned its name was not because of its formulas but its originality of modelling a financial market in a stochastic fashion, which motivated more stochastic models to be created to model financial markets and national economies.

The BSM model assumes transaction in a market is efficient and free of transactional cost and tax. Its key assumption is that the dynamics a share price $S^{(i)}$ is the continuous stochastic process characterized by the following stochastic differential equation (SDE).[1]

$$\begin{cases} dS^{(i)} = (r - q_i)S^{(i)}dt + \sigma_i S^{(i)}dw_i, \\ dw_i \sim N(0, dt), \end{cases}$$

[1]The SDE is the form obtained after change of measure to risk-neutral (probability) measure.

where $r > 0$ is the interest/riskfree rate, $q_i \in [0, r]$ is the dividend rate of $S^{(i)}$ and w_i is a Brownian Motion, or Wiener Process, such that $dw_i \sim N(0, dt)$. When more than one asset is considered, i.e. $i = 1, 2, \ldots$, it also assumes that $E(dw_i dw_j) = \rho_{ij} dt$ and $\sigma_{ij} := \rho_{ij}\sigma_i\sigma_j$.

2.1.2 Other models

The BSM model assumes the volatility $\sigma_i := \sqrt{\sigma_{ii}}$ to be a constant. In contrast, the local volatility model assumes the volatility is an unknown deterministic function while the Heston model assumes it is also stochastic. For example, one can assume the square of volatility follows the dynamics, cf. [47],

$$\begin{cases} d\sigma_{ii} = \tilde{\mu}_i(\tilde{\sigma}_{ii} - \sigma_{ii})dt + \tilde{\sigma}_i\sigma_i d\tilde{w}_i, \\ d\tilde{w}_i \sim N(0, dt), \end{cases}$$

where the mean-reverting rate $\tilde{\mu}_i$, the long-term variance $\tilde{\sigma}_{ii}$, the volatility of (the square of) volatility $\tilde{\sigma}_i$ are all constants and $E(dw_i d\tilde{w}_i) = \tilde{\rho}_{ij} dt$.

Another popular stochastic process for financial models is the Levy process which adds jumps in the SDE and allows a share price to be discontinuous in time, cf. [53, 7, 58]. One example of a Levy process is

$$dS = (r - q)Sdt + \sigma S dw + S\sum_{i=1}^{n_t} Y_i,$$

where $\{Y_i\}_{i=1,\ldots,n}$ follows specific normal distributions.

Merton proposed another Levy process of the form, c.f. [64],

$$\begin{aligned} dS &= (r - q)Sdt + \sigma S dw + S(\eta - 1)dp, \\ dp &= \begin{cases} 0 \text{ with the probability } 1 - \lambda dt \\ 1 \text{ with the probability } \lambda dt \end{cases} \end{aligned}$$

where λ is the frequency of Poisson distribution, dp follows a Poisson process and $\eta - 1$ is the impulse function giving a jump from S to ηS.

The books by Tankov and Lewis [89, 63] investigate the role of jump process and stochastic volatility in option pricing respectively. Besides, there are more variants which change one or more assumptions, cf. [98].

2.2 Black-Scholes-Merton Partial Differential Equation and Inequality

We now briefly explain how to derive the celebrated Black-Scholes-Merton partial differential equation (BSM PDE) and inequality (BSM PDI). Suppose there exists an option v

linked to a portfolio S^p composed of d shares. An individual in the market can create a self-financing portfolio by longing a smaller portfolio π and selling/shorting cash worth π when a trading account is opened. The small portfolio π can be created by buying/longing one unit of the option and shorting Δ_i lots of $S^{(i)}$ for $i = 1, \ldots, d$. Hence the value of π at any future time prior to the expiry date is $\pi = v - \sum_{i=1}^{d} \Delta_i S^{(i)}$. Applying Ito's lemma[2], cf. [98, p.80], the dynamics of the portfolio becomes

$$d\pi = \left(\frac{\partial v}{\partial t} + \frac{1}{2} \sum_{i=1}^{d} \sum_{j=1}^{d} \sigma_{ij} S^{(i)} S^{(j)} \frac{\partial^2 v}{\partial S^{(i)} \partial S^{(j)}} - \sum_{i=1}^{d} \Delta_i q_i S^{(i)} \right) dt + \sum_{i=1}^{d} \left(\frac{\partial v}{\partial S^{(i)}} - \Delta_i \right) dS^{(i)}.$$

Let $\Delta_i = \frac{\partial v}{\partial S^{(i)}}$ to hedge against the uncertain $dS^{(i)}$. The no-arbitrage argument claims $r\pi dt = d\pi$ in the case of European options. We then reach the deterministic BSM PDE

$$\dot{v} + \mathcal{L}v := \frac{\partial v}{\partial t} + \frac{1}{2} \sum_{i=1}^{d} \sum_{j=1}^{d} \sigma_{ij} S^{(i)} S^{(j)} \frac{\partial^2 v}{\partial S^{(i)} \partial S^{(j)}} + \sum_{i=1}^{d} (r - q_i) S^{(i)} \frac{\partial v}{\partial S^{(i)}} - rv = 0. \quad (2.1)$$

When an early exercise property is provided in American and perpetual options, the no-arbitrage argument simply implies that the return of a portfolio is no more than a riskfree investment, i.e. $r\pi dt \geq d\pi$. Hence, the BSM PDE turns to a BSM PDI

$$\dot{v} + \mathcal{L}v \leq 0. \quad (2.2)$$

Since a perpetual option has no expiry restriction, its value is insensitive to time, i.e. $\dot{v} = \frac{\partial v}{\partial t} = 0$. As a result, the BSM PDI is

$$\mathcal{L}v = \frac{1}{2} \sum_{i=1}^{d} \sum_{j=1}^{d} \sigma_{ij} S^{(i)} S^{(j)} \frac{\partial^2 v}{\partial S^{(i)} \partial S^{(j)}} + \sum_{i=1}^{d} (r - q_i) S^{(i)} \frac{\partial v}{\partial S^{(i)}} - rv \leq 0, \quad (2.3)$$

in the perpetual case.

[2]Ito's lemma is a result of stochastic calculus based on geometric Brownian motion.

2.3 Transformation from the BSM Model to a Diffusion Model

With the change of variables

$$\begin{aligned}
&\mathbf{x} := \ln(\mathbf{S}/E), \sigma := \max_{i=1\sim n}\{\sigma_i\}, \tau := (T-t)\frac{\sigma^2}{2},\\
&\tilde{r} := \frac{r}{\sigma/2}, \tilde{q} := \frac{q}{\sigma/2}, \tilde{\sigma}_{ij} := \frac{\sigma_{ij}}{\sigma/2}, \tilde{\mathbf{\Sigma}} := [\tilde{\sigma}_{ij}]_{d\times d},\\
&\tilde{u}(\mathbf{x},\tau) = \frac{v(\mathbf{S},t)}{E}, u(\mathbf{x},\tau) = e^{-\boldsymbol{\alpha}^T\mathbf{x}-\beta\tau}\tilde{u}(\mathbf{x},\tau),\\
&\boldsymbol{\alpha} = \frac{-1}{2}\cdot\tilde{\mathbf{\Sigma}}^{-1}\cdot\mathbf{1}_{(\tilde{r}-\tilde{q}_i-\tilde{\sigma}_{ii})}, \beta := \frac{-1}{4}\cdot\mathbf{1}^T_{(\tilde{r}-\tilde{q}_i-\tilde{\sigma}_{ii})}\cdot\tilde{\mathbf{\Sigma}}^{-1}\cdot\mathbf{1}_{(\tilde{r}-\tilde{q}_i-\tilde{\sigma}_{ii})} - \tilde{r},\\
&\mathbf{1}_{(\tilde{r}-\tilde{q}_i-\tilde{\sigma}_{ii})} := [(\tilde{r}-\tilde{q}_1-\tilde{\sigma}_{11}),\ldots,(\tilde{r}-\tilde{q}_d-\tilde{\sigma}_{dd})]',
\end{aligned}$$

the BSM PDE/PDI can be transformed into a simple diffusion PDE/PDI as below, cf. [34, p.66].

$$\begin{aligned}
u_\tau &= \sum_{i=1}^{n}\sum_{j=1}^{n}\tilde{\sigma}_{ij}u_{x_ix_j} \text{ for European options,}\\
u_\tau &\geq \sum_{i=1}^{n}\sum_{j=1}^{n}\tilde{\sigma}_{ij}u_{x_ix_j} \text{ for American options,}\\
0 &\geq \sum_{i=1}^{n}\sum_{j=1}^{n}\tilde{\sigma}_{ij}u_{x_ix_j} + \beta u \text{ for perpetual options.}
\end{aligned}$$

where $u, x_i, \tau, \tilde{\sigma}_{ij}$ are the transformed counterparts of $v, S^{(i)}, t, \sigma_{ij}$ and β is a constant created in transformation. Instead of studying the original BSM PDE/PDI, some references consider the transformed problems.

2.4 Results from Other Models

While the BSM PDE/PDI arise from the typical BSM model, different partial differential equations/inequalities and partial integro-differential equations/inequalities (PIDEs/PIDIs) result from different stochastic models.

Under the assumption of a stochastic volatility, Heston (1993) [47] obtained another PDE for one-asset European options without dividend

$$\frac{\partial v}{\partial t} + \frac{\sigma_{11}S^2}{2}\frac{\partial^2 v}{\partial S^2} + \tilde{\rho}\tilde{\sigma}S\sigma_{11}\frac{\partial^2 v}{\partial S\partial\sigma_{11}} + \frac{\tilde{\sigma}^2\sigma_{11}}{2}\frac{\partial^2 v}{\partial {\sigma_{11}}^2} + rS\frac{\partial v}{\partial S} + \big(\tilde{\mu}(\tilde{\sigma}^2-\sigma_{11}) - \Lambda\big)\frac{\partial v}{\partial\sigma_{11}} - rv = 0$$

where Λ is called the price of volatility risk and can be a function of t, S, σ_{11}.

Below is the PIDE for one-asset European options without dividend obtained in the framework of a Levy process associated with a Poisson process, [64],

$$\frac{\partial v}{\partial t} + \frac{\sigma^2 S^2}{2}\frac{\partial^2 v}{\partial S^2} + rS\frac{\partial v}{\partial S} - rv + \lambda\left(\int_0^\infty v(\eta S)\tilde{\Gamma}_\delta(\eta)d\eta - v\right) = 0$$

where

$$\tilde{\Gamma}_\delta(\eta) = \frac{\exp(\frac{-1}{2}(\frac{\log\eta}{\delta})^2)}{\sqrt{2\pi}\delta\eta}$$

is the probability density function (p.d.f.) of η.

Bahlali [3], Liming [33] and Yong and Otmani [79] have further discussed the PIDEs in the frame work of a Levy process.

One should bear in mind that not all models produce a deterministic equation/inequality as a necessary condition for option pricing. In those cases, stochastic analysis and simulation is the only way to investigate the pricing problems.

2.5 Sampling-based Approach for Option Pricing Problems

As mentioned previously, most models start from a stochastic process. If one can sample sufficiently many stochastic paths which are generated to some extent of accuracy, theoretically one can approximate an option's value up to a given tolerance. [43, 2] provide comprehensive discussion of simulation algorithms and error analysis. There are two branches to generate paths, tree-based methods and Monte-Carlo methods. At each time step, the former produce specific share prices fitted in a tree graph while the latter allow all possible values over $\mathbb{R}_+^d$.

2.5.1 Solutions In Terms of Expectation

For European options, the aim is to find the expected payoff on expiry time and discount the value back to the current time, i.e.,

$$v(t, \mathbf{S}_t) = E\big(e^{-r(T-t)} \cdot g(\mathbf{S}_T)\big|\mathbf{S}_t\big), \tag{2.4}$$

where $E(\cdot)$ is the operator of expected value dependent on the conditional probability distribution at exercise time, and $e^{-r(T-t)}$ is the continuous discounting factor with at the rate r from time T to t.

For American options, the aim is adjusted to find the maximum value of all possible values at time $\tau \in [t, T]$ and can be expressed as

$$v(t, \mathbf{S}_t) = \sup_{\tau \in \Theta_{t,T}} E\big(e^{-r(\tau - t)} \cdot g(\mathbf{S}_\tau) \big| \mathbf{S}_t\big), \tag{2.5}$$

where $\Theta_{t,T}$ denotes the set of stopping times. The pricing problem turns to an *optimal stopping time* problem in stochastic analysis, c.f. [14].

2.5.2 Tree Simulation

The tree-based methods generate a branched-tree[3] structure for finitely many paths, so one can compute all possible optimal option values along all paths, discount their values from exercising date and obtain the expected (optimal) value at the current time t. The book by Shreve describes the theories on martingale measure in discrete tree models, cf. [85, ch.1,4].

2.5.3 Monte Carlo Simulation

When implementing Monte Carlo methods, paths are generated separately and not restricted to a tree framework. [101, 85, 20] describe most algorithms of Monte Carlo simulation applied in mathematical finance. Broadie, Glasserman and Ha et al. proposed the use of stochastic meshes combined with Monte Carlo methods to price American options, cf. [13, 12]. The so-called Least Square Monte Carlo (LSMC) methods project both $v(t_k, \mathbf{S}_{t_k})$ and $E\big(v(t_{k+1}, \mathbf{S}_{t_{k+1}}) | \mathbf{S}_{t_k}\big)$ onto the same functional space spanned by a set of basis functions and then employ regression to obtain the time-dependent projection coefficients. Using the approximated coefficients and basis functions, one can thus estimate the value of an American option. Firth (2005) [34] gave details of these methods. Barraquand and Martineau (1995) [6] adopted regression-like methods to perform numerical experiments up to 400 assets. Giles (2007, 2008) [38, 39] employed the multi-level Monte Carlo simulation along with Milstein scheme to reduce the computational complexity. [40, 42, 22, 103] then extended such scheme to a multi-dimensional framework, a random coefficient situation, non-globally Lipschitz payoff and a jump-diffusion process individually. Caramellino and Zanette (2011) [17] performed the numerical comparison among some recent Monte Carlo algorithms for pricing and hedging American options in the high-dimensional Black-Scholes-Merton framework.

2.5.4 Comment

Recall that not every stochastic model can produce a PDE/PDI as a necessary condition of no arbitrage. On these circumstances, simulation-based methods are widely used to price

[3]There are two and three branches at each node in a binomial and trinomial tree methods respectively.

a financial derivative. However, simulation-based methods need extremely many paths to obtain one convergent option value, which cause expensive computational cost for path-dependent and multi-dimensional models. Moreover, the simulation results are dependent on an initial state $\mathbf{S}_t$, so one needs to simulate each time when $\mathbf{S}_t$ varies, which is not convenient in practice.

2.6 Equation-based Approach for Option Pricing Problems

When a PDE, PDI, PIDE or PIDI can be obtained from a model, the option pricing problems turn to tackling these (integro-)differential equations. Mostly numerical methods are required to solve the problems due to their complicated (integro-)differential structures and restrictions.

2.6.1 Discretization

In terms of discretization, there are three main numerical methods - finite difference method (FDM), finite element method (FEM) and finite volume method (FVM). Roughly speaking, FDM is mainly based on Taylor's expansion of the object function, FEM is founded on the properties of selected functional spaces and FVM exploits the conservation of physical volume on the computational domain. Two classical references for FDM and FEM in mathematical finance are [31] and [90] which introduce basic theorems and implementation of algorithms. [95, 109, 1] provide a critique of discretization of option pricing problems with FVM.

2.6.2 Log Transformation

In terms of a PDE, the European option problems can be solved similarly as most physical problems. Nevertheless they become challenging high-dimensional problems as the number of shares increases. To make them easier to solve, they are generally transformed into simpler ones by a change of variables if possible. However, such change of variables usually involves a log transformation, c.f. [34, 78], so the numerical error in the transformed domain may be expanded exponentially in the original problem. Besides, the degeneration condition on $S^{(i)} = 0$ in the BSM model, which corresponds to $x_i := \log(S^{(i)}) = \infty$ in the transformed diffusion model, must be replaced by some artificial condition on $x_i = -x_{\max} << 0$. Angermann and Wang (2007) commented on the error and convergence due to the truncation. More inaccuracy may occur in a high-dimensional case because of such transformation.

2.6.3 Early Exercise Issue

Due to the fact that American and perpetual option have the early-exercise property, their values should not be lower than their payoffs at any time; otherwise, one may buy such an option whose value is lower than its payoff and exercise it immediately to gain the risk-free arbitrage. Such an option either follows BSM PDE or has the value equal to its payoff. The domain hence can be separated into *early-exercise* and *non-early-exercise* regions where the values are equal to and greater than payoffs respectively. They are also named *stopping* and *continuation* regions when viewed as an optimal stopping time problem. The intersection between the two regions is called *free boundary*, *early-exercise boundary* or *optimal-exercise boundary* which is a $(d-1)-$dimensional manifold, c.f. [36, 10], in a $d-$dimensional domain and may evolve as time changes.

2.6.4 Strategy for Early Exercise

There are four essential approaches to solving the early-exercise issue:

1. Front-tracking approach,
2. Penalty approach,
3. Early-exercise premium approach,
4. Complementarity approach.

The front fixing is a front-tracking method. The idea is to fix the location of free boundary on some transformed domain by a change of variables. To do so, some properties on the free boundaries are needed to be known. Wu and Kwok (1997) and Houstis and Kortesis (1998) gave the details of its implementation. In that manner, one needs to solve a nonlinear PDE on the transformed domain and transform the solution back to the original domain. Muthuraman (2008) proposed a guess-and-correct method to track the free boundary in the one-asset case. The front-tracking methods can be applied successfully to the one-asset American call and put. However, there may exist more than one free boundaries for options with exotic payoffs such as straddle and supershare options having the payoff function $g(S) = S \cdot \mathbb{1}_{\{S\in[L,H]\}}$. The properties of the free boundary (or even free boundaries) are not well-known for exotic or multi-asset options. This restricts the applicability of these methods.

Zvana, Forsytha and Vetzalb (1998) firstly introduced the penalty method for pricing American options, which adds an extra term to turn a PDI into a PDE and to avoid the free boundary technically, cf. [111]. New penalty functions were proposed by Wang, Yang and Teo (2006) and Fenga, Kovalovb, Linetskyc and Marcozzid (2007), cf. [96, 59]. Nielsen (2001) used both front-tracking and penalty methods and compared their performances, cf. [71]. Difficulties in choosing proper penalty functions come to light again

in the circumstances of exotic payoffs and multi-asset cases. Moreover such an approach actually perturbs originally PDI and cause extra penalty errors.

The value of an American option can be viewed as the sum of its European counterpart and an early-exercise premium, i.e.

$$v^A(\mathbf{S},t) = v^E(\mathbf{S},t) + p(\mathbf{S},t),$$

where superscripts A and E distinguish American and European options and $p(\cdot)$ is an unknown early-exercise premium function. There are several methods to formulate the early-exercise premium function. For example, Kim (1990) formulated the premium in the case of one-asset call economically and mathematically as

$$\begin{aligned}
p(S,t) &= \int_0^{T-t} qSe^{-q(T-t-\tilde{t})}N(d_+(\tilde{t})) - rEe^{-r(T-t-\tilde{t})}N(d_-(\tilde{t}))d\tilde{t},\\
d_+ &:= \frac{\ln\frac{S}{S_f(\tilde{t})} + (r-q+\frac{\sigma^2}{2})(T-t-\tilde{t})}{\sigma\sqrt{T-t-\tilde{t}}},\\
d_- &:= \frac{\ln\frac{S}{S_f(\tilde{t})} + (r-q-\frac{\sigma^2}{2})(T-t-\tilde{t})}{\sigma\sqrt{T-t-\tilde{t}}} \equiv d_+ - \sigma(T-t-\tilde{t}),
\end{aligned}$$

where $S_f(\tilde{t})$ is the free boundary at time $\tilde{t}$. Jacka (1991), Carr et al.(1992), Gao et al. (2000) and Karatzas and Wang (2000) discussed other formulations of the early-exercise premium. Poitras and Veld (2009) exploited the put-call parity to estimate the early exercise premium for American currency options. Generally this approach makes extra economic assumptions to formulate the early-exercise premium.

The early-exercise issue can be viewed as the *complementarity condition* (CC) in the following form in the BSM framework.

$$\begin{cases} v \geq g, \\ (\dot{v} + \mathcal{L}v)(v-g) = 0 \text{ or } (\mathcal{L}v)(v-g) = 0. \end{cases}$$

Wilmott, Dewynne and Howison (1993) described how to numerically solve the one-asset problem in a classical sense using the projected successive over-relaxation (PSOR) method. Jaillet, Lamberton and Lapeyre (1990) adopted a variational approach to analyze the complementarity problem. Their approach is based on the weighted Sobolev space $V_\mu := \{w : e^{-\mu|\mathbf{x}|}D^m w(\mathbf{x}) \in L_2(\mathbb{R}^d); m = 0,1\}$ where $\mu \in (0,\infty)$, $\mathbf{x} = log\mathbf{S}$ and D^m is the weak derivative of order m. Their work also showed the existence of unique solution on the transformed d-dimensional semi-infinite/unbounded domain by linking the formulation to the properties from optimal stopping time analysis. Mautner (2006) estimated the error arising from computational domain truncation in the framework of one-dimensional weighted Sobolev space. Huang and Pang (1998) discussed the approach under different one-asset models. Fenga (2007) considered the variational formulation with asset price following a Markov

jump-diffusion process. Zhang (2007) investigated the variational complementarity problems after log transformation and showed numerical convergence results up to 2 assets.

A recent survey on one-asset American options is carried out by Se Ryoong Ahn, etc. (2011). Mathematically the complementarity approach is the most genuine way to formulate the early-exercise problem. Based on this nature, we adopted this approach but focused on a bounded computational domain in the next chapter.

2.7 Analytical Approach for Option Pricing Problems

The pricing problems can also be investigated analytically from different aspects. We first look at the fundamental solutions for European options. Their fundamental solutions can be obtained by finding expected value with proper probability measure or using the fundamental solution of the transformed diffusion equation.

2.7.1 One-asset Non-path-dependent European Options

Recall the value of a European option can be expressed as (2.4). For a one-asset non-path-dependent European option with a non-negative convex payoff function $g(S)$, its value can be further expressed in the integral form, cf. [86, p.218],

$$v(t,S) = e^{-r\tau}\int_{-\infty}^{\infty}\frac{1}{\sqrt{2\pi}}\,e^{-\frac{\eta^2}{2}}\,g(Se^{(r-q-\frac{\sigma^2}{2})\tau+\sigma\sqrt{\tau}\,\eta})\,d\eta.$$

where $\tau = T-t \geq 0$ is called the *time to maturity*.

2.7.2 Multi-asset Non-path-dependent European Options

The multi-dimensional BSM PDE can be transformed to a multi-dimensional simple diffusion equation which has a fundamental solution in terms of cumulative density function of multi-dimensional standard normal distribution. After converting the solution back to the original BSM model, the fundamental solution to a $d-$asset non-path-dependent European option is of the integral form, cf. [99, p.187],

$$v(t,\mathbf{S}) = e^{-r\tau}\big(2\pi\tau\big)^{-d/2}\big(\det\boldsymbol{\Sigma}\big)^{-1/2}\big(\prod_{i=1}^{d}\sigma_i\big)^{-1}\int_0^{\infty}\cdots\int_0^{\infty}\frac{g(\tilde{\mathbf{S}})}{\prod_{i=1}^{d}\tilde{S}_i}\exp\big(\frac{-\boldsymbol{\zeta}^T\boldsymbol{\Sigma}^{-1}\boldsymbol{\zeta}}{2}\big)d\tilde{S}_1\cdots d\tilde{S}_d,$$

where

$$\tilde{\mathbf{S}} := \big[\tilde{S^{(1)}}\cdots\tilde{S}_d\big]^T,\ \boldsymbol{\zeta} := \big[\zeta_1\cdots\zeta_d\big]^T,\ \boldsymbol{\Sigma} := \big[\sigma_{ij}\big]_{d\times d},$$
$$\zeta_i := \frac{1}{\sqrt{\sigma_i^2\tau}}\Big(\ln\big(\frac{S^{(i)}}{\tilde{S^{(i)}}}\big)+(r-q_i-\frac{\sigma_i^2}{2})\tau\Big).$$

The solution exists when $\frac{1}{\prod_{i=1}^{d}\tilde{S}_i}\exp\left(\frac{-\zeta^T\boldsymbol{\Sigma}^{-1}\zeta}{2}\right)$ goes to zero faster than $g(\tilde{\mathbf{S}})$ goes to infinity as $\tilde{\mathbf{S}}$ approaches infinity, which is never violated by all known options. Note that the τ next to 2π in the equation will disappear after a change of variable in the one-dimensional case. In practice, the fundamental integral solutions can be obtained by approximation. [106] proposes the use of hyper-triangles to approximate a multi-variate integral. [37] employs hyper-cubes along with sparse grids and provides examples of integration up 32 and 256 dimensions.

2.7.3 American Options In Terms of Stopping Time

A stopping time is a random time for a stochastic process to stop under some conditions, cf. [86, p.341, 361, 364]. In mathematical finance, it can be interpreted as the time when an American option owner faces the early-exercise values which are higher than the expected values of keeping the option afterwards. In this manner, the value of American option is the highest of all the values at stopping times. Bensoussan (1984) and Karatzas (1988) formulated the value of American options using no-arbitrage argument and stopping time from stochastic aspect as (2.5).

2.7.4 American Options In Terms of Free Boundary

The free boundaries of American options refer to the intersected boundaries or hypersurfaces between early-exercise and non-early-exercise regions. Simple options such as call and put have only one free boundary but there may exist more than one in exotic and high dimensional cases. Generally, free boundaries are time-dependent in most cases of American options but time-independent in those of perpetual ones.

The regularity of of the free boundaries in variational inequalities was first analyzed by Caffarelli and Rivire (1976) and Kinderlehrer (1978), cf. [15, 55]. Shahgholian (2008) analyzed the behavior of free boundary arising in one-asset American option, cf. [84]. Laurence and Salsa (2009) proved the C^∞ regularity for the free boundaries in the multi-asset case, cf. [61]. In recent years, there are particular interest in the study of the α-stable[4] Levy process, which generally leads to a bilinear form involving a fractional Laplacian. Particularly, [87, 16] investigated the regularity of its solution and free boundary in the framework of its variational inequality.

2.7.5 Asymptotic Analysis for Option Pricing Problems

Instead of tackling original problems, an alternative is to explore the limit behavior of solution provided an extremely large or small number for one of the parameters in a model.

[4] A linear combination of two independent copies of its variable has the same distribution as the variable with scaling and shifting.

For example, one can investigate the solution to an option pricing problem when given an extreme E (strike price), r (riskfree rate), q (dividend rate), T (expiry date) and σ (volatility) in the BSM model. [97, 45, 76] performed different asymptotic analysis in a framework of small/high drift, volatility or transaction cost. Kuske and Keller (1998) investigated the solutions when time approaches maturity date, cf. [60]. Firth (2005) approximated the solutions provided $\frac{\sigma^2}{|r-q|} << 1$, cf. [34, p.111]. Another popular application is to approximate the free boundary asymptotically, cf. [60, 19, 104].

2.8 Closed-form Formulas

The analytical solutions may be further expressed in closed-form formulas in some cases. The book by E. G. Haug [46] summarizes most well-known formulas. We introduce some of them below.

2.8.1 Black-Scholes-Merton Formulas

Below are the celebrated BSM formulas derived from a standard BSM model.

$$C(t,S) = Se^{-q\tau}N(d_1) - Ee^{-r\tau}N(d_2),$$
$$P(t,S) = Ee^{-r\tau}N(-d_2) - Se^{-q\tau}N(-d_1),$$

where

$$d_1 := \frac{\ln\frac{S}{E} + (r - q + \frac{\sigma^2}{2})\tau}{\sqrt{\sigma^2\tau}},$$
$$d_2 \triangleq \frac{\ln\frac{S}{E} + (r - q - \frac{\sigma^2}{2})\tau}{\sqrt{\sigma^2\tau}}.$$

The $C(t,S)$ and $P(t,S)$ stand for the values of one-asset European call and put and $N(\cdot)$ is the cumulative density function (CDF) of standard univariate normal distribution.

2.8.2 Multi-asset minimum and maximum options

Exact closed-form formulas are hardly obtained in a multi-asset model except for European maximum and minimum options. Stulz (1982) first derived the formulas of two-asset European call and put on minimum and maximum, cf. [88]. The formulas are then generalized to the higher dimensional cases by Johnson (1987) and Rich and Chance (1993) , [54, 80]. We summarize the formulas of two-asset call on minimum, call on maximum,

put on minimum and put on maximum as follows.

$$
\begin{aligned}
C_{min}(t,S^{(1)},S^{(2)}) = \quad & S^{(1)}e^{-q_1\tau}N_2(d_{1,S^{(1)}};-\tilde{d}_1;-\tilde{\rho}_1)+S^{(2)}e^{-q_2\tau}N_2(d_{1,S^{(2)}};\tilde{d}_2;-\tilde{\rho}_2)\\
- \quad & Ee^{-r\tau}N_2(d_{2,S^{(1)}};d_{2,S^{(2)}};\rho),\\
C_{max}(t,S^{(1)},S^{(2)}) = \quad & S^{(1)}e^{-q_1\tau}N_2(d_{1,S^{(1)}};\tilde{d}_1;\tilde{\rho}_1)+S^{(2)}e^{-q_2\tau}N_2(d_{1,S^{(2)}};-\tilde{d}_2;\tilde{\rho}_2)\\
- \quad & Ee^{-r\tau}\big(1-N_2(-d_{2,S^{(1)}};-d_{2,S^{(2)}};\rho)\big),\\
P_{min}(t,S^{(1)},S^{(2)}) = \quad & Ee^{-r\tau}-\tilde{C}_{min}(t,S^{(1)},S^{(2)})+C_{min}(t,S^{(1)},S^{(2)}),\\
P_{max}(t,S^{(1)},S^{(2)}) = \quad & Ee^{-r\tau}-\tilde{C}_{max}(t,S^{(1)},S^{(2)})+C_{max}(t,S^{(1)},S^{(2)}),
\end{aligned}
$$

where

ρ : correlation coefficient between log returns,
$N_2(x;y;\rho)$: cdf of standard bivariate normal distribution with correlation coefficient ρ (integral over $[\infty,x]\times[\infty,y]$),

$$\sigma_w=\sqrt{\sigma_1^2+\sigma_2^2-2\rho\sigma_1\sigma_2},\ \rho_1=\frac{\sigma_1-\rho\sigma_2}{\sigma_w},\ \rho_2=\frac{\sigma_2-\rho\sigma_1}{\sigma_w},$$

$$d_{1,S^{(i)}}:=\frac{\ln\frac{S^{(i)}}{E}+(r-q_i+\frac{\sigma_i^2}{2})\tau}{\sqrt{\sigma_i^2\tau}},d_{2,S^{(i)}}:=\frac{\ln\frac{S^{(i)}}{E}+(r-q_i-\frac{\sigma_i^2}{2})\tau}{\sqrt{\sigma_i^2\tau}}=d_{1,S^{(i)}}-\sigma_i\sqrt{\tau},$$

$$\tilde{d}_1:=\frac{\ln\frac{S^{(1)}}{S^{(2)}}+(-q_1+q_2+\frac{\sigma_w^2}{2})\tau}{\sqrt{\sigma_w^2\tau}},\ \tilde{d}_2:=\tilde{d}_1-\sigma_w\sqrt{\tau},$$

$$\tilde{C}_{min}(t,S^{(1)},S^{(2)}):=S^{(1)}e^{-q_1\tau}\big(1-N(\tilde{d}_1)\big)+S^{(2)}e^{-q_2\tau}N(\tilde{d}_2),$$

$$\tilde{C}_{max}(t,S^{(1)},S^{(2)}):=S^{(2)}e^{-q_2\tau}\big(1-N(\tilde{d}_2)\big)+S^{(1)}e^{-q_1\tau}N(\tilde{d}_1).$$

2.8.3 One-asset Perpetual Call and Put

As perpetual options are not restrained by expiry date, their one-dimensional BSM PDE decays to an Euler-Cauchy equation without time term involved in the non-early-exercise regions, i.e. $[0,S_f]$ and $[S_f,\infty]$ for call and put respectively. We consider the pricing models as follows. Recall $\mathcal{L}:=\frac{\partial^2}{\partial S^2}+(r-q)S\frac{\partial}{\partial S}-r$.

Model 2.1 – One-asset Perpetual Put

- *Early-exercise region:*
  $\mathcal{L}P<0,\ P(S)=g(S)=E-S>0,\forall S\in[0,S_f]$,
- *non-early-exercise region*
  $\mathcal{L}P=0,\ P(S)>g(S)\geq 0,\forall S\in[S_f,\infty]$,

- *At the optimal/early exercise boundary*
  $P(S_f) = E - S_f$ *(continuity) and* $\frac{\partial P}{\partial S}\Big|_{S=S_f} = \frac{\partial g}{\partial S}\Big|_{S=S_f} = -1$ *(smooth-pasting),*

- *At the right boundary:*
  $P(S \to \infty) = 0$.

The value of a perpetual put can be expressed in the form of, cf. [98, p.153],

$$P(S) = \begin{cases} g(S) = E - S \text{ if } S \leq S_f \\ BS^{m_2} \text{ if } S \geq S_f \end{cases}$$

where

$$m_2 = \frac{-(r - q - \frac{\sigma^2}{2}) - \sqrt{(r - q - \frac{\sigma^2}{2})^2 + 2r\sigma^2}}{\sigma^2},$$
$$S_f = \frac{E}{1 - \frac{1}{m_2}},\ B = \frac{E - S_f}{S_f^{m_2}}.$$

Particularly, for $q = 0 : m_2 = \frac{-2r}{\sigma^2}$ and $S_f = \frac{E}{1 + \frac{\sigma^2}{2r}}$.

A perpetual call can be handled analogously.

Model 2.2 – One-asset Perpetual Call

- *Early-exercise region:*
  $\mathcal{L}C < 0$, $C(S) = g(S) = S - E > 0, \forall S \in [S_f, \infty]$,

- *non-early-exercise region*
  $\mathcal{L}C = 0$, $C(S) > g(S) \geq 0, \forall S \in [0, S_f]$,

- *At the optimal/early exercise boundary*
  $C(S_f) = S_f - E$ *(continuity) and* $\frac{\partial C}{\partial S}\Big|_{S=S_f} = \frac{\partial g}{\partial S}\Big|_{S=S_f} = 1$ *(smooth-pasting),*

- *At the left boundary:*
  $C(S = 0) = 0$.

The value of perpetual put can be expressed in the form of, cf. [98, p.155],

$$C(S) = \begin{cases} g(S) = S - E \text{ if } S \geq S_f \\ AS^{m_1} \text{ if } S \leq S_f \end{cases}$$

where

$$m_1 = \frac{-(r - q - \frac{\sigma^2}{2}) + \sqrt{(r - q - \frac{\sigma^2}{2})^2 + 2r\sigma^2}}{\sigma^2},$$
$$S_f = \frac{E}{1 - \frac{1}{m_1}},\ A = \frac{S_f - E}{S_f^{m_1}}.$$

Particularly, for $q = 0 : m_1 = 1$ and $S_f \to \infty$. As well, $A = 1$ and $C(S) = S$ in the special case. This implies never to exercise a one-asset perpetual call on a non-dividend-paying asset is the optimal decision since holding the option amounts to holding the underlying asset for an owner.

2.8.4 Other formulas

Rubinstein and Reiner (1991) derived the values of one-asset European barrier options, cf. [81]. In the two-asset framework, Margrabe (1978) provided the pricing formulas of European exchange options and Wu and Zhang (1999) solved the the problems on the minimum or maximum of geometric averages, cf. [66, 102].

2.9 Dividend Issue In One-asset Case

For an American put, if $S < S_f(t) < E$, then the option value is its payoff value, i.e. $v = (E - S)$ and thus we have

$$\begin{aligned} & \frac{\partial v}{\partial t} + \frac{1}{2}S^2\frac{\partial^2 v}{\partial S^2} + (r-q)S\frac{\partial v}{\partial S} - rv \\ = \; & 0 + 0 + (r-q)S(-1) - r(E-S) = qS - rE. \end{aligned}$$

Without dividend, $-rE$ makes the strict inequality. In the dividend-paying case, the early-exercise boundary should be low enough such that $qS - rE \leq 0 \leftrightarrow S \leq S_f(t) \leq \min\{\frac{rE}{q}, E\}$ holds. In general $r \geq q \leftrightarrow \frac{r}{q} \geq 1$, so $S_f(t) \leq \min\{\frac{rE}{q}, E\}$ is satisfied provided $S_f(t) \leq E$ for a put.

On the other hand, an American call with the payoff $S - E$ satisfies

$$\begin{aligned} & \frac{\partial v}{\partial t} + \frac{1}{2}S^2\frac{\partial^2 v}{\partial S^2} + (r-q)S\frac{\partial v}{\partial S} - rv \\ = \; & 0 + 0 + (r-q)S(+1) - r(S-E) = -qS + rE \leq 0 \\ \Leftrightarrow \; & S \geq S_f(t) \geq \max\{\frac{rE}{q}, E\}. \end{aligned} \tag{2.6}$$

It implies $S_f(t) > E$ strictly when a dividend rate is considered and $r \geq q$. Since $S_f(t) \to \infty$ as $q \to 0$, it implies never to exercise an American call is the optimal decision for its owner when no dividend is paid to the underlying asset. Due to the non-early-exercise property given $q = 0$, the value of a one-asset American call simply follows the BSM PDE all the time and it shares the same value as its European counterpart. The same conclusion can be reached based on stochastic analysis, cf. [86, p.363].

We should also bear in mind that for both American call and put the free boundaries $\lim_{t \to T} S_f(t)$ may not be consistent with the exercise price E at maturity time T.

2.10 Summary

Option pricing problems can be investigated from different aspects such as stochastic analysis, partial differential problems and their variational variants. There are very different approaches to tackle such problems. These problems become dramatically challenging in a multi-asset framework and more challenging if an equality is replaced by an inequality in the early-exercise cases. In this research, we look for a variational approach to deal with both situations. Before reformulating problems in variational form, in the next chapter we will describe the necessary conditions for solving the problems.

Chapter 3

Auxiliary Conditions

When option pricing problems are considered from the aspect of differential equations, the proper terminal/final condition (TC/FC) and boundary conditions (BCs) are requested for solving them. In the early-exercise cases, no-arbitrage argument must also be considered. The setup of these conditions must make both financial and mathematical sense. For some exotic options such as barrier options, the conditions also depend on their payoffs and contract restrictions, c.f. [112, 93]. These conditions may vary from model to model, cf. [32, 23]. In our work, we focus on the d-asset European/American/perpetual minimum/maximum/basket call/put/straddle options in the BSM model.

3.1 Conditions for Early-exercise Property

3.1.1 Complementarity Condition

Recall that the value of an option with the early-exercise property either follows the BSM PDE in the non-early-exercise region or must be equal to its payoff in the early-exercise region. This can be expressed as the complementarity condition (CC) in the forms below.

$$\text{American options:} \quad \begin{cases} v(\mathbf{S},t) \geq g(\mathbf{S}), \\ (\dot{v} + \mathcal{L}v)(v-g) = 0. \end{cases}$$

$$\text{Perpetual options:} \quad \begin{cases} v(\mathbf{S}) \geq g(\mathbf{S}), \\ (\mathcal{L}v)(v-g) = 0. \end{cases}$$

3.1.2 Conditions on Early-exercise Boundary

Recall in the previous chapter we use *continuity condition* and *smooth-pasting condition* on the free boundary to analytically solve the pricing problems for one-asset perpetual call and put. In general, the free boundary $S_f(t)$ is a $(d-1)-$dimensional evolutionary manifold in a $d-$asset case. The continuity condition $v = g$ will be satisfied automatically if

only continuous functions are considered for our solutions. The smooth-pasting condition $\frac{\partial v}{\partial S^{(i)}} = \frac{\partial v}{\partial S^{(i)}}$ is not necessary if the pricing problem is formulated as a complementarity problem. Moreover, it may fail in a general scenario, cf. [67] and [108, Remark 3.20]. Based on these, we will not pose the smooth-pasting condition in our later formulation.

3.2 Terminal Condition

Different from most physical problems, in the BSM model without transformation we have the terminal/final condition (TC/FC) at expiry time $t = T$. On the expiry date, an option's value v simply equals its payoff value g, i.e.

$$v(\mathbf{S}, t = T) = g(\mathbf{S}).$$

3.3 Boundary Conditions

In this research, we will work on the spatial domain of bounded $d-$dimensional rectangle/cube . In this manner, we need conditions on $S^{(i)} = 0$ and $S^{(i)} = S_{\max}$ where $S_{\max}$ is a relatively large value.

3.3.1 Choice of $S_{\max}$

A rule of thumb is to take $S_{\max}$ at least three time lager than E, cf. [74, 21]. Intuitively, as the volatility or the time to maturity increases, the probability that a share/portfolio price reach an extreme value is higher. This implies the $S_{\max}$ should be set bigger in these cases. Moreover, the idea of "far enough" should depend on an option's payoff and contract restrictions as well. For example, a vanilla put's $S_{\max}$ can be set smaller than that of its call counterpart. Kangort and Nicolaides (2000) derived the point-wise bounds arising from the setup of $S_{\max}$; in particular, they suggested

$$S_{\max} = Ee^{\sqrt{2\sigma^2 T \ln 100}},$$

for a one-asset European call which coincides with the intuitive guess.

In what follows, there are three types of boundary conditions to be defined − degeneration and deterministic and almost-sure boundary conditions.

3.3.2 Degeneration Condition

A boundary condition is said to be a *degeneration condition* if the value of a $d-$asset option simply degenerates to that of its $(d-1)-$asset counterpart on the boundary. In this case, the boundary condition is of Dirichlet type.

3.3.3 Deterministic Condition

If the option value on a boundary can be expressed by its payoff with a constant portfolio price S^p, we call such Dirichlet conditions *deterministic condition*.

3.3.4 Almost-sure Condition

If the option value on a boundary can be expressed by its payoff with a variable portfolio price S^p or share prices $\mathbf{S}$, we call such Dirichlet conditions *almost-sure condition*. This name is coined because as a share value tends to zero or becomes extremely large, the probability measure to exercise (or not to) is almost equal to 1 or 0. Another approach is to define the almost-sure condition of Neumann type which claims the sensitivity of the option w.r.t. $S^{(i)}$ is equal to that of its payoff for $i = 1, \ldots, d$.

We now give details of how to set our boundary conditions from financial and mathematical aspects. We will take the discount factor into account for European options as they can be exercised only on expiry date.

3.3.5 Near-field Condition on $S^{(i)} = 0$

Once $S^{(i)}$ reaches 0, it remains at 0 afterwards and a $d-$dimensional BSM PDE degenerates to a $(d-1)-$dimensional counterpart. Due to this, basket and maximum options have degeneration conditions while minimum options have the deterministic condition with $S^p = 0$. That is,

- Basket and maximum options: $v(\ldots, S^{(i-1)}, S^{(i)}, S^{(i+1)}, \ldots) = v(\ldots, S^{(i-1)}, S^{(i+1)}, \ldots)$.
- Minimum options:

$$v = \begin{cases} e^{-r(T-t)} g(S^p = 0) & \text{for European options,} \\ g(S^p = 0) & \text{for American and perpetual options.} \end{cases}$$

3.3.6 Far-field Condition on $S^{(i)} = S_{\max}$

We now assume $S_{\max}$ is large enough such that provided $S_t^{(i)} = S_{\max} \to \infty$,

- the probability that a basket option is to be exercised (prior to or on expiry date) is close to either 1 or 0.
- the probability that $S^{(i)}(t^+)$ becomes the minimum of all share prices (prior to or on expiry date) is close to 0 for $t^+ \in (t, T]$.
- the probability that $S^{(i)}(t^+)$ becomes the maximum of all share prices (prior to or on expiry date) is close to 1 for $t^+ \in (t, T]$.

Hence on $S^{(i)} = S_{\max}$ a basket option has an almost-sure condition, a minimum option possesses a degeneration condition and a maximum options is given deterministic conditions.

- Basket options:

$$v = \begin{cases} e^{-r(T-t)} g(\mathbf{S}) & \text{for European options,} \\ g(\mathbf{S}) & \text{for American and perpetual options,} \end{cases}$$

  or in the following Neumann form for European, American and perpetual types.

$$\nabla v = \nabla g.$$

- Minimum options: $v(\ldots, S^{(i-1)}, S^{(i)}, S^{(i+1)}, \ldots) = v(\ldots, S^{(i-1)}, S^{(i+1)}, \ldots)$.

- Maximum option:

$$v = \begin{cases} e^{-r(T-t)} g(S^p = S_{\max}) & \text{for European options,} \\ g(S^p = S_{\max}) & \text{for American and perpetual options.} \end{cases}$$

  An alternative is to have the Neumann form as Basket cases.

$$\nabla v = \nabla g.$$

3.4 Two-asset Examples

3.4.1 BCs of Basket Options

Consider positive weights $w_i > 0$ of underlying asset $S^{(i)}$ to form a portfolio. Start with the payoff of a basket call, for $i, j = 1, 2$

$$\big((w_i S^{(i)} + w_j S^{(j)}) - E\big)^+ = \begin{cases} (w_j S^{(j)} - E)^+ = w_j (S^{(j)} - \frac{E}{w_j})^+ \text{ on } S^{(i)} = 0, \\ (w_i S^{(i)} - E) + w_j S^{(j)} = (w_i S_{\max} - E) + w_j S^{(j)} >> 0 \text{ on } S^{(i)} = S_{\max}. \end{cases}$$

Analogously, a basket put has

$$\big(E - (w_i S^{(i)} + w_j S^{(j)})\big)^+ = \begin{cases} (E - w_j S^{(j)})^+ = w_j (\frac{E}{w_j} - S^{(j)})^+ \text{ on } S^{(i)} = 0, \\ 0 \text{ on } S^{(i)} = S_{\max}. \end{cases}$$

A straddle is simply a call plus a put, thus its payoff is

$$\begin{aligned} & \big((w_i S^{(i)} + w_j S^{(j)}) - E\big)^+ + \big(E - (w_i S^{(i)} + w_j S^{(j)})\big)^+ \\ = & \begin{cases} w_j \big((S^{(j)} - \frac{E}{w_j})^+ + (\frac{E}{w_j} - S^{(j)})^+\big) \text{ on } S^{(i)} = 0, \\ (w_i S_{\max} - E) + w_j S^{(j)} >> 0 \text{ on } S^{(i)} = S_{\max}. \end{cases} \end{aligned}$$

Along $S^{(i)} = 0$ the payoff of one unit of basket option with exercise price E turns to that of w_j lots of one-asset counterpart on remaining $S^{(j)}$ with the different exercise price $\frac{E}{w_j}$. No-arbitrage argument implies the two-asset option's value is equal to w_j units of one-asset counterpart with the exercise price $\frac{E}{w_j}$, so we have the degeneration condition on $S^{(i)} = 0$ in this case.

Along $S^{(i)} = S_{\max}$ we hence have the almost-sure condition of Dirichlet type depending on $(S^{(i)} = S_{\max}, S^{(j)})$ where $S^{(j)} \in [0, S_{\max}]$. As suggested by the literal meaning of almost-sure condition, on $S^{(i)} = S_{\max} \to \infty$ the payoff values above are equal to those of American options while European options share the same payoffs but multiplied by a discount factor. Another choice is to adopt Neumann condition as the almost-sure condition. The basket call and straddle are to be exercised almost surely as $S^{(i)} = S_{\max} \to \infty$, so their Neumann condition reads

$$\nabla v = (w_1,\ w_2)^T.$$

However, a basket put is not to be exercised almost surely, so its Neumann condition is simply

$$\nabla v = \mathbf{0}.$$

3.4.2 BCs of Minimum Options

Minimum options can be interpreted analogously by observing the payoff values below.

Minimum Call

$$\big(\min\{S^{(i)}, S^{(j)}\} - E\big)^+ = \begin{cases} (0-E)^+ = 0 \text{ on } S^{(i)} = 0, \\ (S^{(j)} - E)^+ \text{ on } S^{(i)} = S_{\max}. \end{cases}$$

Minimum Put

$$\big(E - \min\{S^{(i)}, S^{(j)}\}\big)^+ = \begin{cases} (E-0)^+ = E \text{ on } S^{(i)} = 0, \\ (E - S^{(j)})^+ \text{ on } S^{(i)} = S_{\max}. \end{cases}$$

Minimum Straddle

$$\begin{aligned} & \big(\min\{S^{(i)}, S^{(j)}\} - E\big)^+ + \big(E - \min\{S^{(i)}, S^{(j)}\}\big)^+ \\ = & \begin{cases} 0 + E = E \text{ on } S^{(i)} = 0, \\ (S^{(j)} - E)^+ + (E - S^{(j)})^+ \text{ on } S^{(i)} = S_{\max}. \end{cases} \end{aligned}$$

As a result, we can exploit the deterministic conditions on $S^{(i)} = 0$ and the degeneration conditions on $S^{(i)} = S_{\max}$ for $i = 1, 2$.

3.4.3 BCs of Maximum Options

Similarly we observe the payoffs below first.

Maximum Call

$$\left(\text{Max}\{S^{(i)}, S^{(j)}\} - E\right)^+ = \begin{cases} (S^{(j)} - E)^+ \text{ on } S^{(i)} = 0, \\ S_{\max} - E >> 0 \text{ on } S^{(i)} = S_{\max}. \end{cases}$$

Maximum Put

$$\left(E - \text{Max}\{S^{(i)}, S^{(j)}\}\right)^+ = \begin{cases} (E - S^{(j)})^+ \text{ on } S^{(i)} = 0, \\ (E - S_{\max})^+ = 0 \text{ on } S^{(i)} = S_{\max}. \end{cases}$$

Maximum Straddle

$$\begin{aligned} & \left(\text{Max}\{S^{(i)}, S^{(j)}\} - E\right)^+ + \left(E - \text{Max}\{S^{(i)}, S^{(j)}\}\right)^+ \\ = & \begin{cases} (S^{(j)} - E)^+ + (E - S^{(j)})^+ \text{ on } S^{(i)} = 0, \\ (S_{\max} - E) + 0 = S_{\max} - E \text{ on } S^{(i)} = S_{\max}. \end{cases} \end{aligned}$$

Different from Basket options on the boundary of $S^{(i)} = 0$, the value of two-asset Maximum options degenerates to that of one unit of one-asset counterpart linked to the remaining share $S^{(j)}$ with identical exercise price.

An alternative on $S^{(i)} = S_{\max}$ is the Neumann type of almost-sure condition in the following form.

$$\left(\frac{\partial v}{\partial S^{(i)}}, \frac{\partial v}{\partial S^{(j)}}\right) = \begin{cases} (1, 0) \text{ for Maximum call/straddle}, \\ (0, 0) \text{ for Maximum put}. \end{cases}$$

3.5 Other Choices

In the above, the $S_{\max} - E$ and $w_i S_{\max} - E$ may be replaced by $S_{\max}$ and $w_i S_{\max}$ respectively as $S_{\max} >> E$ and $w_i S_{\max} >> E$ respectively. When taking the discount factor into account, some literatures use the dividend and interest rates to discount the share and strike prices separately in the financial point of view. That is, $e^{-r(T-t)} g(\mathbf{S}; E)$ may be replaced by $g(\tilde{\mathbf{S}}; \tilde{E})$ where $\tilde{\mathbf{S}} = \left(e^{-q_1(T-t)} S^{(1)}, \ldots, e^{-q_d(T-t)} S_d\right)^T$ and $\tilde{E} = e^{-r(T-t)} E$. Such idea can also be justified theoretically to some extent by the one-asset BSM formulas.

Some references propose the so-called *linearity boundary condition* at the far field $S^{(i)} = S_{\max}$, cf. [100, 26]. Such approach assumes

$$\left.\frac{\partial^2 v}{\partial {S^{(i)}}^2}\right|_{S^{(i)} = S_{\max}} = 0,$$

which can be viewed as the relaxation of the Neumann BCs mentioned earlier. In one-asset case, this implies using

$$v(t) = c_0(t) + c_1(t)S,$$

on $S^{(i)} = S_{\max}$ which coincides with the form of BSM formulas. In higher dimensional scenarios, it implies to find the value satisfying $\dot{v} + \tilde{\mathcal{L}}v = 0$ on $S^{(i)} = S_{\max}$ where

$$\tilde{\mathcal{L}}v := \frac{1}{2}\sum_{j=1}^{d}\sum_{\substack{k=1 \\ k\neq j=i}}^{d} \sigma_{jk}S^{(j)}S^{(k)}\frac{\partial^2 v}{\partial S^{(j)}\partial S^{(k)}} + \sum_{j=1}^{d}(r-q_j)S^{(j)}\frac{\partial v}{\partial S^{(j)}} - rv,$$

in the European cases.

3.6 Summary

We have seen how to set the auxiliary conditions in financial and mathematical senses. The boundary conditions are more complicated than others since we need to consider payoffs and other contract restrictions (if any). By using replication and no-arbitrage argument, the fair values on boundary are hence presented. Particularly, the degeneration conditions are of the form of their counterparts of one asset less. In the next chapter, we will consider either "all Dirichlet BCs on $S^{(i)} = 0$ and $S^{(i)} = S_{\max}$" or "(half) Dirichlet on $S^{(i)} = 0$ and (half) Neumann BCs $S^{(i)} = S_{\max}$" and incorporate them in variational formulations.

Chapter 4

Reformulation

4.1 Classical Formulation

From now on we pose our problems in the bounded domain $[0,T] \times \Omega$ where $\Omega \subset \mathbb{R}^d_+$. We first recall the Black-Scholes-Merton (BSM) operator of the form

$$\mathcal{L}v := \frac{1}{2}\sum_{i=1}^{d}\sum_{j=1}^{d}\sigma_{ij}S^{(i)}S^{(j)}\frac{\partial^2 v}{\partial S^{(i)}\partial S^{(j)}} + \sum_{i=1}^{d}(r-q_i)S^{(i)}\frac{\partial v}{\partial S^{(i)}} - rv.$$

The option pricing problems of our interest are formulated in a standard BSM model as follows.

European Options

A partial differential equation (PDE):

$$\dot{v} + \mathcal{L}v = 0,$$

along with a terminal condition (TC) and proper boundary conditions (BCs).

American Options

A partial differential inequality (PDI):

$$\dot{v} + \mathcal{L}v \leq 0,$$

along with the complementarity condition (CC)

$$\begin{cases} v - g \geq 0, \\ (\dot{v} + \mathcal{L}v)(v-g) = 0, \end{cases}$$

and a TC and proper BCs.

Perpetual Options

A partial differential inequality (PDI):

$$\mathcal{L}v \leq 0,$$

along with the CC

$$\begin{cases} v - g \geq 0, \\ (\mathcal{L}v)(v - g) = 0, \end{cases}$$

and proper BCs.

Note that g is a payoff function. The forms above are referred to as the *classical* or *strong* formulations of option pricing problems.

4.2 BSM Operator in Divergence Form

Matrix Notations

In order to tackle high-dimensional problems in terms of matrices, we would like to express the BSM operator in the divergence form as shown later. For convenience, the row i, column j and (i, j) minor matrix of an arbitrary matrix $\mathbf{m}$ are denoted by $\mathcal{R}_{\mathbf{m}}^{(i)}$, $\mathcal{C}_{\mathbf{m}}^{(j)}$ and $\mathcal{M}_{\mathbf{m}}^{(i,j)}$ in what follows. A $d \times d$ symmetric tensor matrix $\mathbf{T}$ is defined as a matrix with the (i, j) component

$$\mathbf{T}_{ij} = \frac{\sigma_{ij} S^{(i)} S^{(j)}}{2}.$$

We further define the following vectors.

$$\begin{aligned}
\mathbf{D} &:= \Big((r-q_1)S^{(1)},\ldots,(r-q_d)S^{(d)}\Big)^T,\\
\tilde{\mathbf{D}} &:= \mathbf{D}-\sum_{j=1}^{d}\frac{\partial \mathcal{C}_{\mathbf{T}}^{(j)}}{\partial S_j} = \left(\Big(r-q_i-\sigma_{ii}-\sum_{\substack{j=1\\ j\neq i}}\frac{\sigma_{ij}}{2}\Big)S^{(i)}\right)_{d\times 1}\\
&= \begin{pmatrix} r-q_1-\sigma_{11}-\sum\limits_{\substack{j=1\\ j\neq 1}}\frac{\sigma_{1j}}{2}\\ \vdots\\ r-q_i-\sigma_{ii}-\sum\limits_{\substack{j=1\\ j\neq i}}\frac{\sigma_{ij}}{2}\\ \vdots\\ r-q_d-\sigma_{dd}-\sum\limits_{\substack{j=1\\ j\neq d}}\frac{\sigma_{dj}}{2}\end{pmatrix}\odot\begin{pmatrix}S^{(1)}\\ \vdots\\ S^{(i)}\\ \vdots\\ S^{(d)}\end{pmatrix} = \begin{pmatrix}\bar{D}^{(1)}\\ \vdots\\ \bar{D}^{(i)}\\ \vdots\\ \bar{D}^{(d)}\end{pmatrix}\odot\begin{pmatrix}S^{(1)}\\ \vdots\\ S^{(i)}\\ \vdots\\ S^{(d)}\end{pmatrix}\\
&=: \bar{\mathbf{D}}\odot\mathbf{S}
\end{aligned}$$

where $\odot$ is the entry-by-entry product, also called the Hadamard product. We also denote the maximum of $\bar{D}^{(i)}$ by

$$\bar{D}^{\max} := \max_{1\le i\le d}\left\{\left|\bar{D}^{(i)}\right|\right\}.$$

Divergence Form

The BSM operator can hence be written in the divergence form below.

$$\mathcal{L}(v) = \nabla\cdot(\mathbf{T}\nabla v)+\tilde{\mathbf{D}}\cdot\nabla v - rv.$$

4.3 Variational Formulation

Instead of seeking a solution in the classical sense, the pricing problems can be reformulated in integral form and the weak solutions can then be found in certain functional spaces, generally Hilbert spaces. We will look in detail at European, American and perpetual cases individually.

4.3.1 Notation

Recall our problems of interest are over the bounded domain $[0,T]\times\Omega$ where $\Omega := [0,S_{\max}]^d \subset \mathbb{R}^d_+$ along with the auxiliary conditions introduced in the previous chapter.

We denote the set of Dirichlet boundaries and that of Neumann boundaries by Γ_D and Γ_N respectively. And their union $\Gamma = \Gamma_D \cup \Gamma_N$ refers to the whole boundary. Recall that we use either *all-Dirichlet BCs* or *Dirichlet-Neumann BCs*in this work. In the former case, the Γ_N is an empty set and $\Gamma = \Gamma_D$. If Γ_N is not empty, we then have $\nabla v\Big|_{\Gamma_N} = \nabla g\Big|_{\Gamma_N}$ over Γ_N.

4.3.2 European Options

We multiply $\dot{v} + \mathcal{L}v$ by a test function w such that $w\big|_{\Gamma_D} = 0$ and integrate their product over Ω, i.e.

$$\int_\Omega w(\dot{v} + \mathcal{L}v)d\Omega = 0.$$

One-asset case

With chain rule and integration by parts, we then reach the variational form below.

$$\begin{aligned}
&\int_\Omega w\left(\dot{v} + \Big(\frac{\partial}{\partial S}\big(\frac{\sigma^2 S^2}{2}\frac{\partial v}{\partial S}\big) + (r - q - \sigma^2)S\frac{\partial v}{\partial S} - rv\Big)\right)dS = 0. \\
\Leftrightarrow\quad &\int_\Omega w\dot{v}dS + \int_\Omega w\frac{\partial}{\partial S}\big(\frac{\sigma^2 S^2}{2}\frac{\partial v}{\partial S}\big)dS + \int_\Omega w(r - q - \sigma^2)S\frac{\partial v}{\partial S}dS - \int_\Omega wrvdS = 0 \\
\Leftrightarrow\quad &-(w, \dot{v}) + b(w, v) = \ell(w).
\end{aligned}$$

where

$$\begin{aligned}
&(w, v) := \int_\Omega wvdS, \\
&b(w, v) := r \cdot (w, v) + (w', v')_{\mathbf{T}} - (w, \tilde{\mathbf{D}}v'), \\
&w' := \frac{\partial w}{\partial S}, \\
&(w', v')_{\mathbf{T}} := \int_\Omega w'\mathbf{T}v'dS, \\
&\ell(w) := \Big[w\frac{\sigma^2 S^2}{2}v'\Big]_0^{S_{\max}} = \begin{cases} 0 \text{ if } S_{\max} \in \Gamma_D, \\ \Big[w\frac{\sigma^2 S^2}{2}g'\Big]_0^{S_{\max}} = \frac{\sigma^2 {S_{\max}}^2 \cdot w(S_{\max}) \cdot g'(S_{\max})}{2} \text{ if } S_{\max} \in \Gamma_N. \end{cases}
\end{aligned} \tag{4.1}$$

Multi-asset case

For simplicity, we denote $\int_{\Omega} \cdot \, d\mathbf{S}$ by $\int d\Omega$ in what follows. With the divergence form, integration by parts and Divergence theorem, we then reach the variational form below.

$$\begin{aligned}
& \int w(\dot{v} + \nabla \cdot (\mathbf{T}\nabla v) + \tilde{\mathbf{D}} \cdot \nabla v - rv) d\Omega = 0. \\
\Leftrightarrow \quad & \int w\dot{v} d\Omega + \int \mathbf{n} \cdot \big(w(\mathbf{T}\nabla v)\big) d\Gamma_N - \int \big(\nabla w \cdot (\mathbf{T}\nabla v)\big) d\Omega + \int w\tilde{\mathbf{D}} \cdot \nabla v d\Omega - \int wrv d\Omega = 0 \\
\Leftrightarrow \quad & -(w, \dot{v}) + b(w, v) = \ell(w).
\end{aligned}$$

where

$$(w, v) := \int wv d\Omega, \tag{4.2}$$

$$b(w, v) := r \cdot (w, v) + (\nabla w, \nabla v)_{\mathbf{T}} - (w, \tilde{\mathbf{D}} \cdot \nabla v), \tag{4.3}$$

$$(\nabla w, \nabla v)_{\mathbf{T}} := \int \nabla w \mathbf{T} \nabla v d\Omega, \tag{4.4}$$

$$\ell(w) := \int w\mathbf{n} \cdot \mathbf{T}\nabla v d\Gamma_N = \begin{cases} 0 \text{ if } \Gamma_N = \phi, \\ < w, \mathbf{n} \cdot \mathbf{T}\nabla g > := \int w\mathbf{n} \cdot \mathbf{T}\nabla g d\Gamma_N \text{ o.w.} \end{cases} \tag{4.5}$$

Also note that

$$b(w, v) \equiv (w, -\mathcal{L}v) + \ell(w). \tag{4.6}$$

4.3.3 American Options

We consider a test function w such that $w\big|_{\Gamma_D} = 0$ and $w \geq g$ over Ω. Since $\dot{v} + \mathcal{L}v \leq 0$ and $w - g \geq 0$, we have

$$(\dot{v} + \mathcal{L}v)(w - g) \leq 0. \tag{4.7}$$

Recall the complementarity condition

$$(\dot{v} + \mathcal{L}v)(v - g) = 0. \tag{4.8}$$

(4.8)-(4.7) leads to

$$(\dot{v} + \mathcal{L}v)(v - w) \geq 0 \Leftrightarrow (w - v)(\dot{v} + \mathcal{L}v) \leq 0.$$

As this product is non-positive over Ω, we have

$$\int (w - v)(\dot{v} + \mathcal{L}v) d\Omega \leq 0.$$

The LHS can be manipulated in the same manner as European cases and we hence obtain

$$(w - v, \dot{v}) - b(w - v, v) \leq -\ell(w - v) \Leftrightarrow -(w - v, \dot{v}) + b(w - v, v) \geq \ell(w - v).$$

4.3.4 Perpetual Options

The time term is not involved in perpetual models. With the same argument as the above American option case but without $\dot{v}$, perpetual problems can be reformulated as the following variational form.

$$b(w - v, v) \geq \ell(w - v).$$

4.3.5 Summary

We briefly recapitulate the reformulations of our option pricing problems as follows.

Problem 4.1 *Dynamic Variational Equality (DVE)* (*European Options*)
Find $v(t) \in \mathbb{V}$ such that for all $t \in [0, T]$, $v(t)$ is a solution to

$$-(w, \dot{v}) + b(w, v) = \ell(w), \ \forall w \in \mathbb{V}, \tag{4.9}$$

along with a TC and proper BCs are satisfied.

Problem 4.2 *Dynamic Variational Inequality (DVI)* (*American Options*)
Find $v(t) \in \mathbb{K} \subset \mathbb{V}$, where $\mathbb{K}$ is a closed and convex subset, such that for all $t \in [0, T]$, $v(t)$ is a solution to

$$-(w - v, \dot{v}) + b(w - v, v) \geq \ell(w - v), \ \forall w \in \mathbb{K}, \tag{4.10}$$

along with a TC and proper BCs and CCs are satisfied.

It is worth to mention that if $\mathbb{K} = \mathbb{V}$, then the DVI reduces to the DVE, cf. [44, Remark 2.2].

Problem 4.3 *Steady Variational Inequality (SVI)* (*Perpetual Options*)
Find $v \in \mathbb{K} \subset \mathbb{V}$, where $\mathbb{K}$ is a closed and convex subset, such that v is a solution to

$$b(w - v, v) \geq \ell(w - v), \ \forall w \in \mathbb{K}, \tag{4.11}$$

along with proper BCs and CCs are satisfied.

Mathematically, the perpetual problem can be viewed as the steady state of its American counterpart.

Note that if one replaces t by the *time to maturity* $\tau := T - t$, the time term $-(w - v, \dot{v})$ can be replaced by $(w - v, \frac{\partial v}{\partial \tau})$. Recall that the linear form $\ell(\cdot)$ comes from the Neumann BCs (if used) and $\ell(\cdot) = 0$ can be used if all BCs are of Dirichlet type. $\mathbb{V}$ and $\mathbb{K}$ above are certain solution space/set for our problems. Naturally one may ask: what are the space/set? does a solution exist in that space/set? if it exists, is it unique? Generally, once a space/set is selected, the latter two questions depend on the properties of bilinear form $b(\cdot, \cdot)$ and linear form $\ell(\cdot)$ in the problems. In the next section, we will answer these with three powerful theorems.

4.4 Unique Solution to Variational Problems

Definition 4.4 [Gelfand Triple, cf. [68, Def. 3.12]]
We say $\mathbb{B} \subseteq \mathbb{H} = \mathbb{H}^* \subseteq \mathbb{B}^*$ forms a *Gelfand triple* if $\mathbb{B}$ is a real separable and reflexive Banach space, $\mathbb{H}$ is a real separable Hilbert space and $\mathbb{B}$ is dense in $\mathbb{H}$ with continuous embedding $\mathbb{B} \subseteq \mathbb{H}$, i.e. $\forall v \in \mathbb{B}, \exists c < \infty$ such that

$$||v||_{\mathbb{H}} \leq c||v||_{\mathbb{B}}.$$

We denote such relation by $\mathbb{B} \hookrightarrow \mathbb{H} \hookrightarrow \mathbb{B}^*$.

Note that $\mathbb{B} = H^1(\Omega)$ and $\mathbb{H} = L^2(\Omega)$ forms a Gelfand triple, i.e.

$$H^1(\Omega) \hookrightarrow L^2(\Omega) \hookrightarrow H^{-1}(\Omega) := H^1(\Omega)^*.$$

. Notice that the Gelfand triple is one of the assumptions to ensure the unique solution of variational time-dependent problems, cf. [107, Ch.23,55] and [68, Thm.3.3 and 3.7, Remark 3.14].

4.4.1 Theorems on Unique Solution

Provided $H^1(\Omega) \hookrightarrow L^2(\Omega) \hookrightarrow H^{-1}(\Omega)$ with the induced norms $||\cdot||_H = ||\cdot||_{H^1(\Omega)}$ and $||\cdot||_L = ||\cdot||_{L^2(\Omega)}$ and a subspace $\mathbb{V}$ such that $H_0^1(\Omega) \subseteq \mathbb{V} \subset H^1(\Omega)$ where $H_0^1(\Omega)$ is the subspace with homogeneous/zero Dirichlet boundary conditions, the following theorems will be used to justify the unique solutions to the DVE, DVI and SVI problems mentioned earlier.

Theorem 4.5 (Unique Solution to the DVE with Homogeneous Dirichlet BC) *There exists a unique solution $v \in L_2(0,T;\mathbb{V}) \cap C^0([0,T];\Omega)$ to the DVE if for all $w \in \mathbb{V}$, $\exists c_1, c_2, c_H > 0$ and $\exists c_L \geq 0$ such that*

- $|\ell(w)| \leq c_1||w||_H$ *(boundedness/continuity),*
- $|b(w,v)| \leq c_2||w||_H||v||_H$ *(boundedness/continuity),*
- $b(w,w) \geq c_H||w||_H^2 - c_L||w||_L^2$ *(weak coercivity or Garding's Inequality).*

This conclusion is stated in various references, such as [107, 68], [18], [75, Sec.11.1.1] and [11, Thm.5.6.8]. Actually, it a generalization of the Lax-Milgram theorem with the strong coercivity ($c_L = 0$ in coercivity) and no time term involved. Note that $|\ell(w)| \leq c_1||w||_H$ implies $|\ell(w)| \leq c_3||w||_L$ for some $c_3 > 0$.

Theorem 4.6 (Unique Solution to the DVI with Homogeneous Dirichlet BC) *There exists a unique solution $v \in L_2(0,T;\mathbb{K}) \cap C^0([0,T];\Omega)$, where $\mathbb{K} \subset \mathbb{V}$ is a* **closed and convex nonempty subset***, to the DVE if for all $w \in \mathbb{K}$, the three conditions above are satisfied.*

This result is stated in [107, 68, 56, 5] and [44, Ch.3] along with the references of its proof herein.

Theorem 4.7 (Unique Solution to the SVI with Homogeneous Dirichlet BC) *There exists a unique solution $v \in L_2(\mathbb{K}) \cap C^0(\Omega)$, where $\mathbb{K} \subset \mathbb{V}$ is a* **closed and convex nonempty subset**, *to the DVE if $r > 0$ and for all $w \in \mathbb{K}$, the three conditions above are satisfied.*

This result and its proof is adapted from [27].[1] We leave the lengthy proof in the appendix. In general one of the sufficient conditions to unique solution to the SVI is the *strong coercivity*, cf. [44, Ch.1]. When the loose condition (Garding's Inequality) is applied, we need the extra condition $r > 0$ to compensate. The compensation condition $r > 0$ (positive interest rate) is automatically satisfied in practice.

4.4.2 Assumption for Nonhomogeneous Dirichlet BCs

Proposition 4.8 *In general the pricing problems do not possess homogeneous Dirichlet BCs. In this case we assume there exists another continuous function u which coincides with v on all Dirichlet BCs, i.e. $v(t)\big|_{\Gamma_D} = u(t)\big|_{\Gamma_D}$, in the solution space $\mathbb{V}$ or $\mathbb{K}$. It can be proved that there exists a unique solution v to the pricing problems if such u exists.*

Proof.
Existence: $\tilde{v} := v - u$ has zero Dirichlet BCs and has a solution which implies $v = \tilde{v} + u$ is a solution to the original nonhomogeneous problem.[2]
Uniqueness: Assume v_1 and v_2 are two solutions to the nonhomogeneous problem. By taking identical u, we know $\tilde{v}_1 := v_1 - u$ and $\tilde{v}_2 := v_2 - u$ are solutions to a corresponding homogeneous problems and hence they are identical because of uniqueness. We hence conclude $v_1 = v_2$. ■

4.4.3 Boundedness and Coercivity of Linear and Bilinear Forms

Solution Spaces

For convenience of derivation, [94] considers a weighted Sobolev space and an inner product which are equivalent to the ordinary Sobolev spaces and its inner product on a bounded

[1] I would like to express my deep appreciation to the author of [27], P. Feehan, for his kindly help via email communication.

[2] In the inequality cases we also need to replace thefunction g by $\tilde{g} = g - u$.

domain Ω. We extend their definition in $d-$dimesional sense as below.

$$
\begin{aligned}
&(w,v)_{H^w} := (w,v) + (\mathbf{S}\odot\nabla w, \mathbf{S}\odot\nabla v),\\
&H^{1,\omega}(\Omega) := \left\{w : ||w||_H^2 := (w,w)_{H^w} < \infty\right\},\\
&H_0^{1,\omega}(\Omega) := \left\{w : w\in H^{1,\omega}(\Omega), w\big|_{\Gamma} = 0\right\},\\
&H_D^{1,\omega}(\Omega) := \left\{w : w\in H^{1,\omega}(\Omega), w\big|_{\Gamma_D} = 0\right\}.
\end{aligned}
$$

Given homogeneous Dirichlet BCs, we consider the bilinear form $b(w,v) : H^{1,\omega}(\Omega)\times H^{1,\omega}(\Omega)\to\mathbb{R}$ and the linear form $l(w) : H^{1,\omega}(\Omega)\to\mathbb{R}$ and seek solutions in a subspace

$$
\mathbb{V} := \left\{w : w\in H_D^{1,\omega}(\Omega), \nabla w\big|_{\Gamma_N} = \nabla g\big|_{\Gamma_N}\right\} \text{ such that } H_0^{1,\omega}(\Omega)\subset\mathbb{V}\subset H^{1,\omega}(\Omega),
$$

or a closed and convex nonempty subset

$$
\mathbb{K} := \{w : w\in\mathbb{V}, w(\mathbf{S})\geq g(\mathbf{S}) \text{ over } \Omega\}\subset\mathbb{V}.
$$

One-asset case

[1] Boundedness of Linear Form:
With the definition (4.1), we have

$$
\begin{aligned}
|\ell(w)| &= \begin{cases} 0 \text{ if } S_{\max}\in\Gamma_D,\\ |\frac{\sigma^2 {S_{\max}}^2\cdot w(S_{\max})\cdot g'(S_{\max})}{2}| < |\frac{\sigma^2 {S_{\max}}^2\cdot g'(S_{\max})}{2}|\cdot\sup\limits_{\Omega}|w| \text{ if } S_{\max}\in\Gamma_N. \end{cases}\\
&\leq c_1||w||_{H^\omega} \text{ for some } c_1>0.
\end{aligned}
$$

[2] Boundedness of Bilinear Form:
With the definition (4.3) in one-asset case, we have

$$
\begin{aligned}
|b(w,v)| &= |r\cdot(w,v) + \frac{\sigma^2}{2}\cdot(sw', sv') - (r-q-\sigma^2)\cdot(w, sv')|\\
&\leq 2\cdot\max\{r, \frac{\sigma^2}{2}, |r-q-\sigma^2|\}\cdot||w||_{H^\omega}\cdot||v||_{H^\omega}\\
&=: c_2\cdot||w||_{H^\omega}\cdot||v||_{H^\omega}.
\end{aligned}
$$

[3] Weak Coercivity of Bilinear Form:

Substituting $v = w$ into (4.3) gives

$$\begin{aligned} b(w,w) &= r\cdot(w,w) + \frac{\sigma^2}{2}\cdot(sw', sw') - (r - q - \sigma^2)\cdot(w, sw') \\ &= (r+\frac{r}{2})\cdot(w,w) - \frac{q+\sigma^2}{2}\cdot(w,w) + \frac{\sigma^2}{2}\cdot(sw', sw') \\ &\qquad -r\cdot\frac{S_{\max}}{2}\cdot w(S_{\max})^2 + (q+\sigma^2)\cdot\frac{S_{\max}}{2}\cdot w(S_{\max})^2 \\ &= \min\{\frac{3r}{2}, \frac{\sigma^2}{2}\}\cdot||w||^2_{H^\omega} - \left(\frac{q+\sigma^2}{2} + \frac{rS_{\max}}{2}\right)\cdot||w||^2_L \text{ (for some } c>0) \\ &=: c_H\cdot||w||^2_{H^\omega} - c_L\cdot||w||^2_L \text{ (with } c_H \geq 0 \text{ and } c_L \geq 0). \end{aligned}$$

Multi-asset case

Recall that $\mathbf{\Sigma}$ is symmetric with positive entries. We denote its eigenvalues by λ_i such that $0 < \lambda_1 \leq \lambda_2 \leq \ldots \leq \lambda_d < \infty$.
[1] Boundedness of Linear Form:
With the definition (4.5) and $\int w^2\, d\Gamma_N < \infty$ guaranteed by Trace Theorem, we have

$$\begin{aligned} |\ell(w)| &= |< w, \mathbf{n}\cdot\mathbf{T}\nabla g >| \\ &\leq \lambda_d\cdot|< w, (\mathbf{S}\odot\mathbf{n})\cdot(\mathbf{S}\odot\nabla g) >| \\ &= \lambda_d\cdot||(\mathbf{S}\odot\mathbf{n})\cdot(\mathbf{S}\odot\nabla g)||_{L^2(\Gamma_N)}\cdot||w||_{L^2(\Gamma_N)} \\ &\leq c_1||w||_H. \end{aligned}$$

[2] Boundedness of Bilinear Form:
With the definition (4.3), we have

$$\begin{aligned} b(w,v) &\leq \max\{r,\lambda_d\}\cdot\Big((w,v) + (\mathbf{S}\odot\underline{\nabla w}, \mathbf{S}\odot\underline{\nabla v})\Big) + \max_i\{\big|\bar{D}^{(i)}\big|\}\cdot\sum_{i=1}^{d}\int w\cdot S^{(i)}\cdot\frac{\partial v}{\partial S^{(i)}}d\Omega \\ &\leq \max\{r,\lambda_d, d\cdot\bar{D}^{\max}\}\cdot(||w||_{H^\omega}\cdot||v||_{H^\omega} + ||w||_{H^\omega}\cdot||v||_{H^\omega}) \\ &= 2\cdot\max\{r,\lambda_d, d\cdot\bar{D}^{\max}\}\cdot||w||_{H^\omega}\cdot||v||_{H^\omega} \\ &=: c_2||w||_{H^\omega}\cdot||v||_{H^\omega} \end{aligned}$$

[3] Weak Coercivity of Bilinear Form:

Substituting $v = w$ into (4.3) gives

$$\begin{aligned} b(v,v) &\geq r\cdot(v,v) + \lambda_1 \cdot (\mathbf{S}\odot\underline{\nabla w}, \mathbf{S}\odot\underline{\nabla v}) \\ &\quad - \left(\frac{\bar{D}^{\max}\cdot S_{\max}}{2}\cdot < v,v > -\frac{1}{2}\cdot\sum_{i=1}^{d}\left(r - q_i - \sigma_{ii} - \sum_{\substack{j=1\\ j\neq i}} \frac{\sigma_{ij}}{2}\right)\cdot(v,v)\right) \\ &= (r+\frac{dr}{2})\cdot(v,v) - \frac{1}{2}\cdot\sum_{i=1}^{d}\left(q_i + \sigma_{ii} + \sum_{\substack{j=1\\ j\neq i}} \frac{\sigma_{ij}}{2}\right)\cdot(v,v) + \lambda_1\cdot(\mathbf{S}\odot\underline{\nabla v}, \mathbf{S}\odot\underline{\nabla v}) \\ &\quad - \frac{\bar{D}^{\max}\cdot S_{\max}}{2}\cdot < v,v > . \end{aligned}$$

We define the following operators.

$$\begin{aligned} A^+ &:= \max\{A,0\} = \begin{cases} A > 0 \text{ if } A > 0 \\ 0 \qquad \text{o.w.} \end{cases} \\ A^- &:= \max\{-A,0\} = \begin{cases} -A = |A| > 0 \text{ if } A < 0 \\ 0 \qquad\qquad \text{o.w.} \end{cases} \end{aligned}$$

Note $A \equiv A^+ - A^-$. We further define

$$Q := \sum_{i=1}^{d}\left(q_i + \sigma_{ii} + \sum_{\substack{j=1\\ j\neq i}} \frac{\sigma_{ij}}{2}\right) \equiv Q^+ - Q^-. \tag{4.12}$$

With the new notation and Trace Theorem, we can rewrite

$$\begin{aligned} b(w,v) &\geq (r+\frac{dr}{2})\cdot(v,v) - \frac{1}{2}\cdot(Q^+ - Q^-)\cdot(v,v) + \lambda_1\cdot(\mathbf{S}\odot\underline{\nabla v}, \mathbf{S}\odot\underline{\nabla v}) - \frac{\bar{D}^{\max}\cdot S_{\max}}{2}\cdot < v,v > \\ &\geq \min\{r+\frac{dr}{2}+\frac{Q^-}{2}, \lambda_1\}\cdot||v||^2_{H^\omega} - \left(\frac{Q^+}{2} + \frac{\bar{D}^{\max}\cdot S_{\max}}{2}\cdot c^2\right)\cdot||v||^2_L \quad \text{(for some } c>0) \\ &=: c_H||v||^2_{H^\omega} - c_L||v||^2_L \end{aligned}$$

Note that c_L in one-asset and multi-asset could be very large due to the large $S_{\max}$.

4.5 Summary

In this chapter we reformulate the pricing problems from the classical Black-Scholes-Merton equation to its variational form. Following that, we show the boundedness and weak

coercivity of our linear and bilinear forms. With the practical assumption $r > 0$, unique solutions to European, American and perpetual option pricing problems can be justified by the use of theorems 4.5, 4.6 and 4.7. In the next chapter, we shall see how to obtain the the discrete systems deriving from the variational formulations introduced previously and understand their solvability.

Chapter 5

Discrete Weak Formulation and Solvability

In the previous chapter, we have discussed the conditions for unique solutions for the infinite-dimensional variational formulations of option pricing problems. In order to find their values numerically, we shall introduce how to approximate the problems in discrete forms in this chapter.

5.1 Finite-dimensional Formulations

Recall that in terms of infinite-dimensional problems, we have $H^1(\Omega) \hookrightarrow L^2(\Omega) \hookrightarrow H^{-1}(\Omega)$, a solution space $\mathbb{V}$ such that $H_0^1(\Omega) \subseteq \mathbb{V} \subset H^1(\Omega)$ and a closed and convex nonempty solution subset $\mathbb{K} \subset \mathbb{V}$. We now assume the infinite-dimensional space/set $\mathbb{V}$ and $\mathbb{K}$ can be approximated by the finite-dimensional families $(\mathbb{V}_h)_h$ and $(\mathbb{K}_h)_h$ as $h \to 0$ where $\mathbb{K}_h \subset \mathbb{V}_h$. We also assume $v_h(t, \mathbf{S}) \in \mathbb{V}_h$ in the European case and $v_h(t, \mathbf{S}) \in \mathbb{K}_h$ in the American and perpetual cases. In terms of terminal and boundary conditions, we assume $v_h(t = T, \mathbf{S}) \to v(t = T, \mathbf{S})$ and $v_h(t, \mathbf{S})\big|_\Gamma \to v(t, \mathbf{S})\big|_\Gamma$ strongly in $\mathbb{V}$.
Similar to the infinite-dimensional variational formulations of our option pricing problems, we now build their finite-dimensional counterparts as follows.

Problem 5.1 *(European Options)*
Find $v_h(t, \mathbf{S}) \in \mathbb{V}_h$ such that for all $t \in [0, T]$, v_h is a solution to

$$-(w_h, \dot{v_h}) + b(w_h, v_h) = \ell(w_h),\ \forall w_h \in \mathbb{V}_h,$$

provided a terminal condition (TC) and proper boundary conditions (BCs) are satisfied.

Problem 5.2 *(American Options)*
Find $v_h(t, \mathbf{S}) \in \mathbb{K}_h \subset \mathbb{V}_h$, where $\mathbb{K}_h$ is a closed and convex subset whose member functions

are at least equal to a payoff function $g(\mathbf{S})$, such that for all $t \in [0,T]$, v_h is a solution to

$$-(w_h - v_h, \dot{v_h}) + b(w_h - v_h, v_h) \geq \ell(w_h - v_h),\ \forall w_h \in \mathbb{K}_h,$$

provided a TC and proper BCs and complementarity conditions (CCs) are satisfied.

Problem 5.3 *(Perpetual Options)*
Find $v_h(\mathbf{S}) \in \mathbb{K}_h \subset \mathbb{V}_h$, where $\mathbb{K}_h$ is a closed and convex subset whose member functions are at least equal to a payoff function $g(\mathbf{S})$, such that v_h is a solution to

$$b(w_h - v_h, v_h) \geq \ell(w_h - v_h),\ \forall w_h \in \mathbb{K}_h,$$

provided proper BCs and CCs are satisfied.

5.2 Domain Partition and Nodes Numbering

We assume the spatial domain is partitioned by non-overlapping *(interior) elements*, say $\Omega^{(1)}, \ldots, \Omega^{(n_E)}$, which are geometric simplexes such that $\Omega = \cup_{e=1}^{n_E} \Omega^{(e)}$. Similarly we can divide the Neumann and Dirichlet boundaries respectively by non-overlapping *boundary elements*, say $\Gamma_N^{(1)}, \ldots, \Gamma_N^{(n_N)}$ and $\Gamma_D^{(1)}, \ldots, \Gamma_D^{(n_D)}$, such that $\Gamma_N = \cup_{e=1}^{n_N} \Gamma_N^{(e)}$ and $\Gamma_D = \cup_{e=1}^{n_D} \Gamma_D^{(e)}$.

Every mesh point/node of an element in our spatial domain $[0, S_{\max}]^d$ is given a unique global index $i \in \{1, \ldots, n_3\}$ and denoted by $\mathbf{S}^{(i)}$. We number all mesh points on the interior domain, Neumann boundary and Dirichlet boundary in the order of $i = 1, \ldots, n_1$, $i = n_1 + 1, \ldots, n_2$ and $i = n_2 + 1, \ldots, n_3$ individually.

We partition the time domain $[0,T]$ with the uniform segment length $h_t > 0$ and the points $t_i := i \cdot h_t$ for $i = 0, \ldots, N_t$ with $N_t \in \mathbb{N}$.

5.3 Semi-discretization

In what follows, we rewrite the problems in a discrete sense and express the equations in matrix form by finite element approximation.

5.3.1 Finite Element Approximation

A shape function is a function defined over an element which can be linear, quadratic or higher-order w.r.t. each dimension/axis. A *node/basis function*, denoted by $N^{(i)}(\cdot)$ for $i = 1, \ldots, n_3$, is subsequently defined as a small union of a few shape functions sharing a joint node over some connected elements and has support only over those elements. Namely a basis function will be centered at that joint node and so we can number it simply with the number of the central node.

Generally a basis function has the unit value at its central node and zeros at others. We will show the explicit forms and relevant properties of these functions in the next chapter chapter. At this stage, we simply need to bear in mind that these shape functions will be used to construct finite-dimensional approximation of our functional space.

A finite-dimensional (closed) subspace $\mathbb{V}_h \subset \mathbb{V}$ and a (closed and convex) subset $\mathbb{K}_h \subset \mathbb{K}$ can be spanned by these node/basis functions. We aim to approximate our problems from infinite-dimensional space $\mathbb{V}$ and set $\mathbb{K}$ into their finite-dimensional subspace $\mathbb{V}_h$ and subset $\mathbb{K}_h$. Such technique of approximation is referred to as the *finite element method* (FEM). An approximation w_h in $\mathbb{V}_h$ or $\mathbb{K}_h$ can be expressed/spanned by $w_h = \sum_{i=1}^{n_3} w^{(i)} N^{(i)}$ where $w^{(i)} \in \mathbb{R}$.

5.3.2 Approximation

We now approximate all functions into the finite-dimensional spaces using

$$\begin{aligned} w_h(t, \mathbf{S}) &:= \sum_{i=1}^{n_3} w^{(i)}(t) N^{(i)}(\mathbf{S}), \\ v_h(t, \mathbf{S}) &:= \sum_{j=1}^{n_3} v^{(j)}(t) N^{(j)}(\mathbf{S}), \\ (w_h - v_h)(t, \mathbf{S}) &:= \sum_{i=1}^{n_3} \left(w^{(i)}(t) - v^{(i)}(t) \right) N^{(i)}(\mathbf{S}), \end{aligned}$$

to rewrite the following operators in matrix form.

L^2 Inner Product

$$(w_h, \dot{v}_h) := \sum_i \sum_j w^{(i)} \dot{v}^{(j)} (N^{(i)}, N^{(j)}) =: \mathbf{W}^T \mathbf{M} \dot{\mathbf{V}}$$

where $\mathbf{M}$'s (i, j) entry is defined as $\mathbf{M}_{ij} := (\, N^{(i)}, N^{(j)}\,)$.

Bilinear Form

$$b(w_h, v_h) = \sum_i \sum_j w^{(i)} v^{(j)} b(N^{(i)}, N^{(j)}) =: \mathbf{W}^T \mathbf{B} \mathbf{V}$$

where $\mathbf{B}$'s (i, j) entry is defined as $\mathbf{B}_{ij} := b(\, N^{(i)}, N^{(j)}\,)$.

Linear Form

$$\ell(w_h) = \sum_j w^{(j)} \ell(N^{(j)}) =: \mathbf{W}^T \mathbf{L}$$

where $\mathbf{L}$'s $j^{th.}$ entry is defined as $\mathbf{L}_j := \ell(N^{(j)})$.

We will discuss the detailed computation of $\mathbf{M}, \mathbf{B}, \mathbf{L}$ in the next chapter.

5.3.3 Weak Formulation in Discrete Form

We now express the discrete form of the variational equations for option pricing problems as below.

European options: $-(\mathbf{W}^T \mathbf{M} \dot{\mathbf{V}}) + \mathbf{W}^T \mathbf{B} \mathbf{V} = \mathbf{W}^T \mathbf{L}$.

American options: $-(\mathbf{W} - \mathbf{V})^T \mathbf{M} \dot{\mathbf{V}} + (\mathbf{W} - \mathbf{V})^T \mathbf{B} \mathbf{V} \geq (\mathbf{W} - \mathbf{V})^T \mathbf{L}$.

Perpetual options: $(\mathbf{W} - \mathbf{V})^T \mathbf{B} \mathbf{V} \geq (\mathbf{W} - \mathbf{V})^T \mathbf{L}$.

5.4 Reduced System

We define the collections of (global) indices for the interior, Neumann and Dirichlet nodes by I, N and D respectively. We use IN and D as the subscripts of matrices to denote their minor matrices decided by the selected collections. Following our previous numbering, we have $IN := \{1, \ldots, n_1, n_1 + 1, \ldots, n_2\}$ and $D := \{n_2 + 1, \ldots, n_3\}$. Since the Dirichlet data $\mathbf{V}_D$ are known, we could reduce the systems with only the unknown $\mathbf{V}_{IN}$ remained to be solved as follows.

European options:

$$\begin{aligned} - \quad & \mathbf{W}_{IN}{}^T \left(\mathbf{M}_{IN,IN} \dot{\mathbf{V}}_{IN} + \mathbf{M}_{IN,D} \dot{\mathbf{V}}_D \right) \\ + \quad & \mathbf{W}_{IN}{}^T \left(\mathbf{B}_{IN,IN} \mathbf{V}_{IN} + \mathbf{B}_{IN,D} \mathbf{V}_D \right) = \mathbf{W}_{IN}{}^T \mathbf{L}_{IN}. \end{aligned} \tag{5.1}$$

American options:

$$\begin{aligned} - \quad & (\mathbf{W}_{IN} - \mathbf{V}_{IN})^T \left(\mathbf{M}_{IN,IN} \dot{\mathbf{V}}_{IN} + \mathbf{M}_{IN,D} \dot{\mathbf{V}}_D \right) \\ + \quad & (\mathbf{W}_{IN} - \mathbf{V}_{IN})^T \left(\mathbf{B}_{IN,IN} \mathbf{V}_{IN} + \mathbf{B}_{IN,D} \mathbf{V}_D \right) \geq (\mathbf{W}_{IN} - \mathbf{V}_{IN})^T \mathbf{L}_{IN}. \end{aligned} \tag{5.2}$$

Perpetual options:

$$(\mathbf{W}_{IN} - \mathbf{V}_{IN})^T \left(\mathbf{B}_{IN,IN} \mathbf{V}_{IN} + \mathbf{B}_{IN,D} \mathbf{V}_D \right) \geq (\mathbf{W}_{IN} - \mathbf{V}_{IN})^T \mathbf{L}_{IN}. \tag{5.3}$$

5.5 Full-discretization

5.5.1 Finite Difference Method

We would like to discretize the reduced systems in time by finite difference method (FDM), which is mainly based on the Taylor's expansion. As well as the equalities of European cases, the FDM is also employable to the inequalities of American and perpetual counterparts, cf. [44].

Three popular types are the θ-method, the Rannacher Method and the Runge-Kutta methods. The Runge-Kutta (RK) method adopts multi-step approximation for higher accuracy while the $\theta-$method uses one-step approximation. When $\theta = 0, 1/2$ and 1 in the $\theta-$method of our formulation, it corresponds to explicit Euler, Crank-Nicolson (semi-implicit) and implicit Euler method individually. The semi-implicit and implicit Euler method are proved unconditionally stable for both equality and inequality cases, cf. [75] and [44, Ch.3, Sec.4]. In generally, a $s-$step RK method has the accuracy of order s and $2s$ for explicit and implicit methods respectively with $s \leq 4$. If $s > 4$, then most $s-$step explicit RK methods have the order less than s.

Generally, Crank-Nicolson method with $\theta = 1/2$ is widely used in numerical computation due to its unconditional stability and second-order accuracy. However, it may cause numerical oscillation to the solutions of v, v_s and v_{ss}. The Rannacher method uses implicit Euler ($\theta = 1$) in the first few steps and probably with a smaller time step length and turns to Crank-Nicolson method afterwards. It retains the same unconditional stability and asymptotically second-order accuracy as the Crank-Nicolson method but avoids numerical oscillation, cf. [41]. For simplicity and generality, the problems are to be discretized by the $\theta-$method with a general choice of $\theta \in [0, 1]$. In what follows, the superscript k is used to represent the information at time step t_k.

5.5.2 Coefficient Matrix and Right-Hand-Side Vector

To simplify the expression of equations, we define the following notations.

$$
\begin{aligned}
\mathbf{C} :=& \quad \frac{1}{h_t}\mathbf{M}_{IN,IN} + \theta\mathbf{B}_{IN,IN}, \\
\mathbf{R}^k :=& \quad \left(\frac{1}{h_t}\mathbf{M}_{IN,IN} - (1-\theta)\mathbf{B}_{IN,IN}\right)\mathbf{V}_{IN}^{k+1} + \left(\frac{1}{h_t}\mathbf{M}_{IN,D} - (1-\theta)\mathbf{B}_{IN,D}\right)\mathbf{V}_{D}^{k+1} \\
&+ \quad \left(\frac{-1}{h_t}\mathbf{M}_{IN,D} - \theta\mathbf{B}_{IN,D}\right)\mathbf{V}_{D}^{k} + \mathbf{L}_{IN}, \\
\tilde{\mathbf{C}} :=& \quad \mathbf{B}_{IN,IN}, \\
\tilde{\mathbf{R}} :=& \quad \mathbf{B}_{IN,D}\mathbf{V}_D - \mathbf{L}_{IN}.
\end{aligned}
$$

We notice that:

- $\mathbf{C}$ and $\tilde{\mathbf{C}}$ are constant banded matrices with 3^d bands if globally numbering the nodes in lexicographical order.
- Computationally $\mathbf{R}^k$ must be re-computed at every time step with the known information from previous time step and the data on the Dirichlet boundary.

In order to get rid of the subscripts and to express the problems in the canonical form of linear complementarity problems, we further define the following linear transformation.

$$\begin{aligned} \mathbf{z}^k &:= \mathbf{V}_{IN}^k - \mathbf{G}_{IN}, \\ \mathbf{q}^k &:= \mathbf{C}\mathbf{G}_{IN} - \mathbf{R}^k, \\ \mathbf{z} &:= \mathbf{V}_{IN} - \mathbf{G}_{IN}, \\ \mathbf{q} &:= \tilde{\mathbf{C}}\mathbf{G}_{IN} - \tilde{\mathbf{R}}. \end{aligned}$$

With these notations, we are ready to discretize the systems in time. Note that the fully-discretized systems can be solved backward numerically at each time step, from $k = n_t - 1$ to $k = 0$.

5.5.3 European Options

As (5.1) holds for all $\mathbf{W}_{IN} \in \mathbb{R}^{n_2 \times 1}$, discretizing it with one-step $\theta-$method and time step length $h_t > 0$ gives us

$$\mathbf{C}\mathbf{z}^k + \mathbf{q}^k = \mathbf{0}$$

5.5.4 American Options

Tackling inequality case needs some extra effort. First discretizing (5.2) leads to the

$$\left(\mathbf{W}_{IN}^k - \mathbf{V}_{IN}^k\right)^T \left(\mathbf{C}\mathbf{V}_{IN}^k - \mathbf{R}^k\right) \geq 0. \tag{5.4}$$

We now employ the following lemma to convert the system to a (dynamic/sequential) *linear complementarity problem* (LCP).

Lemma 5.4
Provided $w_h \in \mathbb{K}_h$ whose member functions are at least equal to a payoff function $g(\mathbf{S})$, the (dynamic/sequential) finite-dimensional variational inequality problem (5.4) is equivalent to the (dynamic/sequential) linear complementarity problem (LCP) below

$$\begin{aligned} \mathbf{z}^k &\geqq \mathbf{0}, \\ \boldsymbol{\omega}^k &= \mathbf{C}\mathbf{z}^k + \mathbf{q}^k \geqq \mathbf{0} \\ (\mathbf{z}^k)^T\boldsymbol{\omega} &= 0. \end{aligned}$$

where $\geqq$ is an entry-wise inequality, $\mathbf{0}$ is an $n_2 \times 1$ zero vector.

Proof.
Suppose $\mathbf{z}^k = \mathbf{V}_{IN}^k$ is the solution to the LCP, then it is trivial to satisfy the variational inequality (5.4). Now we suppose the variational inequality (5.4) is satisfied. The first inequality (5.5) is implied by (5.4). The second inequality (5.5) comes from $w_h \in \mathbb{K}_h$. The last equality (5.5) is obtained by multiplying (5.5) by (5.5) and substituting $\mathbf{W}_{IN}^k = \mathbf{G}_{IN}$ into the variational inequality (5.4).

■

5.5.5 Perpetual Options

Recall $\dot{\mathbf{V}}$ is taken off from the formulation of perpetual options, we do not need to discretize in time in this case. Instead, we simply rearrange the formulation in the following finite-dimensional variational from.

$$(\mathbf{W}_{IN} - \mathbf{V}_{IN})^T \left(\tilde{\mathbf{C}}\mathbf{V}_{IN} - \tilde{\mathbf{R}}\right) \geq 0. \tag{5.5}$$

.

Similarly we utilize the lemma below to convert the system to a (static) linear complementarity problem (LCP).

Lemma 5.5
Provided $w_h \in \mathbb{K}_h$ whose member functions are at least equal to a payoff function $g(\mathbf{S})$, the (static) finite-dimensional variational inequality problem (5.5) is equivalent to the (static) linear complementarity problem (LCP) below

$$\begin{aligned} \mathbf{z} &\geqq \mathbf{0}, \\ \boldsymbol{\omega} &= \tilde{\mathbf{C}}\mathbf{z} + \mathbf{q} \geqq \mathbf{0}, \\ (\mathbf{z})^T\boldsymbol{\omega} &= 0. \end{aligned}$$

where $\geqq$ is an entry-wise inequality, $\mathbf{0}$ is an $n_2 \times 1$ zero vector.

Proof. This can be adapted straight from the proof of lemma 5.4. ■

Mathematically the solution to this static LCP can be viewed as the steady state of the dynamic LCP in lemma 5.4.

5.5.6 Summary of Discrete Systems

Provided the terminal conditions $\mathbf{z}^k = \mathbf{0}$ and the proper boundary conditions for the computation of $\mathbf{q}^k$ and $\mathbf{q}$, we can summarize the discrete problems as below. Notice that the boldface $\mathbf{q}^k$ and $\mathbf{q}$ do not refer to the dividend rates in the LCP systems.

- **European options:** find the sequential solutions $\mathbf{V}_{IN}^k$ to the system of equalities below

$$\mathbf{C}\mathbf{z}^k + \mathbf{q}^k = \mathbf{0}, \tag{5.6}$$

at each time step t_k for $k = n_t - 1, \ldots, 1$.

- **American options:** find the sequential solutions $\mathbf{V}_{IN}^k$ to the system of linear complementarity problem (LCP) below

$$\begin{aligned} \mathbf{z}^k &\geqq \mathbf{0}, & (5.7)\\ \boldsymbol{\omega}^k &= \mathbf{C}\mathbf{z}^k + \mathbf{q}^k \geqq \mathbf{0} & (5.8)\\ (\mathbf{z}^k)^T\boldsymbol{\omega} &= 0. & (5.9) \end{aligned}$$

  at each time step t_k for $k = n_t - 1, \ldots, 1$.

- **Perpetual options:** find the solution $\mathbf{V}_{IN}$ to the system of linear complementarity problem below

$$\begin{aligned} \mathbf{z} &\geqq \mathbf{0}, & (5.10)\\ \boldsymbol{\omega} &= \tilde{\mathbf{C}}\mathbf{z} + \mathbf{q} \geqq \mathbf{0}, & (5.11)\\ (\mathbf{z})^T\boldsymbol{\omega} &= 0. & (5.12) \end{aligned}$$

5.6 Coefficient Matrix and Solvability

It is well-know that a system of equalities is uniquely solvable if its coefficient matrix is non-singular. A positive-definite $\mathbf{C}$ will suffice for this in the European case.

A LCP system is uniquely solvable if its coefficient matrix is a P-matrix, cf. [24]. A matrix is said to be a P-matrix if all its principal minors are positive. It is known that a positive-definite matrix is a P-matrix, cf. [24, Thm.3.1.6,p.141] and [49, p.18]. In terms of American and perpetual options, this can be achieved by assuming $\mathbf{C}$ and $\tilde{\mathbf{C}} := \mathbf{B}_{IN,IN}$ are positive definite or asymptotically being so as $h_t \to 0$. We will review the definitions of some matrix classes and their relation to a LCP system in detail in the later chapter 7.

5.6.1 Matrix M

As the mass matrix derives from L_2-norm (L_2-inner product), it follows that $\mathbf{M}$ is strictly positive-definite and hence it is a P-matrix.

5.6.2 Matrix B

We recall that $b(w,w) = r\cdot(w,w) + (\nabla w, \nabla w)_{\mathbf{T}} - (w, \tilde{\mathbf{D}}\cdot\nabla w)$gives $\mathbf{B} \equiv r\mathbf{M} + \mathbf{K} - \mathbf{A}$.

Provided the covariance matrix $\boldsymbol{\Sigma}$ is a symmetric positive definite matrix, the part $r\cdot(w,w) + (\mathbf{S}\odot\nabla w, \mathbf{S}\odot\nabla w)_{\boldsymbol{\Sigma}}$ forms an induced norm over Ω. It then follows that the matrix $(r\mathbf{M} + \mathbf{K})$ is consequently strongly positive definite.

Since the part of $(r\mathbf{M}+\mathbf{K})$ is strongly positive definite, there are various assumptions to make the whole $\mathbf{B}=r\mathbf{M}+\mathbf{K}-\mathbf{A}$ positive definite. Below we explore three possibilities.

1. We assume *the convection term is not dominant in the BSM operator*. In terms of the discrete system, it implies the minimum of the (positive) eigenvalues of $(r\mathbf{M}+\mathbf{K})$is strictly greater than the maximum of those of $\mathbf{A}$. It then follows that $\mathbf{B}$ is positive definite.

2. A stronger assumption is to assume *the convection term in variational produces non-positive values*, i.e. $(w, \tilde{\mathbf{D}}\cdot\nabla v) < 0$. In terms of the discrete system, it implies the asymmetric $\mathbf{A}$ is *semi-negative definite*. We then have $-\mathbf{A}$ being semi-positive definite and $\mathbf{B}$ being strongly positive definite.

3. Actually the above assumption can be guaranteed if we pose a more strict assumption on the coefficients from the trace theorem. With the trace theorem, we can assume $\exists c_i > 0$ such that

$$\int w^2 d\Gamma_N^{(i)} \le c_i \int w^2 d\Omega.$$

   Moreover, by assuming $S_{\max} c_i < 1$ for all $i = 1, \cdots, d$ as $S_{\max} \to \infty$, we can obtain the semi-negative definite $\mathbf{A}$ as shown below.

$$\begin{aligned}
\mathbf{W}^T\mathbf{A}\mathbf{W} &= \sum_{i=1}^{d} \bar{\mathbf{D}}^{(i)} \cdot \frac{1}{2} \cdot \left(S_{\max} \cdot \int w_h^2 d\Gamma_N^{(i)} - \int 1 \cdot w_h^2 d\Omega \right) \\
&\le \sum_{i=1}^{d} \underbrace{\left|\bar{\mathbf{D}}^{(i)}\right|}_{(+)} \cdot \frac{1}{2} \cdot \underbrace{(S_{\max} c_i - 1)}_{(-)} \cdot \underbrace{\int w_h^2 d\Omega}_{(+)} \; < \; 0
\end{aligned}$$

Note that the any one of three assumptions guarantees a positive definite $\mathbf{B}$.

5.6.3 Matrix C

If $\mathbf{B}_{IN,IN}$ is positive definite (and thus P-matrix), it follows $\mathbf{C} := \frac{1}{h_t}\mathbf{M}_{IN,IN} + \theta\mathbf{B}_{IN,IN}$ is positive definite (and thus P-matrix). If the definiteness of $\mathbf{B}_{IN,IN}$ is unknown, at least $\mathbf{C}$ is asymptotically dominated by $\mathbf{M}_{IN,IN}$ (as $h_t \to 0$) and thus asymptotically being positive-definite and a P-matrix.

5.7 Summary

We have seen how to discretize the infinite-dimensional problems into their finite-dimensional counterparts with finite element method in space and finite difference method in time. The

discrete systems can be uniquely solved if their coefficient matrices are positive-definite and accordingly a P-matrix, which can be satisfied at least asymptotically. In the next chapter, we shall see the detailed computation of the matrices arising from finite element approximation.

Chapter 6

Finite Element Matrices

In the previous chapter, we have seen how to discretize the variational formulation of our pricing problems. However, the finite element matrices used in discretized systems have not been explained in detail. This chapter is devoted to the computation of these matrices with conventional quadrature method and newly-derived formulas.

6.1 Numbering System

To implement the finite element method (FEM), we first need to partition the computational domain into finitely many subdomains, namely *computational elements*. Such elements are generally simplexes. Since our computational domain $\Omega = [0, S_{\max}]^d$ is regular, we can choose $d-$dimensional hypercubes[1] as our elements. Following this, we obtain a boundary subdivision of $\Gamma := \Gamma_N \cup \Gamma_D$. We denote the interior elements, Neumann boundary elements and Dirichlet boundary elements by $\Omega^{(e)}, \Gamma_N^{(e)}, \Gamma_D^{(e)}$ individually. We note that

$$\Omega = \bigcup_{e=1}^{n_E} \Omega^{(e)}, \quad \Gamma_N = \bigcup_{e=1}^{n_N} \Gamma_N^{(e)}, \quad \Gamma_D = \bigcup_{e=1}^{n_D} \Gamma_D^{(e)}.$$

Particularly a $d-$dimensional *reference element* is denoted and defined by

$$\Omega^* := [0, 1]^d.$$

If we apply Neumann boundary conditions, a face, say $\Gamma_{N^{(B)}}$, of the whole computational domain is defined in the following way. For each $B \in \{1, \ldots, d\}$,

$$\Gamma_{N^{(B)}} := \left\{ \mathbf{S} \in \Gamma_N : \mathbf{S} = (S^{(1)}, \ldots, S^{(d)}) \text{ and } S^{(B)} = S_{\max} \right\}.$$

[1] They are segments, squares and cubes in $1, 2, 3$ dimensions, respectively.

Each face $\Gamma_{N^{(B)}}$ has freedom in $(d-1)$ dimensions and is divided by its non-overlapping boundary elements $\Gamma^{(b)}_{N^{(B)}}$ for $b = 1, \ldots, m_B$ such that

$$\begin{aligned}\Gamma_N &= \bigcup_{e=1}^{n_N} \Gamma_N^{(e)} \\ &\equiv \bigcup_{B=1}^{d} \Gamma_{N^{(B)}} = \bigcup_{B=1}^{d} \left(\bigcup_{b=1}^{m_B} \Gamma^{(b)}_{N^{(B)}} \right).\end{aligned}$$

Note that $n_N = \sum_{B=1}^{d} m_B$.

We denote a node by $\mathbf{S}^{(g)}$ and number all the nodes with a global index, say $g = 1, \ldots, n_1$, $g = n_1 + 1, \ldots, n_2$ and $g = n_2 + 1, \ldots, n_3$ for the nodes on the interior domain, Neumann boundary and Dirichlet boundary individually. We remind the reader that in this chapter the global numbering system will use g as the notation of index while ℓ will be used to denote that of the local numbering system introduced later.

In addition to the global indices of the nodes over the whole computational domain, it is convenient to number the nodes locally over a common element. A node $\mathbf{S}^e := [S_e^{(1)}, \ldots, S_e^{(d)}] \in \Omega^{(e)}$ is said to be a local origin of an element $\Omega^{(e)}$ if for any $\mathbf{S} := [S^{(1)}, \ldots, S^{(d)}] \in \Omega^{(e)}$,

$$S^{(i)} \in [S_e^{(i)}, S_e^{(i)} + h_i].$$

where h_i refers to the elemental edge length along $S^{(i)}$. If a uniform mesh is employed, we have $h_1 = \ldots = h_d =: h_s > 0$ where the subscript s stands for space (or share/stock) to distinguish from the time step $h_t > 0$. Obviously $\mathbf{0} \in \mathbb{R}^d$ is also a local origin of the reference element Ω^*.

We know that a $d-$dimensional hypercube element has $n_\ell := 2^d$ vertices. Such n_ℓ vertices can be numbered later with $\ell = 1, 2, \ldots, n_\ell$ from its local origin in lexicographical order. Furthermore, we associate each local index ℓ with a $d-$tuple $(\delta_1, \ldots, \delta_d)$ with $\delta_i \in \{0, 1\}$ in the following lexicographical order.

ℓ	$\leftrightarrow$	$(\delta_1,$	$\delta_2,$	$\ldots,$	$\delta_{d-1},$	$\delta_d)$
1	$\leftrightarrow$	$(0,$	$0,$	$\ldots,$	$0,$	$0)$
2	$\leftrightarrow$	$(1,$	$0,$	$\ldots,$	$0,$	$0)$
3	$\leftrightarrow$	$(0,$	$1,$	$\ldots,$	$0,$	$0)$
4	$\leftrightarrow$	$(1,$	$1,$	$\ldots,$	$0,$	$0)$
$\vdots$	$\leftrightarrow$	$\vdots$	$\vdots$	$\ldots,$	$\vdots$	$\vdots$
$n_\ell := 2^d$	$\leftrightarrow$	$(1,$	$1,$	$\ldots,$	$1,$	$1)$

Suppose a node $\mathbf{S}^{(g)}$ is also a vertex of a $d-$dimensional hypercube element. The we can number it locally with a local index ℓ and the corresponding tuple $(\delta_1, \ldots, \delta_d)$ as follows.

$$\mathbf{S}^{(g)}\big|_{\Omega^{(e)}} \equiv \mathbf{S}_\ell^{(e)} \quad := \quad \mathbf{S}^e_{(\delta_1,\ldots,\delta_d)} := (S_e^{(1)} + \delta_1 h_1, \ldots, S_e^{(d)} + \delta_i h_d)^T,$$

and similarly

$$\mathbf{S}^{(g)}\big|_{\Omega^*} \equiv \mathbf{S}^*_\ell \;:=\; \mathbf{S}^*_{(\delta_1,\ldots,\delta_d)} := (\delta_1,\ldots,\delta_i)^T,$$

where $\ell \in \{1,\ldots,n_\ell := 2^d\}, \delta_i \in \{0,1\}$ and $i \in \{1,\ldots,d\}$. For convenience, these notations will be used interchangeably in the rest of this chapter. We will also omit the subscript/superscript e and $*$ if there is no confusion.

6.2 Shape Functions

We first recall that *a shape function* is a function defined over an element and a *node/basis function* is subsequently defined as a small union of a few shape functions sharing a joint node over some connected elements and has support only over those elements. We now define the following shape and node functions which will be used in the later derivation.

6.2.1 One-dimensional hat function

We define two hat functions along $S^{(i)}$ direction over $\Omega^{(e)}$ as follows.

$$H^e_\delta(S^{(i)}) := \begin{cases} \frac{S^{(i)}-S^{(i)}_e}{h_i} \text{ for } \delta = 1, \\ 1 - \frac{S^{(i)}-S^{(i)}_e}{h_i} \text{ for } \delta = 0. \end{cases}$$

Those over Ω^* can be defined in the same manner.

$$H^*_\delta(S^{(i)}) := \begin{cases} S^{(i)} \quad \text{for } \delta = 1, \\ 1 - S^{(i)} \text{ for } \delta = 0. \end{cases}$$

We remind the reader that the superscript e and $*$ (associated with an element) will be omitted if there is no confusion. The one-dimensional hat functions will be used to construct a shape function in one- and higher-dimensional cases.

6.2.2 $d-$linear shape function

A $d-$linear shape function over $\Omega^{(e)}$, denoted by $N^{(\ell)}_e$, reaching one at the node $\mathbf{S}^{(e)}_\ell \in \Omega^{(e)}$ and zero at others vertices is defined as[2]

$$N^{(\ell)}_e(\mathbf{S}) := N^e_{\delta_1,\ldots,\delta_d}(\mathbf{S}) := \prod_{i=1}^{d} H^e_{\delta_i}(S^{(i)}).$$

[2]In a similar way, we can define $d-$quadratic or $d-$cubic shape functions once a one-dimensional quadratic or cubic function is defined.

Analogously, a shape function over Ω^* has the form

$$N_*^{(\ell)}(\mathbf{S}) := N^*_{\delta_1,\ldots,\delta_d}(\mathbf{S}) := \prod_{i=1}^{d} H^*_{\delta_i}(S^{(i)}).$$

and reaches one at $\mathbf{S}^*_\ell$ and zero at the other vertices.

Figures 6.1, 6.2 and 6.3 are the visualization of shape functions in one, two and three dimensions individually.

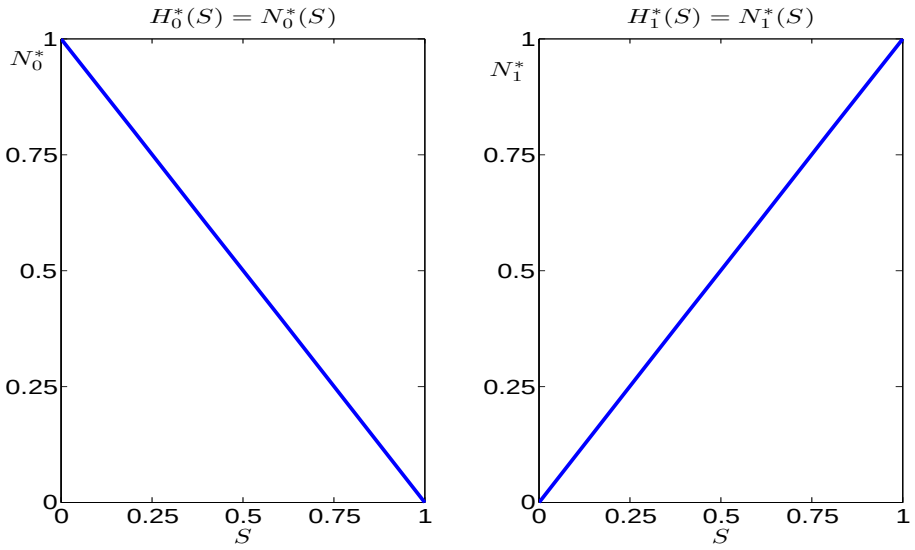

Figure 6.1: Two linear shape functions over a common 1D reference element domain.

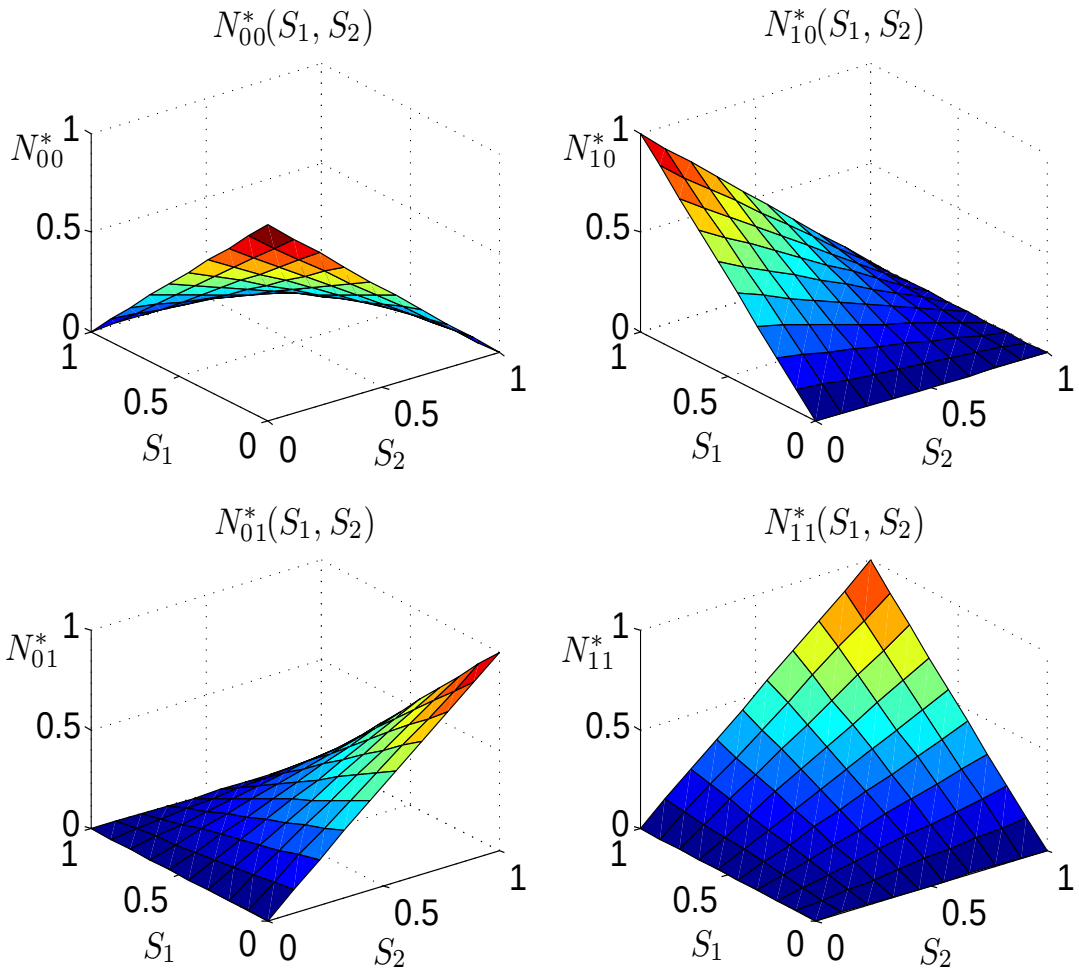

Figure 6.2: Four bilinear shape functions over a common 2D reference element domain.

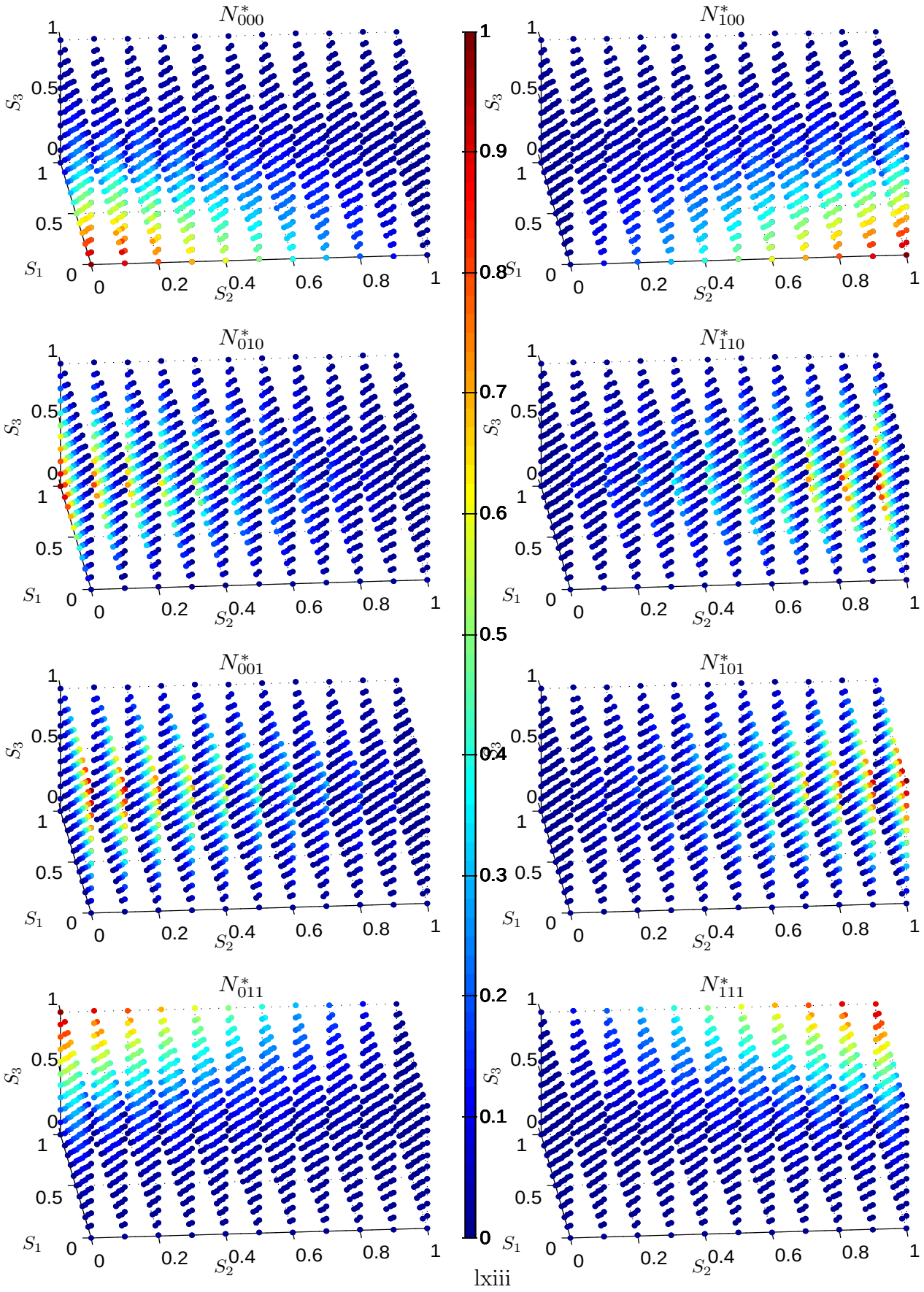

Figure 6.3: Eight trilinear shape functions over a common 3D reference element domain.

6.3 Problem Summary

We recall the infinite-dimensional variational equations of our pricing problems.

European options: $-(w, \dot{v}) + b(w, v) = \ell(w)$,

American options: $-(w - v, \dot{v}) + b(w - v, v) \geq \ell(w - v)$,

Perpetual options: $b(w - v, v) \geq \ell(w - v)$,

where

- $b(w, v) := r \cdot (w, v) + (\nabla w, \nabla v)_{\mathbf{T}} - (w, \tilde{\mathbf{D}}^T \nabla v)$.
- $\mathbf{T}$ is a $d \times d$ symmetric tensor matrix with the (i, j) component

$$\mathbf{T}_{ij} = \frac{\sigma_{ij} S^{(i)} S^{(j)}}{2},$$

  and $\mathbf{T} \equiv \frac{1}{2} \cdot \Sigma \odot (\mathbf{S}\,\mathbf{S}^T)$

- $$\tilde{\mathbf{D}} = \begin{pmatrix} r - q_1 - \sigma_{11} - \sum\limits_{\substack{j=1 \\ j \neq 1}} \frac{\sigma_{1j}}{2} \\ \vdots \\ r - q_i - \sigma_{ii} - \sum\limits_{\substack{j=1 \\ j \neq i}} \frac{\sigma_{ij}}{2} \\ \vdots \\ r - q_d - \sigma_{dd} - \sum\limits_{\substack{j=1 \\ j \neq d}} \frac{\sigma_{dj}}{2} \end{pmatrix} \odot \begin{pmatrix} S^{(1)} \\ \vdots \\ S^{(i)} \\ \vdots \\ S^{(d)} \end{pmatrix} =: \bar{\mathbf{D}} \odot \mathbf{S}.$$

- $\ell(w) \equiv 0$ if all boundary conditions are of Dirichlet type. If the the Neumann boundary conditions are applied , then

$$\ell(w) := \int_{\Gamma_N} w \mathbf{n} \cdot \mathbf{T} \nabla g d\Gamma_N.$$

After spatial discretization with finite element method, we obtain the following systems.

European options: $-(\mathbf{W}^T \mathbf{M} \dot{\mathbf{V}}) + \mathbf{W}^T \mathbf{B} \mathbf{V} = \mathbf{W}^T \mathbf{L}$,

American options: $-(\mathbf{W} - \mathbf{V})^T \mathbf{M} \dot{\mathbf{V}} + (\mathbf{W} - \mathbf{V})^T \mathbf{B} \mathbf{V} \geq (\mathbf{W} - \mathbf{V})^T \mathbf{L}$,

Perpetual options: $(\mathbf{W}-\mathbf{V})^T\mathbf{B}\mathbf{V} \geq (\mathbf{W}-\mathbf{V})^T\mathbf{L}$,

where

- $\mathbf{W} := (w^{(1)}, \cdots, w^{(n_3)})^T$,
- $\mathbf{V} := (v^{(1)}, \cdots, v^{(n_3)})^T$,
- $\mathbf{M}_{ij} := (\, N^{(i)}, N^{(j)}\,)$,
- $\mathbf{B}_{ij} := b(\, N^{(i)}, N^{(j)}\,)$,
- $\mathbf{L}_j := \ell(N^{(j)})$.

Furthermore, $\mathbf{B} \equiv r\mathbf{M} + \mathbf{K} - \mathbf{A}$ because

$$b(N^{(i)}, N^{(j)}) := r \cdot (N^{(i)}, N^{(j)}) + (\nabla N^{(i)}, \nabla N^{(j)})_{\mathbf{T}} - (N^{(i)}, \tilde{\mathbf{D}}\nabla N^{(j)}) =: r\mathbf{M}_{ij} + \mathbf{K}_{ij} - \mathbf{A}_{ij}.$$

Global and Elemental Matrices

We call $\mathbf{L}$ the *global load vector*. The symmetric matrices $\mathbf{M}$ and $\mathbf{K}$ are referred to as *global mass matrix* and *global stiffness matrix*, and we note that $\mathbf{A}$ is a nonsymmetric global matrix. We would like to find their entry values, so we can proceed with the solution of the fully-discretized reduced systems as shown in the previous chapter.

Conventionally, the global matrices and load vector are computed *element by element*. Namely,

$$\mathbf{M}_{ij} \;:=\; \int_{\Omega} N^{(i)}N^{(j)}d\Omega = \sum_{e=1}^{n_E} \int_{\Omega^{(e)}} N^{(i)}N^{(j)}d\Omega^{(e)} =: \sum_{e=1}^{n_E} \mathbf{M}_{ij}^{(e)}.$$

and similarly $\mathbf{K}_{ij} = \sum_{e=1}^{n_E} \mathbf{K}_{ij}^{(e)}$, $\mathbf{A}_{ij} = \sum_{e=1}^{n_E} \mathbf{A}_{ij}^{(e)}$ and $\mathbf{L}_j = \sum_{e=1}^{n_N} \mathbf{L}_j^{(e)}$.

Since there are only $n_\ell := 2^d$ node functions with support over a common $d-$dimensional element, zeros fill into most entries of the global matrices associated with the element numbered by (e). Accordingly we focus on the nonzero entries, reduce the matrix (and vector) size from $n_3 \times n_3$ (and $n_3 \times 1$) to $2^d \times 2^d$ (and $2^{d-1} \times 1$) and call the reduced counterparts *elemental matrices* (and *elemental load vector*).

Instead of the straight computation of global matrices and load vector, we focus on that of their elemental counterparts. Following the computation of elemental matrices and load vector, we then sum up their results to obtain the full-sized global counterparts. To map the computed values from elemental matrices to global counterparts, we can build a connectivity table linking local and global numbering systems for the use of assembly.

6.4 Elemental Computation by Closed-form Formula

Most people adopt numerical computation to approximate the elemental matrices up to satisfactory accuracy when using the finite element method. We describe how this can be performed and comment on this approach in our appendix.

Since our problem is specifically on the Black-Scholes-Merton equation, we alternatively describe how to obtain their exact component values by using the closed-form formulas derived below. These formulas can save substantial pre-processing time from numerical integration especially in high-dimensional cases and provide exact results of integration for our elemental matrices.

A key advantage of choosing $d-$linear shape functions is that the integrals over a $d-$dimensional hypercube element can be split into the sums or products of integrals along each dimension. Equipped with a well-defined local numbering system, closed-form formulas are consequently available for all elemental matrices .

6.4.1 Preliminaries

After some efforts of manual computation, we obtain the following results. For $\delta, \delta_j, \delta_k \in \{0, 1\}$,

$$\begin{aligned}
\int_{S_e^{(i)}}^{S_e^{(i)}+h_i} H_\delta(S^{(i)})\, dS^{(i)} &= \frac{h_i}{2}, \\
\int_{S_e^{(i)}}^{S_e^{(i)}+h_i} H_{\delta_j}(S^{(i)}) H_{\delta_k}(S^{(i)})\, dS^{(i)} &= \frac{h_i}{6} \cdot (1 + \mathbb{1}_{\{\delta_j=\delta_k\}}), \\
\int_{S_e^{(i)}}^{S_e^{(i)}+h_i} S^{(i)} H_\delta(S^{(i)})\, dS^{(i)} &= \frac{h_i S_e^{(i)}}{2} + \frac{{h_i}^2(1 + \mathbb{1}_{\{\delta=1\}})}{6}.
\end{aligned}$$

6.4.2 Integrals over interior elements in the two-dimensional case

We first recall the following two-dimensional node functions.

$$\begin{aligned}
N_e^{(\ell_1)}(\mathbf{S}) &:= N_{\delta_1\delta_2}(\mathbf{S}) := H_{\delta_1}(S^{(1)}) \cdot H_{\delta_2}(S^{(2)}), \\
N_e^{(\ell_2)}(\mathbf{S}) &:= N_{\delta_3\delta_4}(\mathbf{S}) := H_{\delta_3}(S^{(1)}) \cdot H_{\delta_4}(S^{(2)}).
\end{aligned}$$

Component of Elemental Mass Matrix $\mathbf{M}^{(e)}$

$$\mathbf{M}_{\ell_1,\ell_2}^{(e)} := \int_{\Omega^{(e)}} N_e^{(\ell_1)}\, N_e^{(\ell_2)}\, d\Omega^{(e)} = \frac{h_1 h_2 \Big(1 + \mathbb{1}_{\{\delta_1=\delta_3\}}\Big) \cdot \Big(1 + \mathbb{1}_{\{\delta_2=\delta_4\}}\Big)}{36}.$$

It is worth mentioning that the local mass matrix is "element-independent"; that is, all elements share a common 4×4 local mass matrix of the form below.

$$\mathbf{M}^{(e)} = \frac{h_1 h_2}{36} \begin{bmatrix} 4 & 2 & 2 & 1 \\ 2 & 4 & 1 & 2 \\ 2 & 1 & 4 & 2 \\ 1 & 2 & 2 & 4 \end{bmatrix}.$$

Component of Elemental Stiffness Matrix $\mathbf{K}^{(e)}$

$$\begin{aligned}
\mathbf{K}^{(e)}_{\ell_1,\ell_2} &:= \int_{\Omega^{(e)}} (\nabla N_e^{(\ell_1)})^T \, \mathbf{T} (\nabla N_e^{(\ell_2)}) \, d\Omega^{(e)} \\
&= \frac{\sigma_{11} H'_{\delta_1}(S^{(1)}) H'_{\delta_3}(S^{(1)})}{2} \cdot \int_{S_e^{(1)}}^{S_e^{(1)}+h_1} {S^{(1)}}^2 \, dS^{(1)} \cdot \int_{S_e^{(2)}}^{S_e^{(2)}+h_2} H_{\delta_2}(S^{(2)}) H_{\delta_4}(S^{(2)}) \, dS^{(2)} + \\
&\quad \frac{\sigma_{12} H'_{\delta_1}(S^{(1)}) H'_{\delta_4}(S^{(2)})}{2} \cdot \int_{S_e^{(1)}}^{S_e^{(1)}+h_1} S^{(1)} H_{\delta_3}(S^{(1)}) \, dS^{(1)} \cdot \int_{S_e^{(2)}}^{S_e^{(2)}+h_2} S^{(2)} H_{\delta_2}(S^{(2)}) \, dS^{(2)} + \\
&\quad \frac{\sigma_{21} H'_{\delta_2}(S^{(2)}) H'_{\delta_3}(S^{(1)})}{2} \cdot \int_{S_e^{(1)}}^{S_e^{(1)}+h_1} S^{(1)} H_{\delta_1}(S^{(1)}) \, dS^{(1)} \cdot \int_{S_e^{(2)}}^{S_e^{(2)}+h_2} S^{(2)} H_{\delta_4}(S^{(2)}) \, dS^{(2)} + \\
&\quad \frac{\sigma_{22} H'_{\delta_2}(S^{(2)}) H'_{\delta_4}(S^{(2)})}{2} \cdot \int_{S_e^{(1)}}^{S_e^{(1)}+h_1} H_{\delta_1}(S^{(1)}) H_{\delta_3}(S^{(1)}) \, dS^{(1)} \cdot \int_{S_e^{(2)}}^{S_e^{(2)}+h_2} {S^{(2)}}^2 \, dS^{(2)} \\
&= \frac{\sigma_{11}}{72} \cdot \frac{h_2}{h_1} \cdot \left(1 - 2 \cdot \mathbb{1}_{\{\delta_1 \neq \delta_3\}}\right) \cdot \left(6 {S_e^{(1)}}^2 + 6 S_e^{(1)} h_1 + 2 h_1^2\right) \cdot \left(1 + \mathbb{1}_{\{\delta_2 = \delta_4\}}\right) + \\
&\quad \frac{\sigma_{12}}{72} \cdot \left(1 - 2 \cdot \mathbb{1}_{\{\delta_1 \neq \delta_4\}}\right) \cdot \left(3 S_e^{(1)} + h_1 (1 + \mathbb{1}_{\{\delta_3 = 1\}})\right) \cdot \left(3 S_e^{(2)} + h_2 (1 + \mathbb{1}_{\{\delta_2 = 1\}})\right) + \\
&\quad \frac{\sigma_{21}}{72} \cdot \left(1 - 2 \cdot \mathbb{1}_{\{\delta_2 \neq \delta_3\}}\right) \cdot \left(3 S_e^{(1)} + h_1 (1 + \mathbb{1}_{\{\delta_1 = 1\}})\right) \cdot \left(3 S_e^{(2)} + h_2 (1 + \mathbb{1}_{\{\delta_4 = 1\}})\right) + \\
&\quad \frac{\sigma_{22}}{72} \cdot \frac{h_1}{h_2} \cdot \left(1 - 2 \cdot \mathbb{1}_{\{\delta_2 \neq \delta_4\}}\right) \cdot \left(1 + \mathbb{1}_{\{\delta_1 = \delta_3\}}\right) \cdot \left(6 {S_e^{(2)}}^2 + 6 S_e^{(2)} h_2 + 2 h_2^2\right).
\end{aligned}$$

It is obvious that stiffness matrix is "element-dependent".

Component of Elemental Matrix $\mathbf{A}^{(e)}$

$$
\begin{aligned}
\mathbf{A}^{(e)}_{\ell_1,\ell_2} &:= \int\limits_{\Omega^{(e)}} N_e^{(\,)} d\Omega^{(e)} \ell_1 \tilde{\mathbf{D}}^T (\nabla N_e^{(\ell_2)}) d\Omega^{(e)} \\
&= (r - q_1 - \sigma_{11} - \frac{\sigma_{12}}{2}) H'_{\delta_3}(S^{(1)}) \cdot \int_{S_e^{(1)}}^{S_e^{(1)}+h_1} S^{(1)} H_{\delta_1}(S^{(1)})\, dS^{(1)} \cdot \int_{S_e^{(2)}}^{S_e^{(2)}+h_2} H_{\delta_2}(S^{(2)}) H_{\delta_4}(S^{(2)})\, dS^{(2)} \; + \\
&\quad (r - q_2 - \frac{\sigma_{21}}{2} - \sigma_{22}) H'_{\delta_4}(S^{(2)}) \cdot \int_{S_e^{(1)}}^{S_e^{(1)}+h_1} H_{\delta_1}(S^{(1)}) H_{\delta_3}(S^{(1)})\, dS^{(1)} \cdot \int_{S_e^{(2)}}^{S_e^{(2)}+h_2} S^{(2)} H_{\delta_2}(S^{(2)})\, dS^{(2)} \\
&= \frac{(r - q_1 - \sigma_{11} - \frac{\sigma_{12}}{2})}{36} \Big(1 - 2 \cdot \mathbb{1}_{\{\delta_3=0\}}\Big) \Big(3S_e^{(1)} + h_1(1 + \mathbb{1}_{\{\delta_1=1\}})\Big) \Big(h_2(1 + \mathbb{1}_{\{\delta_2=\delta_4\}})\Big) + \\
&\quad \frac{(r - q_2 - \frac{\sigma_{21}}{2} - \sigma_{22})}{36} \Big(1 - 2 \cdot \mathbb{1}_{\{\delta_4=0\}}\Big) \Big(h_1(1 + \mathbb{1}_{\{\delta_1=\delta_3\}})\Big) \Big(3S_e^{(2)} + h_2(1 + \mathbb{1}_{\{\delta_2=1\}})\Big).
\end{aligned}
$$

It follows by observation that components of $\mathbf{A}^{(e)}$ are "element-dependent".

6.4.3 Integrals over Interior Elements in $d-$dimensional Case with $d \geq 3$

Similarly we first define the d-dimensional node functions.

$$
\begin{aligned}
N_e^{(\ell_1)}(\mathbf{S}) &:= N_{\delta_1 \ldots \delta_d}(\mathbf{S}) \quad := H_{\delta_1}(S^{(1)}) \ldots H_{\delta_d}(S^{(d)}), \\
N_e^{(\ell_2)}(\mathbf{S}) &:= N_{\delta_{d+1} \ldots \delta_{2d}}(\mathbf{S}) := H_{\delta_{d+1}}(S^{(1)}) \ldots H_{\delta_{d+d}}(S^{(d)}).
\end{aligned}
$$

Recall the elemental matrices are of size $n_\ell \times n_\ell$ for a general $d-$dimensional element $\Omega^{(e)}$ and consequently $\ell_1, \ell_2 \in \{1, 2, 3, 4, \ldots, n_\ell\}$ and $\delta_1, \delta_2, \delta_3, \delta_4, \ldots, \delta_{d+d} \in \{0, 1\}$. With the same logic, general formulas in high-dimensional cases can be derived. As we will see soon, components of matrices $\mathbf{M}^{(e)}$ are element-independent while those of $\mathbf{K}^{(e)}$ and $\mathbf{A}^{(e)}$ are element-dependent.

Component values of mass matrix $\mathbf{M}^{(e)}$:

$$
\begin{aligned}
\mathbf{M}^{(e)}_{\ell_1,\ell_2} &:= \int\limits_{\Omega^{(e)}} N_e^{(\ell_1)}\, N_e^{(\ell_2)}\, d\Omega^{(e)} \\
&= \Big(\int_{S_e^{(1)}}^{S_e^{(1)}+h_1} H_{\delta_1}(S^{(1)}) H_{\delta_{d+1}}(S^{(1)})\, dS^{(1)}\Big) \cdots \Big(\int_{S_e^{(d)}}^{S_e^{(d)}+h_d} H_{\delta_d}(S^{(d)}) H_{\delta_{d+d}}(S^{(d)})\, dS^{(d)}\Big) \\
&= \prod_{i=1}^{d} \frac{h_i}{6} \cdot (1 + \mathbb{1}_{\{\delta_i=\delta_{d+i}\}}).
\end{aligned}
$$

In particular the three-dimensional counterpart is in the specific form below.

$$\mathbf{M}^{(e)} = \frac{h_1 h_2 h_3}{216} \begin{bmatrix} 8 & 4 & 4 & 2 & 4 & 2 & 2 & 1 \\ 4 & 8 & 2 & 4 & 2 & 4 & 1 & 2 \\ 4 & 2 & 8 & 4 & 2 & 1 & 4 & 2 \\ 2 & 4 & 4 & 8 & 1 & 2 & 2 & 4 \\ 4 & 2 & 2 & 1 & 8 & 4 & 4 & 2 \\ 2 & 4 & 1 & 2 & 4 & 8 & 2 & 4 \\ 2 & 1 & 4 & 2 & 4 & 2 & 8 & 4 \\ 1 & 2 & 2 & 4 & 2 & 4 & 4 & 8 \end{bmatrix}$$

Component of Elemental Stiffness Matrix $\mathbf{K}^{(e)}$:

$$
\begin{aligned}
\mathbf{K}^{(e)}_{\ell_1,\ell_2} &:= \int_{\Omega^{(e)}} (\nabla N_e^{(\ell_1)})^T \, \mathbf{T} (\nabla N_e^{(\ell_2)}) \, d\Omega^{(e)} \\
&= \sum_{i=1}^{d-1} \sum_{j=i+1}^{d} \frac{\sigma_{ij} H'_{\delta_i} H'_{\delta_{d+j}}}{2} \cdot \Big(\prod_{\substack{k=1 \\ k\neq i,j}}^{d} \int_{S_e^{(k)}}^{S_e^{(k)}+h_k} H_{\delta_k}(S^{(k)}) H_{\delta_{d+k}}(S^{(k)}) \, dS^{(k)} \Big) \\
&\qquad \cdot \Big(\int_{S_e^{(i)}}^{S_e^{(i)}+h_i} S^{(i)} H_{\delta_{d+i}}(S^{(i)}) \, dS^{(i)} \Big) \Big(\int_{S_e^{(j)}}^{S_e^{(j)}+h_j} S^{(j)} H_{\delta_j}(S^{(j)}) \, dS^{(j)} \Big) + \\
&\quad \sum_{i=1}^{d} \frac{\sigma_{ii} H'_{\delta_i} H'_{\delta_{d+i}}}{2} \cdot \Big(\prod_{\substack{k=1 \\ k\neq i}}^{d} \int_{S_e^{(k)}}^{S_e^{(k)}+h_k} H_{\delta_k}(S^{(k)}) H_{\delta_{d+k}}(S^{(k)}) \, dS^{(k)} \Big) \cdot \Big(\int_{S_e^{(i)}}^{S_e^{(i)}+h_i} {S^{(i)}}^2 \, dS^{(i)} \Big) + \\
&\quad \sum_{i=2}^{d} \sum_{j=1}^{i-1} \frac{\sigma_{ij} H'_{\delta_i} H'_{\delta_{d+j}}}{2} \cdot \Big(\prod_{\substack{k=1 \\ k\neq i,j}}^{d} \int_{S_e^{(k)}}^{S_e^{(k)}+h_k} H_{\delta_k}(S^{(k)}) H_{\delta_{d+k}}(S^{(k)}) \, dS^{(k)} \Big) \\
&\qquad \cdot \Big(\int_{S_e^{(j)}}^{S_e^{(j)}+h_j} S^{(j)} H_{\delta_j}(S^{(j)}) \, dS^{(j)} \Big) \Big(\int_{S_e^{(i)}}^{S_e^{(i)}+h_i} S^{(i)} H_{\delta_{d+i}}(S^{(i)}) \, dS^{(i)} \Big) \\
&= \sum_{i=1}^{d-1} \sum_{j=i+1}^{d} \frac{\sigma_{ij}}{2} \frac{1 - 2 \cdot \mathbb{1}_{\{\{\delta_i \neq \delta_{d+j}\}\}}}{h_i h_j} \cdot \Big(\prod_{\substack{k=1 \\ k\neq i,j}}^{d} \frac{h_k}{6} \cdot (1 + \mathbb{1}_{\{\delta_k = \delta_{d+k}\}}) \Big) \\
&\qquad \cdot \Big(\frac{h_i S_e^{(i)}}{2} + \frac{{h_i}^2 (1 + \mathbb{1}_{\{\delta_{d+i}=1\}})}{6} \Big) \Big(\frac{h_j S_e^{(j)}}{2} + \frac{{h_j}^2 (1 + \mathbb{1}_{\{\delta_j=1\}})}{6} \Big) + \\
&\quad \sum_{i=1}^{d} \frac{\sigma_{ii}}{2} \frac{1 - 2 \cdot \mathbb{1}_{\{\{\delta_i \neq \delta_{d+i}\}\}}}{h_i h_i} \cdot \Big(\prod_{\substack{k=1 \\ k\neq i}}^{d} \frac{h_k}{6} \cdot (1 + \mathbb{1}_{\{\delta_k = \delta_{d+k}\}}) \Big) \cdot \Big(\frac{h_i (3{S_e^{(i)}}^2 + 3 S_e^{(i)} h_i + {h_i}^2)}{3} \Big) + \\
&\quad \sum_{i=2}^{d} \sum_{j=1}^{i-1} \frac{\sigma_{ji}}{2} \frac{1 - 2 \cdot \mathbb{1}_{\{\{\delta_i \neq \delta_{d+j}\}\}}}{h_j h_i} \cdot \Big(\prod_{\substack{k=1 \\ k\neq i,j}}^{d} \frac{h_k}{6} \cdot (1 + \mathbb{1}_{\{\delta_k = \delta_{d+k}\}}) \Big) + \\
&\qquad \cdot \Big(\frac{h_j S_e^{(j)}}{2} + \frac{{h_j}^2 (1 + \mathbb{1}_{\{\delta_j=1\}})}{6} \Big) \Big(\frac{h_i S_e^{(i)}}{2} + \frac{{h_i}^2 (1 + \mathbb{1}_{\{\delta_{d+i}=1\}})}{6} \Big).
\end{aligned}
$$

Notice that there are no $\prod_{\substack{k=1 \\ k\neq i,j}}^{d} \int_{S_e^{(k)}}^{S_e^{(k)}+h_k} H_{\delta_k}(S^{(k)}) H_{\delta_{d+k}}(S^{(k)}) \, dS^{(k)}$ terms for both $i < j$ and $i > j$ in two-dimensional cases.

Component of Elemental Matrix $\mathbf{A}^{(e)}$

$$
\begin{aligned}
\mathbf{A}^{(e)}_{\ell_1,\ell_2} &:= \int N_e^{(\ell_1)} \tilde{\mathbf{D}}^T (\nabla N_e^{(\ell_2)}) d\Omega^{(e)} \\
&= \sum_{i=1}^{d} (r - q_i - \frac{\sigma_{ii}}{2} - \sum_{j=1}^{d} \frac{\sigma_{ij}}{2}) H'_{\delta_{d+i}}(S^{(i)}) \\
&\qquad \cdot \left(\prod_{\substack{k=1 \\ k\neq i}}^{d} \int_{S_e^{(k)}}^{S_e^{(k)}+h_k} H_{\delta_k}(S^{(k)}) H_{\delta_{d+k}}(S^{(k)})\, dS^{(k)} \right) \cdot \left(\int_{S_e^{(i)}}^{S_e^{(i)}+h_i} S^{(i)} H_{\delta_i}(S^{(i)})\, dS^{(i)} \right) \\
&= \sum_{i=1}^{d} (r - q_i - \frac{\sigma_{ii}}{2} - \sum_{j=1}^{d} \frac{\sigma_{ij}}{2}) \cdot \frac{1 - 2 \cdot \mathbb{1}_{\{\delta_{d+i}=0\}}}{h_i} \cdot \\
&\qquad \cdot \left(\prod_{\substack{k=1 \\ k\neq i}}^{d} \frac{h_k}{6} \cdot (1 + \mathbb{1}_{\{\delta_k=\delta_{d+k}\}}) \right) \cdot \left(\frac{h_i S_e^{(i)}}{2} + \frac{{h_i}^2 (1 + \mathbb{1}_{\{\delta_i=1\}})}{6} \right).
\end{aligned}
$$

Component of Elemental *Unweighted* Stiffness Matrix $\mathbf{S}^{(e)}$:

6.4.4 Integrals over boundary elements in $d-$dimensional case

General Case of $d \geq 2$

We recall the notations of Neumann edges, its partition and the boundary conditions on them.

$$\begin{aligned}
\Gamma_{N^{(B)}} &:= \left\{\mathbf{S} \in \Gamma_N : \mathbf{S} = (S^{(1)}, \ldots, S^{(d)}) \text{ and } S^{(B)} = S_{\max}\right\} \text{ for } B = 1, \ldots, d, \\
\Gamma_N &= \bigcup_{e=1}^{n_N} \Gamma_N^{(e)} \\
&\equiv \bigcup_{B=1}^{d} \Gamma_{N^{(B)}} = \bigcup_{B=1}^{d} \left(\bigcup_{b=1}^{m_B} \Gamma_{N^{(B)}}^{(b)} \right), \\
\nabla v\Big|_{\Gamma_{N^{(B)}}} &= \nabla g\Big|_{\Gamma_{N^{(B)}}},
\end{aligned}$$

where $n_N = \sum_{B=1}^{d} m_B$ and $\Gamma_{N^{(B)}}$ is a $(d-1)-$dimensional manifold.

Given $B \in \{1, \ldots, d\}$, we define the *adjusted dimension* for $i \in \{1, \ldots, \underline{d} := d-1\}$ as below to link the free dimensions to the original ones,

$$\begin{aligned}
i^B &:= i + \mathbb{1}_{\{i \geq B\}} \\
S^{(i^B)} &:= \begin{cases} S^{(i)} & \text{if } i < B, \\ S^{(i+1)} & \text{if } i \geq B. \end{cases}
\end{aligned}$$

A boundary element $\Gamma_{N^{(B)}}^{(b)}$ is one dimension less than those on an interior element. We define its local origin by

$$\mathbf{S}_{B,b}^{1} := \left(S_{B,b}^{(1^B)}, \cdots, S_{B,b}^{(\underline{d}^B)} \right).$$

We further define other vertices with local indices and their associated $\underline{d}-$tuple in lexicographical order as below.

$$\begin{aligned}
\ell &\in \{1, \ldots, \underline{n_\ell} := 2^{\underline{d}}\}, \\
\mathbf{S}^{(i)}\Big|_{\Gamma_{N^{(B)}}^{(b)}} := \mathbf{S}_{B,b}^{\ell} &:= \mathbf{S}_{\delta_{(1^B)} \cdots \delta_{(\underline{d}^B)}} \\
&:= \left(S^{(1^B)}, \cdots, S^{(\underline{d}^B)} \right)^T \\
&:= \left(S_{B,b}^{(1^B)} + \delta_{(1^B)} \cdot h_{(1^B)}, \cdots, S_{B,b}^{(\underline{d}^B)} + \delta_{(\underline{d}^B)} \cdot h_{(\underline{d}^B)} \right)^T. \\
&\equiv \mathbf{S}_{B,b}^{1} + \left(\delta_{(1^B)} \cdot h_{(1^B)}, \cdots, \delta_{(\underline{d}^B)} \cdot h_{(\underline{d}^B)} \right)^T
\end{aligned}$$

where $\delta_{(i^B)} \in \{0,1\}$ and $h_{(i^B)}$ is the step length along $S^{(i^B)}$ for a given $B \in \{1,\ldots,d\}$ and $i \in \{1,\ldots,\underline{d}\}$. Notice that $\mathbf{S}^1_{B,b}$ has $\delta_{(i^B)} = 0$ for all $i = 1,\ldots,\underline{d}$.
As well, the shape functions over the boundary element can be expressed in the form with one dimension less.
Namely,

$$\begin{aligned} N^{(i)}\Big|_{\Gamma^{(b)}_{N^{(B)}}} &:= N^{\ell}_{B,b}\left(S^{(1^B)},\cdots,S^{(\underline{d}^B)}\right) \\ &:= N_{\delta_{(1^B)}\cdots\delta_{(\underline{d}^B)}}\left(S^{(1^B)},\cdots,S^{(\underline{d}^B)}\right) \\ &:= H_{\delta_{(1^B)}}(S^{(1^B)}) \;\cdots\; H_{\delta_{(\underline{d}^B)}}(S^{(\underline{d}^B)}) \end{aligned}$$

With these notations, we can derive the closed forms of (Neumann boundary) load vector like those of elemental matrices.

Component of Elemental Load vector $\mathbf{L}^{(B,b)}$:

$$\begin{aligned} \mathbf{L}^{(B,b)}_{\ell} &:= \int \mathbf{n}\cdot\mathbf{T}(\nabla g)N^{\ell}_{B,b}\; d\Gamma^{(b)}_{N^{(B)}} \\ &= \frac{\sigma_{BB}S^{(B)}S^{(B)}}{2}\cdot(\partial^{(B)}_B g)\cdot\prod_{j=1}^{\underline{d}}\int_{S^{(j^B)}}^{S^{(j^B)}+h_{(j^B)}} H_{\delta_{(j^B)}}(S^{(j^B)})\; dS^{(j^B)} \\ &\quad+\sum_{i=1}^{\underline{d}}\frac{\sigma_{B(i^B)}S^{(B)}}{2}\cdot(\partial^{(i^B)}_B g)\cdot\left(\int_{S^{(i^B)}}^{S^{(i^B)}+h_{(i^B)}} S^{(i^B)}H_{\delta_{(i^B)}}(S^{(i^B)})\; dS^{(i^B)}\right. \\ &\qquad\left.\times\prod_{\substack{j=1\\ j\neq i}}^{\underline{d}}\int_{S^{(j^B)}}^{S^{(j^B)}+h_{(j^B)}} H_{\delta_{(j^B)}}(S^{(j^B)})\; dS^{(j^B)}\right) \\ &= \frac{\sigma_{BB}S^2_{\max}}{2}\cdot(\partial^{(B)}_B g)\cdot\prod_{j=1}^{\underline{d}}\frac{h_{(j^B)}}{2} \\ &\quad+\sum_{i=1}^{\underline{d}}\frac{\sigma_{B(i^B)}S_{\max}}{2}\cdot(\partial^{(i^B)}_B g)\cdot\left(\left(\frac{h_{i^B}S^{(i^B)}_e}{2}+\frac{{h_{i^B}}^2(1+\mathbb{1}_{\{\delta^B_i=1\}})}{6}\right)\times\prod_{\substack{j=1\\ j\neq i}}^{\underline{d}}\frac{h_{(j^B)}}{2}\right) \end{aligned}$$

where $\nabla g\big|_{\Gamma_{N^{(B)}}} := \left((\partial^{(1)}_B g)\cdots(\partial^{(B)}_B g)\cdots(\partial^{(d)}_B g)\right)^T$ is a constant vector for $B \in \{1,\ldots,d\}$.

An Alternative to Load Vector

Instead of finding the *exact* load vector as above, we can approximate the Neumann boundary function in finite-dimensional sense as before.

$$\begin{aligned}\ell(w_h) &= \sum_{B=1}^{d}\sum_{b=1}^{m_B}\int w_h f_h^B d\Gamma_{N^{(B)}}^{(b)} \\ &= \sum_{B=1}^{d}\sum_{b=1}^{m_B}\mathbf{W}\ \mathbf{M}_{B,b}\mathbf{f^B} \\ &=: \sum_{B=1}^{d}\sum_{b=1}^{m_B}\mathbf{W}\ \mathbf{L}^{(B,b)},\end{aligned}$$

where $\mathbf{M}_{B,b}$ is the boundary elemental mass function of size $n_3\times n_3$, $\mathbf{f^B} := \left(f_h^B(\mathbf{S}^1),\cdots,f_h^B(\mathbf{S}^{n_3})\right)^T$ and $\mathbf{L}^{(B,b)} := \mathbf{M}_{B,b}\ \mathbf{f^B}$ is the *approximated* load vector of size $n_3 \times n_3$.

We recall that most components of the $\mathbf{M}_{B,b}$ are zeros and only the node functions having support over the boundary element $\Gamma_{N^{(B)}}^{(b)}$ will provide non-zero entries when integrating over it. Based on this, the size of the boundary element matrix $\mathbf{M}_{B,b}$ can be reduced to $\underline{n_\ell}\times\underline{n_\ell}$ with all the non-zeros. We now focus on the reduced $\mathbf{M}_{B,b}$ of size $\underline{n_\ell}\times\underline{n_\ell}$.

Analogously we define the following $\underline{d}$-dimensional node functions having support over the boundary element $\mathbf{M}_{B,b}$.

$$\begin{aligned}N^{(i)}\big|_{\Gamma_{N^{(B)}}^{(b)}} := N_{B,b}^{\ell_1}(\mathbf{S}) &:= N_{\delta_{(1^B)}\cdots\delta_{(\underline{d}^B)}}(\mathbf{S}) \qquad := H_{\delta_{(1^B)}}(S^{(1^B)})\cdots H_{\delta_{(\underline{d}^B)}}(S^{(\underline{d}^B)}), \\ N^{(j)}\big|_{\Gamma_{N^{(B)}}^{(b)}} := N_{B,b}^{\ell_2}(\mathbf{S}) &:= N_{\delta_{(\underline{d}+1^B)}\cdots\delta_{(\underline{d}+\underline{d}^B)}}(\mathbf{S}) := H_{\delta_{(\underline{d}+1^B)}}(S^{(1^B)})\cdots H_{\delta_{(\underline{d}+\underline{d}^B)}}(S^{(\underline{d}^B)}).\end{aligned}$$

With these notations, we now derive its non-zero value as those of interior elements.

$$\begin{aligned}\mathbf{M}_{\ell_1,\ell_2}^{(B,b)} &:= \int N_{B,b}^{\ell_1} N_{B,b}^{\ell_2}\ d\Gamma_{N^{(B)}}^{(b)} \\ &= \Big(\int_{S_e^{(1^B)}}^{S_e^{(1^B)}+h_{1^B}} H_{\delta_{(1^B)}}(S^{(1^B)})H_{\delta_{(\underline{d}+1^B)}}(S^{(1^B)})\ dS^{(1^B)}\Big)\cdots \\ &\quad \Big(\int_{S_e^{(\underline{d}^B)}}^{S_e^{(\underline{d}^B)}+h_{\underline{d}}^B} H_{\delta_{(\underline{d}^B)}}(S^{(\underline{d}^B)})H_{\delta_{(\underline{d}+\underline{d}^B)}}(S^{(\underline{d}^B)})\ dS^{(\underline{d}^B)}\Big) \\ &= \prod_{i=1}^{\underline{d}}\frac{h_{(i^B)}}{6}\cdot(1+\mathbb{1}_{\{\delta_{(i^B)}=\delta_{(\underline{d}+i^B)}\}}).\end{aligned}$$

6.5 Summary

A conventional way to obtain the elemental matrices and load vector is to do a change of variable and to carry out numerical integration over a reference element of the same dimension. In the case of the elemental mass matrix, all values are element-independent and such approach can compute values efficiently. However, component values are element-dependent in other elemental matrices. From this point of view, the conventional method can not actually benefit the computation. Furthermore, its error in high dimensional quadrature may influence the accuracy of final option values. The closed-form formulas we propose here are new in mathematical finance. These formulas give us the exact values and avoid the numerical error of coefficient matrices. Technically they are the most straight and efficient way to obtain the values. The technique we use here can be directly extended to combinations of other different elements and shape functions such as hyper-triangles and d-quadratical shape functions.

Chapter 7

Algorithms for Linear Complementarity Problem

We have described in chapter five how to reformulate the multi-asset option pricing problems under the Black-Scholes-Merton model as discrete algebra systems: (sequential) linear system of equations (LSE) for European options and (sequential) linear complementarity problem (LCP) for American and perpetual options. In particular, these discrete systems share identical global matrices and load vectors. However, they may possess different Dirichlet data, generally the option or (discounted) payoff values of one-dimension-less counterparts.

There are two main approaches to numerically solve the discrete algebra systems — *direct methods* and *iterative methods*. The direct methods find the exact solutions by *pivoting*[1] or *factorizing*[2] the discrete systems. Instead, iterative methods provide approximate solutions which converge to the exact solution based on matrix analysis, convex analysis and optimization theories.

Linear System of Equations

Most numerical methods for linear equation systems are well doucmented. For example, Gauss-Jordan elimination and Cholesky, LU, LDL^T decomposition count for the direct method. As well, the widely-used iterative methods include generalized minimum residual (GMERS), conjugate gradient (CG), quasi-minimal residual (QMR), algebraic multigrid (AMG) methods and their variants. We refer the reader to [52, 92, 83] for their details and omit further discussion in our work.

[1] Interchange the rows or columns of a linear systems based on certain rules.

[2] Rewrite the coefficient matrix of a linear system as a product of two or more matrices, such as triangular and diagonal matrices, based on certain rules.

Linear Complementarity Problem

Compared with the numerical methods for linear system of equations (LSE), those for linear complementarity problems are not well introduced, particularly in the field of quantitative finance. Due to these, we decide to select several methods for such problems and introduce their implementing procedure in this chapter. In the next chapter, we will further compare these methods in terms of numerical error and computational time.

7.1 Preliminaries

7.1.1 Canonical Form of LCP

For convenience of discussion, we consider a linear complementarity problem in the standard form below.

Problem 7.1 *Find* $\mathbf{z}, \mathbf{w} \in \mathbb{R}^n$ *such that*

$$\begin{aligned} &\mathbf{z} \geqq \mathbf{0}, \\ &\mathbf{w} = \mathbf{C}\mathbf{z} + \mathbf{q} \geqq \mathbf{0}, \\ &\mathbf{w}^T\mathbf{z} = 0. \end{aligned}$$

For brevity of notation, we denote this problem by LCP$(\mathbf{C}, \mathbf{q})$*. For each* $i = 1, \ldots, n$*, the pair of components* $\mathbf{z}_i$ *and* $\mathbf{w}_i$ *are said to be complements of each other. We also define its feasible set and solution set as follows.*

$$\begin{aligned} FEA(\mathbf{C}, \mathbf{q}) &:= \{\mathbf{z} \big| \mathbf{z} \geqq \mathbf{0} \text{ and } \mathbf{C}\mathbf{z} + \mathbf{q} \geqq \mathbf{0}\}, \\ SOL(\mathbf{C}, \mathbf{q}) &:= \{\mathbf{z} \in FEA(\mathbf{C}, \mathbf{q}) \big| (\mathbf{C}\mathbf{z} + \mathbf{q})^T\mathbf{z} = 0\}. \end{aligned}$$

7.1.2 Matrix Classes

Existence and uniqueness of the solution to LCP$(\mathbf{C}, \mathbf{q})$ strongly depends on the matrix $\mathbf{C}$ and vector q, cf. [24]. The relations between different matrix classes are complicated and yet fully understood. Below we introduce a few relevant matrix classes.

Definition 7.2 (Classes of matrices)

- Submatrix and minor:
  - We define $[n] := \{1, \ldots, n\}$ and consider a *square* matrix $\mathbf{C} \in \mathbb{R}^{n \times n}$.
  - For $\alpha \subset [n]$, $\mathbf{C}_{\alpha\alpha}$ is a principal submatrix extracted from the intersection of rows and columns indexed by α.

- The principal submatrices $\mathbf{C}_{\alpha\alpha}$ where $\alpha = [k]$ for $k = 1, 2, \ldots, n$ are called *leading* principal matrices.
- The determinant of a (leading) principal submatrix of $\mathbf{C}$ is called a (leading) principal *minor* of $\mathbf{C}$ and denoted by $\det(\mathbf{C}_{\alpha\alpha})$.

- Comparison matrix:
  Matrix $\overline{\mathbf{C}}$ is said to be the comparison matrix of $\mathbf{C}$ if its (i, j) component are defined by

$$\overline{\mathbf{C}}_{ij} := \begin{cases} |\mathbf{C}_{ij}| & \forall i = j, \\ -|\mathbf{C}_{ij}| & \forall i \neq j. \end{cases}$$

- Q-matrix:
  - $\mathbf{C}$ is a Q-matrix, denoted by $[\mathbb{Q}]$, if $\mathrm{SOL}(\mathbf{C}, \mathbf{q}) \neq \emptyset, \forall \mathbf{q}$.
  - $\mathbf{C}$ is a Q_0-matrix, denoted by $[\mathbb{Q}_0]$, if $\forall \mathbf{q}, \mathrm{FEA}(\mathbf{C}, \mathbf{q}) \neq \emptyset \Rightarrow \mathrm{SOL}(\mathbf{C}, \mathbf{q}) \neq \emptyset$. Note that $[\mathbb{Q}] \subset [\mathbb{Q}_0]$.

- Co-positive matrix:
  - $\mathbf{C}$ is said to be *co-positive*, denoted by [c-p.], if $\forall \mathbf{x} \geqq \mathbf{0} \Rightarrow \mathbf{x}^T\mathbf{C}\mathbf{x} \geq 0$.
  - $\mathbf{C}$ is said to be *strictly co-positive*, denoted by [s.c-p.], if 'for $\mathbf{0} \neq \mathbf{x} \geqq \mathbf{0} \Rightarrow \mathbf{x}^T\mathbf{C}\mathbf{x} \geq 0$'.
  - $\mathbf{C}$ is said to be *co-positive plus*, denoted by [c-p.p.], if it satisfies the following two conditions:
    1. $\mathbf{C}$ is co-positive.
    2. $\mathbf{x} \geqq \mathbf{0}$ and $\mathbf{x}^T\mathbf{C}\mathbf{x} = 0 \Rightarrow (\mathbf{C} + \mathbf{C}^T)\mathbf{x} = \mathbf{0}$.

- P-matrix:
  $\mathbf{C}$ is a P-matrix, denoted by $[\mathbb{P}]$, if *all* its principal minors, including leading and non-leading ones, are positive.

- H-matrix:
  - $\mathbf{C}$ is called a H-matrix, denoted by $[\mathbb{H}]$, if $\overline{\mathbf{C}} \in [\mathbb{P}]$.

- Z-matrix:
  - $\mathbf{C}$ is a Z-matrix, denoted by $[\mathbb{Z}]$, if all its off-diagonal entries are non-positive.

- M-matrix:
  - The intersection set of $[\mathbb{Z}]$ and $[\mathbb{P}]$ is called M-matrix set or K-matrix set, denoted by $[\mathbb{M}]$ or $[\mathbb{K}]$.

- If all the entries of the inverse of a matrix are all non-negative, say $\mathbf{C}^{-1} \geqq \mathbf{0}$, then $\mathbf{C} \in [\mathbb{M}]$.

- R-matrix:
  - Given a non-negative vector $\mathbf{d} \in \mathbb{R}^n_+$ but $\mathbf{d} \neq \mathbf{0}.$, we say $\mathbf{C}$ is $\mathbf{d}$-regular if for all $\tau \geq 0$, $\mathrm{SOL}(\mathbf{C}, \tau\mathbf{d}) = \{\mathbf{0}\}$.
  - $\mathbf{C}$ is called regular, denoted by $[\mathbb{R}]$, if $\mathbf{C}$ is $\mathbf{d}$-regular for some $\mathbf{d} > 0$ (component-wise).
  - $\mathbf{C}$ is called pseudo-regular, denoted by $[\mathbb{R}_0]$, if $\mathrm{SOL}(\mathbf{C}, \mathbf{0}) = \{\mathbf{0}\}$.

- Interval matrix:
  - The set

$$[\mathbb{I}] := \{\mathbf{C} \in \mathbb{R}^{n\times n} : \mathbf{C}_l \leqq \mathbf{C} \leqq \mathbf{C}_u \quad \text{for some } \mathbf{C}_l, \mathbf{C}_u \in \mathbb{R}^{n\times n}\}$$

    is called an *interval matrix* where the inequalities are component-wise.
  - We define

$$\mathbf{C}_p := \frac{\mathbf{C}_u + \mathbf{C}_l}{2}\,,\ \mathbf{C}_m := \frac{\mathbf{C}_u - \mathbf{C}_l}{2}.$$

    Obviously,

$$[\mathbb{I}] = [\mathbf{C}_p - \mathbf{C}_m, \mathbf{C}_p + \mathbf{C}_m].$$

  - $[\mathbb{I}]$ is called *regular* if all $\mathbf{C} \in [\mathbb{I}]$ are regular; moreover, $[\mathbb{I}]$ is called *strongly regular* if the interval matrix $\left(\mathbf{C}_P^{-1}[\mathbb{I}]\right)$ is regular.
  - Consider a regular $[\mathbb{I}]$ and any element $\mathbf{y}$ in the set $Y := \{\mathbf{y} \in \mathbb{R}^n : |y_i| = 1\,, \forall i = 1, \ldots, n\}$. We then define a class of matrix

$$M_{\mathbf{y}}([\mathbb{I}]) := (\mathbf{C}_p - D_{\mathbf{y}}\mathbf{C}_m)^{-1}(\mathbf{C}_p + D_{\mathbf{y}}\mathbf{C}_m),$$

    where $D_{\mathbf{y}}$ is the diagonal matrix with main diagonal $\mathbf{y}$.

7.2 Algorithms for Linear Complementarity Problem

As mentioned previously, numerical methods for LCP can be divided into two categories – direct and iterative methods. Direct methods solve the LCP exactly by pivoting or factorizing matrices while iterative methods approximate the solution repeatedly. In what follows, we assume there exists a solution to the problem $\mathrm{LCP}(\mathbf{C}, \mathbf{q})$, i.e. $\mathbf{C} \in [\mathbb{Q}]$, and introduce algorithms of both types to find it.

7.2.1 PSOR Method

Let $\mathbf{C}_{ij}$, $\mathbf{q}_i$ and $\mathbf{z}_i^k$ be the (i,j) component of $\mathbf{C}$ and i component of $\mathbf{q}$ and $\mathbf{z}^k$ respectively. Given arbitrary $\mathbf{z}^0 \in \mathbb{R}^n$, the algorithm of *projected successive over-relaxation (PSOR)* reads

$$\mathbf{z}_i^{k+1} = \max\{0, \mathbf{z}_i^k - w\mathbf{C}_{ii}^{-1}(\sum_{j<i} \mathbf{C}_{ij}\mathbf{z}_j^{k+1} + \sum_{j\geq i} \mathbf{C}_{ij}\mathbf{z}_j^k + \mathbf{q}_i)\} \quad \text{for } k = 1, 2, \ldots.$$

Note that this formula is expressed in terms of components and can not be converted into an *explicit* matrix form between k and $k+1$. Readers are referred to [65], which explains the relations between PSOR method and the classical SOR method.

The PSOR is an iterative method. Its convergence depends on the type of $\mathbf{C}$.

- If $\mathbf{C}$ is *symmetric and positive definite*, such as those coefficient matrices of the d-dimensional diffusion equations simplified from their BSM PDE counterparts, the convergence of PSOR is guaranteed with $w \in (0, 2)$, cf [25].
- If $\mathbf{C} \in [\mathbb{H}]$, the the PSOR is convergent with $w \in (0, \tilde{w})$, cf. [49, p.19], where

  $$1 < \tilde{w} := 2 \min_i \frac{\mathbf{C}_{ii}\mathbf{d}_i}{\sum_j |\mathbf{C}_{ij}|\mathbf{d}_j} \leq 2, \quad \text{and} \quad \mathbf{d} \in \{\mathbf{x} \in \mathbb{R}^n | \, \overline{\mathbf{C}}\mathbf{x} > 0\} \text{ which is not empty.}$$

It is shown that the convergence is at its fastest speed when taking

$$w = w^* := \frac{2}{1 + \sqrt{1 - \rho_G^2}}$$

where ρ_G is the spectral radius of the matrix $G := D^{-1}(\mathbf{C} - D)$and D is the diagonal matrix formed by the diagonal entries of $\mathbf{C}$; moreover, ρ_G can be approximated by, cf. [51, p.114],

$$\rho_G \approx \max_i \frac{1}{\mathbf{C}_{ii}} \sum_{j \neq i} |\mathbf{C}_{ij}|.$$

7.2.2 Modulus method

Provided $w \in (0, +\infty)$ and $(wI + \mathbf{C})$ is nonsingular, the *(extrapolated) Cayley transform* of a matrix $\mathbf{C}$ is defined as

$$\mathcal{C}_w(\mathbf{C}) := (wI + \mathbf{C})^{-1}(wI - \mathbf{C}).$$

With the Cayley transform, solving the LCP$(\mathbf{C}, \mathbf{q})$ is equivalent to solving the following *fixed point problem (FPP)*, cf. [70, Thm.9.1] and [28, Thm3.1],

$$\mathbf{x} = f(\mathbf{x}) := \mathcal{C}_w(\mathbf{C})|\mathbf{x}| - (wI + \mathbf{C})^{-1}\mathbf{q}$$

If $\mathbf{x}^*$ is a solution of the FPP, then

$$\mathbf{w}^* := w\left(|\mathbf{x}^*| - \mathbf{x}^*\right) \quad \text{and} \quad \mathbf{z}^* := |\mathbf{x}^*| + \mathbf{x}^*$$

is a solution to the LCP.

With the equivalence, the modulus method approximates the solution $\mathbf{x}^*$ using

$$\mathbf{x}^{k+1} := f(\mathbf{x}^k) \quad \text{for all } \mathbf{x}^0 \in \mathbb{R}^n.$$

The convergence is guaranteed if one of the following conditions is satisfied, cf. [70, 82, 28].

- $w = 1$ and $\mathbf{C} \in [\mathbb{H}_+]$
- $w = 1$ and $\mathbf{C} \in M_{\mathbf{y}}([\mathbb{I}])$
- $w \in (0, +\infty)$ and $\mathbf{C}$ is symmetric positive-definite

Furthermore, [28, Prop 3.1] proves that the optimal choice in the symmetric positive-definite case is

$$w^* := \sqrt{\lambda_{\min}\lambda_{\max}},$$

where $\lambda_{\min}$ and $\lambda_{\max}$ are the minimum and maximum eigenvalues of $\mathbf{C}$. The optimal choice minimizes the contraction factor of the spectral radius of $\mathcal{C}_w(\mathbf{C})$ and makes the convergence faster.

[4, 110] consider the variants of the modulus methods by splitting $\mathbf{C} = \mathbf{M} - \mathbf{N}$.

7.2.3 Lemke's method

Problem 7.3 Almost complementarity problem
An almost complementarity problem is formed by augmenting a LCP$(\mathbf{C}, \mathbf{q})$ *with an artificial variable* $z_0 \in \mathbb{R}_+$ *and a covering vector* $\mathbf{e} \in \mathbb{R}^n_+$. *An almost complementarity problem, denoted by ACP*$(\mathbf{C}, \mathbf{q}; \mathbf{e})$*, states:*
Given $\mathbf{e} \in \mathbb{R}^n_+$*, find the* $(\mathbf{w}, \mathbf{z}, z_0) \in \mathbb{R}^n_+ \times \mathbb{R}^n_+ \times \mathbb{R}_+$ *such that*

$$\begin{aligned} \mathbf{w} &= z_0\mathbf{e} + \mathbf{C}\mathbf{z} + \mathbf{q} \\ \mathbf{w}^T\mathbf{z} &= 0 \end{aligned}$$

We notice that the solution to ACP$(\mathbf{C}, \mathbf{q}; \mathbf{e})$ coincides with the that of LCP$(\mathbf{C}, \mathbf{q})$ when $z_0 = 0$. The ACP$(\mathbf{C}, \mathbf{q}; \mathbf{e})$ can be expressed in the following canonical tableau with independent (or nonbasic) variables on the top and dependent (or basic) variables on the left.

	z_0	z_1	$\dots$	z_n	1
w_1	e_1	$\mathbf{C}_{11}$	$\dots$	$\mathbf{C}_{1n}$	q_1
$\vdots$	$\vdots$	$\vdots$	$\ddots$	$\vdots$	$\vdots$
w_n	e_n	$\mathbf{C}_{mn}$	$\dots$	$\mathbf{C}_{mn}$	q_n

The above idea is used in the Lemke's method, which was first introduced in [62]. There are some variants designed after its introduction. Below is a simplified version, called (streamlined) Lemke method, cf.[24, p.271] and [105].

Step 0

Trivial case:

If $\mathbf{q} \geqq \mathbf{0}$, then $(\mathbf{z}^*, \mathbf{w}^*) = (\mathbf{0}, \mathbf{q})$ is a solution to the LCP$(\mathbf{C}, \mathbf{q})$.

Non-trivial case:

If $\mathbf{q}^0 := \mathbf{q} \ngeqq \mathbf{0}$, then consider the canonical tableau of ACP$(\mathbf{C}, \mathbf{q}; \mathbf{D})$ and do the following.

1. Driving items:
   (a) Define the driving index $d^0 = 0$.
   (b) Denote the driving variable at the initial step by v^0 and let it equal to the artificial variable, i.e. $v^0 := z_{d^0} = z_0$.
   (c) Denote the driving column which is the column beneath the driving variable by $\mathbf{D}^0$.[3]
2. Blocking items:
   (a) We choose some row number b^0 as the blocking index such that[4]

$$\frac{-q_{b^0}}{D^0_{b^0}} \equiv \max_j \left\{ \frac{-q_j}{D^0_j} : q_j < 0 \right\} = -\min_j \left\{ \frac{q_j}{D^0_j} : q_j < 0 \right\}.$$

   (b) Denote by c^0 the blocking variable at the initial step. Let $c^0 = w_{b^0}$ be the blocking variable.
3. Pivoting items:
   Pivot driving and blocking variables, rewrite the canonical tableau with new coefficients and denote by $\mathbf{q}^1$ the column beneath independent variable 1.
4. Go to the next step.

Step k (for $k = 1, 2, \ldots$)

Continuation:

1. Driving items:
   (a) Define the driving index $d^k = b^{k-1}$.
   (b) Set $v^k = z_{d^k}$ as the new driving variable if its complement variable is the previous blocking variable; otherwise, set $v^k = w_{d^k}$ as the new driving variable.

[3]The driving column at the initial step is provided by users and also referred to "covering vector".

[4]This is the minimum ratio test at the initial step. And it amounts to choosing the row with the *most* negative q_j provided $D^0_j = 1$.

(c) Denote the new driving column by $\mathbf{D}^k$ which is the column beneath the new driving variable v^k.

2. Blocking items:
   (a) We choose some row number b^k as the blocking index such that[5]

$$\frac{-q^k_{b^k}}{D^k_{b^k}} \equiv -\max_j \left\{ \frac{q^k_j}{D^k_j} : D^k_j < 0 \right\} = \min_j \left\{ \frac{-q^k_j}{D^k_j} : D^k_j < 0 \right\}.$$

   This is the so-called *minimum ratio test* at the step k.[6]
   (b) Let the blocking variable be the variable in row b^k among all dependent variables, which is either w_{b^k} or z_{b^k} and denote it by c^k.
3. Pivoting items:
   We pivot the driving and blocking variables at step k and then rewrite the canonical tableau with new coefficients and let the column beneath the independent variable 1 be $\mathbf{q}^{k+1}$.

Solution found or next step:

1. If the new independent variable is z_0, then the solution $\mathbf{z}^*$ is found where

$$z^*_i := \begin{cases} q^{k+1}_i & \text{if } z_i \text{ is one of the dependent variables.} \\ 0 & \text{o.w.} \end{cases}$$

2. If the new independent variable is not z_0, then go to next step $k+1$.

Theorem 7.4 (Convergence of Lemke method, cf. [105, Thm.2.1])
If ACP$(\mathbf{C}, \mathbf{q}; \mathbf{e})$ *has non-degenerate solution, i.e. all the solutions of dependent/basis variables are strictly positive and* $\mathbf{C}$ *is co-positive plus, then Lemke method is stopped after finitely many steps with either no solution or exact solution.*

According to the theorem, Lemke's method is a direct algorithm for LCP problems, which can actually produce an exact solution (if any) when given a proper covering vector.

7.2.4 Lagrange Multiplier Method

The Lagrange Multiplier Method is a Newton-type iterative algorithm. Provided an initial guess, say $\mathbf{z}^0$, this algorithm provides an approximation at each iteration step by using a *direction vector* and a proper *step length*, denoted by $\mathbf{d}^k$ and t^k respectively, cf. [91]. Namely,

$$\mathbf{z}^{k+1} = \mathbf{z}^k + t^k \mathbf{d}^k.$$

[5] This is the minimum ratio test at the step k.

[6] This amounts to choosing the row with the *least* negative $\frac{q^k_j}{D^k_j}$.

The direction vector and step length at step can be computed with the assistance of the following vector-valued and single-valued functions.

- $\hat{\mathbf{w}} = \hat{\mathbf{w}}(\mathbf{z}) := \mathbf{C}\mathbf{z} + \mathbf{q}$,
- $\hat{\boldsymbol{\lambda}} = \hat{\boldsymbol{\lambda}}(\mathbf{z}) := \mathbb{1}_{\{\mathbf{z} < \hat{\mathbf{w}}(\mathbf{z})\}}$,
- The *Lagrangian of the LCP*$(\mathbf{C}, \mathbf{q})$ is defined by

$$\hat{\mathbf{L}} = \hat{\mathbf{L}}(\mathbf{z}, \boldsymbol{\lambda}) := \boldsymbol{\lambda} \odot \mathbf{z} + (1 - \boldsymbol{\lambda}) \odot \hat{\mathbf{w}}(\mathbf{z}),$$

- $\hat{\mathbf{H}} = \hat{\mathbf{H}}(\mathbf{z}) := \min\{\mathbf{z}, \hat{\mathbf{w}}(\mathbf{z})\}$,
- $\hat{\boldsymbol{\Phi}} = \hat{\boldsymbol{\Phi}}(\mathbf{z}, \boldsymbol{\lambda}) := \hat{\mathbf{H}}(\mathbf{z}) - \hat{\mathbf{L}}(\mathbf{z}, \boldsymbol{\lambda})$,
- $\hat{\mathbf{M}} = \hat{\mathbf{M}}(\mathbf{z}, \boldsymbol{\lambda}) := (\hat{\boldsymbol{\lambda}}(\mathbf{z}) - \boldsymbol{\lambda}) \odot \mathbb{1}_{\{\mathbf{z} \neq \hat{\mathbf{w}}(\mathbf{z})\}}$,
- The *merit function* of the Newton-type algorithm is defined by

$$\hat{\theta} = \hat{\theta}(\mathbf{z}, \boldsymbol{\lambda}) := \frac{1}{2}\left(||\hat{\mathbf{L}}(\mathbf{z}, \boldsymbol{\lambda})||^2 + ||\hat{\boldsymbol{\Phi}}(\mathbf{z}, \boldsymbol{\lambda})||^2\right),$$

- $\tilde{\boldsymbol{\lambda}} = \tilde{\boldsymbol{\lambda}}(\mathbf{z}) := \left(\left(\hat{\mathbf{H}}(\mathbf{z}) - 2\hat{\mathbf{w}}(\mathbf{z})\right) \oslash 2\left(\mathbf{z} - \hat{\mathbf{w}}(\mathbf{z})\right)\right) \odot \mathbb{1}_{\{\mathbf{z} \neq \hat{\mathbf{w}}(\mathbf{z})\}}$,
- $$\begin{aligned} \bar{\boldsymbol{\lambda}} = \bar{\boldsymbol{\lambda}}(\mathbf{z}, \boldsymbol{\lambda}) := \quad & \min\left\{1,\ \tilde{\boldsymbol{\lambda}}(\mathbf{z}) + |\tilde{\boldsymbol{\lambda}}(\mathbf{z}) - \boldsymbol{\lambda}|\right\} \odot \mathbb{1}_{\{\mathbf{z} < \hat{\mathbf{w}}(\mathbf{z})\}} \\ + \quad & \max\left\{0,\ \tilde{\boldsymbol{\lambda}}(\mathbf{z}) - |\tilde{\boldsymbol{\lambda}}(\mathbf{z}) - \boldsymbol{\lambda}|\right\} \odot \mathbb{1}_{\{\mathbf{z} > \hat{\mathbf{w}}(\mathbf{z})\}} \\ + \quad & \boldsymbol{\lambda} \odot \mathbb{1}_{\{\mathbf{z} = \hat{\mathbf{w}}(\mathbf{z})\}}, \end{aligned}$$
- $$\hat{\boldsymbol{\tau}} = \hat{\boldsymbol{\tau}}(\mathbf{z}, \boldsymbol{\lambda}) = \boldsymbol{\lambda} + \left(\hat{\boldsymbol{\Phi}}(\mathbf{z}, \boldsymbol{\lambda}) \odot \hat{\mathbf{M}}(\mathbf{z}, \boldsymbol{\lambda}) \oslash \hat{\mathbf{L}}(\mathbf{z}, \boldsymbol{\lambda})\right) \odot \mathbb{1}_{\left\{\hat{\mathbf{L}}(\mathbf{z}, \boldsymbol{\lambda}) \neq \mathbf{0}\right\}},$$

where the $\mathbb{1}_{\{\cdot\}}$, min and $\odot$ and $\oslash$ are *componentwise* indicator function, minimum function, multiplication and division individually.

Provided $(\mathbf{z}^0, \boldsymbol{\lambda}^0) \in \mathbb{R} \times [0,1]^n$, constant parameters $\sigma \in (0, 2/3), \rho \in (\sigma, 1 - 0.5\sigma)$ and the information from iteration k, the Lagrangian Multiplier method proceeds with the following computation until certain criteria is met during iterations.

1. Modification of $\boldsymbol{\lambda}^{k+1} = \bar{\boldsymbol{\lambda}}\left(\mathbf{z}^k, \boldsymbol{\lambda}^k\right)$

2. Direction vector $\mathbf{d}^{k+1}$:

   (a) $\hat{\boldsymbol{\tau}}^k = \hat{\boldsymbol{\tau}}\left(\mathbf{z}^k,\, \boldsymbol{\lambda}^{k+1}\right)$

   (b) $\mathbf{D}_{\hat{\boldsymbol{\tau}}^k} := \operatorname{diag}(\hat{\boldsymbol{\tau}}_1^k, \cdots, \hat{\boldsymbol{\tau}}_n^k)$ is a diagonal matrix with $\hat{\boldsymbol{\tau}}^k$ as its main diagonal

   (c) $\mathbf{d}^{k+1}$ is the solution to following system

$$\left(\mathbf{D}_{\hat{\boldsymbol{\tau}}^k} \,+\, (I - \mathbf{D}_{\hat{\boldsymbol{\tau}}^k})\mathbf{C}\right)\mathbf{d}^{k+1} \,=\, -\hat{\mathbf{H}}\left(\mathbf{z}^k\right),$$

   which can be solved exactly or numerically (even with a pre-conditioner).

3. Step length is chosen by $t^k := \rho^{p_k}$ where

$$p_k := \min_p \left\{ p \in \mathbb{N} \cup \{0\} : \hat{\theta}\left(\mathbf{z}^k + \rho^p \mathbf{d}^k,\, \boldsymbol{\lambda}^{k+1}\right) \leq (1 - \sigma\rho^p) \cdot \hat{\theta}\left(\mathbf{z}^k,\, \boldsymbol{\lambda}^{k+1}\right) \right\}$$

4. Update the approximate solution by $\mathbf{z}^{k+1} = \mathbf{z}^k + t^k \mathbf{d}^k$.

It is proved that *if* $\mathbf{C} \in [\mathbb{P}]$*, then this algorithm converges linearly.* In addition, if the solution is *degenerate* (not non-degenerate), then it converges in finitely many steps.

7.2.5 Active Set of Linear Complementarity Problem

Suppose $\mathbf{z}^*$ is the solution to the problem LCP$(\mathbf{C}, \mathbf{q})$. It is notable that the LCP$(\mathbf{C}, \mathbf{q})$ can be equivalently expressed as

$$\min\left\{\mathbf{z}^*,\ \mathbf{w}^* := \mathbf{C}\mathbf{z}^* + \mathbf{q}\right\} = \mathbf{0}.$$

As a result, there exists an *active set/indices* $\alpha \subset [n]$ and an *inactive set/indices* $\bar{\alpha} = [n]/\alpha$ such that

$$\begin{aligned} \mathbf{0} &:= \mathbf{z}_\alpha^*, \\ \mathbf{0} &:= \mathbf{w}_{\bar{\alpha}}^*. \end{aligned}$$

7.2.6 Howard's Method

Howard's method, also known as *policy iteration*, is an *active-set-based* iterative algorithm, which is equivalent to the *Primal-dual active set* algorithm developed in [48], cf. [9, Thm 4.7]. It finds an approximate solution $\mathbf{z}^{k+1}$ in the following two steps at each iteration when provided an initial guess and information of $\mathbf{z}^k$, cf, [9, 35, 77].

1. We define $\hat{\mathbf{w}}^k := \hat{\mathbf{w}}\left(\mathbf{z}^k\right) := \mathbf{C}\mathbf{z}^k + \mathbf{q}$ and the *proxy active sets* below.

$$\begin{aligned} \alpha &:= \{i :\ \mathbf{z}_i^k < \hat{\mathbf{w}}_i^k\} \\ \bar{\alpha} &:= \{j :\ \hat{\mathbf{w}}_j^k \leq \mathbf{z}_j^k\} \end{aligned}$$

2. Substitute $\mathbf{z}_{\alpha}^{k+1} = \mathbf{0}$ and solve the following reduced *proxy system*

$$\mathbf{C}_{\bar{\alpha}\bar{\alpha}}\mathbf{z}_{\bar{\alpha}}^{k+1} + \mathbf{q}_{\bar{\alpha}} = \mathbf{0}$$

   Notice that this system can be solved directly or iteratively and, probably, with a pre-conditioner.

If $\exists!\mathbf{C}^{-1} \geqq \mathbf{0}$ (componentwise)[7], it is guaranteed to be *globally super-linearly* convergent by [9, Thm3.4], namely

$$\lim_{k\to\infty} ||\mathbf{z}^{k+1} - \mathbf{z}^*||_p = 0 \text{ and } \lim_{k\to\infty} \frac{||\mathbf{z}^{k+1} - \mathbf{z}^*||}{||\mathbf{z}^k - \mathbf{z}^*||} = 0.$$

Moreover, it converges to the *exact solution* $\mathbf{z}^*$ in at most $n+1$ iterations if $\mathbf{z} \in \mathbb{R}^n$ for arbitrary initial guess $\mathbf{z}^0$, cf. [9, Thm4.3].

7.2.7 Hybrid Method with Active Set

A hybrid method is an *active-set-assisted* iterative method, which speeds up a selected iterative method (the main algorithm) by fine-tuning its values with the assistance of active set. It *replaces* $\mathbf{z}^{k+1}$ *by* $\tilde{\mathbf{z}}^{k+1} := \mathbf{z}^{k+1} + \Delta$ *once every one/several iterations* after initial warm-up iterations, where Δ is an adjuster based on active set.

Given a small nonnegative ϵ, a *proxy active set* α and *its complement* $\bar{\alpha}$ are defined as follows.

$$\begin{aligned} \alpha &:= \{i : |\mathbf{z}_i^{k+1}| \leq \epsilon\}, \\ \bar{\alpha} &:= \{j : |\mathbf{z}_j^{k+1}| > \epsilon\}. \end{aligned}$$

Generally such a method is efficient only if

1. the $\mathbf{z}^{k+1}$ obtained from main iterative algorithm can provide good approximations of active sets;

2. the cost to find Δ is cheap.

The convergence of the hybrid method depends on both the selected LCP algorithm and the class of matrix $\mathbf{C}$.

[57] defines the adjustor Δ as below

- $\Delta_{\alpha} = \mathbf{0}$

[7] In this case, it belongs to $[\mathbb{M}]$

- $\Delta_{\bar{\alpha}}$ is the solution to the following system.

$$\mathbf{C}_{\bar{\alpha}\bar{\alpha}} \left(\Delta^{k+1}\right)_{\bar{\alpha}} + r(\mathbf{q}_{\bar{\alpha}} + \mathbf{C}_{\bar{\alpha}\cdot}\mathbf{z}^{k+1}) = \mathbf{0} \tag{7.1}$$
$$\text{where } \cdot := [n] \text{ and } r \leq 1 \text{ is } \textit{the largest real} \text{ such that } \tilde{\mathbf{z}}^{k+1} \geqq \mathbf{0}$$

[57] chooses *the PSOR* as its iterative algorithm and numerically solves the reduced linear system of equalities (7.1) with *pre-conditioned conjugate gradient method*. If $\mathbf{C}_{\alpha\alpha}$ is *symmetric and positive definite*, then its convergence is guaranteed by [57, Thm.2.1].

7.3 Summary

The author of classical reference *"The Linear Complementarity Problem"* [24] once stated: *..., the convergence of a PSOR method for solving the LCP with an asymmetric positive definite matrix* $\mathbf{C}$ *is not very well understood; at best, the convergence requires highly restrictive conditions. Indeed, it is not common in the LCP community to apply this method for solving such a LCP; instead, alternative methods such as Lemke's method or other recent algorithms can be used*, cf. [49, p.19]. This statement motivates us to seek more methods to benchmark against the PSOR, which is the most popular LCP solver when pricing the options with early-exercise property. As we saw already, the solvability of LCP$(\mathbf{C}, \mathbf{q})$ highly depends on the classes of matrix $\mathbf{C}$. However, at present there is still no efficient way to judge the class of a matrix, even for the broad classes such as Q-matrices and P-matrices, cf. [24, p.146, 149].

Since the class of its coefficient matrix is vital to the solvability of a LCP, the approximate coefficient matrix computed by numerical integration (when discretized by finite element techniques) may disturb the solvability of LCP systems if the class of matrix is sensitive to some certain entry values. However, if we use the exact closed-form formulas derived from previous chapter for the computation of elemental matrices, such problems can certainly be avoided.

We have surveyed several algorithms for solving the LCPs arising from the option pricing problems with early-exercise property. In the next chapter, the numerical experiments will be performed in one, two and three-asset frameworks. We are interested to see whether the solutions are convergent against different options and parameters, how large the errors will be and the computational efficiency of different LCP solvers. We would also benchmark the different LCP algorithms against the PSOR in terms of computational cost and speed.

Chapter 8

Numerical Experiments

In our research, we have built a variety of Matlab programs based on the reformulation, discretization and algorithms introduced previously to price options linked with up to three assets. We are able to price an option of any type of the following combinations.

- Number of assets: one-asset, two-asset or three-asset;
- Exercise restriction: European, American or perpetual;
- Portfolio price: basket, minimum or maximum;
- Payoff type: call, put or straddle.

Notice that in the one-asset case, the basket, minimum and maximum options are actually of the same type. For simplicity, we employ Dirichlet boundary conditions through this chapter.

We recall that the expiry date is denoted by T. For convenience of comparison, we will present the computational results in terms of the time to maturity, i.e. $\tau := T - t$. The option value at $\tau = 0$ is actually its payoff. Notice that the expiry restriction $T > 0$ only applies to European and American options and so their $\tau \in [0, T]$. As to perpetual options, they possess $T = \infty$, or equivalently $\tau = \infty$.

All the experiments presented in this chapter were performed on a Sun X4600 server with 8 dual-core processors (AMD Opteron 8220) running at 2.8GHz (16 cores in total) and 64GB memory.

8.1 Visualization

In this section, we present our computational results visually. For simplicity, we select minimum put, maximum call and basket straddle options for demonstration.

8.1.1 One-asset Examples

We use the following parameters for our one-dimensional options.

- Exercise price: $E = 300$;
- Interest rate: $r = 0.05$;
- (Continuous) dividend rate: $q = 0.02$;
- Expiry date: $T = 1$ (year);
- (Annualized) variance: $\sigma^2 = 0.2^2 = 0.04$.

We partition the spatial and time axes uniformly with the numerical parameters set below.

- The far-field bound: $S_{\max} = 2000$;
- Number of partition points in S-axis: $N_1 + 1 = 201$;
- Number of partition points in t-axis: $N_t + 1 = 21$.

Figures [8.1, 8.2], [8.3, 8.4] and [8.5, 8.6] are the visualization of one-asset put, call and straddle options at $\tau = 0, 0.5, 1$ (w.r.t European and American ones) and ∞ (w.r.t. perpetual ones). We can observe that parts of European option values fall below their payoffs while the values of all American options are greater than or equal to payoffs.

8.1.2 Two-asset Examples

We use the following parameters for our two-dimensional options.

- Exercise price: $E = 300$;
- Interest rate: $r = 0.05$;
- (Continuous) dividend rates: $\mathbf{q} = \begin{pmatrix} 0.02 & 0.03 \end{pmatrix}^T$;
- Expiry date: $T = 1$ (year);
- (Annualized) volatilities: $\sigma_1 = 0.2, \sigma_2 = 0.4$ with correlation coefficient $\rho = 0.5$; namely the (annualized) covariance is

$$\mathbf{\Sigma} = \begin{pmatrix} 0.04 & 0.04 \\ 0.04 & 0.16 \end{pmatrix};$$

- Weights for basket option: $\begin{pmatrix} 0.4 & 0.6 \end{pmatrix}$.

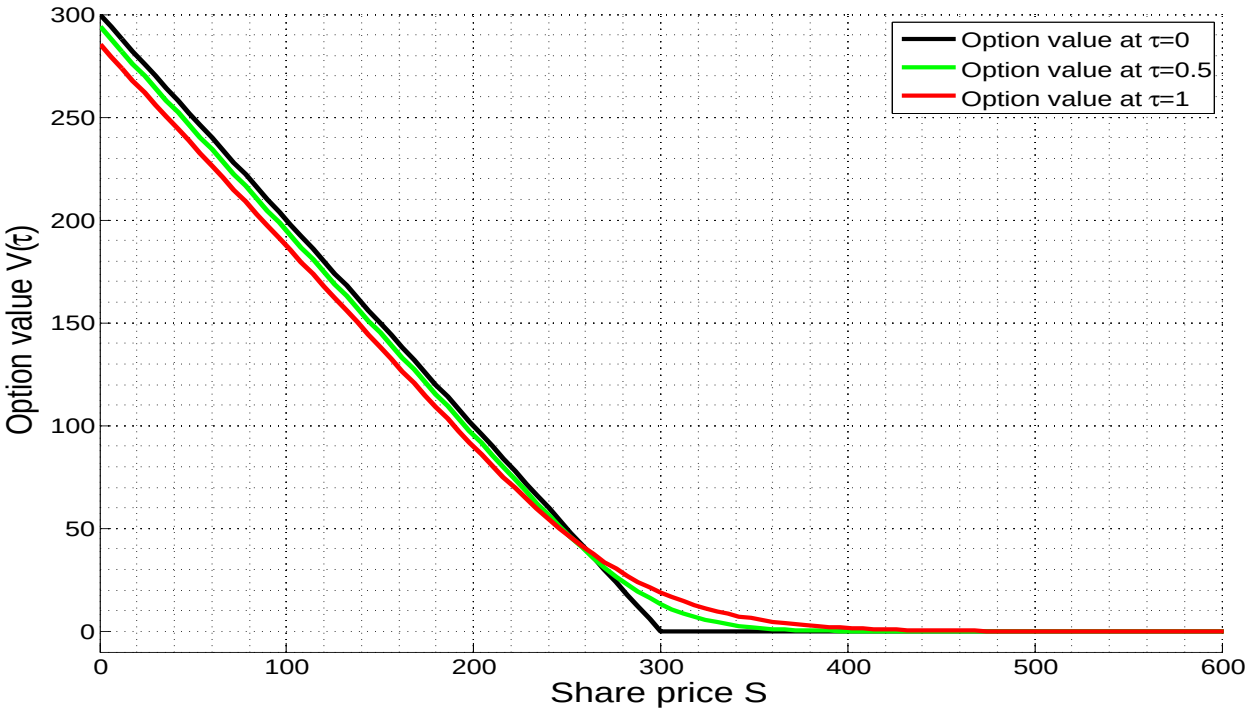

Figure 8.1: One-asset European Put.

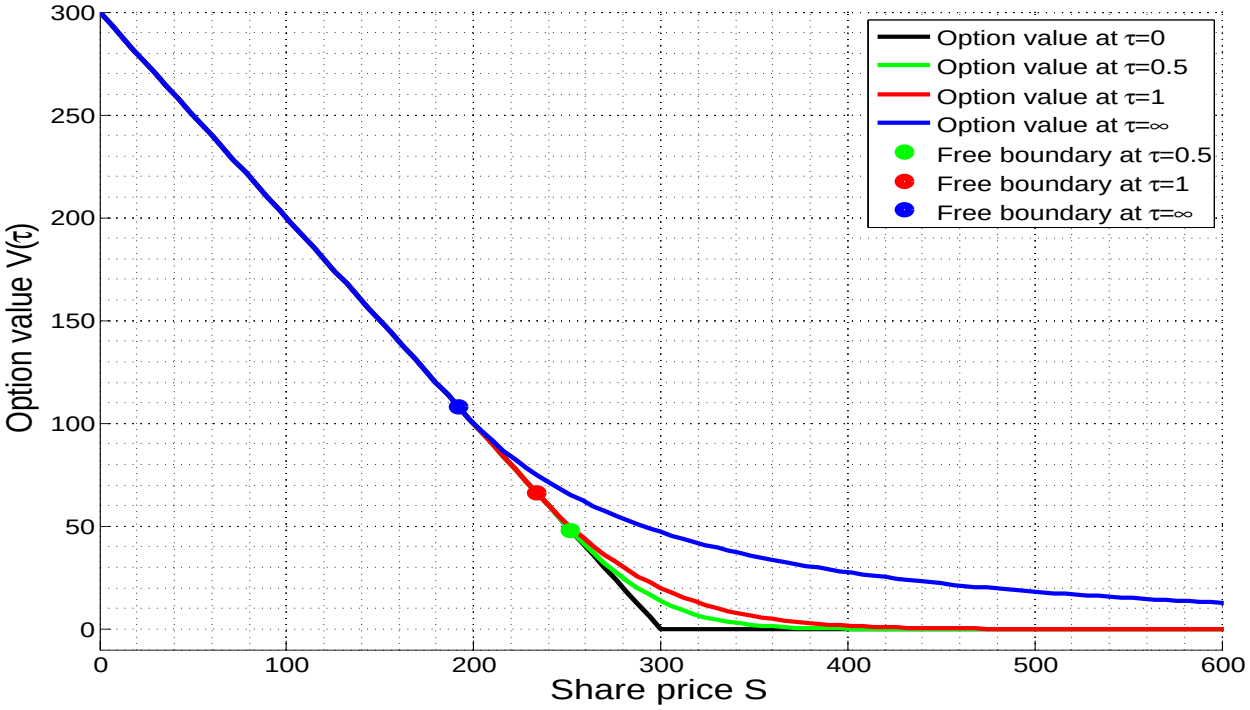

Figure 8.2: One-asset American and Perpetual Puts.

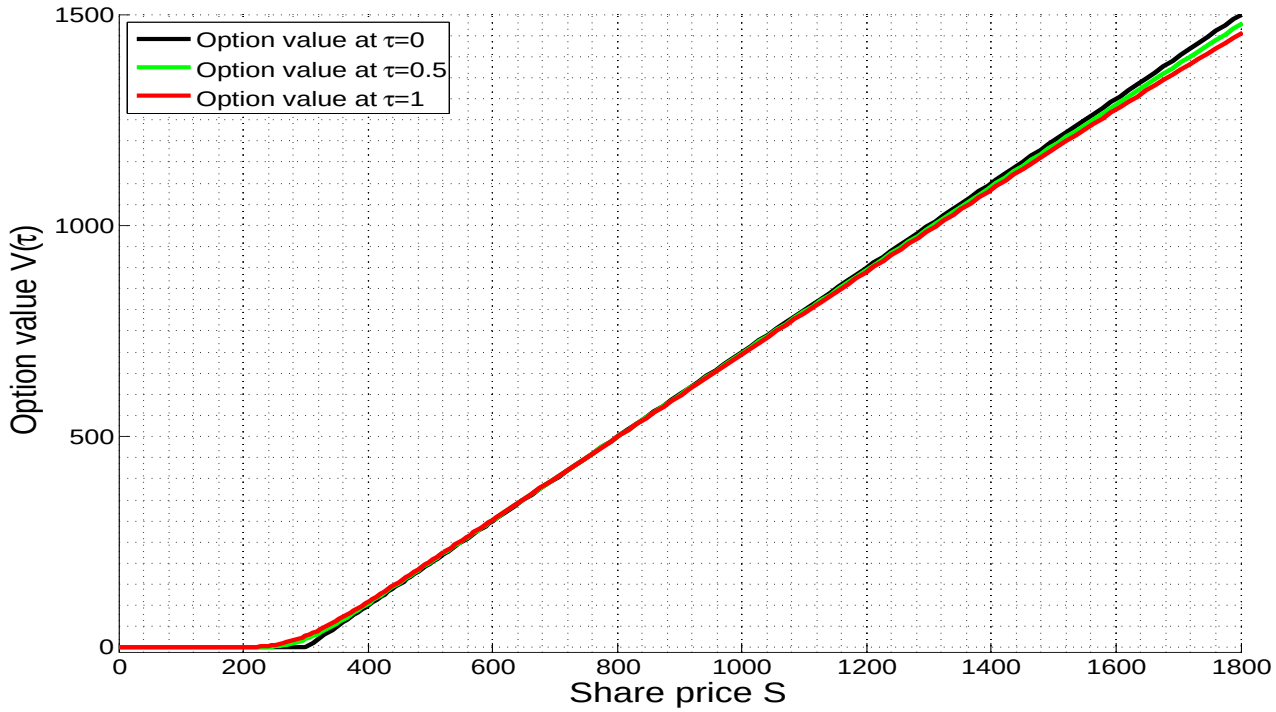

Figure 8.3: One-asset European Call.

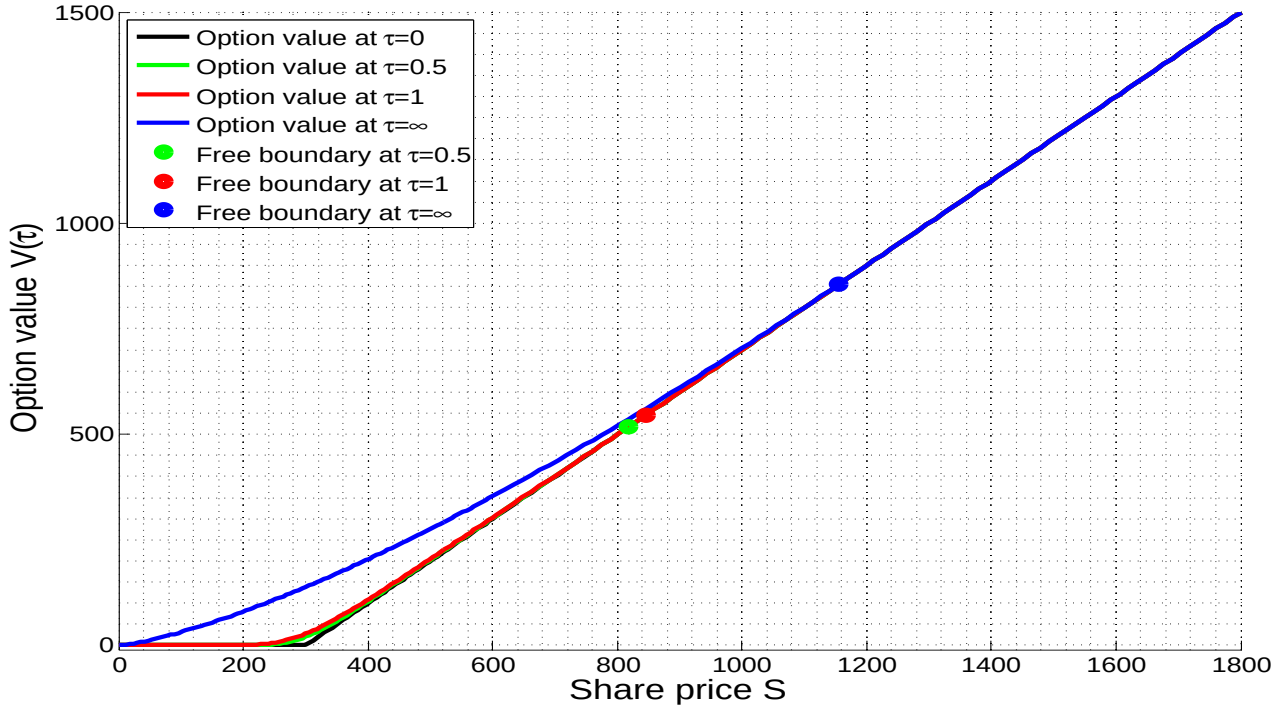

Figure 8.4: One-asset American and Perpetual Calls.

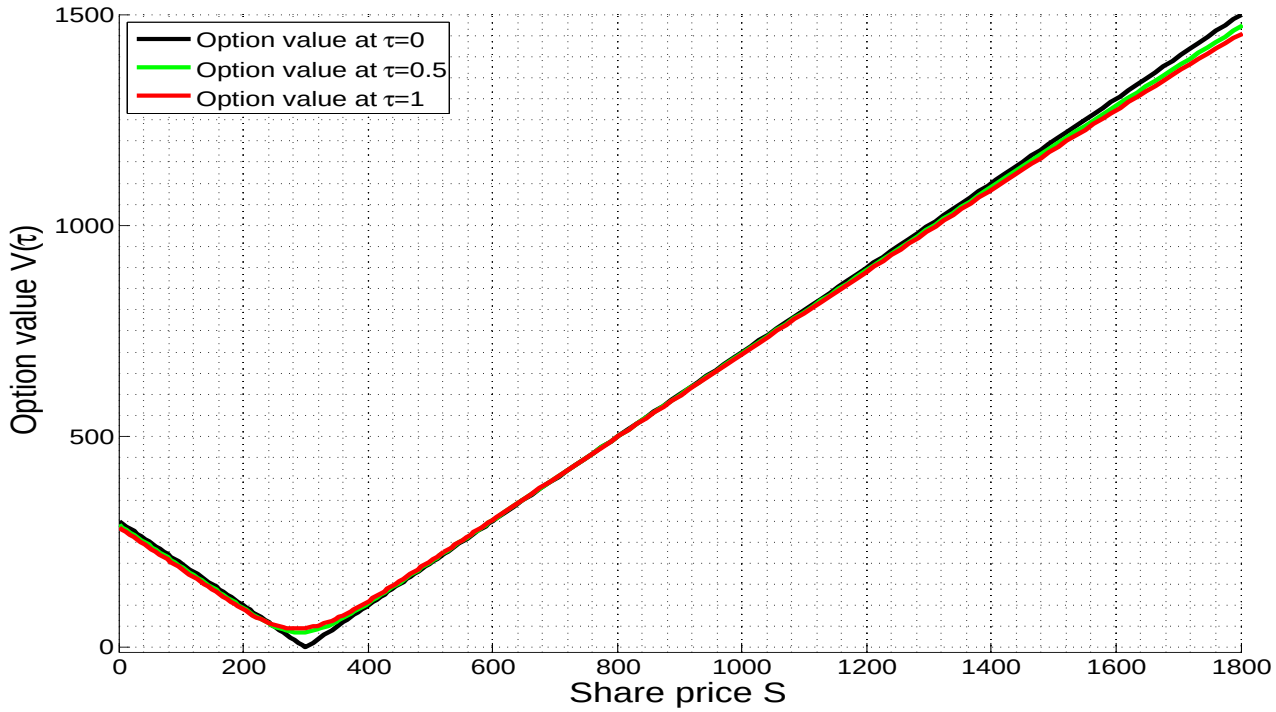

Figure 8.5: One-asset European Straddle.

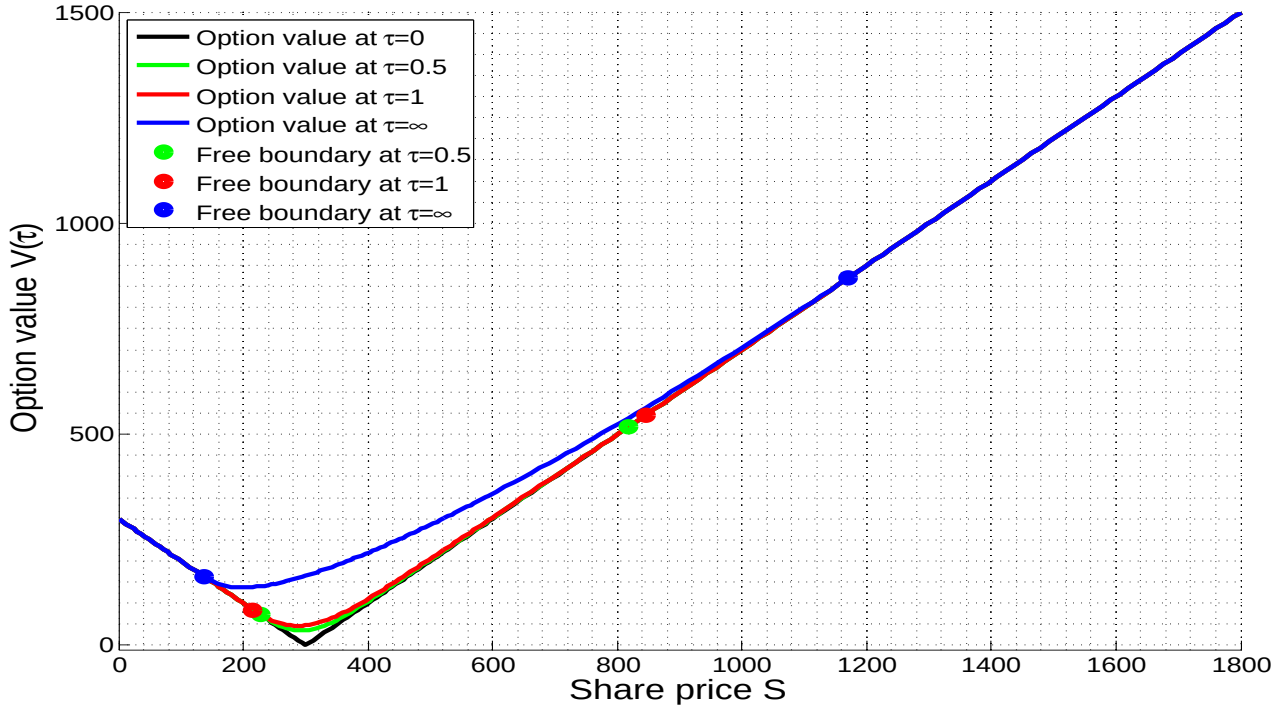

Figure 8.6: One-asset American and Perpetual Straddles.

We partition the spatial and time axes uniformly with the numerical parameters set below.

- The far-field bound: $S_{\max} = 2000$;
- Number of partition points in $S^{(i)}$-axis: $N_i + 1 = 101$ for $i = 1, 2$;
- Number of partition points in t-axis: $N_t + 1 = 21$.

Figures 8.7, 8.8 and 8.9 visualize the option values of two-asset minimum put, maximum call and basket straddle individually. Recall that the values for $\tau = 0$ and $\tau = \infty$ stand for those of payoff and perpetual option respectively. For the options with early-exercise property, we identify their free boundaries and the nodes in the early-exercise region with red and black points respectively.

We provide the cross sections at $S_1 = 300$ to locally compare the European, American and perpetual values in figures 8.10, 8.11 and 8.12. Notice that in terms of payoff values, the kink points are $(S_1 = 200, v = 100)$, $(S_1 = 300, v = 0)$ and $(S_1 = 600, v = 0)$ for minimum put, maximum call and basket straddle individually. Similar to one-asset options, we can find the cross-section values of European options may fall below their payoffs while their American counterparts stay at least equal to payoffs.

8.1.3 Three-asset Examples

We use the following parameters for our three-dimensional options.

- Exercise price: $E = 300$;
- Interest rate: $r = 0.05$;
- (Continuous) dividend rates: $\mathbf{q} = \begin{pmatrix} 0.01 & 0.02 & 0.03 \end{pmatrix}^T$;
- Expiry date: $T = 1$ (year);
- (Annualized) volatilities: $\sigma_1^2 = 0.3, \sigma_2^2 = 0.4, \sigma_3^2 = 0.5$ with correlation coefficient $\rho_{12} = 0.25, \rho_{13} = 0.5, \rho_{23} = 0.75$; namely the (annualized) covariance is

$$\mathbf{\Sigma} = \begin{pmatrix} 0.3000 & 0.0866 & 0.1936 \\ 0.0866 & 0.4000 & 0.3354 \\ 0.1936 & 0.3354 & 0.5000 \end{pmatrix};$$

- Weights for basket option: $\begin{pmatrix} 0.2 & 0.3 & 0.5 \end{pmatrix}$.

We partition the spatial and time axes uniformly with the numerical parameters set below.

- The far-field bound: $S_{\max} = 2000$;

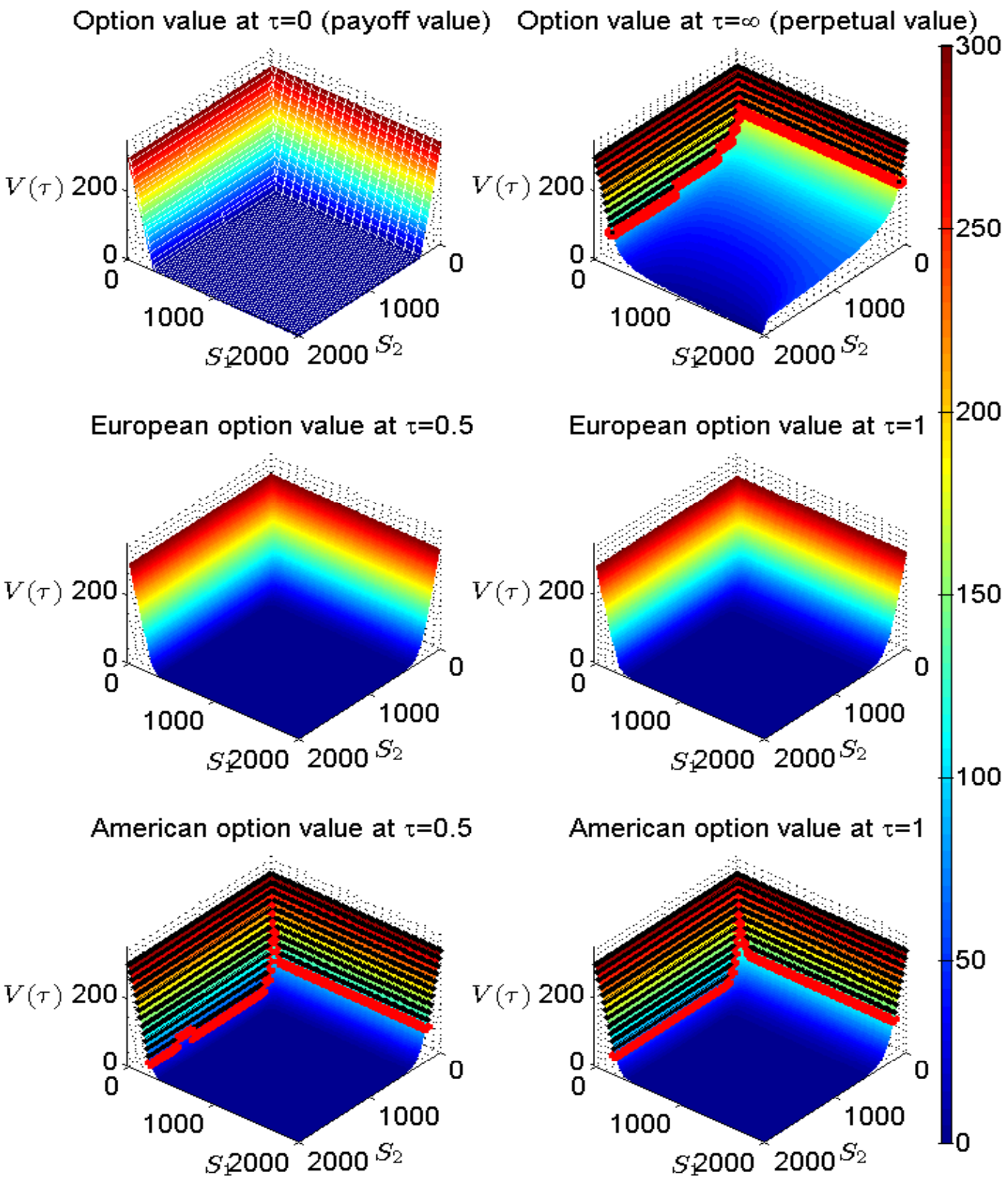

Figure 8.7: Two-asset Minimum Put.

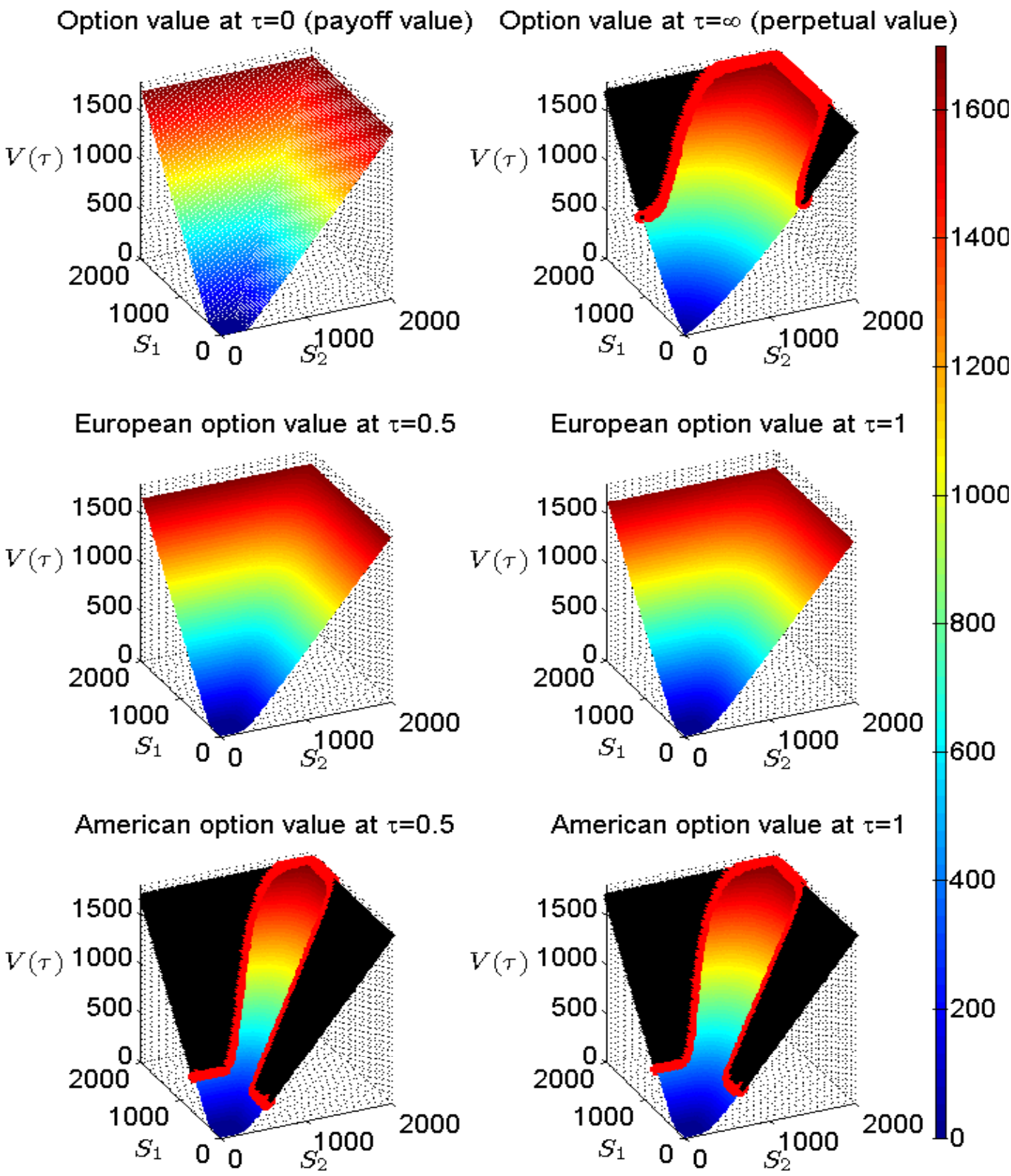

Figure 8.8: Two-asset Maximum Call.

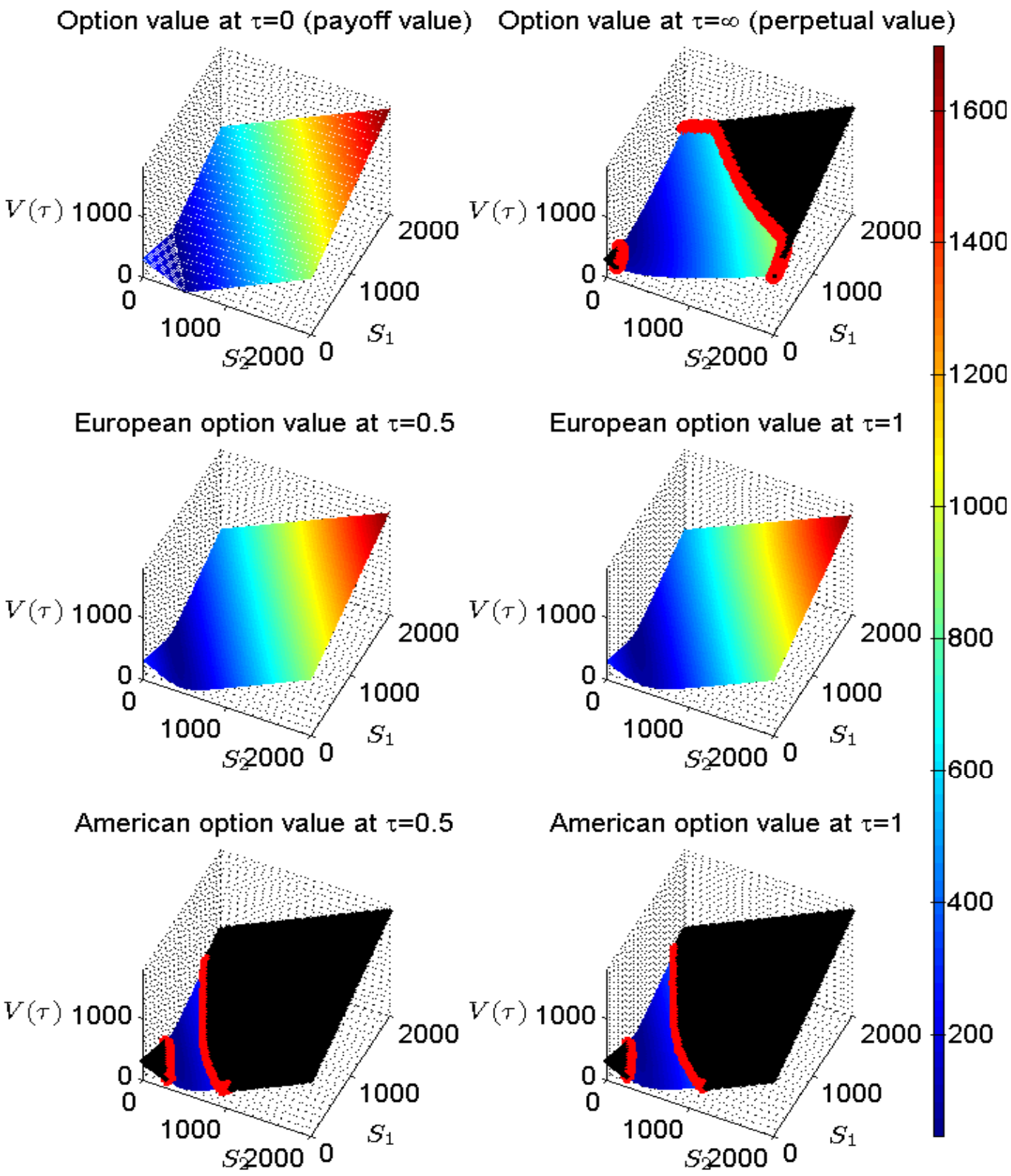

Figure 8.9: Two-asset Basket Straddle.

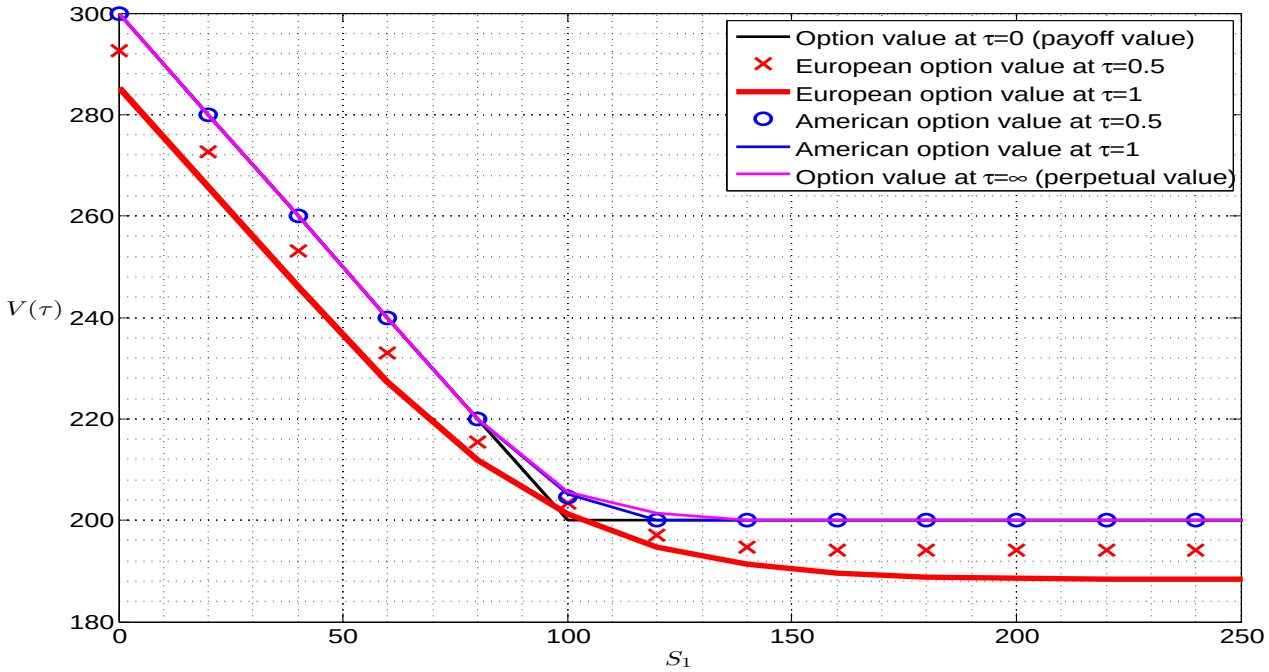

Figure 8.10: Cross Section of Two-asset Minimum Put at $S_2 = 100$.

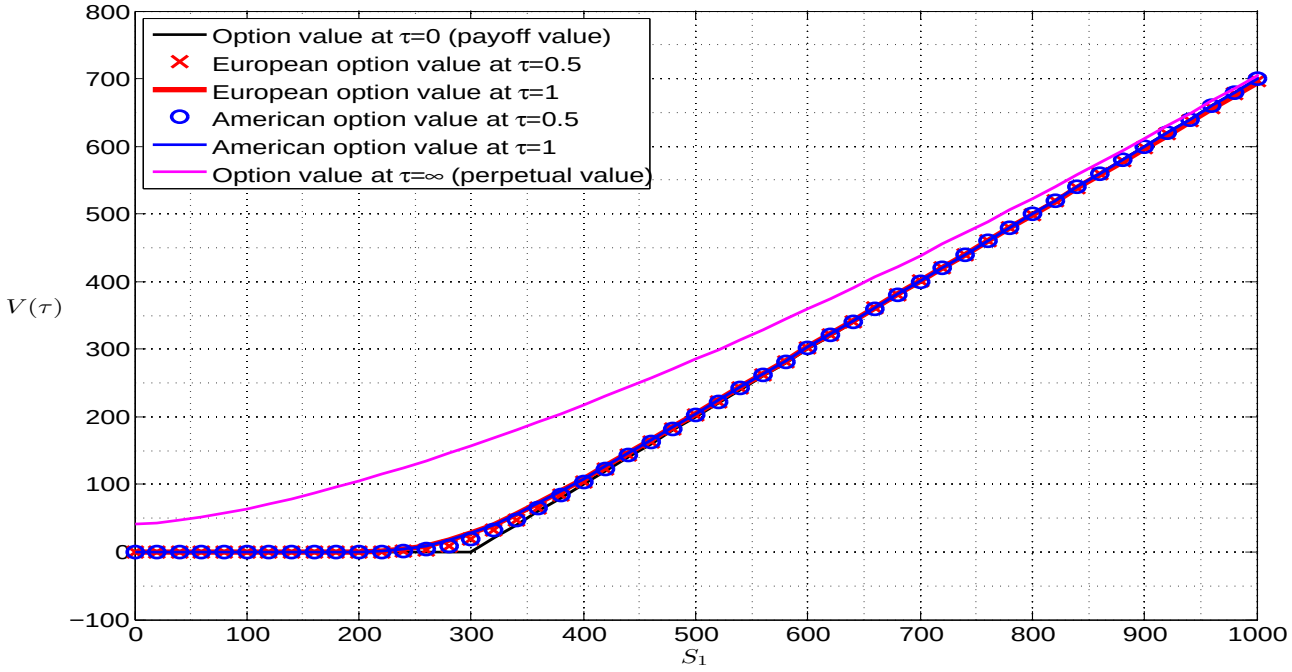

Figure 8.11: Cross Section of Two-asset Max Call at $S_2 = 100$.

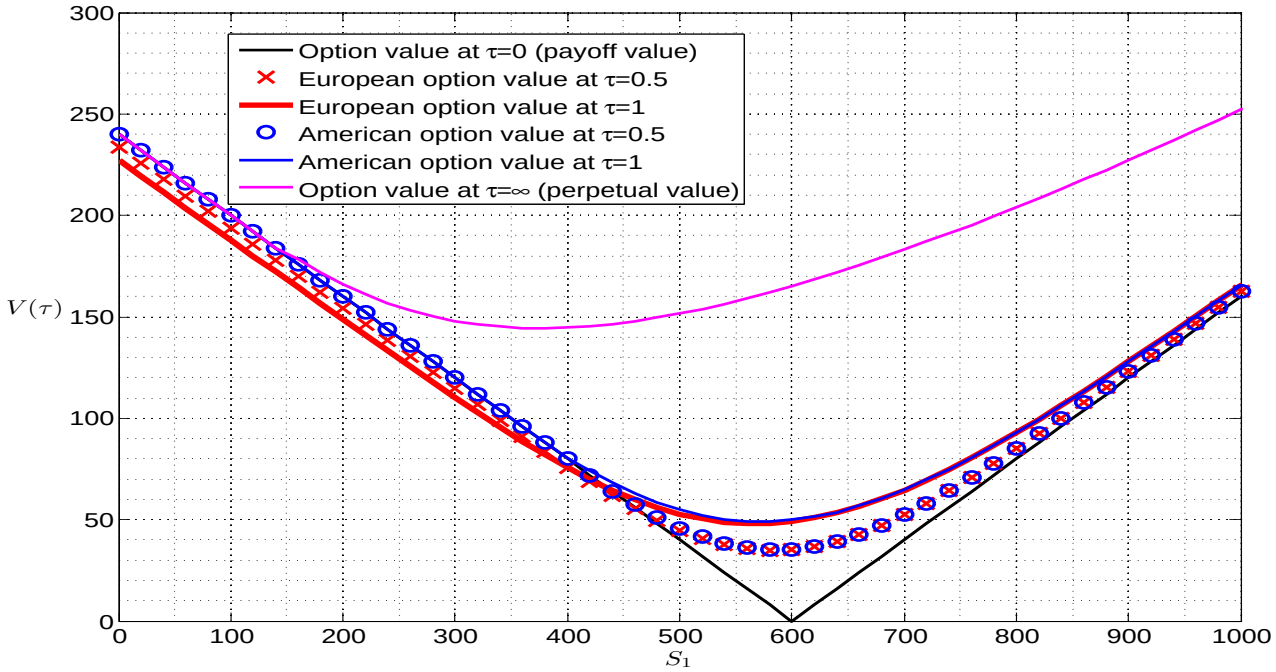

Figure 8.12: Cross Section of Two-asset Basket Straddle at $S_2 = 100$.

- Number of partition points in $S^{(i)}$-axis: $N_i + 1 = 26$ for $i = 1, 2, 3$;
- Number of partition points in t-axis: $N_t + 1 = 21$.

The option values are visualized in terms of different colorful points for three-asset minimum put, maximum call and basket straddle in figures 8.13, 8.15 and 8.17 separately. Following each figure is the free boundaries identified at $\tau = 0.25, 0.5, 1$ for the American type and at ∞ for the perpetual one as shown in figures 8.14, 8.16 and 8.18.

Figures 8.19, 8.20 and 8.21 present the cross sections at $S_1 = 400$ and $S_2 = 320$ for the comparison of local values among European, American and perpetual types. Notice that the kink points of the payoffs in the cross sections are $(S_3 = 300, v = 0)$, $(S_3 = 400, v = 100)$ and $(S_3 = 248, v = 0)$ for minimum put, maximum call and basket straddle individually.

8.1.4 Free Boundary as Manifold

It is interesting to observe the evolution of the free boundaries of American and perpetual options in the above three cases. We notice that in one-dimensional problems, the put and call have their free boundary points located behind and beyond their exercise price (kink-point) respectively. The straddle counterpart has the exercise rights of both call and put and accordingly its free boundary points lie on both sides of its kink point. As the time to maturity (τ) tends to ∞, those free boundary points numerically approach to their perpetual counterparts, namely the numerical steady state of free boundaries. Such phenomenon can also be observed in high-dimensional cross sections.

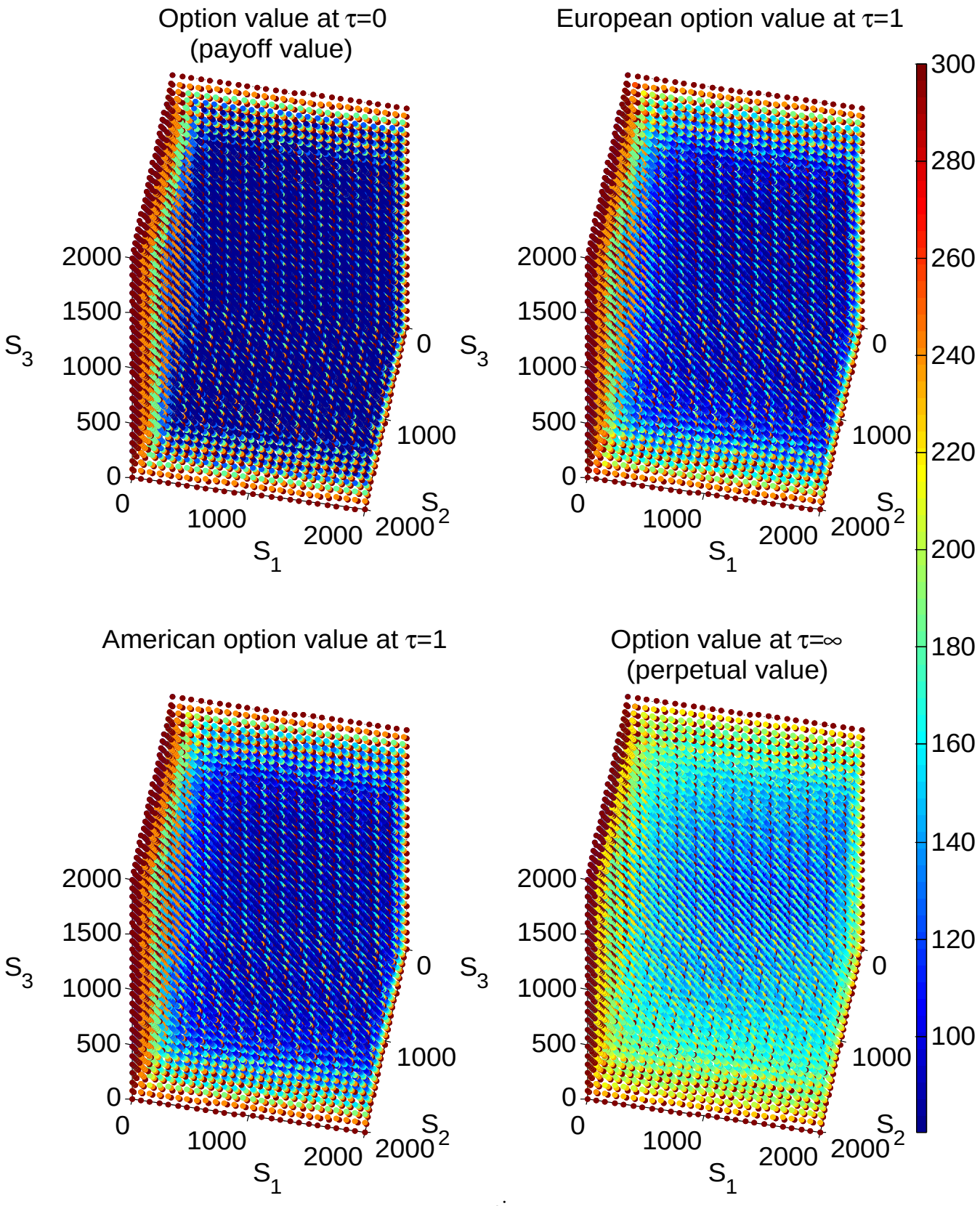

Figure 8.13: Three-asset Minimum Put.

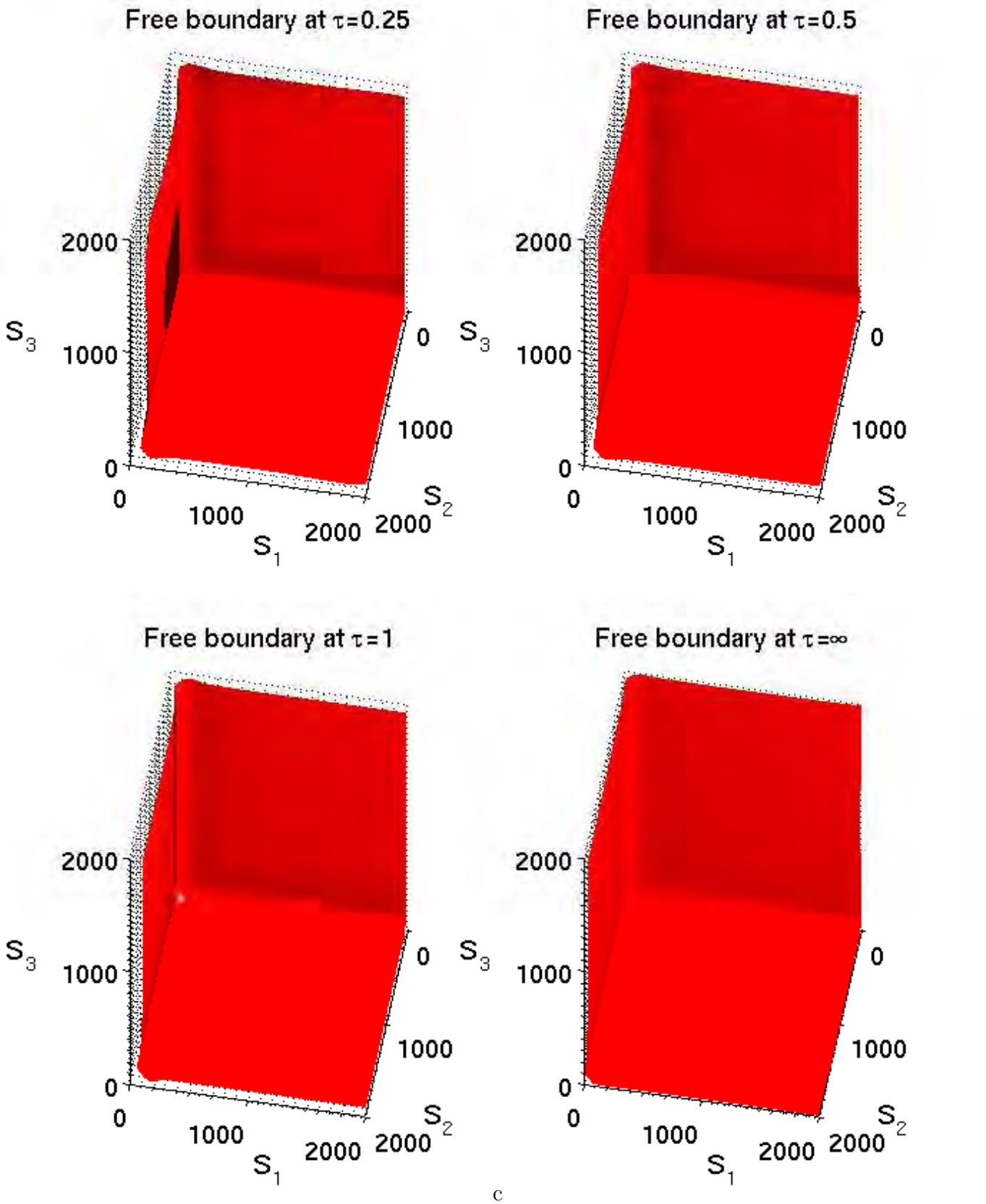

c

Figure 8.14: Free Boundary of Three-asset Minimum Put.

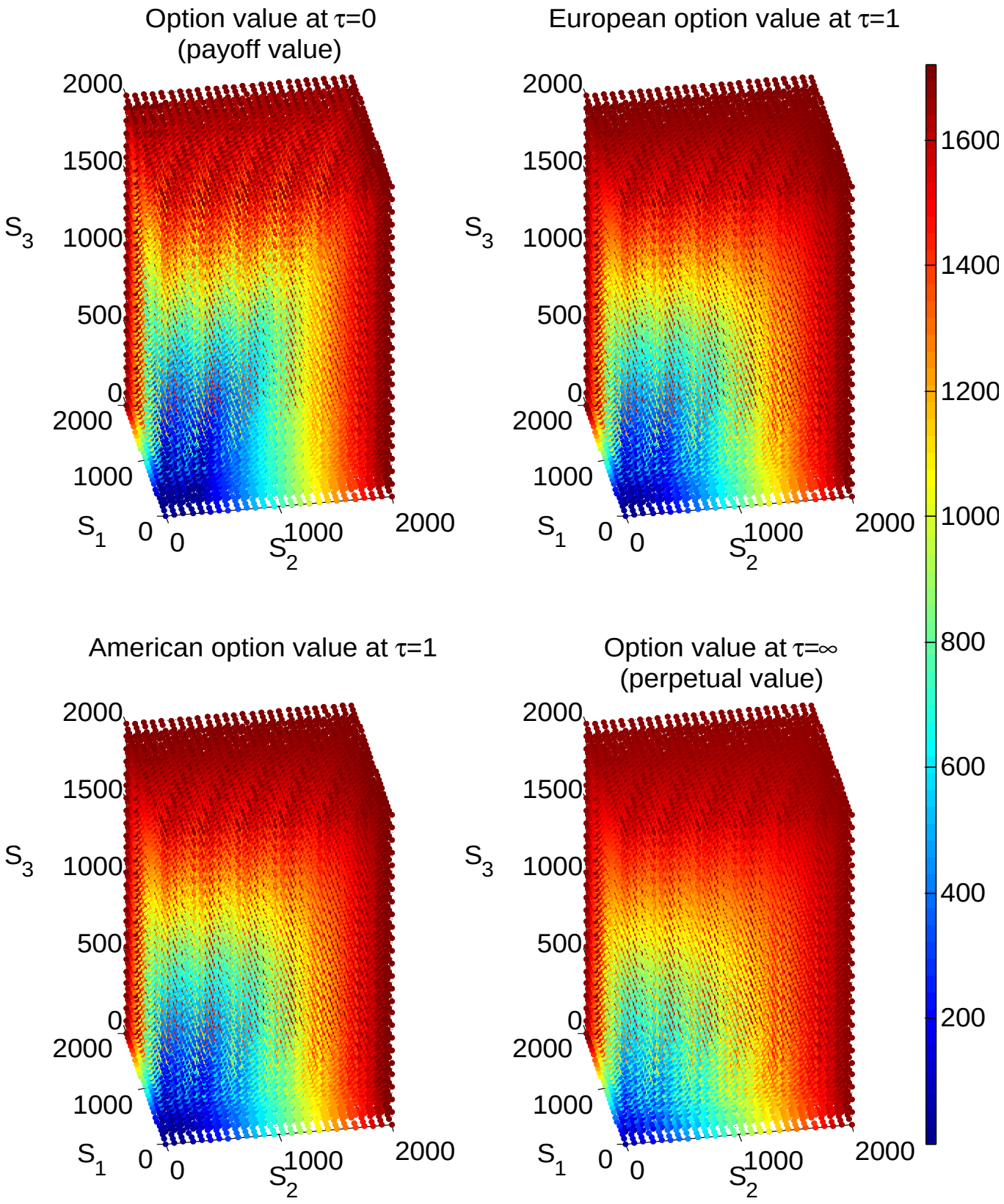

ci

Figure 8.15: Three-asset Maximum Call.

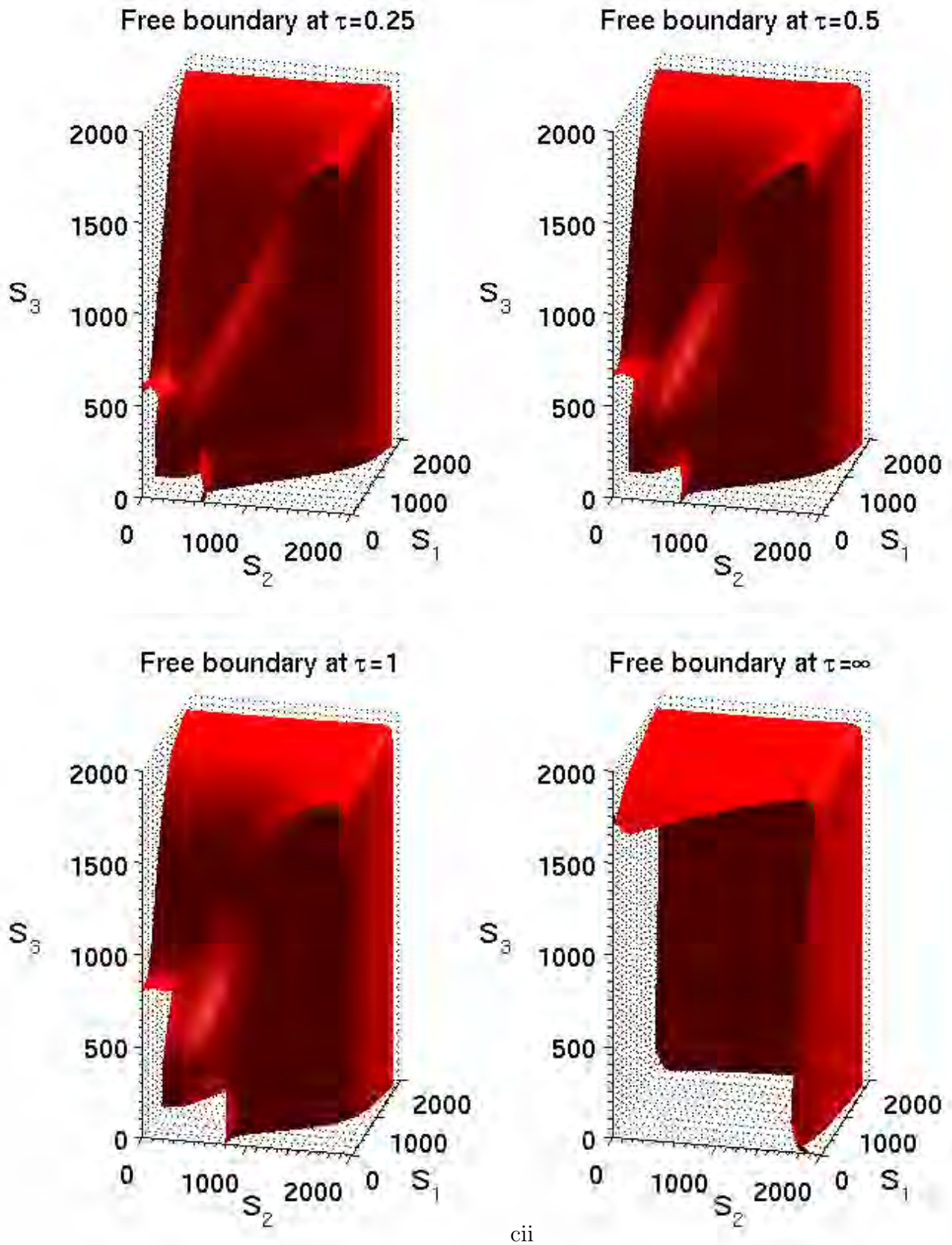

cii

Figure 8.16: Free Boundary of Three-asset Maximum Call.

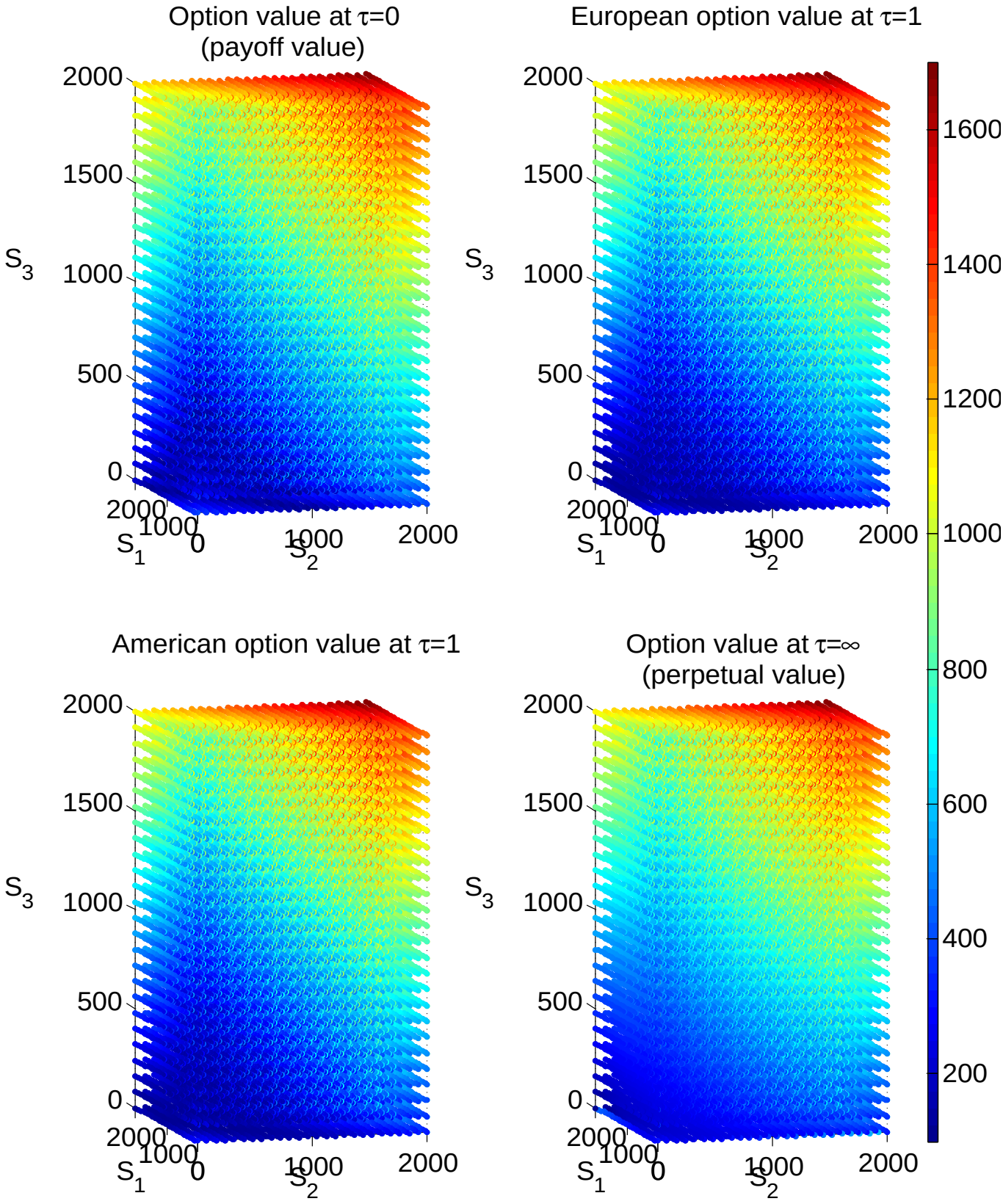

Figure 8.17: Three-asset Basket Straddle.

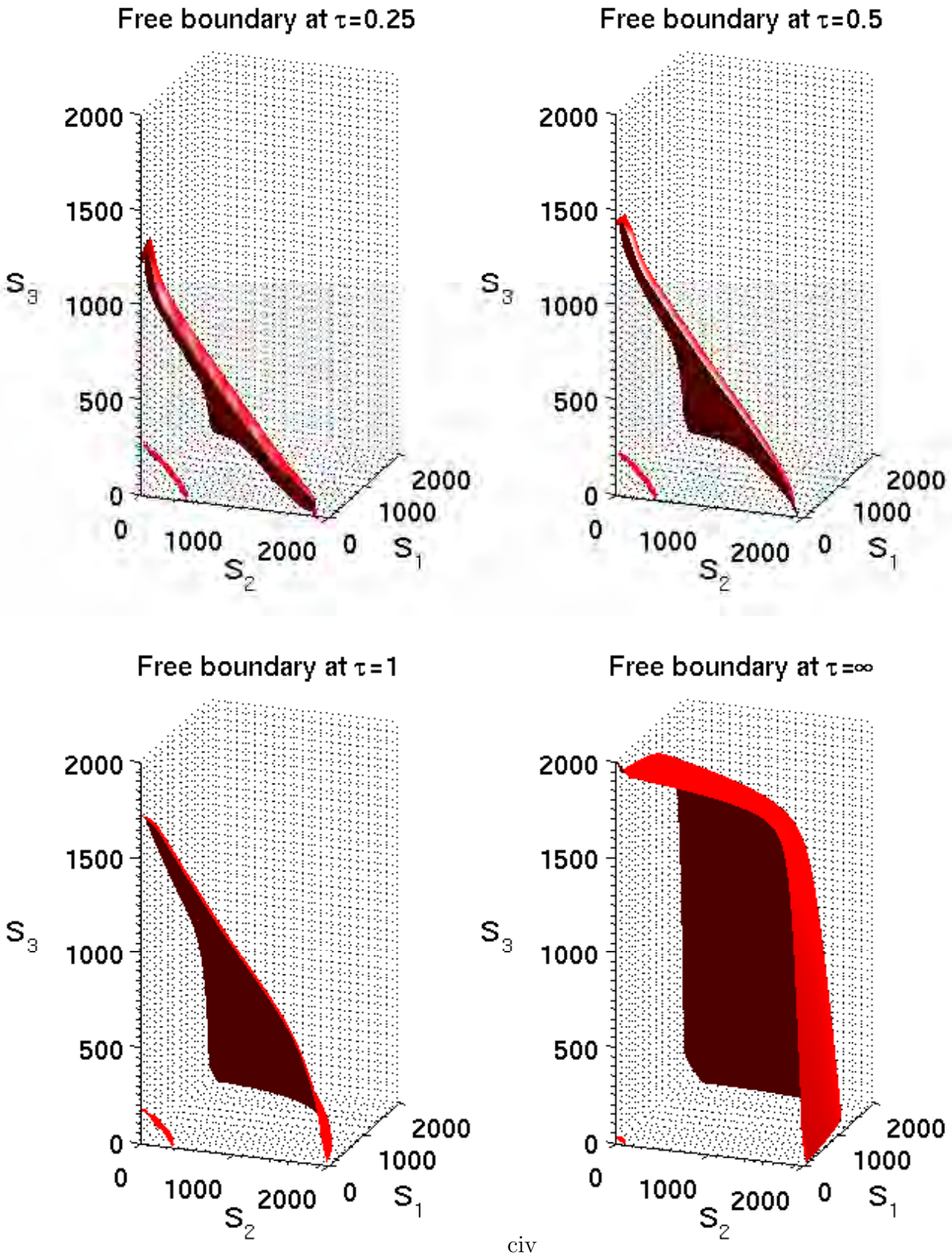

Figure 8.18: Free Boundary of Three-asset Basket Straddle.

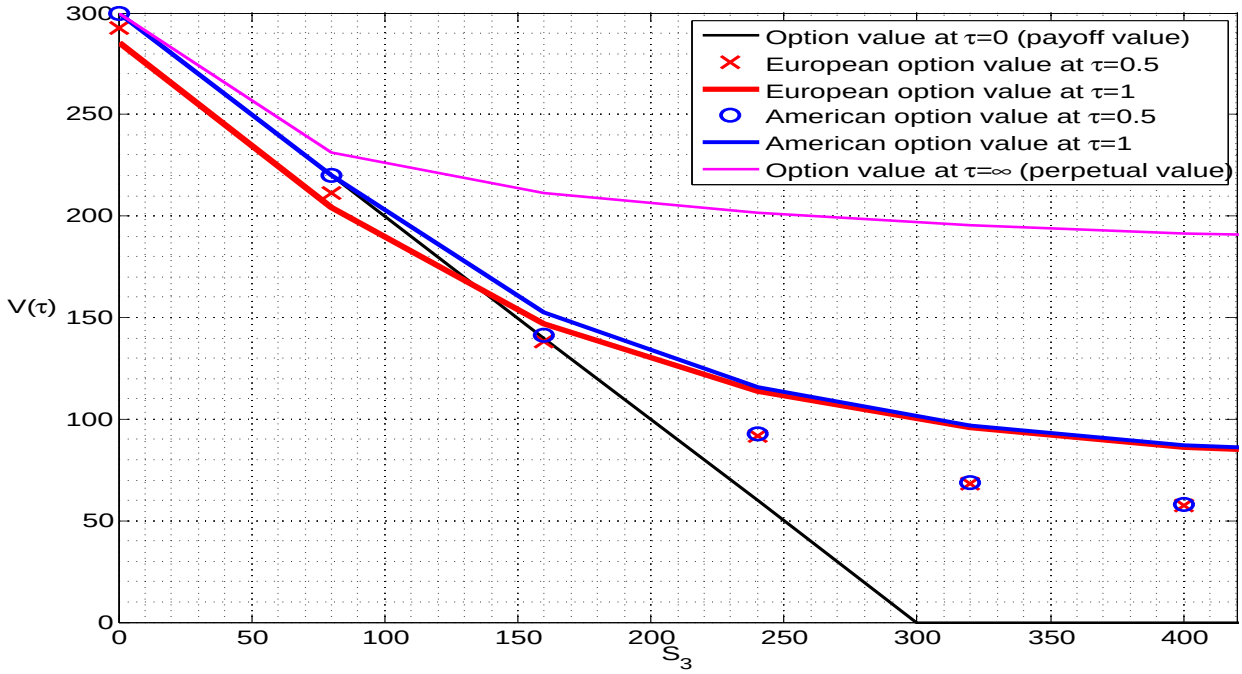

Figure 8.19: Cross Section of Three-asset Minimum Put at $S_1 = 400$ and $S_2 = 320$.

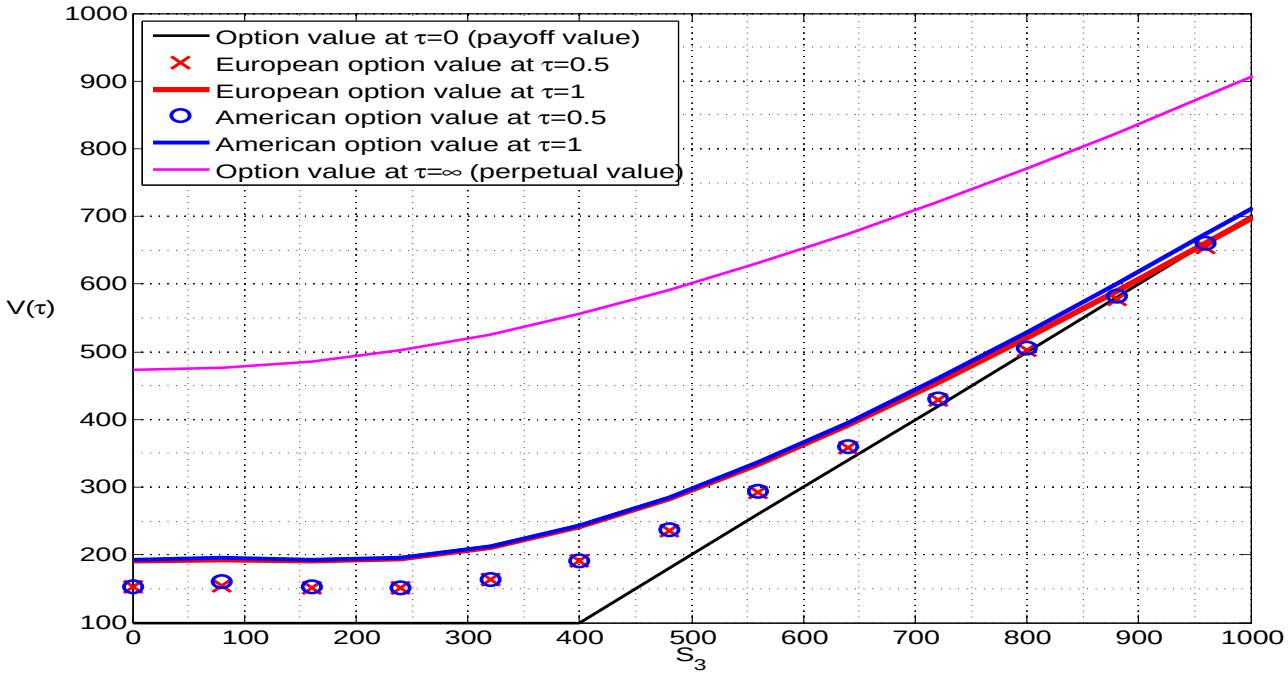

Figure 8.20: Cross Section of Three-asset Maximum Call at $S_1 = 400$ and $S_2 = 320$.

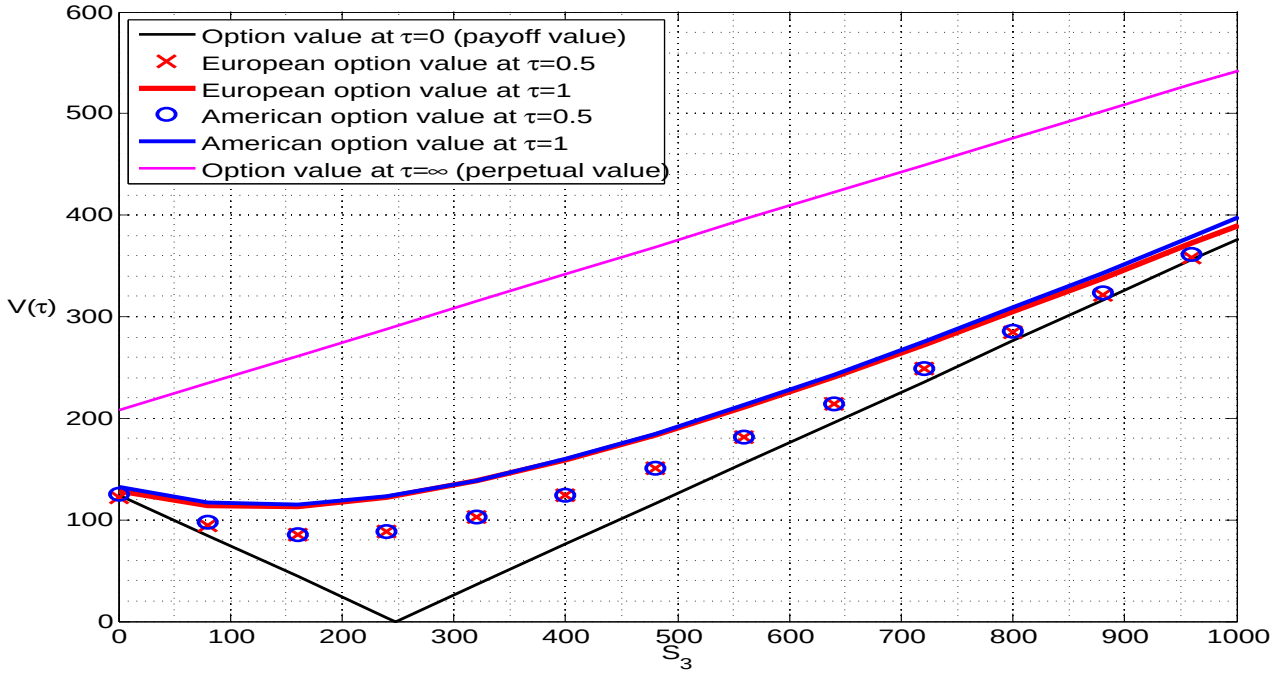

Figure 8.21: Cross Section of Three-asset Basket Straddle at $S_1 = 400$ and $S_2 = 320$.

Generally, the free-boundary of a $d-$asset option is a $(d-1)-$dimensional manifold. As we have seen, they are the points, curves or surfaces separating the early-exercise region and non-early-exercise region. Economically the payoffs in the early-exercise region must be high enough to incentivize an option owner to exercise his right early. In the (minimum) put part, the early-exercise region is the part closer to the $d-$dimensional origin while that of a (maximum) call is the part closer to the $d-$dimensional infinite point, i.e. $(S_{\max}, \ldots, S_{\max})$ numerically or $(\infty, \ldots, \infty)$ analytically. It follows that a basket option has its early-exercise regions in both parts. As time goes backward (or equivalently τ increases), we find different parts of a free boundary move at different rates, which may result from the interaction of the different parameters associated with different assets such as q_i, σ_{ii} and ρ_{ij} for $i = 1, \cdots, d$.

In terms of shapes, the free boundary of the two-dimensional minimum put seems L-shaped, with corner stretching from the origin, while that of the maximum call appears to be fish-shaped with the fish mouth towards the infinite point. However, the free boundaries of a basket straddle are different. They consist of two curves, of which the call part seems to change its convexity in the (numerical) steady state. The shapes of free boundaries remain in any 2D cross-section of higher dimensional counterparts.

8.2 Numerical Setup

We introduce the following notations and terminologies for further discussion of LCP algorithms and numerical errors.

Time Discretization

We have introduced explicit, semi-implicit, implicit and the Rannacher Method for time discretization in chapter 5. To avoid numerical oscillations, we adopt the Rannacher method which finds the solution of the first backward step by dividing the step into 5 substeps and using implicit Euler in these substeps then switches to semi-implicit method from the second backward step onward. [41] suggests this scheme is unconditionally stable and asymptotically second-order accurate.

Number of Unknowns

In the following experiments, we partition each spatial axis uniformly into N_s segments, namely $(N_s)^d$ hypercube elements in our $d-$dimensional computational domain, and N_t segments in the time axis. Notice that we do not need time discretization in perpetual cases. In this manner, we will have a total of $N_u := (N_s - 1)^d$ unknown nodal values in $\Omega := (0, S_{\max})^d$ when provided all Dirichlet boundary conditions (at each time step). For convenience of comparison cross dimensions, we simply show the value of N_s instead of $(N_s - 1)^d$ in the comparison of LCP algorithms. However, one should bear in mind that when provided the same N_s, a higher-dimensional problem is far larger than its lower-dimensional counterparts.

Algorithms

We shall focus on the LCP algorithms introduced in the previous chapter. For the hybrid method with active set, we choose the PSOR method to distinguish the active and inactive nodes at each iteration. Once they are separated, the subsequent system of equation (of smaller size) is solved in three different ways. The first choice is to use the backslash operator in Matlab, which has been automatically optimized for sparse matrices. The second and third one will be solved by the BICGSTAB solver in Matlab, which is based on the biconjugate gradients stabilized method, with and without preconditioning respectively. The preconditioners of the third choice are obtained by the ILU program in Matlab, which attains the sparse incomplete LU factorization, and then fed into the BICGSTAB solver.

In the following, we compare the previous methods, abbreviated as PSOR-BS, PSOR-BICGSTAB and PSOR-BICGSTAB-Pre, the PSOR method, Modulus method, (Lagrangian) Multiplier method, Lemke's method and Howard's method in the problems of different sizes in a $d-$asset framework for $d = 1, 2, 3$.

Initial Guess for LCPs

Recall we performed a linear transformation to obtain the canonical LCP forms (5.7-5.9) and (5.10-5.12) for American and perpetual option pricing problems. We have tried three types of initial guess for solving for the vector $\mathbf{z}$ of a canonical LCP at each time step k: $\mathbf{0}$, $\mathbf{V}_A^{k+1} - \mathbf{G}$ and $\max\{\mathbf{0}, \mathbf{V}_E^{k+1} - \mathbf{G}\}$ where $\mathbf{G}$ is the vector of payoff values, $\mathbf{V}_A^{k+1}$ and $\mathbf{V}_E^{k+1}$ are the American and European Option values at time step $k+1$. Our results suggest that generally $\mathbf{V}_A^{k+1} - \mathbf{G}$ is a better choice[1] for American options when the size of time step is small. For simplicity of presentation, we will only show the results by using the initial guesses $\mathbf{V}_A^{k+1} - \mathbf{G}$ and $\mathbf{0}$ for the American and perpetual option pricing problems respectively in the following experiments.

Stopping Criteria

We define *tol* as the maximum tolerance for all the relative changes after every iteration or pivoting, which are measured in absolute value at each entry, i.e., we impose

$$\frac{|(\mathbf{z}^{\ell})_i - (\mathbf{z}^{\ell+1})_i|}{\max\{1, (\mathbf{z}^{\ell+1})_i\}} \leq tol \text{ for all } i$$

where $\mathbf{z}$ is the non-negative vector considered in a canonical LCP, ℓ is the iteration number[2] in an algorithm and i refers to the $i^{\text{th.}}$ entry of the vector. Notice that in our option pricing problems, the above criterion is stricter than

$$\frac{||\mathbf{z}^{\ell} - \mathbf{z}^{\ell+1}||_{\infty}}{||\mathbf{z}^{\ell+1}||_{\infty}} \leq tol$$

which is also widely used in the literature. We also remind the reader that $\max\{1, (\mathbf{z}^{\ell+1})_i\}$ instead of $(\mathbf{z}^{\ell+1})_i$ is adopted as the denominator to avoid the singularity caused by $(\mathbf{z}^{\ell+1})_i = 0$. This also affects those values less than 1, but in pratical cases their number is a very tiny proportion compared to the total number N_u, when given an exercise price $E \gg 1$.

A stopping criterion to find a numerical/exact solution is set to be $tol = 0.01\%$ (in the sense of each entry) when comparing different LCP algorithms in the next section. Following that, we set up a stricter criterion as $tol = 10^{-6}$ for higher accuracy to measure the discretization and truncation errors. In addition to the *tol*, we also set 10^5 as the maximum iteration number for iterative solvers.[3] An iterative algorithm will stop when either all the relative entry errors are smaller than *tol* or when it reaches the maximum iteration number.

[1] When the time to maturity is small, the non-negative European option values can be a good guess. But when the time is far away from maturity date, such choice is not sensible since many of its component values may be smaller than payoffs.

[2] In time-dependent cases, we have $\mathbf{z}^{k,\ell+1}$ instead, where k refers to the time step t_k.

[3] As we shall see later, an iterative algorithm may reach the limit in a large-scale problem involved with multiple assets.

Benchmark Solution

To compare solutions in various scenarios, we define different benchmark solutions, denoted by $v_* = v_*(t, \mathbf{S})$ when given time t and share prices $\mathbf{S}$, in accordance with the purposes of the following sections. If exact solutions are available, their linear interpolants on a fixed finite element mesh are taken as the benchmark solutions; otherwise, we consider the numerical solution computed by a specified method, on the finest mesh or with the largest far-field bound in each case and take their linear interpolants on a fixed, and generally coarser, finite element mesh as the benchmark solutions. The definition of the benchmark solutions will be further specified in the following sections.

Errors

One can calculate different errors when given a benchmark solution $v_* = v_*(t, \mathbf{S})$ and a numerical solution obtained by a different method or on a different mesh, denoted by $v_h = v_h(t, \mathbf{S})$. Conventionally, in the field of mathematical finance the numerical errors are considered in a discrete sense such as the mean square error (MSE) and maximum relative error (MRE) defined below

$$\begin{aligned} \text{MSE} &:= \frac{1}{N_u} \sum_{\substack{\mathbf{S}\in\mathcal{N}_h \\ \mathbf{S}\notin\Gamma_h}} \left(v_h(0,\mathbf{S}) - v_*(0,\mathbf{S})\right)^2, \\ \text{MRE} &:= \max_{\substack{\mathbf{S}\in\mathcal{N}_h \\ \mathbf{S}\notin\Gamma_h}} \left\{ \frac{|v_h(0,\mathbf{S}) - v_*(0,\mathbf{S})|}{\max\{1, v_*(0,\mathbf{S})\}} \right\} \quad (\text{provided } E >> 1). \end{aligned}$$

where $\mathcal{N}_h$ is the collection of the nodes in a $d-$dimensional uniform grid of mesh size h, Γ_h is the boundary of computational domain and time $t = 0$ can be omitted in time-independent cases.

In addition to these two discrete errors, since the finite element methods are implemented in our research, we shall calculate the errors in a functional sense. We define an error function

$$e_h(t, \mathbf{S}) := v_h(t, \mathbf{S}) - v_*(t, \mathbf{S}),$$

and its canonical H_0-(or L_2-) and H_1-norm errors

$$\begin{aligned} ||e_h||_0^2 &:= (e_h, e_h) := \int_\Omega e_h^2 \, d\Omega, \\ ||e_h||_1^2 &:= (e_h, e_h) + (\nabla e_h, \nabla e_h) := ||e_h||_0^2 + |e_h|_1^2 \\ &:= \int_\Omega e_h^2 \, d\Omega + \sum_{i=1}^{d} \int_\Omega \left(\frac{\partial e_h}{\partial S^{(i)}} \right)^2 d\Omega. \end{aligned}$$

Additionally, we also define the following weighted $H_{1,w}$-norm error

$$\begin{aligned} ||e_h||^2_{1,w} &:= (e_h, e_h) + (\nabla e_h, \nabla e_h)_{\mathbf{T}} := ||e_h||^2_0 + |e_h|^2_{1,w} \\ &:= \int_\Omega e_h^2 \, d\Omega + \sum_{i=1}^{d} \sum_{j=1}^{d} \int_\Omega \frac{\sigma_{ij} S^{(i)} S^{(j)}}{2} \frac{\partial e_h}{\partial S^{(i)}} \frac{\partial e_h}{\partial S^{(j)}} d\Omega. \end{aligned}$$

The five errors will be investigated in the following experiments for comprehensive comparison.

Computational Cost

The computational cost of our numerical schemes is measured from the following aspects.

- (Average) runtime:
  The runtime is defined as the solution time on a scale of seconds, excluding preprocessing time, to achieve a numerical solution satisfying the above stopping criteria. If an American option is considered, then the runtime is defined as the average values of all time steps.

- (Average) iteration number:
  The iteration number is defined as the average number of iteration needed to achieve a numerical solution satisfying the above stopping criteria. If a solver has two-layer iterations, the number refers to that of outer iteration. And the average value of all time steps is taken when considering time-dependent American models.

- (Average) runtime per iteration (RPI):
  The (average) runtime per iteration refers to the ratio of (average) runtime to (average) iteration number. It is used to measure how expensive for each iteration of an algorithm.

8.3 Robustness of LCP Solvers

As mentioned in the previous chapter, the solvability of a LCP solver heavily depends on the class of coefficient matrix $\mathbf{C}$ (and the values of vector $\mathbf{q}$ and $\mathbf{q}^k$ in Chapter 5). Also mentioned earlier is that up to date there is no efficient numerical test to check the class of the coefficient matrix for the convergence of LCP algorithms. A natural question then follows: whether the numerical algorithms introduced earlier are robust to solve the LCPs arising from the Black-Scholes-Merton partial differential inequalities when dealing with

American and perpetual option pricing problems? Are the numerical solutions convergent and accurate to satisfactory extent?[4]

Since the closed-form formulas are known in the cases of one-asset American call without dividend paying and one-asset perpetual call/put with general setup of dividends, the exact values can be used as benchmark solutions to examine the robustness of different LCP algorithms. In what follows, we present the numerical results obtained by exact formulas, the PSOR method, the Modulus method, the Lemke method, the Lagrangian Multiplier method, the Howard method and the hybrid PSOR-BS method. The following analytical and numerical parameters are used in our tests.

- Exercise price: $E = 300$;
- Interest rate: $r = 0.05$;
- Expiry date: $T = 1$ (in time-dependent cases);
- (Annualized) variance: $\sigma^2 = 0.2^2 = 0.04$.
- The far-field bound: $S_{\max} = 2000$;
- Number of partition points in S-axis: $N_1 + 1 = 51$;
- Number of partition points in t-axis: $N_t + 1 = 21$ (in time-dependent cases).

To focus on the robustness of LCP solvers and to avoid the truncation errors, we will use the exact solutions as the far-field boundary conditions in the following tests. In the trials, the stopping criterion is set by $tol = 0.01\%$ and the benchmark solutions are set as

$$v_* = I_h v$$

where $I_h : \mathbb{V} \to \mathbb{V}_h$ is a $d-$dimensional piecewise interpolation operator on a mesh of mesh size h such that given a fixed t_k,

$$I_h v(t_k, S_j) = v(t_k, S_j) \text{ for } S_j \in \{0, 40, 80, \ldots, 2000\}.$$

We recall that $t_k = 0$ in the American case while the t_k can be omitted in the perpetual cases.

[4]Recall that the values of lower-dimensional options may serve as the boundary conditions of its high-dimensional counterparts. In this case, a LCP solver influences the accuracy of option values on both the boundary and the interior domain.

	Methods					
Errors	PSOR	Modulus	Lemke	Multiplier	Howard	Hybrid
MSE	$3.5645 \cdot 10^{-4}$	$1.8514 \cdot 10^{2}$	$6.5103 \cdot 10^{-4}$	$6.5103 \cdot 10^{-4}$	$6.5103 \cdot 10^{-4}$	$3.5645 \cdot 10^{-4}$
MRE	0.5698%	99.8641%	0.1932%	0.1932%	0.1932%	0.5698
H_0	$8.3984 \cdot 10^{-1}$	$4.8348 \cdot 10^{2}$	$9.1505 \cdot 10^{-1}$	$9.1505 \cdot 10^{-1}$	$9.1505 \cdot 10^{-1}$	$8.2896 \cdot 10^{-1}$
H_1	$8.3987 \cdot 10^{-1}$	$4.8349 \cdot 10^{2}$	$9.1509 \cdot 10^{-1}$	$9.1509 \cdot 10^{-1}$	$9.1509 \cdot 10^{-1}$	$8.2899 \cdot 10^{-1}$
$H_{1,w}$	$9.0662 \cdot 10^{-1}$	$5.0516 \cdot 10^{2}$	$9.6866 \cdot 10^{-1}$	$9.6866 \cdot 10^{-1}$	$9.6866 \cdot 10^{-1}$	$8.9644 \cdot 10^{-1}$

Table 8.1: The errors for one-asset perpetual put with nonzero dividend.

8.3.1 Time-independent Case

We have introduced the closed-form formulas of one-asset perpetual call and put in Chapter 1. Here we take the nonzero dividend $q = 0.02$ for our tests. Figures 8.22 and 8.23 show that for all the selected LCP solvers except for the Modulus method, the absolute error $|v_h(t_k, S_j) - I_h v(t_k, S_j)|$ is well below 1 (given $E = 300 >> 1$) at an arbitrary node, or equivalently its MRE $< 0.1\%$, in both time-independent cases. The Modulus method produces significant differences from others in terms of the MSE, MRE, H_0-norm, H_1-norm and $H_{1,w}$-norm errors. Actually the errors of numerical solution of Modulus method remain almost unchanged even if we increase the partition number N_1 from 50 to 1000, which suggests the numerical solution of Modulus method may be inaccurate in a general case.

8.3.2 Time-dependent Case

Since numerical errors accumulate when time integration is performed in a numerical scheme, we would like to investigate the robustness of LCP algorithms in time-dependent cases. It is well-known that an American call is equivalent to a European call if there is no dividend payment. In this case, we set $q = 0$ for our American option and compare its numerical values with the exact values of its European counterpart. As figure 8.24 shows, the relative errors of all the selected LCP solvers are well below 0.05%, or equivalently the absolute errors are less than 1 given $E = 300$, at $\tau = 1$. Such accuracy provided by only 51 partition points in S-axis is sufficient for practical use. Surprisingly in this particular time-dependent case, the Modulus method provides smaller errors than others from the aspects of MSE, MRE, H_0-norm, H_1-norm and $H_{1,w}$-norm.

8.3.3 Comment

We have seen that when there is no dividend paying to a share, the Modulus method and all others seems to provide a decent numerical solution. However, in a more generalized

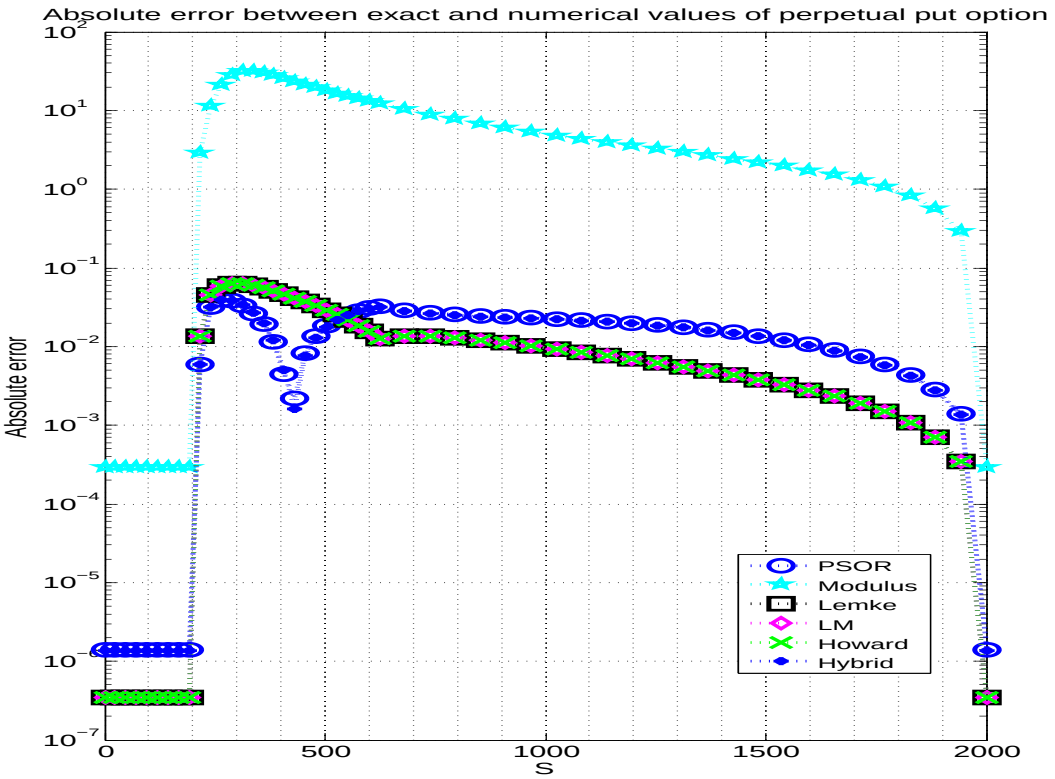

Figure 8.22: Exact and numerical perpetual put values with dividend.

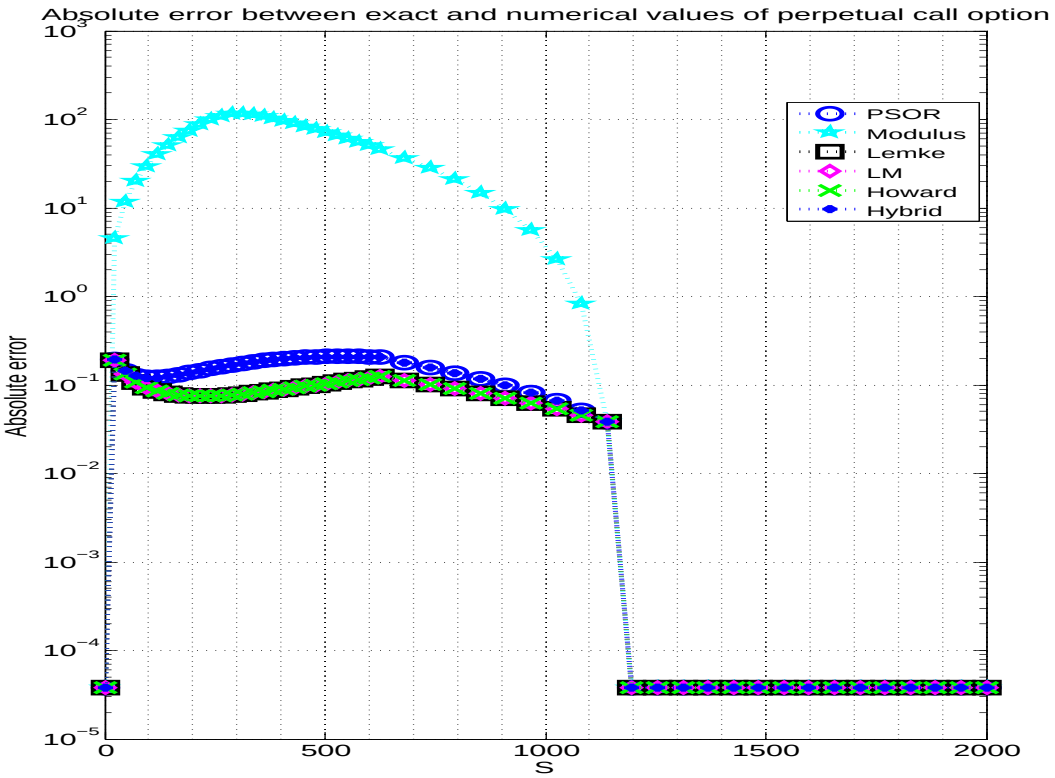

Figure 8.23: Exact and numerical perpetual call values with dividend.

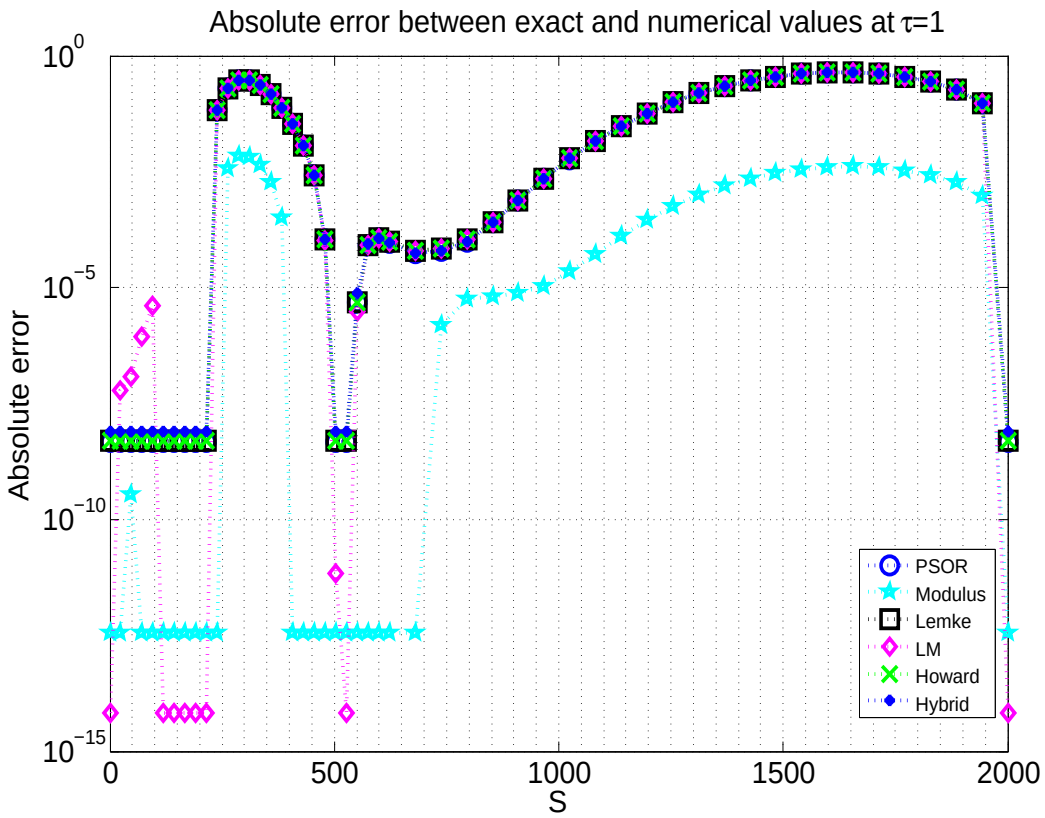

Figure 8.24: Exact and numerical American call values without dividend.

	Methods					
Errors	PSOR	Modulus	Lemke	Multiplier	Howard	Hybrid
MSE	$1.8364 \cdot 10^{-2}$	$3.1719 \cdot 10^{3}$	$6.2050 \cdot 10^{-3}$	$6.2050 \cdot 10^{-3}$	$6.2050 \cdot 10^{-3}$	$1.8110 \cdot 10^{-2}$
MRE	4.2886%	100%	4.1958%	4.1958%	4.1958%	4.2872%
H_0	$5.1783 \cdot 10^{0}$	$2.0068 \cdot 10^{3}$	$3.0666 \cdot 10^{0}$	$3.0666 \cdot 10^{0}$	$3.0666 \cdot 10^{0}$	$5.1435 \cdot 10^{0}$
H_1	$5.1785 \cdot 10^{0}$	$2.0068 \cdot 10^{3}$	$3.0669 \cdot 10^{0}$	$3.0669 \cdot 10^{0}$	$3.0669 \cdot 10^{0}$	$5.1437 \cdot 10^{0}$
$H_{1,w}$	$5.3245 \cdot 10^{0}$	$2.0484 \cdot 10^{3}$	$3.2177 \cdot 10^{0}$	$3.2177 \cdot 10^{0}$	$3.2177 \cdot 10^{0}$	$5.2895 \cdot 10^{0}$

Table 8.2: The errors for one-asset perpetual call with nonzero dividend.

	Methods					
Errors	PSOR	Modulus	Lemke	Multiplier	Howard	Hybrid
MSE	$2.0521 \cdot 10^{-2}$	$1.2376 \cdot 10^{-5}$	$2.0536 \cdot 10^{-2}$	$2.0531 \cdot 10^{-2}$	$2.0536 \cdot 10^{-2}$	$2.0529 \cdot 10^{-2}$
MRE	1.5743%	0.0614%	1.5744%	1.5732%	1.5744%	1.5744%
H_0	7.0417	0.1270	7.0447	7.0443	7.0447	7.0433
H_1	7.0419	0.1271	7.0449	7.0445	7.0449	7.0434
$H_{1,w}$	9.4342	0.1797	9.4377	9.4373	9.4377	9.4361

Table 8.3: The finite element errors for one-asset American call without dividend.

circumstance with dividend payment, the Modulus method may produce bias in its numerical solution even though its numerical solution is convergent. Such bias is significant around the exercise price (kink point), which is the so-called hotspot area in practice. Since the values of one-asset options serve as boundary conditions in higher-dimensional cases, its bias may propagate into the interior domain of multi-dimensional circumstances. Actually, in our other experiments and as we shall see later, the Modulus method usually generates a notably different numerical solution from other methods, which can not be reduced by using smaller mesh sizes (h_s and h_t) and larger far-field bound value ($S_{\max}$). Our results suggest that the Modulus method may not be a suitable algorithm when solving a generalized Black-Scholes-Merton partial differential inequality along with finite element techniques.

8.4 Performance of LCP Algorithms

From the comparison with the exact solutions of previous section, we have learnt that our LCP algorithms are robust for solving option pricing problems except that the Modulus method may produce incorrect solutions. However, exact solutions for American and perpetual option problems are generally unknown when given more complicated payoffs, nonzero dividends or in multi-asset cases. Since the size of LCP problems grow exponentially as N_s and d increase linearly, we are interested to see how different and how expensive the numerical solutions would be when fixing N_s, N_t and d and provided identical stopping criteria. For simplicity, we fix $N_t = 20$ and set $tol \leq 0.01\%$ in this section. We shall observe their costs for solving a LCP with $N_u = (N_s - 1)^d$ unknowns (at each time step if time-dependent) and compare the differences of their numerical solutions in terms of MSE, MRE, H_0-norm, H_1-norm and $H_{1,w}-$norm errors by taking the numerical solution obtained by Howard's method as the benchmark solution given the same N_s in a d-asset framework for $d = 1, 2, 3$. As (basket) straddles have more complicated payoffs than calls and puts, we consider American/perpetual (basket) straddle options in what follows. We reminder readers the aim of this section is to compare the LCP solvers when provided identical problems, numerical parameters and stopping criteria instead of investigating the convergence of numerical errors, which will be discussed following this section.

8.4.1 Option Parameters

For convenience, we shall use the following parameter values for all numerical experiments from this section on. Note that the weights $\boldsymbol{\omega}$ are only for (multi-asset) basket options and the expiry date T is applicable only to European and American options. Also recall that a covariance is defined as $\sigma_{ij} = \rho_{ij}\sigma_i\sigma_j$ where $\rho_{ii} = 1$.

One-asset Case

$E = 300$, $r = 0.05$, $q = 0.02$, $T = 1$ and $\sigma^2 = 0.2^2 = 0.04$.

Two-asset Case

$\boldsymbol{\omega} = (0.4,\ 0.6)^T$, $E = 300$, $r = 0.05$, $\mathbf{q} = (0.02,\ 0.03)^T$, $T = 1$ and $\sigma_1^2 = 0.2^2, \sigma_2^2 = 0.4^2$ and the correlation coefficient $\rho_{12} = 0.5$.

Three-asset Case

$\boldsymbol{\omega} = (0.2,\ 0.3,\ 0.5)^T$, $E = 300$, $r = 0.05$, $\mathbf{q} = (0.01,\ 0.02,\ 0.03)^T$, $T = 1$ and $\sigma_1^2 = 0.3, \sigma_2^2 = 0.4, \sigma_3^2 = 0.5$ and the correlation coefficients $\rho_{12} = 0.25, \rho_{13} = 0.5, \rho_{23} = 0.75$.

8.4.2 Observation

Tables [8.4], [8.6] and [8.8] manifest the comparison results of time-dependent American cases while tables [8.5], [8.7] and [8.9] reveal those of time-independent perpetual cases.

Computational Cost

It is obvious that the runtimes, iterations and RPI increase as N_s doubles (and correspondingly N_u grows almost 2^d larger each time). However their increase rates are different and dependent on the choice of algorithms, and option types. We recall that the one-dimensional problems are relatively smaller and with less complexity[5] than those of higher-dimensional ones. As a result, the runtime increases significantly as the number of assets d increases with respect to each algorithm.We remind readers that the coefficient matrices have $3, 9, 27$ bands for one-, two- and three-asset cases.

Overall, Howard's method has the most satisfactory runtimes, followed by the Multiplier and Lemke's methods. However, the Multiplier method prevails over Howard's method at $N_s = 640$ in two-asset (both American and perpetual) cases. This suggests the Multiplier method may outperform Howard's method when problems become extremely large and more complicated (with 9 bands). This may even be true in three-dimensional cases (with 27 bands), but we will need further experiments to verify it.

In general, the runtimes of perpetual cases are much longer than their American counterparts (the total of all time steps). This may result from the fact that the initial guesses (the previous solutions) provide more information when the time step is small in the case of American options while the payoffs provide less information when serving as the initial guess of the perpetual counterparts.

As for the PSOR method and its variants, they generally consume much more computational time. The PSOR-BS method, the PSOR-BICGSTAB method and the PSOR-BICGSTAB-Pre methods do not seem benefit from the separation of active/inactive nodes in one-dimensional small-scaled problems due to the fact that they are implemented in two phases and need extra operations. However, when the problems become more complicated and larger in multi-asset cases, their extra effort is rewarded with slight reduction of runtimes. Overall, the PSOR-BS method and the PSOR-BICGSTAB method have almost equal performance in each case; and the PSOR-BICGSTAB-Pre method provides subtle improvement in one-dimensional problems (or tri-diagonal systems) but have uncertain improvement in higher-dimensional ones (or multi-band systems). However, the PSOR-BICGSTAB-Pre method needs less iterations than the PSOR-BS method and the PSOR-BICGSTAB method. This suggests that if one can simplify the procedures of the PSOR-BICGSTAB-Pre method from programming or mathematical point of view, it may overwhelm the PSOR method, the PSOR-BS method and the PSOR-BICGSTAB method.

[5]We have tri-diagonal systems in one-dimensional problems and a 3^d-band system in a generalized $d-$dimesional cases for $d \geq 1$.

In terms of iteration and RPI, Howard's method, Multiplier method and Lemke's method are still the most favourite in all cases. It is noticeable that the needed number of iterations of Lemke's method increase at about the rate of 2^d as N_s doubles in d-dimensional experiments. In contrast, those of Howard's method and Multiplier method increase slowly, around $1.8 \sim 2$ times for one-asset perpetual, two-asset American and perpetual cases and around 1.5 times for three-asset American and perpetual cases. As to one-asset American option, due to good initial guess and its small size, the increase of its iteration number is not not significant for Howard's method and Multiplier method.

Errors among Algorithms

Beware that even given an identical stopping criterion and an identical numerical mesh, there still exist slight differences among the numerical solutions obtained by different algorithms. If we take the solution of Howard's method as the benchmark solution, we can not find significant differences/errors from those by other methods when provided the same partition numbers, except for that by the Modulus method.

Particularly, most of the MREs of Multiplier and Lemke's methods are less than 0.1% in our experiments and thus negligible in practice. However, in two-asset perpetual cases, Lemke's method stops at the maximum iteration limit (10^5) and thus fails to satisfy the criterion $tol = 10^{-4}$ as shown in table 8.10. This suggests Lemke's method needs a higher maximum iteration limit in large-scale problems and will consume more time to achieve satisfactory accuracy.

In contrast, the Modulus method produces convergent but incorrect numerical solutions, measured by all five types of errors, in all cases. Its MRE even reaches 91.5411% when given $N_s = 80$ in two-asset American case. Such differences/errors result from the algorithm of Modulus method itself and can not be remedied with smaller tol, mesh size and lager far-field bound. We summarize the errors with its largest N_s in each case in table 8.11.

Comment

Interestingly, even though Howard's method and the Multiplier method are designed based on different theories, they have quite similar performances from all the aspects of runtimes, iterations, RPI and errors in all our experiments. Based on our results, Howard's, Multiplier and Lemke's method deserve further investigation in the future especially in large-scale multi-band problems. In contrast, the Modulus method may not be suitable for option pricing with BSM partial differential inequality due to its incorrect numerical solutions while the PSOR and its variants produce quite disappointing performance even though they are widely introduced for option pricing problems.

		Methods							
	N_s	PSOR	Modulus	Multiplier	PSOR-BS	PSOR-BICGSTAB	PSOR-BICGSTAB-Pre	Lemke	Howard
Runtime	10	$2.0177 \cdot 10^{-3}$	$1.1107 \cdot 10^{-1}$	$1.6554 \cdot 10^{-2}$	$6.2676 \cdot 10^{-3}$	$3.1819 \cdot 10^{-2}$	$2.2307 \cdot 10^{-2}$	$1.2176 \cdot 10^{-2}$	$7.2475 \cdot 10^{-3}$
	20	$2.8595 \cdot 10^{-3}$	$8.2706 \cdot 10^{-2}$	$1.5520 \cdot 10^{-2}$	$1.5495 \cdot 10^{-2}$	$2.2344 \cdot 10^{-2}$	$2.2321 \cdot 10^{-2}$	$1.7934 \cdot 10^{-3}$	$2.1385 \cdot 10^{-3}$
	40	$4.9657 \cdot 10^{-3}$	$1.4877 \cdot 10^{-1}$	$3.7831 \cdot 10^{-2}$	$2.1075 \cdot 10^{-2}$	$2.2494 \cdot 10^{-2}$	$9.4094 \cdot 10^{-3}$	$2.0675 \cdot 10^{-3}$	$2.4217 \cdot 10^{-3}$
	80	$9.3820 \cdot 10^{-3}$	$8.3854 \cdot 10^{-2}$	$3.1528 \cdot 10^{-2}$	$1.3038 \cdot 10^{-2}$	$2.2584 \cdot 10^{-2}$	$1.4381 \cdot 10^{-2}$	$3.8034 \cdot 10^{-3}$	$2.4130 \cdot 10^{-3}$
	160	$4.2646 \cdot 10^{-2}$	$8.2647 \cdot 10^{-2}$	$3.4440 \cdot 10^{-2}$	$5.4713 \cdot 10^{-2}$	$7.5306 \cdot 10^{-2}$	$5.3188 \cdot 10^{-2}$	$8.4146 \cdot 10^{-3}$	$2.5588 \cdot 10^{-3}$
	320	$3.0568 \cdot 10^{-1}$	$1.2075 \cdot 10^{-1}$	$1.7170 \cdot 10^{-2}$	$3.5127 \cdot 10^{-1}$	$3.6104 \cdot 10^{-1}$	$2.9261 \cdot 10^{-1}$	$2.0604 \cdot 10^{-2}$	$8.2994 \cdot 10^{-3}$
	640	$1.8563 \cdot 10^{0}$	$2.5922 \cdot 10^{-1}$	$2.2869 \cdot 10^{-2}$	$1.9478 \cdot 10^{0}$	$2.0506 \cdot 10^{0}$	$1.8033 \cdot 10^{0}$	$1.0163 \cdot 10^{-1}$	$4.4102 \cdot 10^{-3}$
	1280	$1.1220 \cdot 10^{1}$	$6.3973 \cdot 10^{-1}$	$3.8651 \cdot 10^{-2}$	$1.2389 \cdot 10^{1}$	$1.2903 \cdot 10^{1}$	$1.1505 \cdot 10^{1}$	$2.2312 \cdot 10^{-1}$	$8.5119 \cdot 10^{-3}$
Iteration	10	4.40	14.90	3.75	3.00	3.00	3.00	3.00	3.75
	20	5.75	14.50	4.10	3.00	3.00	3.00	2.29	4.10
	40	5.95	10.05	4.45	3.00	3.00	3.00	3.65	4.45
	80	5.90	7.75	3.60	3.00	3.00	3.00	10.75	3.60
	160	12.20	8.40	3.60	4.65	4.65	3.05	23.15	3.70
	320	30.25	10.80	4.00	8.15	8.15	3.00	45.75	4.05
	640	75.85	14.10	4.45	17.20	17.20	3.00	91.25	4.45
	1280	166.15	18.25	5.65	35.15	35.15	3.00	182.45	5.65
RPI	10	$4.5856 \cdot 10^{-4}$	$7.4545 \cdot 10^{-3}$	$4.4143 \cdot 10^{-3}$	$2.0892 \cdot 10^{-3}$	$1.0606 \cdot 10^{-2}$	$7.4357 \cdot 10^{-3}$	$4.0587 \cdot 10^{-3}$	$1.9327 \cdot 10^{-3}$
	20	$4.9730 \cdot 10^{-4}$	$5.7038 \cdot 10^{-3}$	$3.7853 \cdot 10^{-3}$	$5.1649 \cdot 10^{-3}$	$7.4479 \cdot 10^{-3}$	$7.4402 \cdot 10^{-3}$	$7.8463 \cdot 10^{-4}$	$5.2159 \cdot 10^{-4}$
	40	$8.3458 \cdot 10^{-4}$	$1.4803 \cdot 10^{-2}$	$8.5013 \cdot 10^{-3}$	$7.0250 \cdot 10^{-3}$	$7.4980 \cdot 10^{-3}$	$3.1365 \cdot 10^{-3}$	$5.6644 \cdot 10^{-4}$	$5.4421 \cdot 10^{-4}$
	80	$1.5902 \cdot 10^{-3}$	$1.0820 \cdot 10^{-2}$	$8.7578 \cdot 10^{-3}$	$4.3459 \cdot 10^{-3}$	$7.5280 \cdot 10^{-3}$	$4.7936 \cdot 10^{-3}$	$3.5381 \cdot 10^{-4}$	$6.7026 \cdot 10^{-4}$
	160	$3.4956 \cdot 10^{-3}$	$9.8389 \cdot 10^{-3}$	$9.5666 \cdot 10^{-3}$	$1.1766 \cdot 10^{-2}$	$1.6195 \cdot 10^{-2}$	$1.7439 \cdot 10^{-2}$	$3.6348 \cdot 10^{-4}$	$6.9158 \cdot 10^{-4}$
	320	$1.0105 \cdot 10^{-2}$	$1.1181 \cdot 10^{-2}$	$4.2926 \cdot 10^{-3}$	$4.3100 \cdot 10^{-2}$	$4.4299 \cdot 10^{-2}$	$9.7537 \cdot 10^{-2}$	$4.5037 \cdot 10^{-4}$	$2.0492 \cdot 10^{-3}$
	640	$2.4473 \cdot 10^{-2}$	$1.8384 \cdot 10^{-2}$	$5.1392 \cdot 10^{-3}$	$1.1325 \cdot 10^{-1}$	$1.1922 \cdot 10^{-1}$	$6.0110 \cdot 10^{-1}$	$1.1137 \cdot 10^{-3}$	$9.9106 \cdot 10^{-4}$
	1280	$6.7527 \cdot 10^{-2}$	$3.5054 \cdot 10^{-2}$	$6.8408 \cdot 10^{-3}$	$3.5246 \cdot 10^{-1}$	$3.6708 \cdot 10^{-1}$	$3.8349 \cdot 10^{0}$	$1.2229 \cdot 10^{-3}$	$1.5065 \cdot 10^{-3}$

Table 8.4: Comparison of LCP solvers for One-asset American Straddle.

		Methods							
	N_s	PSOR	Modulus	Multiplier	PSOR-BS	PSOR-BICGSTAB	PSOR-BICGSTAB-Pre	Lemke	Howard
Runtime	10	$2.1865 \cdot 10^{-2}$	$9.7696 \cdot 10^{-1}$	$2.1973 \cdot 10^{-1}$	$5.6053 \cdot 10^{-2}$	$2.5699 \cdot 10^{-1}$	$1.0595 \cdot 10^{-1}$	$5.3716 \cdot 10^{-2}$	$3.2912 \cdot 10^{-1}$
	20	$3.9820 \cdot 10^{-2}$	$1.3519 \cdot 10^{-1}$	$6.6018 \cdot 10^{-2}$	$1.2916 \cdot 10^{-1}$	$1.6486 \cdot 10^{-1}$	$5.5961 \cdot 10^{-2}$	$6.4370 \cdot 10^{-3}$	$3.4260 \cdot 10^{-3}$
	40	$2.7515 \cdot 10^{-1}$	$7.5744 \cdot 10^{-2}$	$7.5488 \cdot 10^{-2}$	$4.5986 \cdot 10^{-1}$	$7.5408 \cdot 10^{-1}$	$2.8917 \cdot 10^{-1}$	$1.1012 \cdot 10^{-2}$	$4.9250 \cdot 10^{-3}$
	80	$2.0967 \cdot 10^{0}$	$7.3248 \cdot 10^{-2}$	$1.4632 \cdot 10^{-1}$	$1.8601 \cdot 10^{0}$	$3.1200 \cdot 10^{0}$	$1.9401 \cdot 10^{0}$	$2.3855 \cdot 10^{-2}$	$8.4450 \cdot 10^{-3}$
	160	$6.7614 \cdot 10^{0}$	$1.1064 \cdot 10^{-1}$	$3.2731 \cdot 10^{-1}$	$8.0451 \cdot 10^{0}$	$1.3119 \cdot 10^{1}$	$6.1879 \cdot 10^{0}$	$5.2293 \cdot 10^{-2}$	$1.6649 \cdot 10^{-2}$
	320	$4.0183 \cdot 10^{1}$	$4.5060 \cdot 10^{-1}$	$7.8261 \cdot 10^{-1}$	$4.1015 \cdot 10^{1}$	$1.0903 \cdot 10^{2}$	$3.7767 \cdot 10^{1}$	$1.4731 \cdot 10^{-1}$	$4.1804 \cdot 10^{-2}$
	640	$2.6982 \cdot 10^{2}$	$1.8552 \cdot 10^{0}$	$1.5044 \cdot 10^{0}$	$5.4090 \cdot 10^{2}$	$5.1661 \cdot 10^{2}$	$2.7038 \cdot 10^{2}$	$4.8282 \cdot 10^{-1}$	$1.2665 \cdot 10^{-1}$
	1280	$1.7633 \cdot 10^{3}$	$6.1811 \cdot 10^{0}$	$2.9770 \cdot 10^{0}$	$2.1468 \cdot 10^{3}$	$2.8262 \cdot 10^{3}$	$1.7353 \cdot 10^{3}$	$1.7482 \cdot 10^{0}$	$4.8822 \cdot 10^{-1}$
Iteration	10	14	12	4	5	5	3	5	4
	20	35	21	5	9	9	3	8	5
	40	122	39	8	26	26	3	16	8
	80	440	70	15	90	90	3	33	15
	160	1376	123	29	277	277	4	64	28
	320	4243	189	58	851	851	7	130	56
	640	11780	270	111	2358	2358	14	259	109
	1280	25796	413	217	5161	5161	28	517	214
RPI	10	$1.5618 \cdot 10^{-3}$	$8.1413 \cdot 10^{-2}$	$5.4933 \cdot 10^{-2}$	$1.1211 \cdot 10^{-2}$	$5.1399 \cdot 10^{-2}$	$3.5316 \cdot 10^{-2}$	$1.0743 \cdot 10^{-2}$	$8.2280 \cdot 10^{-2}$
	20	$1.1377 \cdot 10^{-3}$	$6.4377 \cdot 10^{-3}$	$1.3204 \cdot 10^{-2}$	$1.4351 \cdot 10^{-2}$	$1.8318 \cdot 10^{-2}$	$1.8654 \cdot 10^{-2}$	$8.0463 \cdot 10^{-4}$	$6.8520 \cdot 10^{-4}$
	40	$2.2553 \cdot 10^{-3}$	$1.9422 \cdot 10^{-3}$	$9.4360 \cdot 10^{-3}$	$1.7687 \cdot 10^{-2}$	$2.9003 \cdot 10^{-2}$	$9.6389 \cdot 10^{-2}$	$6.8825 \cdot 10^{-4}$	$6.1562 \cdot 10^{-4}$
	80	$4.7652 \cdot 10^{-3}$	$1.0464 \cdot 10^{-3}$	$9.7549 \cdot 10^{-3}$	$2.0668 \cdot 10^{-2}$	$3.4666 \cdot 10^{-2}$	$6.4669 \cdot 10^{-1}$	$7.2288 \cdot 10^{-4}$	$5.6300 \cdot 10^{-4}$
	160	$4.9138 \cdot 10^{-3}$	$8.9955 \cdot 10^{-4}$	$1.1287 \cdot 10^{-2}$	$2.9044 \cdot 10^{-2}$	$4.7362 \cdot 10^{-2}$	$1.5470 \cdot 10^{0}$	$8.1708 \cdot 10^{-4}$	$5.9461 \cdot 10^{-4}$
	320	$9.4704 \cdot 10^{-3}$	$2.3841 \cdot 10^{-3}$	$1.3493 \cdot 10^{-2}$	$4.8196 \cdot 10^{-2}$	$1.2812 \cdot 10^{-1}$	$5.3952 \cdot 10^{0}$	$1.1332 \cdot 10^{-3}$	$7.4650 \cdot 10^{-4}$
	640	$2.2905 \cdot 10^{-2}$	$6.8711 \cdot 10^{-3}$	$1.3553 \cdot 10^{-2}$	$2.2939 \cdot 10^{-1}$	$2.1909 \cdot 10^{-1}$	$1.9313 \cdot 10^{1}$	$1.8642 \cdot 10^{-3}$	$1.1619 \cdot 10^{-3}$
	1280	$6.8356 \cdot 10^{-2}$	$1.4966 \cdot 10^{-2}$	$1.3719 \cdot 10^{-2}$	$4.1596 \cdot 10^{-1}$	$5.4762 \cdot 10^{-1}$	$6.1975 \cdot 10^{1}$	$3.3815 \cdot 10^{-3}$	$2.2814 \cdot 10^{-3}$

Table 8.5: Comparison of LCP solvers for One-asset Perpetual Straddle.

		Methods							
	N_s	PSOR	Modulus	Multiplier	PSOR-BS	PSOR-BICGSTAB	PSOR-BICGSTAB-Pre	Lemke	Howard
Runtime	10	$1.7518 \cdot 10^{-2}$	$5.2598 \cdot 10^{-2}$	$1.6923 \cdot 10^{-2}$	$1.5408 \cdot 10^{-2}$	$2.9959 \cdot 10^{-2}$	$2.1863 \cdot 10^{-2}$	$2.2819 \cdot 10^{-3}$	$3.5211 \cdot 10^{-3}$
	20	$9.9036 \cdot 10^{-2}$	$7.0295 \cdot 10^{-1}$	$1.8312 \cdot 10^{-2}$	$9.7140 \cdot 10^{-2}$	$1.1061 \cdot 10^{-1}$	$1.1778 \cdot 10^{-1}$	$4.4398 \cdot 10^{-3}$	$4.1280 \cdot 10^{-3}$
	40	$1.3873 \cdot 10^{0}$	$5.4902 \cdot 10^{0}$	$5.5385 \cdot 10^{-2}$	$1.1643 \cdot 10^{0}$	$1.1527 \cdot 10^{0}$	$1.6286 \cdot 10^{0}$	$3.3882 \cdot 10^{-2}$	$2.8300 \cdot 10^{-2}$
	80	$4.6628 \cdot 10^{1}$	$1.5269 \cdot 10^{2}$	$4.5533 \cdot 10^{-1}$	$2.3037 \cdot 10^{1}$	$2.0993 \cdot 10^{1}$	$5.0168 \cdot 10^{1}$	$1.3296 \cdot 10^{0}$	$1.4281 \cdot 10^{-1}$
	160	—	—	$2.7300 \cdot 10^{0}$	—	—	—	$3.6502 \cdot 10^{1}$	$9.6595 \cdot 10^{-1}$
	320	—	—	$2.0708 \cdot 10^{1}$	—	—	—	$5.4959 \cdot 10^{2}$	$1.4190 \cdot 10^{1}$
	640	—	—	$1.5017 \cdot 10^{2}$	—	—	—	$7.4306 \cdot 10^{3}$	$1.5938 \cdot 10^{2}$
Iteration	10	6.75	15.95	4.00	3.00	3.00	3.00	2.57	3.90
	20	7.65	11.40	3.95	3.00	3.00	3.00	4.26	4.10
	40	8.65	8.00	4.00	3.00	3.00	3.00	13.00	4.00
	80	17.40	8.40	4.15	3.55	3.55	3.00	50.65	4.15
	160	—	—	6.60	—	—	—	206.80	6.60
	320	—	—	11.10	—	—	—	841.90	11.10
	640	—	—	20.00	—	—	—	3397.40	20.00
RPI	10	$2.5953 \cdot 10^{-3}$	$3.2977 \cdot 10^{-3}$	$4.2308 \cdot 10^{-3}$	$5.1361 \cdot 10^{-3}$	$9.9862 \cdot 10^{-3}$	$7.2877 \cdot 10^{-3}$	$8.8739 \cdot 10^{-4}$	$9.0285 \cdot 10^{-4}$
	20	$1.2946 \cdot 10^{-2}$	$6.1662 \cdot 10^{-2}$	$4.6358 \cdot 10^{-3}$	$3.2380 \cdot 10^{-2}$	$3.6872 \cdot 10^{-2}$	$3.9262 \cdot 10^{-2}$	$1.0406 \cdot 10^{-3}$	$1.0068 \cdot 10^{-3}$
	40	$1.6038 \cdot 10^{-1}$	$6.8628 \cdot 10^{-1}$	$1.3846 \cdot 10^{-2}$	$3.8810 \cdot 10^{-1}$	$3.8423 \cdot 10^{-1}$	$5.4286 \cdot 10^{-1}$	$2.6063 \cdot 10^{-3}$	$7.0749 \cdot 10^{-3}$
	80	$2.6798 \cdot 10^{0}$	$1.8177 \cdot 10^{1}$	$1.0972 \cdot 10^{-1}$	$6.4892 \cdot 10^{0}$	$5.9135 \cdot 10^{0}$	$1.6723 \cdot 10^{1}$	$2.6251 \cdot 10^{-2}$	$3.4412 \cdot 10^{-2}$
	160	—	—	$4.1364 \cdot 10^{-1}$	—	—	—	$1.7651 \cdot 10^{-1}$	$1.4636 \cdot 10^{-1}$
	320	—	—	$1.8656 \cdot 10^{0}$	—	—	—	$6.5280 \cdot 10^{-1}$	$1.2784 \cdot 10^{0}$
	640	—	—	$7.5083 \cdot 10^{0}$	—	—	—	$2.1871 \cdot 10^{0}$	$7.9691 \cdot 10^{0}$

Table 8.6: Comparison of LCP solvers for Two-asset American Basket Straddle.

		Methods							
	N_s	PSOR	Modulus	Multiplier	PSOR-BS	PSOR-BICGSTAB	PSOR-BICGSTAB-Pre	Lemke	Howard
Runtime	10	$8.3401 \cdot 10^{-2}$	$3.4235 \cdot 10^{-1}$	$1.0703 \cdot 10^{-1}$	$1.2334 \cdot 10^{-1}$	$2.2829 \cdot 10^{-1}$	$1.1828 \cdot 10^{-1}$	$2.1652 \cdot 10^{-2}$	$6.7278 \cdot 10^{-2}$
	20	$2.4616 \cdot 10^{0}$	$7.3832 \cdot 10^{-1}$	$9.2621 \cdot 10^{-2}$	$2.7551 \cdot 10^{0}$	$3.4185 \cdot 10^{0}$	$2.2954 \cdot 10^{0}$	$1.4685 \cdot 10^{-1}$	$2.2101 \cdot 10^{-1}$
	40	$1.0408 \cdot 10^{2}$	$5.5434 \cdot 10^{0}$	$1.0228 \cdot 10^{0}$	$1.1887 \cdot 10^{2}$	$1.0104 \cdot 10^{2}$	$1.0163 \cdot 10^{2}$	$1.4413 \cdot 10^{1}$	$4.4164 \cdot 10^{0}$
	80	$4.8280 \cdot 10^{3}$	$2.0041 \cdot 10^{2}$	$1.2486 \cdot 10^{1}$	$4.9043 \cdot 10^{3}$	$4.8997 \cdot 10^{3}$	$4.6279 \cdot 10^{3}$	$2.2409 \cdot 10^{2}$	$1.3036 \cdot 10^{1}$
	160	—	—	$8.8312 \cdot 10^{1}$	—	—	—	$5.3384 \cdot 10^{3}$	$6.4107 \cdot 10^{1}$
	320	—	—	$6.3204 \cdot 10^{2}$	—	—	—	$7.3340 \cdot 10^{4}$	$8.0182 \cdot 10^{2}$
	640	—	—	$6.6321 \cdot 10^{3}$	—	—	—	$8.0399 \cdot 10^{5}$	$4.0091 \cdot 10^{4}$
Iteration	10	37	25	9	9	9	3	35	8
	20	155	38	15	33	33	3	166	15
	40	567	67	28	103	103	3	729	26
	80	1797	112	52	361	361	4	3018	49
	160	—	—	104	—	—	—	12370	96
	320	—	—	207	—	—	—	49964	189
	640	—	—	387	—	—	—	100000	375
RPI	10	$2.2541 \cdot 10^{-3}$	$1.3694 \cdot 10^{-2}$	$1.1892 \cdot 10^{-2}$	$1.3704 \cdot 10^{-2}$	$2.5365 \cdot 10^{-2}$	$3.9427 \cdot 10^{-2}$	$6.1863 \cdot 10^{-4}$	$8.4098 \cdot 10^{-3}$
	20	$1.5881 \cdot 10^{-2}$	$1.9430 \cdot 10^{-2}$	$6.1747 \cdot 10^{-3}$	$8.3489 \cdot 10^{-2}$	$1.0359 \cdot 10^{-1}$	$7.6513 \cdot 10^{-1}$	$8.8463 \cdot 10^{-4}$	$1.4734 \cdot 10^{-2}$
	40	$1.8355 \cdot 10^{-1}$	$8.2737 \cdot 10^{-2}$	$3.6529 \cdot 10^{-2}$	$1.1541 \cdot 10^{0}$	$9.8093 \cdot 10^{-1}$	$3.3876 \cdot 10^{1}$	$1.9771 \cdot 10^{-2}$	$1.6986 \cdot 10^{-1}$
	80	$2.6867 \cdot 10^{0}$	$1.7894 \cdot 10^{0}$	$2.4011 \cdot 10^{-1}$	$1.3585 \cdot 10^{1}$	$1.3572 \cdot 10^{1}$	$1.1570 \cdot 10^{3}$	$7.4253 \cdot 10^{-2}$	$2.6605 \cdot 10^{-1}$
	160	—	—	$8.4916 \cdot 10^{-1}$	—	—	—	$4.3156 \cdot 10^{-1}$	$6.6778 \cdot 10^{-1}$
	320	—	—	$3.0533 \cdot 10^{0}$	—	—	—	$1.4678 \cdot 10^{0}$	$4.2424 \cdot 10^{0}$
	640	—	—	$1.7137 \cdot 10^{1}$	—	—	—	$8.0399 \cdot 10^{0}$	$1.0691 \cdot 10^{2}$

Table 8.7: Comparison of LCP solvers for Two-asset Perpetual Basket Straddle.

		Methods							
	N_s	PSOR	Modulus	Multiplier	PSOR-BS	PSOR-BICGSTAB	PSOR-BICGSTAB-Pre	Lemke	Howard
Runtime	10	$6.7343 \cdot 10^{-1}$	$7.9973 \cdot 10^{0}$	$5.1347 \cdot 10^{-2}$	$5.4540 \cdot 10^{-1}$	$5.3120 \cdot 10^{-1}$	$7.3544 \cdot 10^{-1}$	$1.2305 \cdot 10^{-1}$	$3.1608 \cdot 10^{-2}$
	20	$2.8760 \cdot 10^{2}$	$2.2979 \cdot 10^{3}$	$2.3688 \cdot 10^{0}$	$1.5165 \cdot 10^{2}$	$1.5041 \cdot 10^{2}$	$3.1000 \cdot 10^{2}$	$4.3469 \cdot 10^{1}$	$6.7820 \cdot 10^{-1}$
	40	—	—	$7.3888 \cdot 10^{1}$	—	—	—	$1.1608 \cdot 10^{4}$	$5.1400 \cdot 10^{1}$
	80	—	—	$8.5453 \cdot 10^{3}$	—	—	—	—	$5.5469 \cdot 10^{3}$
Iteration	10	8.80	17.95	4.25	3.00	3.00	3.00	17.80	4.00
	20	15.65	23.80	5.45	3.60	3.60	3.00	155.55	5.00
	40	—	—	6.65	—	—	—	1366.60	6.35
	80	—	—	9.80	—	—	—	—	9.75
RPI	10	$7.6526 \cdot 10^{-2}$	$4.4553 \cdot 10^{-1}$	$1.2082 \cdot 10^{-2}$	$1.8180 \cdot 10^{-1}$	$1.7707 \cdot 10^{-1}$	$2.4515 \cdot 10^{-1}$	$6.9129 \cdot 10^{-3}$	$7.9020 \cdot 10^{-3}$
	20	$1.8377 \cdot 10^{1}$	$9.6551 \cdot 10^{1}$	$4.3464 \cdot 10^{-1}$	$4.2124 \cdot 10^{1}$	$4.1781 \cdot 10^{1}$	$1.0333 \cdot 10^{2}$	$2.7945 \cdot 10^{-1}$	$1.3564 \cdot 10^{-1}$
	40	—	—	$1.1111 \cdot 10^{1}$	—	—	—	$8.4942 \cdot 10^{0}$	$8.0944 \cdot 10^{0}$
	80	—	—	$8.7197 \cdot 10^{2}$	—	—	—	—	$5.6892 \cdot 10^{2}$

Table 8.8: Comparison of LCP solvers for Three-asset American Basket Straddle.

		Methods							
	N_s	PSOR	Modulus	Multiplier	PSOR-BS	PSOR-BICGSTAB	PSOR-BICGSTAB-Pre	Lemke	Howard
Runtime	10	$5.1667 \cdot 10^{0}$	$9.8826 \cdot 10^{0}$	$1.5129 \cdot 10^{0}$	$1.7822 \cdot 10^{0}$	$2.7351 \cdot 10^{0}$	$3.3486 \cdot 10^{0}$	$1.4584 \cdot 10^{1}$	$4.3977 \cdot 10^{-1}$
	20	$3.5753 \cdot 10^{3}$	$2.5667 \cdot 10^{3}$	$3.5458 \cdot 10^{1}$	$4.8393 \cdot 10^{2}$	$4.8373 \cdot 10^{2}$	$3.4419 \cdot 10^{3}$	$7.4429 \cdot 10^{3}$	$1.1543 \cdot 10^{1}$
	40	—	—	$2.1605 \cdot 10^{3}$	—	—	—	—	$8.1799 \cdot 10^{2}$
	80	—	—	$7.0672 \cdot 10^{5}$	—	—	—	—	$1.9330 \cdot 10^{5}$
Iteration	10	42	59	12	4	4	3	734	10
	20	179	109	23	7	7	3	6908	18
	40	—	—	42	—	—	—	—	33
	80	—	—	473	—	—	—	—	63
RPI	10	$1.2302 \cdot 10^{-1}$	$1.6750 \cdot 10^{-1}$	$1.2608 \cdot 10^{-1}$	$4.4556 \cdot 10^{-1}$	$6.8377 \cdot 10^{-1}$	$1.1162 \cdot 10^{0}$	$1.9870 \cdot 10^{-2}$	$4.3977 \cdot 10^{-2}$
	20	$1.9974 \cdot 10^{1}$	$2.3547 \cdot 10^{1}$	$1.5417 \cdot 10^{0}$	$6.9134 \cdot 10^{1}$	$6.9104 \cdot 10^{1}$	$1.1473 \cdot 10^{3}$	$1.0774 \cdot 10^{0}$	$6.4125 \cdot 10^{-1}$
	40	—	—	$5.1440 \cdot 10^{1}$	—	—	—	—	$2.4788 \cdot 10^{1}$
	80	—	—	$9.6811 \cdot 10^{3}$	—	—	—	—	$3.0682 \cdot 10^{3}$

Table 8.9: Comparison of LCP solvers for Three-asset Perpetual Basket Straddle.

	Errors of Lemke's Method in Two-asset Perpetual Straddle				
N_s	MSE	MRE	H_0	H_1	$H_{1,w}$
320	$5.0155 \cdot 10^{-25}$	0.0000%	$1.7066 \cdot 10^{-9}$	$1.7151 \cdot 10^{-9}$	$1.7161 \cdot 10^{-8}$
640	$6.0808 \cdot 10^{2}$	47.3560%	$6.2984 \cdot 10^{4}$	$6.3001 \cdot 10^{4}$	$6.7291 \cdot 10^{4}$

Table 8.10: Lemke's method reaches maximum iteration at $N_s = 640$.

		Errors of Modulus Method				
Type	N_s	MSE	MRE	H_0	H_1	$H_{1,w}$
One-asset American	1280	$1.2948 \cdot 10^{-1}$	5.7870%	$1.8184 \cdot 10^{1}$	$1.8207 \cdot 10^{1}$	$3.6889 \cdot 10^{1}$
One-asset Perpetual	1280	$1.5438 \cdot 10^{3}$	71.5119%	$1.9872 \cdot 10^{3}$	$1.9873 \cdot 10^{3}$	$2.0520 \cdot 10^{3}$
Two-asset American	80	$4.9458 \cdot 10^{1}$	91.5411%	$1.7435 \cdot 10^{4}$	$1.7437 \cdot 10^{4}$	$2.3336 \cdot 10^{4}$
Two-asset Perpetual	80	$1.9312 \cdot 10^{3}$	90.9663%	$1.1005 \cdot 10^{5}$	$1.1005 \cdot 10^{5}$	$1.1790 \cdot 10^{5}$
Three-asset American	20	$1.8045 \cdot 10^{2}$	84.3624%	$1.4897 \cdot 10^{6}$	$1.4898 \cdot 10^{6}$	$2.0755 \cdot 10^{6}$
Three-asset Perpetual	20	$7.7012 \cdot 10^{3}$	85.9248%	$9.7790 \cdot 10^{6}$	$9.7792 \cdot 10^{6}$	$1.3563 \cdot 10^{7}$

Table 8.11: Errors of Modulus Method.

8.5 Discretization Error

Overall, Howard's method is the speediest of all the unbiased algorithms compared in the previous section. On the merits of its computational speed, we adopt Howard's method as the default algorithm from this section on to investigate numerical errors. In order to obtain sharp results of numerical errors, we also raise the stopping criteria to $tol = 10^{-6}$ hereafter.

In this section, we shall investigate the discretization errors when given different numbers of partitions (or mesh sizes) in spatial and time axes. Once again, we will consider the (basket) straddle case of European, American and perpetual options in our experiments and summarize their results in the tables [8.12], [8.13], [8.14], [8.15], [8.16], [8.17], [8.18], [8.19] and [8.20]. In each table/case, we define the benchmark solution as the following interpolant

$$v_* := I_h v_{h^*}$$

where I_h is a linear interpolant operator on a uniform coarse mesh with edge size h and v_{h^*} is the numerical solution on the finest mesh with edge size h^* in each table/case. We then take this linear interpolant $v_*(0, \mathbf{S})$ as the benchmark solution against the numerical solution $v_h(0, \mathbf{S})$ computed with the same coarse mesh h for all $\mathbf{S} \in \mathcal{N}_h$. The nodal errors of the coarse mesh are computed and utilized to compute the discretization errors in terms of the five types introduced earlier.

When considering time-dependent cases in tables [8.12], [8.13], [8.15], [8.16], [8.18] and [8.19], we first observe that given a fixed N_t (in each column of each table), the errors decrease and then increase as N_s doubles. This illustrates that when time term is involved, discretization errors can not be reduced by simply using finer spatial mesh. Once the mesh size is reduced to some extent, it starts to bring more time integration errors and raise the overall discretization errors. If the errors are compared column by column (i.e. with increasingly large N_t), it is found that the minimum errors (in red) of each column is actually becoming smaller as N_t and N_s both increase. Particularly, when the time

mesh is fine enough such as the last column with the largest N_t in each table, then the discretization errors are apparently reduced as N_s doubles. Similarly, given the largest N_s (with the finest spatial mesh) on the last row of each case, we observe the discretization errors decrease as N_t increase. As to the perpetual examples shown in tables [8.14], [8.17] and [8.20], it simply shows the monotone descendant trend as N_s ascends because there is no errors caused by time integration in these cases. These observations verify that the discretization errors go to zero as the mesh sizes in space and time becomes smaller and smaller in all cases.

It is also interesting to find the patterns of smallest errors are similar (or even identical) when measured in different types in each case. Take the two-asset American basket straddle option in table [8.16] as an example, we notice the H_0 and H_1 errors both reach their smallest values at $N_s = 160$ when $N_t = 10, 20, 40$ and $N_s = 320$ when $N_t = 80, 160$ while $H_{1,w}$, MSE and MRE errors have similar but slightly different patterns. We also notice that, for all the five errors in the time-dependent cases, the smallest error in a column with smaller N_t (and even smaller N_s) is reduced more than half compared with that in the previous column. However, the convergence rate with doubling N_s is not apparent in our experiments of perpetual options.

8.6 Truncation Error

In the previous section, we fixed the far-field bound $S_{\max} = 2560$ which may introduce truncation errors in each case. To investigate how truncation errors vary, we define the following far-field bounds and corresponding computational domains. For $i = 1, \ldots, 9$,

$$\begin{aligned} S_{\max}^{(i)} &:= 320 + i \cdot 320 \\ \Omega_i &:= [0, S_{\max}^{(i)}]^d \end{aligned}$$

In order to measure the truncation error sharply, we take the finest mesh (in space and time) of each case as below.

- One-asset case: $h_t = 1/320 = 0.003125$ and $h_s = 2560/5120 = 0.5$;
- Two-asset case: $h_t = 1/320 = 0.003125$ and $h_s = 2560/640 = 4$;
- Three-asset case: $h_t = 1/40 = 0.025$ and $h_s = 2560/80 = 32$.

Again the time terms t and h_t are dropped in perpetual cases. With identical option parameters, we can compute option values over each Ω_i and denote a nodal solution at time t by $v_i(t, \mathbf{S})$ where $\mathbf{S}$ is a spatial node of the mesh over Ω_i. To measure the truncation errors properly, we adopt Nielsen's approach in [72] and define

$$TE := \frac{||v_i(0, \mathbf{S}) - v_*(0, \mathbf{S})||_{H(\Omega_i)}}{||v_*(0, \mathbf{S})||_{H(\Omega_i)}}$$

		N_t					
Error Type	(N_s, N_u)	10	20	40	80	160	320
MSE	$(10, 9)$	$3.7992 \cdot 10^{0}$	$3.9897 \cdot 10^{0}$	$4.1192 \cdot 10^{0}$	$4.1929 \cdot 10^{0}$	$4.2320 \cdot 10^{0}$	$4.2522 \cdot 10^{0}$
	$(20, 19)$	$4.5512 \cdot 10^{0}$	$4.6346 \cdot 10^{0}$	$4.7063 \cdot 10^{0}$	$4.7500 \cdot 10^{0}$	$4.7739 \cdot 10^{0}$	$4.7863 \cdot 10^{0}$
	$(40, 39)$	$3.6816 \cdot 10^{-1}$	$3.3294 \cdot 10^{-1}$	$3.4505 \cdot 10^{-1}$	$3.5890 \cdot 10^{-1}$	$3.6783 \cdot 10^{-1}$	$3.7280 \cdot 10^{-1}$
	$(80, 79)$	$1.3832 \cdot 10^{-1}$	$4.8955 \cdot 10^{-2}$	$3.2782 \cdot 10^{-2}$	$3.2188 \cdot 10^{-2}$	$3.3812 \cdot 10^{-2}$	$3.5110 \cdot 10^{-2}$
	$(160, 159)$	$1.3896 \cdot 10^{-1}$	$3.2223 \cdot 10^{-2}$	$7.0097 \cdot 10^{-3}$	$1.8016 \cdot 10^{-3}$	$1.0942 \cdot 10^{-3}$	$1.2206 \cdot 10^{-3}$
	$(320, 319)$	$1.4309 \cdot 10^{-1}$	$3.3852 \cdot 10^{-2}$	$7.2470 \cdot 10^{-3}$	$1.3055 \cdot 10^{-3}$	$2.2189 \cdot 10^{-4}$	$1.5783 \cdot 10^{-4}$
	$(640, 639)$	$1.4565 \cdot 10^{-1}$	$3.5082 \cdot 10^{-2}$	$7.7582 \cdot 10^{-3}$	$1.4437 \cdot 10^{-3}$	$1.7010 \cdot 10^{-4}$	$1.0133 \cdot 10^{-5}$
	$(1280, 1279)$	$1.4550 \cdot 10^{-1}$	$3.5038 \cdot 10^{-2}$	$7.7406 \cdot 10^{-3}$	$1.4325 \cdot 10^{-3}$	$1.6027 \cdot 10^{-4}$	$5.7397 \cdot 10^{-7}$
	$(2560, 2559)$	$1.4543 \cdot 10^{-1}$	$3.5022 \cdot 10^{-2}$	$7.7365 \cdot 10^{-3}$	$1.4312 \cdot 10^{-3}$	$1.5962 \cdot 10^{-4}$	$2.2987 \cdot 10^{-8}$
	$(5120, 5119)$	$1.4540 \cdot 10^{-1}$	$3.5014 \cdot 10^{-2}$	$7.7348 \cdot 10^{-3}$	$1.4309 \cdot 10^{-3}$	$1.5956 \cdot 10^{-4}$	0
MRE	$(10, 9)$	2.6404%	2.6687%	2.6831%	2.6904%	2.6940%	2.6958%
	$(20, 19)$	7.7890%	7.9210%	7.9881%	8.0220%	8.0390%	8.0476%
	$(40, 39)$	4.5210%	5.0718%	5.3484%	5.4870%	5.5564%	5.5910%
	$(80, 79)$	0.7674%	1.3006%	1.5706%	1.7183%	1.7939%	1.8317%
	$(160, 159)$	0.9324%	0.2655%	0.0983%	0.2384%	0.3227%	0.3648%
	$(320, 319)$	1.1602%	0.4897%	0.1525%	0.0240%	0.1022%	0.1446%
	$(640, 639)$	1.3400%	0.6599%	0.3179%	0.1465%	0.0616%	0.0294%
	$(1280, 1279)$	1.3260%	0.6462%	0.3043%	0.1329%	0.0472%	0.0070%
	$(2560, 2559)$	1.3225%	0.6428%	0.3009%	0.1296%	0.0438%	0.0014%
	$(5120, 5119)$	1.3216%	0.6419%	0.3001%	0.1287%	0.0429%	0%
H_0	$(10, 9)$	$8.1146 \cdot 10^{1}$	$8.3427 \cdot 10^{1}$	$8.4970 \cdot 10^{1}$	$8.5841 \cdot 10^{1}$	$8.6302 \cdot 10^{1}$	$8.6538 \cdot 10^{1}$
	$(20, 19)$	$9.5727 \cdot 10^{1}$	$9.6380 \cdot 10^{1}$	$9.7067 \cdot 10^{1}$	$9.7502 \cdot 10^{1}$	$9.7743 \cdot 10^{1}$	$9.7869 \cdot 10^{1}$
	$(40, 39)$	$2.8973 \cdot 10^{1}$	$2.7009 \cdot 10^{1}$	$2.7332 \cdot 10^{1}$	$2.7837 \cdot 10^{1}$	$2.8173 \cdot 10^{1}$	$2.8361 \cdot 10^{1}$
	$(80, 79)$	$1.8667 \cdot 10^{1}$	$1.1007 \cdot 10^{1}$	$8.8915 \cdot 10^{0}$	$8.7639 \cdot 10^{0}$	$8.9721 \cdot 10^{0}$	$9.1414 \cdot 10^{0}$
	$(160, 159)$	$1.8790 \cdot 10^{1}$	$9.0510 \cdot 10^{0}$	$4.2210 \cdot 10^{0}$	$2.1317 \cdot 10^{0}$	$1.6479 \cdot 10^{0}$	$1.7374 \cdot 10^{0}$
	$(320, 319)$	$1.9104 \cdot 10^{1}$	$9.2928 \cdot 10^{0}$	$4.2999 \cdot 10^{0}$	$1.8251 \cdot 10^{0}$	$7.5192 \cdot 10^{-1}$	$6.3314 \cdot 10^{-1}$
	$(640, 639)$	$1.9293 \cdot 10^{1}$	$9.4687 \cdot 10^{0}$	$4.4527 \cdot 10^{0}$	$1.9208 \cdot 10^{0}$	$6.5933 \cdot 10^{-1}$	$1.6089 \cdot 10^{-1}$
	$(1280, 1279)$	$1.9291 \cdot 10^{1}$	$9.4670 \cdot 10^{0}$	$4.4496 \cdot 10^{0}$	$1.9142 \cdot 10^{0}$	$6.4028 \cdot 10^{-1}$	$3.8314 \cdot 10^{-2}$
	$(2560, 2559)$	$1.9291 \cdot 10^{1}$	$9.4668 \cdot 10^{0}$	$4.4494 \cdot 10^{0}$	$1.9137 \cdot 10^{0}$	$6.3912 \cdot 10^{-1}$	$7.6677 \cdot 10^{-3}$
	$(5120, 5119)$	$1.9291 \cdot 10^{1}$	$9.4668 \cdot 10^{0}$	$4.4494 \cdot 10^{0}$	$1.9137 \cdot 10^{0}$	$6.3906 \cdot 10^{-1}$	0
H_1	$(10, 9)$	$8.1147 \cdot 10^{1}$	$8.3428 \cdot 10^{1}$	$8.4971 \cdot 10^{1}$	$8.5842 \cdot 10^{1}$	$8.6303 \cdot 10^{1}$	$8.6539 \cdot 10^{1}$
	$(20, 19)$	$9.5731 \cdot 10^{1}$	$9.6384 \cdot 10^{1}$	$9.7070 \cdot 10^{1}$	$9.7506 \cdot 10^{1}$	$9.7747 \cdot 10^{1}$	$9.7873 \cdot 10^{1}$
	$(40, 39)$	$2.8975 \cdot 10^{1}$	$2.7012 \cdot 10^{1}$	$2.7335 \cdot 10^{1}$	$2.7840 \cdot 10^{1}$	$2.8176 \cdot 10^{1}$	$2.8364 \cdot 10^{1}$
	$(80, 79)$	$1.8667 \cdot 10^{1}$	$1.1008 \cdot 10^{1}$	$8.8928 \cdot 10^{0}$	$8.7654 \cdot 10^{0}$	$8.9737 \cdot 10^{0}$	$9.1430 \cdot 10^{0}$
	$(160, 159)$	$1.8791 \cdot 10^{1}$	$9.0511 \cdot 10^{0}$	$4.2210 \cdot 10^{0}$	$2.1319 \cdot 10^{0}$	$1.6484 \cdot 10^{0}$	$1.7380 \cdot 10^{0}$
	$(320, 319)$	$1.9105 \cdot 10^{1}$	$9.2930 \cdot 10^{0}$	$4.2999 \cdot 10^{0}$	$1.8251 \cdot 10^{0}$	$7.5197 \cdot 10^{-1}$	$6.3328 \cdot 10^{-1}$
	$(640, 639)$	$1.9293 \cdot 10^{1}$	$9.4689 \cdot 10^{0}$	$4.4528 \cdot 10^{0}$	$1.9209 \cdot 10^{0}$	$6.5935 \cdot 10^{-1}$	$1.6091 \cdot 10^{-1}$
	$(1280, 1279)$	$1.9292 \cdot 10^{1}$	$9.4672 \cdot 10^{0}$	$4.4498 \cdot 10^{0}$	$1.9142 \cdot 10^{0}$	$6.4030 \cdot 10^{-1}$	$3.8318 \cdot 10^{-2}$
	$(2560, 2559)$	$1.9292 \cdot 10^{1}$	$9.4671 \cdot 10^{0}$	$4.4495 \cdot 10^{0}$	$1.9138 \cdot 10^{0}$	$6.3914 \cdot 10^{-1}$	$7.6800 \cdot 10^{-3}$
	$(5120, 5119)$	$1.9292 \cdot 10^{1}$	$9.4671 \cdot 10^{0}$	$4.4495 \cdot 10^{0}$	$1.9138 \cdot 10^{0}$	$6.3908 \cdot 10^{-1}$	0
$H_{1,w}$	$(10, 9)$	$8.8208 \cdot 10^{1}$	$9.1307 \cdot 10^{1}$	$9.3488 \cdot 10^{1}$	$9.4732 \cdot 10^{1}$	$9.5392 \cdot 10^{1}$	$9.5732 \cdot 10^{1}$
	$(20, 19)$	$1.0627 \cdot 10^{2}$	$1.0678 \cdot 10^{2}$	$1.0761 \cdot 10^{2}$	$1.0817 \cdot 10^{2}$	$1.0848 \cdot 10^{2}$	$1.0865 \cdot 10^{2}$
	$(40, 39)$	$3.5396 \cdot 10^{1}$	$3.2038 \cdot 10^{1}$	$3.2228 \cdot 10^{1}$	$3.2828 \cdot 10^{1}$	$3.3251 \cdot 10^{1}$	$3.3492 \cdot 10^{1}$
	$(80, 79)$	$2.4572 \cdot 10^{1}$	$1.4196 \cdot 10^{1}$	$1.1236 \cdot 10^{1}$	$1.1028 \cdot 10^{1}$	$1.1302 \cdot 10^{1}$	$1.1532 \cdot 10^{1}$
	$(160, 159)$	$2.4941 \cdot 10^{1}$	$1.2009 \cdot 10^{1}$	$5.5872 \cdot 10^{0}$	$2.8317 \cdot 10^{0}$	$2.2655 \cdot 10^{0}$	$2.4326 \cdot 10^{0}$
	$(320, 319)$	$2.5441 \cdot 10^{1}$	$1.2368 \cdot 10^{1}$	$5.7167 \cdot 10^{0}$	$2.4146 \cdot 10^{0}$	$9.7494 \cdot 10^{-1}$	$8.2751 \cdot 10^{-1}$
	$(640, 639)$	$2.5730 \cdot 10^{1}$	$1.2628 \cdot 10^{1}$	$5.9300 \cdot 10^{0}$	$2.5521 \cdot 10^{0}$	$8.6245 \cdot 10^{-1}$	$1.7729 \cdot 10^{-1}$
	$(1280, 1279)$	$2.5753 \cdot 10^{1}$	$1.2637 \cdot 10^{1}$	$5.9389 \cdot 10^{0}$	$2.5533 \cdot 10^{0}$	$8.5193 \cdot 10^{-1}$	$4.2222 \cdot 10^{-2}$
	$(2560, 2559)$	$2.5763 \cdot 10^{1}$	$1.2643 \cdot 10^{1}$	$5.9407 \cdot 10^{0}$	$2.5549 \cdot 10^{0}$	$8.5290 \cdot 10^{-1}$	$8.4493 \cdot 10^{-3}$
	$(5120, 5119)$	$2.5767 \cdot 10^{1}$	$1.2644 \cdot 10^{1}$	$5.9421 \cdot 10^{0}$	$2.5556 \cdot 10^{0}$	$8.5340 \cdot 10^{-1}$	0

Table 8.12: Discretization Errors for One-asset European Straddle Option.

		N_t					
Error Type	(N_s, N_u)	10	20	40	80	160	320
MSE	$(10, 9)$	$3.8592 \cdot 10^{0}$	$3.9193 \cdot 10^{0}$	$3.9500 \cdot 10^{0}$	$3.9656 \cdot 10^{0}$	$3.9734 \cdot 10^{0}$	$3.9773 \cdot 10^{0}$
	$(20, 19)$	$3.3772 \cdot 10^{0}$	$3.5080 \cdot 10^{0}$	$3.5763 \cdot 10^{0}$	$3.6111 \cdot 10^{0}$	$3.6287 \cdot 10^{0}$	$3.6376 \cdot 10^{0}$
	$(40, 39)$	$1.6775 \cdot 10^{-1}$	$2.0965 \cdot 10^{-1}$	$2.3392 \cdot 10^{-1}$	$2.4695 \cdot 10^{-1}$	$2.5371 \cdot 10^{-1}$	$2.5714 \cdot 10^{-1}$
	$(80, 79)$	$6.6814 \cdot 10^{-3}$	$1.6449 \cdot 10^{-2}$	$2.4871 \cdot 10^{-2}$	$3.0274 \cdot 10^{-2}$	$3.3278 \cdot 10^{-2}$	$3.4857 \cdot 10^{-2}$
	$(160, 159)$	$3.6498 \cdot 10^{-3}$	$1.1743 \cdot 10^{-3}$	$5.3692 \cdot 10^{-4}$	$8.3513 \cdot 10^{-4}$	$1.3903 \cdot 10^{-3}$	$1.7867 \cdot 10^{-3}$
	$(320, 319)$	$3.3934 \cdot 10^{-3}$	$9.7066 \cdot 10^{-4}$	$2.3308 \cdot 10^{-4}$	$3.8754 \cdot 10^{-5}$	$4.5095 \cdot 10^{-5}$	$1.3244 \cdot 10^{-4}$
	$(640, 639)$	$3.4391 \cdot 10^{-3}$	$1.0044 \cdot 10^{-3}$	$2.4707 \cdot 10^{-4}$	$4.8855 \cdot 10^{-5}$	$5.8044 \cdot 10^{-6}$	$1.2324 \cdot 10^{-6}$
	$(1280, 1279)$	$3.4656 \cdot 10^{-3}$	$1.0113 \cdot 10^{-3}$	$2.5297 \cdot 10^{-4}$	$5.0536 \cdot 10^{-5}$	$5.7500 \cdot 10^{-6}$	$7.5104 \cdot 10^{-8}$
	$(2560, 2559)$	$3.4682 \cdot 10^{-3}$	$1.0123 \cdot 10^{-3}$	$2.5492 \cdot 10^{-4}$	$5.1542 \cdot 10^{-5}$	$6.0659 \cdot 10^{-6}$	$2.3412 \cdot 10^{-9}$
	$(5120, 5119)$	$3.4670 \cdot 10^{-3}$	$1.0129 \cdot 10^{-3}$	$2.5521 \cdot 10^{-4}$	$5.1767 \cdot 10^{-5}$	$6.1606 \cdot 10^{-6}$	0
MRE	$(10, 9)$	4.8311%	4.8311%	4.8311%	4.8311%	4.8311%	4.8311%
	$(20, 19)$	8.0413%	8.1987%	8.2794%	8.3202%	8.3408%	8.3511%
	$(40, 39)$	3.7754%	4.4095%	4.7346%	4.8991%	4.9824%	5.0241%
	$(80, 79)$	0.6184%	1.2394%	1.5628%	1.7507%	1.8546%	1.9068%
	$(160, 159)$	0.6728%	0.3213%	0.3277%	0.3270%	0.3772%	0.4481%
	$(320, 319)$	0.6849%	0.3692%	0.1771%	0.0584%	0.0713%	0.1379%
	$(640, 639)$	0.6887%	0.3804%	0.1905%	0.0847%	0.0268%	0.0138%
	$(1280, 1279)$	0.6907%	0.3821%	0.1937%	0.0872%	0.0293%	0.0038%
	$(2560, 2559)$	0.6909%	0.3824%	0.1945%	0.0883%	0.0305%	0.0005%
	$(5120, 5119)$	0.6908%	0.3826%	0.1947%	0.0885%	0.0307%	0%
H_0	$(10, 9)$	$8.5188 \cdot 10^{1}$	$8.5804 \cdot 10^{1}$	$8.6116 \cdot 10^{1}$	$8.6274 \cdot 10^{1}$	$8.6353 \cdot 10^{1}$	$8.6393 \cdot 10^{1}$
	$(20, 19)$	$7.9482 \cdot 10^{1}$	$8.0970 \cdot 10^{1}$	$8.1739 \cdot 10^{1}$	$8.2128 \cdot 10^{1}$	$8.2323 \cdot 10^{1}$	$8.2422 \cdot 10^{1}$
	$(40, 39)$	$1.9403 \cdot 10^{1}$	$2.1608 \cdot 10^{1}$	$2.2771 \cdot 10^{1}$	$2.3368 \cdot 10^{1}$	$2.3671 \cdot 10^{1}$	$2.3823 \cdot 10^{1}$
	$(80, 79)$	$3.9441 \cdot 10^{0}$	$6.3030 \cdot 10^{0}$	$7.7736 \cdot 10^{0}$	$8.5828 \cdot 10^{0}$	$9.0010 \cdot 10^{0}$	$9.2131 \cdot 10^{0}$
	$(160, 159)$	$3.0040 \cdot 10^{0}$	$1.6656 \cdot 10^{0}$	$1.0653 \cdot 10^{0}$	$1.3596 \cdot 10^{0}$	$1.8007 \cdot 10^{0}$	$2.0580 \cdot 10^{0}$
	$(320, 319)$	$2.9345 \cdot 10^{0}$	$1.5699 \cdot 10^{0}$	$7.6916 \cdot 10^{-1}$	$3.1235 \cdot 10^{-1}$	$3.3687 \cdot 10^{-1}$	$5.7912 \cdot 10^{-1}$
	$(640, 639)$	$2.9625 \cdot 10^{0}$	$1.6011 \cdot 10^{0}$	$7.9413 \cdot 10^{-1}$	$3.5312 \cdot 10^{-1}$	$1.2159 \cdot 10^{-1}$	$5.5677 \cdot 10^{-2}$
	$(1280, 1279)$	$2.9768 \cdot 10^{0}$	$1.6081 \cdot 10^{0}$	$8.0429 \cdot 10^{-1}$	$3.5947 \cdot 10^{-1}$	$1.2124 \cdot 10^{-1}$	$1.3748 \cdot 10^{-2}$
	$(2560, 2559)$	$2.9790 \cdot 10^{0}$	$1.6094 \cdot 10^{0}$	$8.0765 \cdot 10^{-1}$	$3.6316 \cdot 10^{-1}$	$1.2458 \cdot 10^{-1}$	$2.4397 \cdot 10^{-3}$
	$(5120, 5119)$	$2.9788 \cdot 10^{0}$	$1.6101 \cdot 10^{0}$	$8.0820 \cdot 10^{-1}$	$3.6400 \cdot 10^{-1}$	$1.2557 \cdot 10^{-1}$	0
H_1	$(10, 9)$	$8.5189 \cdot 10^{1}$	$8.5805 \cdot 10^{1}$	$8.6117 \cdot 10^{1}$	$8.6275 \cdot 10^{1}$	$8.6354 \cdot 10^{1}$	$8.6394 \cdot 10^{1}$
	$(20, 19)$	$7.9487 \cdot 10^{1}$	$8.0974 \cdot 10^{1}$	$8.1743 \cdot 10^{1}$	$8.2132 \cdot 10^{1}$	$8.2328 \cdot 10^{1}$	$8.2426 \cdot 10^{1}$
	$(40, 39)$	$1.9405 \cdot 10^{1}$	$2.1610 \cdot 10^{1}$	$2.2773 \cdot 10^{1}$	$2.3371 \cdot 10^{1}$	$2.3673 \cdot 10^{1}$	$2.3826 \cdot 10^{1}$
	$(80, 79)$	$3.9451 \cdot 10^{0}$	$6.3039 \cdot 10^{0}$	$7.7745 \cdot 10^{0}$	$8.5838 \cdot 10^{0}$	$9.0021 \cdot 10^{0}$	$9.2142 \cdot 10^{0}$
	$(160, 159)$	$3.0050 \cdot 10^{0}$	$1.6671 \cdot 10^{0}$	$1.0678 \cdot 10^{0}$	$1.3620 \cdot 10^{0}$	$1.8026 \cdot 10^{0}$	$2.0598 \cdot 10^{0}$
	$(320, 319)$	$2.9353 \cdot 10^{0}$	$1.5703 \cdot 10^{0}$	$7.6935 \cdot 10^{-1}$	$3.1255 \cdot 10^{-1}$	$3.3709 \cdot 10^{-1}$	$5.7933 \cdot 10^{-1}$
	$(640, 639)$	$2.9634 \cdot 10^{0}$	$1.6015 \cdot 10^{0}$	$7.9434 \cdot 10^{-1}$	$3.5322 \cdot 10^{-1}$	$1.2167 \cdot 10^{-1}$	$5.5846 \cdot 10^{-2}$
	$(1280, 1279)$	$2.9777 \cdot 10^{0}$	$1.6086 \cdot 10^{0}$	$8.0451 \cdot 10^{-1}$	$3.5957 \cdot 10^{-1}$	$1.2129 \cdot 10^{-1}$	$1.3916 \cdot 10^{-2}$
	$(2560, 2559)$	$2.9799 \cdot 10^{0}$	$1.6099 \cdot 10^{0}$	$8.0787 \cdot 10^{-1}$	$3.6326 \cdot 10^{-1}$	$1.2461 \cdot 10^{-1}$	$2.4869 \cdot 10^{-3}$
	$(5120, 5119)$	$2.9798 \cdot 10^{0}$	$1.6106 \cdot 10^{0}$	$8.0843 \cdot 10^{-1}$	$3.6410 \cdot 10^{-1}$	$1.2560 \cdot 10^{-1}$	0
$H_{1,w}$	$(10, 9)$	$9.0270 \cdot 10^{1}$	$9.0959 \cdot 10^{1}$	$9.1309 \cdot 10^{1}$	$9.1485 \cdot 10^{1}$	$9.1574 \cdot 10^{1}$	$9.1619 \cdot 10^{1}$
	$(20, 19)$	$9.2346 \cdot 10^{1}$	$9.4125 \cdot 10^{1}$	$9.5040 \cdot 10^{1}$	$9.5503 \cdot 10^{1}$	$9.5737 \cdot 10^{1}$	$9.5854 \cdot 10^{1}$
	$(40, 39)$	$2.2289 \cdot 10^{1}$	$2.5212 \cdot 10^{1}$	$2.6779 \cdot 10^{1}$	$2.7588 \cdot 10^{1}$	$2.8000 \cdot 10^{1}$	$2.8208 \cdot 10^{1}$
	$(80, 79)$	$5.1202 \cdot 10^{0}$	$7.6242 \cdot 10^{0}$	$9.3159 \cdot 10^{0}$	$1.0265 \cdot 10^{1}$	$1.0757 \cdot 10^{1}$	$1.1008 \cdot 10^{1}$
	$(160, 159)$	$4.3019 \cdot 10^{0}$	$2.8612 \cdot 10^{0}$	$2.5475 \cdot 10^{0}$	$2.9372 \cdot 10^{0}$	$3.2870 \cdot 10^{0}$	$3.5238 \cdot 10^{0}$
	$(320, 319)$	$4.2607 \cdot 10^{0}$	$2.2127 \cdot 10^{0}$	$1.0690 \cdot 10^{0}$	$4.9416 \cdot 10^{-1}$	$5.4584 \cdot 10^{-1}$	$8.2999 \cdot 10^{-1}$
	$(640, 639)$	$4.4363 \cdot 10^{0}$	$2.3426 \cdot 10^{0}$	$1.1424 \cdot 10^{0}$	$4.9976 \cdot 10^{-1}$	$1.9269 \cdot 10^{-1}$	$1.5029 \cdot 10^{-1}$
	$(1280, 1279)$	$4.4943 \cdot 10^{0}$	$2.3830 \cdot 10^{0}$	$1.1757 \cdot 10^{0}$	$5.2261 \cdot 10^{-1}$	$1.8087 \cdot 10^{-1}$	$6.8155 \cdot 10^{-2}$
	$(2560, 2559)$	$4.5183 \cdot 10^{0}$	$2.3992 \cdot 10^{0}$	$1.1895 \cdot 10^{0}$	$5.2982 \cdot 10^{-1}$	$1.8060 \cdot 10^{-1}$	$1.5111 \cdot 10^{-2}$
	$(5120, 5119)$	$4.5243 \cdot 10^{0}$	$2.4026 \cdot 10^{0}$	$1.1916 \cdot 10^{0}$	$5.3209 \cdot 10^{-1}$	$1.8251 \cdot 10^{-1}$	0

Table 8.13: Discretization Errors for One-asset American Straddle Option.

(N_s, N_u)	Error Type				
	MSE	MRE	H_0	H_1	$H_{1,w}$
$(10, 9)$	$1.4474 \cdot 10^{2}$	22.9610%	$5.0954 \cdot 10^{2}$	$5.0955 \cdot 10^{2}$	$5.1988 \cdot 10^{2}$
$(20, 19)$	$4.6516 \cdot 10^{-1}$	1.7377%	$3.0728 \cdot 10^{1}$	$3.0729 \cdot 10^{1}$	$3.2168 \cdot 10^{1}$
$(40, 39)$	$3.2089 \cdot 10^{-2}$	0.8167%	$8.4809 \cdot 10^{0}$	$8.4841 \cdot 10^{0}$	$9.8905 \cdot 10^{0}$
$(80, 79)$	$1.1990 \cdot 10^{-2}$	0.2852%	$5.3331 \cdot 10^{0}$	$5.3334 \cdot 10^{0}$	$5.8284 \cdot 10^{0}$
$(160, 159)$	$1.1649 \cdot 10^{-3}$	0.1865%	$1.6429 \cdot 10^{0}$	$1.6448 \cdot 10^{0}$	$2.2903 \cdot 10^{0}$
$(320, 319)$	$5.5589 \cdot 10^{-4}$	0.1156%	$1.1716 \cdot 10^{0}$	$1.1734 \cdot 10^{0}$	$1.7642 \cdot 10^{0}$
$(640, 639)$	$7.0396 \cdot 10^{-7}$	0.0025%	$4.2351 \cdot 10^{-2}$	$4.2376 \cdot 10^{-2}$	$5.4100 \cdot 10^{-2}$
$(1280, 1279)$	$8.0899 \cdot 10^{-8}$	0.0015%	$1.4356 \cdot 10^{-2}$	$1.4545 \cdot 10^{-2}$	$4.8301 \cdot 10^{-2}$
$(2560, 2559)$	$3.1047 \cdot 10^{-8}$	0.0015%	$8.8054 \cdot 10^{-3}$	$8.9643 \cdot 10^{-3}$	$3.7769 \cdot 10^{-2}$

Table 8.14: Discretization Errors for One-asset Perpetual Straddle Option.

where $\mathbf{S} \in \Omega_i$, $v_i(0, \mathbf{S})$ for $i = 1, \cdots, 8$ is computed numerically and $H(\Omega_i)$ is a finite-element norm defined by one of the H_0, H_1 and $H_{1,w}$ norms over Ω_i. We consider the solutions on the largest computational domain Ω_9 the benchmark solution, i.e. $v_* = v_9$ in this section, and find its values either analytically (if applicable) or numerically.

8.6.1 Observation

One-asset Case

Since closed-form valuation is available for one-asset European put (EP), European call (EC), perpetual put (PP), perpetual call (PC) and European straddle (ES), we use their analytical solutions as benchmarks. Besides, due to the complicated payoff of straddle, we also include its American and perpetual types (AS and PS) in our experiment. All the results are listed in table [8.21].

It is obvious there is no big change after $S^{(i)}_{\max} = 960$ for the put options, EP and PP, no matter whether they have early-exercise property or not. This may be due to the fact that all their option values are all close/equal to zero at hight share prices and thus less sensitive to the increase of $S^{(i)}_{\max}$. In contrast, we find the truncation errors of EC and ES, whose values are far from zero at far-field bounds, decrease slowly as $S^{(i)}_{\max}$ increases.

In the other cases with the early-exercise property, the AS, PC and PS options, their identified/exact free boundaries associated with a call part are at $841.5, 1153$ and 1173 separately. It is known that once a share price exceeds the free boundaries, its corresponding option values are simply equal to its payoffs. Echoed with this property, the AS, PC and PS produce the significant slumps of truncation errors after $S^{(i)}_{\max} = 960, 1280$ and 1280. Our LCP solvers even show no numerical difference for AS and PS after Ω_7 and Ω_3 respectively.

		N_t					
Error Type	(N_s, N_u)	10	20	40	80	160	320
MSE	$(10, 81)$	$4.2386 \cdot 10^{0}$	$4.4668 \cdot 10^{0}$	$4.6048 \cdot 10^{0}$	$4.6800 \cdot 10^{0}$	$4.7192 \cdot 10^{0}$	$4.7392 \cdot 10^{0}$
	$(20, 361)$	$5.5120 \cdot 10^{-1}$	$5.3954 \cdot 10^{-1}$	$5.5435 \cdot 10^{-1}$	$5.6719 \cdot 10^{-1}$	$5.7500 \cdot 10^{-1}$	$5.7926 \cdot 10^{-1}$
	$(40, 1521)$	$1.6413 \cdot 10^{-1}$	$1.0141 \cdot 10^{-1}$	$8.9128 \cdot 10^{-2}$	$8.8014 \cdot 10^{-2}$	$8.8747 \cdot 10^{-2}$	$8.9441 \cdot 10^{-2}$
	$(80, 6241)$	$1.2704 \cdot 10^{-1}$	$5.5269 \cdot 10^{-2}$	$3.7915 \cdot 10^{-2}$	$3.4125 \cdot 10^{-2}$	$3.3485 \cdot 10^{-2}$	$3.3483 \cdot 10^{-2}$
	$(160, 25281)$	$1.1249 \cdot 10^{-1}$	$4.0027 \cdot 10^{-2}$	$2.2090 \cdot 10^{-2}$	$1.7947 \cdot 10^{-2}$	$1.7115 \cdot 10^{-2}$	$1.7013 \cdot 10^{-2}$
	$(320, 101761)$	$1.0853 \cdot 10^{-1}$	$3.6104 \cdot 10^{-2}$	$1.8078 \cdot 10^{-2}$	$1.3863 \cdot 10^{-2}$	$1.2987 \cdot 10^{-2}$	$1.2861 \cdot 10^{-2}$
	$(640, 408321)$	$9.4783 \cdot 10^{-2}$	$2.2871 \cdot 10^{-2}$	$5.0576 \cdot 10^{-3}$	$9.3613 \cdot 10^{-4}$	$1.0441 \cdot 10^{-4}$	0
MRE	$(10, 81)$	12.0871%	12.4160%	12.5835%	12.6680%	12.7105%	12.7318%
	$(20, 361)$	7.6741%	7.9448%	8.0829%	8.1527%	8.1878%	8.2053%
	$(40, 1521)$	2.6369%	2.5227%	2.6025%	2.6420%	2.6616%	2.6713%
	$(80, 6241)$	1.8069%	1.0000%	0.7405%	0.6877%	0.6928%	0.6953%
	$(160, 25281)$	1.7257%	0.8225%	0.5493%	0.5490%	0.5489%	0.5488%
	$(320, 101761)$	1.7731%	0.8661%	0.7041%	0.7039%	0.7039%	0.7038%
	$(640, 408321)$	1.7639%	0.8568%	0.4006%	0.1718%	0.0573%	0%
H_0	$(10, 81)$	$3.9801 \cdot 10^{3}$	$4.0815 \cdot 10^{3}$	$4.1440 \cdot 10^{3}$	$4.1781 \cdot 10^{3}$	$4.1960 \cdot 10^{3}$	$4.2051 \cdot 10^{3}$
	$(20, 361)$	$1.5615 \cdot 10^{3}$	$1.5230 \cdot 10^{3}$	$1.5419 \cdot 10^{3}$	$1.5628 \cdot 10^{3}$	$1.5754 \cdot 10^{3}$	$1.5823 \cdot 10^{3}$
	$(40, 1521)$	$9.3354 \cdot 10^{2}$	$7.0504 \cdot 10^{2}$	$6.5186 \cdot 10^{2}$	$6.4768 \cdot 10^{2}$	$6.5150 \cdot 10^{2}$	$6.5489 \cdot 10^{2}$
	$(80, 6241)$	$8.6033 \cdot 10^{2}$	$5.4015 \cdot 10^{2}$	$4.2968 \cdot 10^{2}$	$4.0242 \cdot 10^{2}$	$3.9812 \cdot 10^{2}$	$3.9846 \cdot 10^{2}$
	$(160, 25281)$	$8.3175 \cdot 10^{2}$	$4.7698 \cdot 10^{2}$	$3.3649 \cdot 10^{2}$	$2.9526 \cdot 10^{2}$	$2.8658 \cdot 10^{2}$	$2.8569 \cdot 10^{2}$
	$(320, 101761)$	$8.2434 \cdot 10^{2}$	$4.5868 \cdot 10^{2}$	$3.0668 \cdot 10^{2}$	$2.5898 \cdot 10^{2}$	$2.4817 \cdot 10^{2}$	$2.4672 \cdot 10^{2}$
	$(640, 408321)$	$7.8651 \cdot 10^{2}$	$3.8635 \cdot 10^{2}$	$1.8168 \cdot 10^{2}$	$7.8164 \cdot 10^{1}$	$2.6105 \cdot 10^{1}$	0
H_1	$(10, 81)$	$3.9802 \cdot 10^{3}$	$4.0816 \cdot 10^{3}$	$4.1441 \cdot 10^{3}$	$4.1782 \cdot 10^{3}$	$4.1960 \cdot 10^{3}$	$4.2052 \cdot 10^{3}$
	$(20, 361)$	$1.5616 \cdot 10^{3}$	$1.5231 \cdot 10^{3}$	$1.5419 \cdot 10^{3}$	$1.5629 \cdot 10^{3}$	$1.5755 \cdot 10^{3}$	$1.5824 \cdot 10^{3}$
	$(40, 1521)$	$9.3365 \cdot 10^{2}$	$7.0517 \cdot 10^{2}$	$6.5200 \cdot 10^{2}$	$6.4781 \cdot 10^{2}$	$6.5163 \cdot 10^{2}$	$6.5503 \cdot 10^{2}$
	$(80, 6241)$	$8.6056 \cdot 10^{2}$	$5.4048 \cdot 10^{2}$	$4.3007 \cdot 10^{2}$	$4.0282 \cdot 10^{2}$	$3.9852 \cdot 10^{2}$	$3.9885 \cdot 10^{2}$
	$(160, 25281)$	$8.3226 \cdot 10^{2}$	$4.7775 \cdot 10^{2}$	$3.3752 \cdot 10^{2}$	$2.9639 \cdot 10^{2}$	$2.8773 \cdot 10^{2}$	$2.8684 \cdot 10^{2}$
	$(320, 101761)$	$8.2588 \cdot 10^{2}$	$4.6119 \cdot 10^{2}$	$3.1026 \cdot 10^{2}$	$2.6312 \cdot 10^{2}$	$2.5245 \cdot 10^{2}$	$2.5100 \cdot 10^{2}$
	$(640, 408321)$	$7.8666 \cdot 10^{2}$	$3.8643 \cdot 10^{2}$	$1.8171 \cdot 10^{2}$	$7.8179 \cdot 10^{1}$	$2.6110 \cdot 10^{1}$	0
$H_{1,w}$	$(10, 81)$	$4.8751 \cdot 10^{3}$	$5.0120 \cdot 10^{3}$	$5.0993 \cdot 10^{3}$	$5.1479 \cdot 10^{3}$	$5.1733 \cdot 10^{3}$	$5.1860 \cdot 10^{3}$
	$(20, 361)$	$2.9235 \cdot 10^{3}$	$2.8857 \cdot 10^{3}$	$2.9036 \cdot 10^{3}$	$2.9204 \cdot 10^{3}$	$2.9313 \cdot 10^{3}$	$2.9374 \cdot 10^{3}$
	$(40, 1521)$	$2.8247 \cdot 10^{3}$	$2.6893 \cdot 10^{3}$	$2.6620 \cdot 10^{3}$	$2.6594 \cdot 10^{3}$	$2.6610 \cdot 10^{3}$	$2.6625 \cdot 10^{3}$
	$(80, 6241)$	$2.9568 \cdot 10^{3}$	$2.7994 \cdot 10^{3}$	$2.7607 \cdot 10^{3}$	$2.7524 \cdot 10^{3}$	$2.7512 \cdot 10^{3}$	$2.7513 \cdot 10^{3}$
	$(160, 25281)$	$3.0742 \cdot 10^{3}$	$2.9158 \cdot 10^{3}$	$2.8756 \cdot 10^{3}$	$2.8664 \cdot 10^{3}$	$2.8646 \cdot 10^{3}$	$2.8644 \cdot 10^{3}$
	$(320, 101761)$	$3.6820 \cdot 10^{3}$	$3.5488 \cdot 10^{3}$	$3.5151 \cdot 10^{3}$	$3.5072 \cdot 10^{3}$	$3.5056 \cdot 10^{3}$	$3.5054 \cdot 10^{3}$
	$(640, 408321)$	$1.1276 \cdot 10^{3}$	$5.5335 \cdot 10^{2}$	$2.6007 \cdot 10^{2}$	$1.1185 \cdot 10^{2}$	$3.7353 \cdot 10^{1}$	0

Table 8.15: Discretization Errors for Two-asset European Basket Straddle Option.

		N_t					
Error Type	(N_s, N_u)	10	20	40	80	160	320
MSE	$(10, 81)$	$5.1865 \cdot 10^{0}$	$5.4141 \cdot 10^{0}$	$5.5636 \cdot 10^{0}$	$5.6262 \cdot 10^{0}$	$5.6648 \cdot 10^{0}$	$5.6832 \cdot 10^{0}$
	$(20, 361)$	$3.2885 \cdot 10^{-1}$	$3.4581 \cdot 10^{-1}$	$3.5988 \cdot 10^{-1}$	$3.6853 \cdot 10^{-1}$	$3.7319 \cdot 10^{-1}$	$3.7562 \cdot 10^{-1}$
	$(40, 1521)$	$3.9369 \cdot 10^{-2}$	$2.8258 \cdot 10^{-2}$	$2.7405 \cdot 10^{-2}$	$2.8540 \cdot 10^{-2}$	$2.9508 \cdot 10^{-2}$	$3.0094 \cdot 10^{-2}$
	$(80, 6241)$	$2.3023 \cdot 10^{-2}$	$6.5699 \cdot 10^{-3}$	$2.4664 \cdot 10^{-3}$	$1.6190 \cdot 10^{-3}$	$1.5695 \cdot 10^{-3}$	$1.6649 \cdot 10^{-3}$
	$(160, 25281)$	$2.2311 \cdot 10^{-2}$	$5.6227 \cdot 10^{-3}$	$1.2974 \cdot 10^{-3}$	$2.8445 \cdot 10^{-4}$	$9.9496 \cdot 10^{-5}$	$9.7239 \cdot 10^{-5}$
	$(320, 101761)$	$2.2553 \cdot 10^{-2}$	$5.7390 \cdot 10^{-3}$	$1.3195 \cdot 10^{-3}$	$2.4820 \cdot 10^{-4}$	$2.8265 \cdot 10^{-5}$	$4.1706 \cdot 10^{-6}$
	$(640, 408321)$	$2.2637 \cdot 10^{-2}$	$5.7950 \cdot 10^{-3}$	$1.3493 \cdot 10^{-3}$	$2.6060 \cdot 10^{-4}$	$3.0057 \cdot 10^{-5}$	0
MRE	$(10, 81)$	19.7082%	19.8307%	19.8820%	19.8914%	19.9121%	19.9232%
	$(20, 361)$	6.9144%	6.4295%	6.1816%	6.0496%	5.9804%	5.9448%
	$(40, 1521)$	3.8507%	3.7519%	3.7002%	3.6713%	3.6543%	3.6447%
	$(80, 6241)$	2.1769%	1.3843%	1.0486%	0.9228%	0.8766%	0.8639%
	$(160, 25281)$	1.9060%	0.9765%	0.5087%	0.2867%	0.2140%	0.2101%
	$(320, 101761)$	1.9488%	0.9805%	0.4780%	0.2173%	0.0877%	0.0438%
	$(640, 408321)$	1.9332%	0.9654%	0.4622%	0.2020%	0.0684%	0%
H_0	$(10, 81)$	$4.3153 \cdot 10^{3}$	$4.4092 \cdot 10^{3}$	$4.4677 \cdot 10^{3}$	$4.4919 \cdot 10^{3}$	$4.5068 \cdot 10^{3}$	$4.5137 \cdot 10^{3}$
	$(20, 361)$	$1.1990 \cdot 10^{3}$	$1.2496 \cdot 10^{3}$	$1.2826 \cdot 10^{3}$	$1.3012 \cdot 10^{3}$	$1.3108 \cdot 10^{3}$	$1.3157 \cdot 10^{3}$
	$(40, 1521)$	$4.4493 \cdot 10^{2}$	$3.6975 \cdot 10^{2}$	$3.6311 \cdot 10^{2}$	$3.7259 \cdot 10^{2}$	$3.8008 \cdot 10^{2}$	$3.8459 \cdot 10^{2}$
	$(80, 6241)$	$3.7293 \cdot 10^{2}$	$1.9759 \cdot 10^{2}$	$1.1904 \cdot 10^{2}$	$9.5402 \cdot 10^{1}$	$9.4116 \cdot 10^{1}$	$9.7307 \cdot 10^{1}$
	$(160, 25281)$	$3.7618 \cdot 10^{2}$	$1.8883 \cdot 10^{2}$	$9.0612 \cdot 10^{1}$	$4.2190 \cdot 10^{1}$	$2.4601 \cdot 10^{1}$	$2.4297 \cdot 10^{1}$
	$(320, 101761)$	$3.8148 \cdot 10^{2}$	$1.9242 \cdot 10^{2}$	$9.2249 \cdot 10^{1}$	$3.9979 \cdot 10^{1}$	$1.3439 \cdot 10^{1}$	$5.1213 \cdot 10^{0}$
	$(640, 408321)$	$3.8374 \cdot 10^{2}$	$1.9416 \cdot 10^{2}$	$9.3692 \cdot 10^{1}$	$4.1176 \cdot 10^{1}$	$1.3984 \cdot 10^{1}$	0
H_1	$(10, 81)$	$4.3154 \cdot 10^{3}$	$4.4093 \cdot 10^{3}$	$4.4678 \cdot 10^{3}$	$4.4920 \cdot 10^{3}$	$4.5069 \cdot 10^{3}$	$4.5138 \cdot 10^{3}$
	$(20, 361)$	$1.1990 \cdot 10^{3}$	$1.2496 \cdot 10^{3}$	$1.2827 \cdot 10^{3}$	$1.3012 \cdot 10^{3}$	$1.3109 \cdot 10^{3}$	$1.3158 \cdot 10^{3}$
	$(40, 1521)$	$4.4500 \cdot 10^{2}$	$3.6981 \cdot 10^{2}$	$3.6317 \cdot 10^{2}$	$3.7266 \cdot 10^{2}$	$3.8014 \cdot 10^{2}$	$3.8466 \cdot 10^{2}$
	$(80, 6241)$	$3.7299 \cdot 10^{2}$	$1.9763 \cdot 10^{2}$	$1.1908 \cdot 10^{2}$	$9.5437 \cdot 10^{1}$	$9.4149 \cdot 10^{1}$	$9.7339 \cdot 10^{1}$
	$(160, 25281)$	$3.7627 \cdot 10^{2}$	$1.8888 \cdot 10^{2}$	$9.0635 \cdot 10^{1}$	$4.2206 \cdot 10^{1}$	$2.4618 \cdot 10^{1}$	$2.4314 \cdot 10^{1}$
	$(320, 101761)$	$3.8165 \cdot 10^{2}$	$1.9251 \cdot 10^{2}$	$9.2292 \cdot 10^{1}$	$4.0000 \cdot 10^{1}$	$1.3450 \cdot 10^{1}$	$5.1289 \cdot 10^{0}$
	$(640, 408321)$	$3.8405 \cdot 10^{2}$	$1.9432 \cdot 10^{2}$	$9.3766 \cdot 10^{1}$	$4.1208 \cdot 10^{1}$	$1.3995 \cdot 10^{1}$	0
$H_{1,w}$	$(10, 81)$	$4.7956 \cdot 10^{3}$	$4.9056 \cdot 10^{3}$	$4.9756 \cdot 10^{3}$	$5.0031 \cdot 10^{3}$	$5.0178 \cdot 10^{3}$	$5.0252 \cdot 10^{3}$
	$(20, 361)$	$1.4449 \cdot 10^{3}$	$1.4726 \cdot 10^{3}$	$1.5011 \cdot 10^{3}$	$1.5193 \cdot 10^{3}$	$1.5293 \cdot 10^{3}$	$1.5345 \cdot 10^{3}$
	$(40, 1521)$	$5.9939 \cdot 10^{2}$	$5.1114 \cdot 10^{2}$	$5.0557 \cdot 10^{2}$	$5.1788 \cdot 10^{2}$	$5.2914 \cdot 10^{2}$	$5.3524 \cdot 10^{2}$
	$(80, 6241)$	$5.0805 \cdot 10^{2}$	$2.6811 \cdot 10^{2}$	$1.6830 \cdot 10^{2}$	$1.4307 \cdot 10^{2}$	$1.4385 \cdot 10^{2}$	$1.4841 \cdot 10^{2}$
	$(160, 25281)$	$5.2803 \cdot 10^{2}$	$2.6254 \cdot 10^{2}$	$1.2577 \cdot 10^{2}$	$6.1897 \cdot 10^{1}$	$4.2480 \cdot 10^{1}$	$4.3160 \cdot 10^{1}$
	$(320, 101761)$	$5.4060 \cdot 10^{2}$	$2.7045 \cdot 10^{2}$	$1.2879 \cdot 10^{2}$	$5.5800 \cdot 10^{1}$	$1.9976 \cdot 10^{1}$	$1.0958 \cdot 10^{1}$
	$(640, 408321)$	$5.4565 \cdot 10^{2}$	$2.7395 \cdot 10^{2}$	$1.3139 \cdot 10^{2}$	$5.7475 \cdot 10^{1}$	$1.9450 \cdot 10^{1}$	0

Table 8.16: Discretization Errors for Two-asset American Basket Straddle Option.

(N_s, N_u)	Error Type				
	MSE	MRE	H_0	H_1	$H_{1,w}$
$(10, 81)$	$8.7429 \cdot 10^{0}$	7.7385%	$6.0772 \cdot 10^{3}$	$6.0773 \cdot 10^{3}$	$6.5314 \cdot 10^{3}$
$(20, 361)$	$4.7840 \cdot 10^{-1}$	4.4712%	$1.4571 \cdot 10^{3}$	$1.4572 \cdot 10^{3}$	$1.6451 \cdot 10^{3}$
$(40, 1521)$	$4.0459 \cdot 10^{-2}$	2.2362%	$4.4058 \cdot 10^{2}$	$4.4067 \cdot 10^{2}$	$6.7590 \cdot 10^{2}$
$(80, 6241)$	$6.2147 \cdot 10^{-3}$	1.1496%	$1.6990 \cdot 10^{2}$	$1.7007 \cdot 10^{2}$	$4.8679 \cdot 10^{2}$
$(160, 25281)$	$7.7160 \cdot 10^{-4}$	0.2741%	$6.3825 \cdot 10^{1}$	$6.3990 \cdot 10^{1}$	$2.8826 \cdot 10^{2}$
$(320, 101761)$	$1.6405 \cdot 10^{-4}$	0.0660%	$2.9440 \cdot 10^{1}$	$2.9758 \cdot 10^{1}$	$1.6380 \cdot 10^{2}$

Table 8.17: Discretization Errors for Two-asset Perpetual Basket Straddle Option.

Two-asset Case

Table [8.22] shows the truncation errors of European minimum put (EMP), European maximum call (EMC), European basket straddle (EBS), American basket straddle (ABS) and perpetual basket straddle (PBS) in our two-asset experiments. We remind readers that only the EMP and EMC have their closed-form analytical solutions valued over Ω_9 as benchmarks.

Similar to one-asset circumstances, we observe the put option (EMP) is less sensitive to the change of far-field bound after $S^{(i)}_{\max} = 1280$ while other cases have the truncation errors reduced slowly as $S^{(i)}_{\max}$ increases. For the ABS and PBS options having their free boundaries in call parts, we once again observe the significant drops of truncation errors after $S^{(i)}_{\max} = 1920$ and 2560 respectively. Analogously this is because any share price of $\mathbf{S} = (S^{(1)}, S^{(2)})$ exceeds those boundaries given by our option parameters, then they fall into the early-exercise region where their option value is equal to their payoff and our LCP solver produces almost no numerical error in the region.

Three-asset Case

There is no closed-form formula available for option pricing in a three-asset framework. Consequently we consider only the basket options of European, American and perpetual types (EBS, ABS and PBS) and record their truncation errors in table [8.23]. As expected, we observe the slow slide of truncation errors when given increasingly large $S^{(i)}_{\max}$. But there is no significant drop observed in the three-asset ABS and PBS options. This suggests that even one of the share prices $\mathbf{S} = (S^{(1)}, S^{(2)}, S^{(3)})$ is greater than $S^{(i)}_{\max} = 3200$, it can not guarantee the triple lies in the early-exercise region, which suggests a larger far-field bound should be taken into account to further reduce the truncation error in the numerical computation of the three-asset American and perpetual option pricing problems.

		N_t		
Error Type	(N_s, N_u)	10	20	40
MSE	$(10, 729)$	3.9998	4.1431	4.3400
	$(20, 6859)$	0.3009	0.2587	0.2599
	$(40, 59319)$	0.0806	0.0206	0.0117
	$(80, 493039)$	0.0676	0.0080	0
MRE	$(10, 729)$	6.7487%	7.1180%	8.1541%
	$(20, 6859)$	4.2117%	4.3065%	4.5255%
	$(40, 59319)$	2.0992%	1.5031%	1.4870%
	$(80, 493039)$	1.7458%	0.5615%	0%
H_0	$(10, 729)$	$2.0150 \cdot 10^5$	$2.0370 \cdot 10^5$	$2.0711 \cdot 10^5$
	$(20, 6859)$	$6.1654 \cdot 10^4$	$5.6880 \cdot 10^4$	$5.6625 \cdot 10^4$
	$(40, 59319)$	$3.3947 \cdot 10^4$	$1.6961 \cdot 10^4$	$1.2530 \cdot 10^4$
	$(80, 493039)$	$3.2468 \cdot 10^4$	$1.1184 \cdot 10^4$	0%
H_1	$(10, 729)$	$2.0150 \cdot 10^5$	$2.0371 \cdot 10^5$	$2.0711 \cdot 10^5$
	$(20, 6859)$	$6.1656 \cdot 10^4$	$5.6882 \cdot 10^4$	$5.6627 \cdot 10^4$
	$(40, 59319)$	$3.3949 \cdot 10^4$	$1.6963 \cdot 10^4$	$1.2531 \cdot 10^4$
	$(80, 493039)$	$3.2472 \cdot 10^4$	$1.1186 \cdot 10^4$	0%
$H_{1,w}$	$(10, 729)$	$2.9302 \cdot 10^5$	$2.9611 \cdot 10^5$	$3.0147 \cdot 10^5$
	$(20, 6859)$	$1.0129 \cdot 10^5$	$9.1650 \cdot 10^4$	$9.0130 \cdot 10^4$
	$(40, 59319)$	$6.6776 \cdot 10^4$	$4.4992 \cdot 10^4$	$4.0636 \cdot 10^4$
	$(80, 493039)$	$5.4830 \cdot 10^4$	$1.8978 \cdot 10^4$	0%

Table 8.18: Discretization Errors for Three-asset European Basket Straddle Option.

		N_t		
Error Type	(N_s, N_u)	10	20	40
MSE	$(10, 729)$	3.1945	3.8864	5.0983
	$(20, 6859)$	0.2813	0.2417	0.3241
	$(40, 59319)$	0.0926	0.0196	0.0171
	$(80, 493039)$	0.0773	0.0101	0
MRE	$(10, 729)$	7.8764%	7.7308%	8.1634%
	$(20, 6859)$	4.7095%	4.6200%	4.5768%
	$(40, 59319)$	2.4109%	1.2357%	1.4767%
	$(80, 493039)$	2.1687%	1.0184%	0%
H_0	$(10, 729)$	$1.7598 \cdot 10^5$	$1.9109 \cdot 10^5$	$2.1510 \cdot 10^5$
	$(20, 6859)$	$5.9325 \cdot 10^4$	$5.4227 \cdot 10^4$	$6.0919 \cdot 10^4$
	$(40, 59319)$	$3.6467 \cdot 10^4$	$1.6661 \cdot 10^4$	$1.4434 \cdot 10^4$
	$(80, 493039)$	$3.4690 \cdot 10^4$	$1.2425 \cdot 10^4$	0
H_1	$(10, 729)$	$1.7598 \cdot 10^5$	$1.9110 \cdot 10^5$	$2.1510 \cdot 10^5$
	$(20, 6859)$	$5.9327 \cdot 10^4$	$5.4228 \cdot 10^4$	$6.0921 \cdot 10^4$
	$(40, 59319)$	$3.6469 \cdot 10^4$	$1.6662 \cdot 10^4$	$1.4437 \cdot 10^4$
	$(80, 493039)$	$3.4693 \cdot 10^4$	$1.2427 \cdot 10^4$	0
$H_{1,w}$	$(10, 729)$	$2.6186 \cdot 10^5$	$2.8503 \cdot 10^5$	$3.2391 \cdot 10^5$
	$(20, 6859)$	$9.7643 \cdot 10^4$	$8.5697 \cdot 10^4$	$9.5093 \cdot 10^4$
	$(40, 59319)$	$6.5343 \cdot 10^4$	$3.3586 \cdot 10^4$	$2.9377 \cdot 10^4$
	$(80, 493039)$	$6.0431 \cdot 10^4$	$2.1452 \cdot 10^4$	0

Table 8.19: Discretization Errors for Three-asset American Basket Straddle Option.

(N_s, N_u)	Error Type				
	MSE	MRE	H_0	H_1	$H_{1,w}$
$(10, 729)$	$1.8370 \cdot 10^{1}$	6.1368%	$4.3360 \cdot 10^{5}$	$4.3360 \cdot 10^{5}$	$6.3447 \cdot 10^{5}$
$(20, 6859)$	$4.1047 \cdot 10^{0}$	6.1126%	$2.3087 \cdot 10^{5}$	$2.3087 \cdot 10^{5}$	$3.8112 \cdot 10^{5}$
$(40, 59319)$	$3.9071 \cdot 10^{-1}$	4.7607%	$7.4274 \cdot 10^{4}$	$7.4279 \cdot 10^{4}$	$1.6777 \cdot 10^{5}$
$(80, 493039)$	0	0%	0	0	0

Table 8.20: Discretization Errors for Three-asset Perpetual Basket Straddle Option.

8.6.2 Comment

We have seen the truncation errors are reduced with increasingly large far-field bounds for the European, American and perpetual options in one-, two- and three-asset frameworks. Such reduction makes mathematical sense because we approximate the Dirichlet boundary conditions on the far-field bounds. The larger the far-field bound is, the better approximation we should have.

Compared with calls and straddles, one-asset European and perpetual puts and a two-asset minimum put generally have much smaller truncation errors. This is because they have (near-)zero option values at high share prices and thus are less sensitive to the increase of far-filed bounds.

When an option tends to be early exercised in the far-field area such as a maximum/basket call/straddle, we find that there exists a bounded value $\max_{t\in[0,T]}\{S_f(t)\}$ such that once any of the share prices $\mathbf{S} = (S^{(1)}, \cdots, S^{(d)})$ falls beyond $\max_{t\in[0,T]}\{S_f(t)\}$, the combination of shares falls into the early-exercise region. Given identical option types, we also observe that the $\max_{t\in[0,T]}\{S_f(t)\}$ becomes larger if

- time to maturity is larger:
  And there exists a limit as $T \to \infty$, which is the maximum bound of the free boundaries of perpetual options.

- number of assets is multiple:
  So the $S^{(i)}_{\max}$ needed to produce significant drop in the two-asset framework is generally larger than that of its one-asset counterpart.

- the payoff is at least equal to that of another option:
  So we observe $S^{(i)}_{\max}$ needed to produce a significant drop of truncation errors for a straddle option is generally larger than that of its call counterpart.

These observations suggest that when given the same far-filed bounds, the American and perpetual options can be approximated better than their European counterparts if the selected far-filed bounds are deeply in the early-exercise region. This is consistent with the

Type	$S_{\max}^{(i)}$	One-asset Options						
		EP	EC	ES	AS	PP	PC	PS
H_0	640	$3.1768 \cdot 10^{-5}$	$2.9859 \cdot 10^{-2}$	$2.3662 \cdot 10^{-2}$	$2.3593 \cdot 10^{-4}$	$4.7257 \cdot 10^{-2}$	$1.1721 \cdot 10^{-1}$	$1.0701 \cdot 10^{-1}$
	960	$3.1754 \cdot 10^{-5}$	$2.0725 \cdot 10^{-2}$	$1.9901 \cdot 10^{-2}$	$9.7746 \cdot 10^{-17}$	$2.8330 \cdot 10^{-2}$	$9.0310 \cdot 10^{-3}$	$1.0563 \cdot 10^{-2}$
	1280	$3.1754 \cdot 10^{-5}$	$1.7757 \cdot 10^{-2}$	$1.7529 \cdot 10^{-2}$	$5.9867 \cdot 10^{-17}$	$1.9402 \cdot 10^{-2}$	$7.9951 \cdot 10^{-8}$	0
	1600	$3.1754 \cdot 10^{-5}$	$1.6298 \cdot 10^{-2}$	$1.6206 \cdot 10^{-2}$	$3.7879 \cdot 10^{-17}$	$1.4408 \cdot 10^{-2}$	$5.3239 \cdot 10^{-8}$	0
	1920	$3.1754 \cdot 10^{-5}$	$1.5432 \cdot 10^{-2}$	$1.5387 \cdot 10^{-2}$	$2.5358 \cdot 10^{-17}$	$1.1283 \cdot 10^{-2}$	$3.8516 \cdot 10^{-8}$	0
	2240	$3.1754 \cdot 10^{-5}$	$1.4859 \cdot 10^{-2}$	$1.4834 \cdot 10^{-2}$	$1.7107 \cdot 10^{-17}$	$9.1707 \cdot 10^{-3}$	$2.9476 \cdot 10^{-8}$	0
	2560	$3.1754 \cdot 10^{-5}$	$1.4453 \cdot 10^{-2}$	$1.4437 \cdot 10^{-2}$	0	$7.6612 \cdot 10^{-3}$	$2.3477 \cdot 10^{-8}$	0
	2880	$3.1754 \cdot 10^{-5}$	$1.4149 \cdot 10^{-2}$	$1.4139 \cdot 10^{-2}$	0	$6.5365 \cdot 10^{-3}$	$1.9264 \cdot 10^{-8}$	0
H_1	640	$3.1778 \cdot 10^{-5}$	$2.9862 \cdot 10^{-2}$	$2.3664 \cdot 10^{-2}$	$6.2607 \cdot 10^{-4}$	$4.7257 \cdot 10^{-2}$	$1.1721 \cdot 10^{-1}$	$1.0701 \cdot 10^{-1}$
	960	$3.1772 \cdot 10^{-5}$	$2.0726 \cdot 10^{-2}$	$1.9902 \cdot 10^{-2}$	$1.4114 \cdot 10^{-16}$	$2.8330 \cdot 10^{-2}$	$9.0310 \cdot 10^{-3}$	$1.0563 \cdot 10^{-2}$
	1280	$3.1772 \cdot 10^{-5}$	$1.7757 \cdot 10^{-2}$	$1.7529 \cdot 10^{-2}$	$8.4766 \cdot 10^{-17}$	$1.9401 \cdot 10^{-2}$	$1.1611 \cdot 10^{-7}$	0
	1600	$3.1772 \cdot 10^{-5}$	$1.6298 \cdot 10^{-2}$	$1.6207 \cdot 10^{-2}$	$5.4549 \cdot 10^{-17}$	$1.4408 \cdot 10^{-2}$	$7.7323 \cdot 10^{-8}$	0
	1920	$3.1772 \cdot 10^{-5}$	$1.5432 \cdot 10^{-2}$	$1.5387 \cdot 10^{-2}$	$3.8385 \cdot 10^{-17}$	$1.1283 \cdot 10^{-2}$	$5.5940 \cdot 10^{-8}$	0
	2240	$3.1772 \cdot 10^{-5}$	$1.4860 \cdot 10^{-2}$	$1.4834 \cdot 10^{-2}$	$2.7773 \cdot 10^{-17}$	$9.1706 \cdot 10^{-3}$	$4.2810 \cdot 10^{-8}$	0
	2560	$3.1772 \cdot 10^{-5}$	$1.4453 \cdot 10^{-2}$	$1.4437 \cdot 10^{-2}$	0	$7.6611 \cdot 10^{-3}$	$3.4098 \cdot 10^{-8}$	0
	2880	$3.1772 \cdot 10^{-5}$	$1.4149 \cdot 10^{-2}$	$1.4139 \cdot 10^{-2}$	0	$6.5364 \cdot 10^{-3}$	$2.7978 \cdot 10^{-8}$	0
$H_{1,w}$	640	$4.5997 \cdot 10^{-5}$	$4.4535 \cdot 10^{-2}$	$3.5935 \cdot 10^{-2}$	$5.0870 \cdot 10^{-2}$	$4.8215 \cdot 10^{-2}$	$1.1721 \cdot 10^{-1}$	$1.0808 \cdot 10^{-1}$
	960	$4.5801 \cdot 10^{-5}$	$3.1615 \cdot 10^{-2}$	$3.0421 \cdot 10^{-2}$	$9.8244 \cdot 10^{-15}$	$2.8749 \cdot 10^{-2}$	$9.0310 \cdot 10^{-3}$	$1.0599 \cdot 10^{-2}$
	1280	$4.5801 \cdot 10^{-5}$	$2.7268 \cdot 10^{-2}$	$2.6932 \cdot 10^{-2}$	$5.6585 \cdot 10^{-15}$	$1.9663 \cdot 10^{-2}$	$1.3023 \cdot 10^{-7}$	0
	1600	$4.5801 \cdot 10^{-5}$	$2.5105 \cdot 10^{-2}$	$2.4969 \cdot 10^{-2}$	$3.7434 \cdot 10^{-15}$	$1.4595 \cdot 10^{-2}$	$8.6818 \cdot 10^{-8}$	0
	1920	$4.5801 \cdot 10^{-5}$	$2.3813 \cdot 10^{-2}$	$2.3746 \cdot 10^{-2}$	$2.7100 \cdot 10^{-15}$	$1.1427 \cdot 10^{-2}$	$6.2878 \cdot 10^{-8}$	0
	2240	$4.5801 \cdot 10^{-5}$	$2.2955 \cdot 10^{-2}$	$2.2917 \cdot 10^{-2}$	$2.1124 \cdot 10^{-15}$	$9.2871 \cdot 10^{-3}$	$4.8159 \cdot 10^{-8}$	0
	2560	$4.5801 \cdot 10^{-5}$	$2.2345 \cdot 10^{-2}$	$2.2321 \cdot 10^{-2}$	0	$7.7580 \cdot 10^{-3}$	$3.8384 \cdot 10^{-8}$	0
	2880	$4.5801 \cdot 10^{-5}$	$2.1888 \cdot 10^{-2}$	$2.1872 \cdot 10^{-2}$	0	$6.6188 \cdot 10^{-3}$	$3.1511 \cdot 10^{-8}$	0

Table 8.21: Nielsen Truncation Errors for One-asset Options.

argument in [72, Sec.5.2] that the multi-asset American options can be solved on a rather small domain with a tolerable truncation error as long as $S_{\max} > \max_{t\in[0,T]} \{S_f(t)\}$.

In sum, we can consider such $\max_{t\in[0,T]} \{S_f(t)\}$ the minimum far-field bound value needed to form a computational domain which provides no significant truncation errors for the options tending to be exercised early in the far-field area.

8.7 Summary

In order to give a rapid feel for different options, we start with visualizing their calibrated values and identifying corresponding (evolutionary) free boundaries (if any). For the first time in literatures, we present the free boundaries of three-asset American and perpetual options. The subsequent computational results are also very encouraging. When given different early-exercise restrictions, different expiry restrictions and multiple assets, our approach reveals positive results in terms of discretization errors and truncation errors.

Type	$S_{\max}^{(i)}$	Two-asset Options				
		EMP	EMC	EBS	ABS	PBS
H_0	640	$1.7093 \cdot 10^{-3}$	$6.7406 \cdot 10^{-2}$	$5.6415 \cdot 10^{-2}$	$4.1311 \cdot 10^{-2}$	$2.5815 \cdot 10^{-1}$
	960	$1.5844 \cdot 10^{-4}$	$4.8473 \cdot 10^{-2}$	$2.4491 \cdot 10^{-2}$	$3.1460 \cdot 10^{-3}$	$9.6344 \cdot 10^{-2}$
	1280	$1.2325 \cdot 10^{-4}$	$4.2202 \cdot 10^{-2}$	$2.0095 \cdot 10^{-2}$	$6.9812 \cdot 10^{-4}$	$3.1905 \cdot 10^{-2}$
	1600	$1.2644 \cdot 10^{-4}$	$3.9093 \cdot 10^{-2}$	$1.7866 \cdot 10^{-2}$	$1.7765 \cdot 10^{-4}$	$1.0107 \cdot 10^{-2}$
	1920	$1.2856 \cdot 10^{-4}$	$3.7240 \cdot 10^{-2}$	$1.6064 \cdot 10^{-2}$	$1.3042 \cdot 10^{-5}$	$2.7816 \cdot 10^{-3}$
	2240	$1.3003 \cdot 10^{-4}$	$3.6011 \cdot 10^{-2}$	$1.3995 \cdot 10^{-2}$	$7.1199 \cdot 10^{-16}$	$5.7801 \cdot 10^{-4}$
	2560	$1.3112 \cdot 10^{-4}$	$3.5137 \cdot 10^{-2}$	$1.1068 \cdot 10^{-2}$	$5.0408 \cdot 10^{-16}$	$1.1236 \cdot 10^{-4}$
	2880	$1.3195 \cdot 10^{-4}$	$3.4483 \cdot 10^{-2}$	$6.6107 \cdot 10^{-3}$	$2.8670 \cdot 10^{-16}$	$4.9309 \cdot 10^{-17}$
H_1	640	$1.7096 \cdot 10^{-3}$	$6.7412 \cdot 10^{-2}$	$5.6465 \cdot 10^{-2}$	$4.1358 \cdot 10^{-2}$	$2.5815 \cdot 10^{-1}$
	960	$1.5851 \cdot 10^{-4}$	$4.8475 \cdot 10^{-2}$	$2.4495 \cdot 10^{-2}$	$3.1517 \cdot 10^{-3}$	$9.6344 \cdot 10^{-2}$
	1280	$1.2331 \cdot 10^{-4}$	$4.2204 \cdot 10^{-2}$	$2.0097 \cdot 10^{-2}$	$6.9947 \cdot 10^{-4}$	$3.1905 \cdot 10^{-2}$
	1600	$1.2649 \cdot 10^{-4}$	$3.9094 \cdot 10^{-2}$	$1.7867 \cdot 10^{-2}$	$1.7840 \cdot 10^{-4}$	$1.0107 \cdot 10^{-2}$
	1920	$1.2860 \cdot 10^{-4}$	$3.7240 \cdot 10^{-2}$	$1.6065 \cdot 10^{-2}$	$1.3671 \cdot 10^{-5}$	$2.7816 \cdot 10^{-3}$
	2240	$1.3007 \cdot 10^{-4}$	$3.6012 \cdot 10^{-2}$	$1.3996 \cdot 10^{-2}$	$7.2257 \cdot 10^{-16}$	$5.7802 \cdot 10^{-4}$
	2560	$1.3115 \cdot 10^{-4}$	$3.5137 \cdot 10^{-2}$	$1.1068 \cdot 10^{-2}$	$5.1498 \cdot 10^{-16}$	$1.1236 \cdot 10^{-4}$
	2880	$1.3198 \cdot 10^{-4}$	$3.4484 \cdot 10^{-2}$	$6.6109 \cdot 10^{-3}$	$2.9250 \cdot 10^{-16}$	$4.9310 \cdot 10^{-17}$
$H_{1,w}$	640	$4.5491 \cdot 10^{-3}$	$9.8246 \cdot 10^{-2}$	$8.9795 \cdot 10^{-2}$	$8.2344 \cdot 10^{-2}$	$2.7340 \cdot 10^{-1}$
	960	$4.2696 \cdot 10^{-4}$	$7.3077 \cdot 10^{-2}$	$3.6800 \cdot 10^{-2}$	$1.2215 \cdot 10^{-2}$	$1.0449 \cdot 10^{-1}$
	1280	$1.8301 \cdot 10^{-4}$	$6.4374 \cdot 10^{-2}$	$3.0154 \cdot 10^{-2}$	$3.3252 \cdot 10^{-3}$	$3.6890 \cdot 10^{-2}$
	1600	$1.8214 \cdot 10^{-4}$	$5.9966 \cdot 10^{-2}$	$2.6847 \cdot 10^{-2}$	$1.6485 \cdot 10^{-3}$	$1.3002 \cdot 10^{-2}$
	1920	$1.8487 \cdot 10^{-4}$	$5.7308 \cdot 10^{-2}$	$2.3993 \cdot 10^{-2}$	$5.3731 \cdot 10^{-4}$	$4.3779 \cdot 10^{-3}$
	2240	$1.8684 \cdot 10^{-4}$	$5.5532 \cdot 10^{-2}$	$2.0633 \cdot 10^{-2}$	$9.3637 \cdot 10^{-15}$	$1.3600 \cdot 10^{-3}$
	2560	$1.8829 \cdot 10^{-4}$	$5.4263 \cdot 10^{-2}$	$1.6023 \cdot 10^{-2}$	$7.5483 \cdot 10^{-15}$	$3.5611 \cdot 10^{-4}$
	2880	$1.8940 \cdot 10^{-4}$	$5.3311 \cdot 10^{-2}$	$9.4855 \cdot 10^{-3}$	$6.6291 \cdot 10^{-15}$	$7.6877 \cdot 10^{-17}$

Table 8.22: Nielsen Truncation Errors for Two-asset Options.

Type	$S_{\max}^{(i)}$	Three-asset Options		
		EBS	ABS	PBS
H_0	640	$2.6493 \cdot 10^{-1}$	$2.4630 \cdot 10^{-1}$	$6.0163 \cdot 10^{-1}$
	960	$9.4376 \cdot 10^{-2}$	$7.4381 \cdot 10^{-2}$	$3.8307 \cdot 10^{-1}$
	1280	$4.4255 \cdot 10^{-2}$	$2.4460 \cdot 10^{-2}$	$2.3729 \cdot 10^{-1}$
	1600	$2.8195 \cdot 10^{-2}$	$9.1403 \cdot 10^{-3}$	$1.4665 \cdot 10^{-1}$
	1920	$2.0591 \cdot 10^{-2}$	$3.8488 \cdot 10^{-3}$	$8.9383 \cdot 10^{-2}$
	2240	$1.4985 \cdot 10^{-2}$	$1.7609 \cdot 10^{-3}$	$5.2255 \cdot 10^{-2}$
	2560	$9.8625 \cdot 10^{-3}$	$8.0723 \cdot 10^{-4}$	$2.7662 \cdot 10^{-2}$
	2880	$4.8785 \cdot 10^{-3}$	$3.0533 \cdot 10^{-4}$	$1.1153 \cdot 10^{-2}$
H_1	640	$2.6493 \cdot 10^{-1}$	$2.4630 \cdot 10^{-1}$	$6.0164 \cdot 10^{-1}$
	960	$9.4377 \cdot 10^{-2}$	$7.4382 \cdot 10^{-2}$	$3.8307 \cdot 10^{-1}$
	1280	$4.4255 \cdot 10^{-2}$	$2.4460 \cdot 10^{-2}$	$2.3729 \cdot 10^{-1}$
	1600	$2.8195 \cdot 10^{-2}$	$9.1405 \cdot 10^{-3}$	$1.4665 \cdot 10^{-1}$
	1920	$2.0591 \cdot 10^{-2}$	$3.8489 \cdot 10^{-3}$	$8.9383 \cdot 10^{-2}$
	2240	$1.4985 \cdot 10^{-2}$	$1.7609 \cdot 10^{-3}$	$5.2255 \cdot 10^{-2}$
	2560	$9.8625 \cdot 10^{-3}$	$8.0724 \cdot 10^{-4}$	$2.7662 \cdot 10^{-2}$
	2880	$4.8786 \cdot 10^{-3}$	$3.0533 \cdot 10^{-4}$	$1.1153 \cdot 10^{-2}$
$H_{1,w}$	640	$3.8038 \cdot 10^{-1}$	$3.6132 \cdot 10^{-1}$	$6.3843 \cdot 10^{-1}$
	960	$1.3344 \cdot 10^{-1}$	$1.0917 \cdot 10^{-1}$	$3.8891 \cdot 10^{-1}$
	1280	$6.2642 \cdot 10^{-2}$	$3.7676 \cdot 10^{-2}$	$2.3637 \cdot 10^{-1}$
	1600	$3.8954 \cdot 10^{-2}$	$1.5054 \cdot 10^{-2}$	$1.4517 \cdot 10^{-1}$
	1920	$2.7566 \cdot 10^{-2}$	$6.6686 \cdot 10^{-3}$	$8.8605 \cdot 10^{-2}$
	2240	$1.9614 \cdot 10^{-2}$	$3.1721 \cdot 10^{-3}$	$5.2273 \cdot 10^{-2}$
	2560	$1.2742 \cdot 10^{-2}$	$1.5084 \cdot 10^{-3}$	$2.8284 \cdot 10^{-2}$
	2880	$6.3297 \cdot 10^{-3}$	$6.2237 \cdot 10^{-4}$	$1.2271 \cdot 10^{-2}$

Table 8.23: Nielsen Truncation Errors for Three-asset Options.

From the aspect of LCP algorithms, we find that the widely-introduced PSOR and its variants deliver quite disappointing performance and the modulus method produces convergent but incorrect solutions. In contrast, Howard's method provids the most satisfactory speed and accuracy, followed by the Lagrangian Multiplier method[6] and Lemke's method, in large-scale multi-asset option pricing problems with an early-exercise property which are highly demanding in terms of numerical computation.

We also observe the decrease of discretization errors with decreasing mesh sizes in space and time even though their convergence order is not always trivial. We recognize there exists a truncation error resulting from a bounded spatial domain but find that once the far-field bound is large enough, say $S_{\max}^{(i)} \geq \max_{t\in[0,T]} \{S_f(t)\}$, then the truncation error is almost ignorable for the options tending to be exercised early in the far-field area. For others with (near-)zero option values in the far-field area, we also observe they are less sensitive to the increase of far-field bounds and a properly large far-field value providing (near-)zero far-field boundary condition values will produce ignorable truncation errors too.

We have seen in the chapter that the complementarity reformulation solvable with LCP algorithms provides almost no numerical error in the early-exercise region and have decreasing discretization errors with increasing mesh nodes in a multi-dimensional framework. In contrast to the use of a penalty method which produces small but probably influential errors propagating into the space-time domain, the reformulation accompanied with LCP algorithms should be considered a genuine approach for the option pricing problems accompanied by an early-exercise property.

[6]The excellent performance of Lagrangian Multiplier method, which is a Newton-type iterative method, suggests that the discrete systems of the transformed equations (as introduced in chapter two) along with a symmetric coefficient matrix may also be efficiently solved by the Conjugate Gradient Methods, c.f. [73, 65]. However, the log transform may cause the numerical errors scaled up exponentially.

Chapter 9

Conclusion

We have presented a range of techniques aimed at solving the multi-asset option pricing problems for European, American and perpetual cases in a unified variational approach. We now flash through the points of this thesis, summarize our contributions, list possibilities of future work and make concluding remarks in the final chapter.

9.1 Summary of Previous Chapters

In chapter two, we reviewed mainstream formulations of option pricing problems. Simulation-based approaches mimic the assumed stochastic processes of the assets linked to an option. They are simple to implement in practice; but for only one convergent option price, one needs to simulate numerous paths, which is time-consuming and must be repeated once an asset price changes. Their computational cost are relatively expensive compared with the PDE/PDI-based approaches, especially in a multi-asset framework. On the account of computational efficiency, our research focuses on the PDE/PDI approaches, which allow us to obtain all possible option values when given different share prices or different time, and accordingly prevent one from repeated computation due to the everyday price change.

Among PDE/PDI approaches, the front-tracking methods aim to track the free boundary at every time step. However, the analytical properties of free boundaries of different options are not well understood yet. The free boundaries of different options behave so distinctively. For example, in one-asset case, the free boundaries of an American call and an American put are located above and below the exercise price respectively while the straddle counterpart has two on both sides. The variant behavior of different free boundaries makes the front-tracking method hard to implement in the generalized cases such as exotic and multi-asset options.

Penalty methods of PDI-based approaches force the awkward inequality become an equality by adding a penalty term into a partial differential inequality. Its idea is straightforward and can be applied even in high-dimensional cases. However, from analytical point

of view, we know little about the possible impact of the artificial penalty term. Will it overestimate or undervalue the option prices? What part of the domain will be influenced most? As time goes by, how will the penalty errors propagate into the space-time domain? All of these questions need to be further investigated from the functional point of view. Besides, the artificial penalty term often makes a partial differential equation becomes a nonlinear problem and demands more computational resources and a powerful numerical algorithm for solution. From these aspects, the penalty method seems an overkill approach for solving the BSM PDI.

To avoid the overkill manipulation, we decided to formulate our pricing problems in variational form. We first describe the boundary conditions used in our models in chapter three. In the following chapter, the pricing problems are rewritten as (4.9), (4.10) and (4.11) for European, American and perpetual cases. The theorems 4.5, 4.6 and 4.7 and proposition 4.8 justify their unique solutions when certain assumptions are met in selected solution spaces. Especially, the theorem 4.7 is adapted from the work of [27] without using a measure function but on a bounded domain.

The discrete weak formulations are presented in the form of linear system of equations (LSE) and linear complementarity problem (LCP) in chapter five by using the finite element method in space and the finite difference method in time. Finite element methods have some favourable geometric and functional properties suitable for all dimensional problems. Using the tensor shape functions along with lexicographical ordering, we derived the closed-form formulas for the exact component values of coefficient matrices in chapter six. These formulas provide exact integral values and speed up the pre-processing procedure of numerical computation.

Numerical algorithms for solving the LSE have been widely introduced and can be found in various literatures and references therein. In contrast, those for the LCP are limitedly understood and rarely used for solving partial differential inequalities. We consequently surveyed up to six algorithms in chapter seven and sketched their implementing procedure.

In chapter eight, we identified and visualized their evolutionary option values and accompanying free boundaries when given different payoffs, exercise restrictions and up to three assets. We also demonstrated the robustness of LCP solvers and compared their performances in various circumstances. In particular, the PSOR method, which is widely introduced for option pricing, manifest unsatisfactory performance. In contrast, the Howard's method, the Lagrangian Multiplier method and Lemke's method solve identical problems much faster and deserve more attention in the future study. The numerical errors were subsequently investigated. As expected, the discretization errors are reduced with increasingly small step sizes in space and time even though their convergence order is not trivial. The reduction of truncation errors are also observed in all our experiments. Particularly, the American and perpetual options can be solved on a small spatial domain as long as the selected far field bound can make the d-tuple of share prices falls into the early-exercise region (decided by the option parameters). The positive results adumbrate the promising

future of variational formulation for option pricing problems.

9.2 Contribution

We now outline our main contributions and detail them in the following subsections.

- Finite Element Reformulation of the Black-Scholes-Merton (BSM) PDE/PDI.
- Adaption of the work of [27] to prove the theorem of unique solution of perpetual option.
- Derivation of the closed-form formulas for elemental matrices.
- Calibration and visualization of various option values and free boundaries.
- Robustness investigation and comparison of LCP algorithms.
- Investigation of numerical errors.
- Achievement in programming.

9.2.1 Reformulation

The BSM PDE/PDI serve as the necessary condition for no-arbitrage argument in the BSM model. By reformulating them in variational form, we obtain a unified and elegant expression to present option pricing problems of European, American and perpetual cases in a generalized multi-asset framework. Such variational forms are accompanied with either all-Dirichlet boundary conditions or half-Dirichlet-half-Neumann boundary conditions. By choosing proper solution spaces/sets and restricting to a large enough but bounded spatial domain, their unique solutions can be guaranteed by the theorems and proposition in chapter four. The subsequent discretization can be performed by projecting the infinite-dimensional spaces/sets into their finite-dimensional counterparts.

9.2.2 Adaption

[27] focuses on a generalized unbounded domain and exploits a measure function to form bounded functionals for variational formulations. Instead of considering unbounded domain, we restrict ourselves on a large (in terms of computation) but bounded domain, its analogy of the theorem for unique solution of perpetual cases can then follows and can be proved by using the same ideas as [27] from the functional point of view.

9.2.3 Elemental Matrices

Conventionally, people adopt numerical integration to compute elemental matrices when working on finite element methods. However, in a high-dimensional case, one needs to select many enough Gaussian points to obtain satisfactory results of numerical integrals, which generally requests for more floating-point operations per second (FLOPs) and is hence time-consuming. Our formulas provide exact results of the integrals to form elemental matrices without spending precious time for the pre-processing procedure of numerical computation. The formulas are derived based on $d-$dimensioanl hyper-cube elements and $d-$linear shape functions. The same idea can be easily extended to $d-$dimensioanl hyper-triangle elements and higher-order shape functions in the future work.

9.2.4 Calibration and Visualization

We have identified and visualized the option values with the same type of payoff for European, American and perpetual cases in one-, two- and three-asset frameworks in chapter eight. We visualize, for the first time, the free boundaries of three-asset options. Generally the free boundary is a $(d-1)-$dimesnional manifold in a $d-$asset framework. We also found the analogy patterns of the free boundaries in different dimensional frameworks. It can be observed that the free boundary of American options move toward to that of its perpetual counterpart, namely the free boundary of steady state, as the time to maturity tends to infinity.

9.2.5 LCP Algorithms

We have tested the robustness of variational inequality approach by comparing the numerical solutions obtained by LCP algorithms with a few well-known exact solutions. The robustness test shows us extremely positive results to support its use. We also compared the performances of different LCP algorithms in terms of iteration number, computational time, cost per iteration, mean-square, maximum-relative, H_0, H_1 and $H_{1,w}$ errors in different payoffs and dimensions with and without time term involved. The widely introduced algorithm, the PSOR method, and its hybrid variants manifest disappointing performance in large-scale and high-dimensional problems. The modulus method produces biased solutions significantly inconsistent from those obtained by other methods in many cases. Our results indicate Howard's method has the most satisfactory performance in terms of computational time and accuracy for solving the large-scale LCP involved with multiple assets. Following Howard's method are the Lagrangian Multiplier method and Lemke's method which also deserve further study in the future.

9.2.6 Numerical Errors

We investigated the numerical errors, including discretization errors and truncation errors, by comparing the numerical solutions on different computational domains and meshes with either numerical or exact solutions on the finest mesh. As expected, their discretization errors are reduced as mesh size becomes finer. The truncation errors are decreased slowly with increasingly large far-field bound values. Moreover, we found if an option has (near-)zero values in the far-field area, such as a minimum put or a basket put, then its numerical solutions are less sensitive to the increase of far-field bound. For the American/perpetual options tending to be exercised almost surely on the far-field bounds, they can be solved on a small spatial domain with satisfactory accuracy if their far-field area is deeply located in the early-exercise region. Our discovery in a multi-dimensional framework is consistent with that of [72, Sec.5.2] in a two-asset framework.

9.2.7 Programming

We have successfully built a Matlab program to price an arbitrary option of following combinations in an objective sense, namely the object-oriented programming (OOP). Our Matlab code can be converted into C++ code straightly to further speed up the computational time in the future.

Dimension:		**Exercise restriction:**		**Portfolio price:**		**Payoff:**
One-asset,	$\times$	European,	$\times$	Basket,	$\times$	Call,
Two-asset,		American,		Minimum,		Put,
Three-asset,		Perpetual,		Maximum		Straddle.

9.3 Future Work

Our current work can be extended and improved from analytical and computational aspects. We list the possible directions to be further investigated by interested researchers.

9.3.1 Analytically

Jump Process:

It is interesting to investigate the pricing problems when stochastic part has a jump process such as a more general α-stable Levy process whose variational inequality may depend on a bilinear form involving a Fractional Laplacian operator, cf. [89, 87, 16].

Error Analysis:

We have seen the numerical behavior of discretization and truncation errors in our

framework. However, the analytical investigation of the errors are very challenging and has not yet been performed in our work. Conventionally, people investigate the errors with coercivity and with an equality. Instead we have weak coercivity and inequality (with complementarity condition) in our framework, these challenges make the analysis even more difficult. If an a prior/posterior error estimate can be derived from functional point of view, it can be further used in mesh refinement to improve numerical computation.

Other Variational Formulations:

There are at least two possibilities to obtain other reformulations. Instead of considering the $d-$linear shape function, one may use the *wavelet* basis function to reformulate the classical BSM operator as the *wavelet BSM operator* and obtain a different reformulation. Another possibility is like [27] to exploit a measure function. However, the measure function may make the computation of elemental matrices more complicated and more time-consuming.

Matrix Analysis:

One can investigated further on the global elemental matrices or the coefficient matrices used in the discrete forms. If their classes or properties can be identified exactly, they may provide useful information to choose/adapt an algorithm to solve option pricing problems more efficiently.

9.3.2 Computationally

Other Models:

It will be interesting to perform numerical experiments under other models and to identify and visualize their option values and free boundaries. For example, the local-volatility, stochastic-volatility and (Levy-)jump models may be suitable candidates.

Improvement of Time Discretization:

It is possible to use a higher-order Runge-Kutta method to improve the accuracy in time discretization. Besides, a non-uniform time mesh may also be applied if an error estimate can be designed.

Improvement of Spatial Discretization:

This can be performed from the following aspects.

1. Higher-order shape functions.
2. Adaptive mesh refinement.
3. Sparse grid multi-level methods.

Banded Sparse System:

A common point of all the discrete systems are the banded structure of their coefficient matrices. They have the pattern of 3^d bands in a $d-$dimensioanl framework. It requires further exploration and research to utilize the banded structure to solve the systems more efficiently, probably with the knowledge of graph theory, cf. [29, 30].

Efficient Utilization of Computational Resources:

As the number of assets increases, the corresponding discrete systems grow exponentially. Their computational capacity and capability are unavoidably highly demanded. These may be manipulated by combining the following techniques.

1. Domain decomposition.
2. Parallel computation.
3. Graphics processing unit (GPU) computation.

9.4 Concluding Remark

Compared with the prevalent use of classical Black-Scholes-Merton partial differential equation/inequality and finite difference method, the variational formulation and finite element method seem less applied in the computation of mathematical finance. As we have seen, the variational formulation is actually a unified approach for multi-asset European, American and perpetual options and the finite element method approximate the solutions in functional sense and with favourable geometric properties. Their merits should draw more attention in the future research of quantitative finance. In terms of numerical computation, we expect more efficient algorithms to be designed for the subsequent discrete systems, especially the large-scale linear complementarity problems of multi-asset American and perpetual options.

Appendix A

Unique Solution to Steady Variational Inequality Problem with Homogeneous Dirichlet BCs

[27] considers a Heston Model with an integro-differential operator A and a static obstacle problem of the form

$$\begin{cases} Av \geq f, \\ v \geq g, \\ (Av - f)(v - g) = 0 \end{cases}$$

where A is an elliptic differential operator, $f \in L^2(\Omega)$ is non-negative and g is an obstacle function. It is further reformulated as the steady variational inequality (SVI) of the form

$$\begin{cases} a(w - v, v) \geq (w - v, f), \\ v \geq g, \end{cases}$$

where $a(\cdot, \cdot)$ is a bilinear form. In the formulation of chapter four, we consider

$$\begin{cases} \mathcal{L}v \leq -f \equiv 0, \\ v \geq g. \end{cases} \Leftrightarrow \begin{cases} -\mathcal{L}v \geq f \equiv 0, \\ v \geq g. \end{cases}$$

where the differential operator is the Black-Scholes-Merton (BSM) operator defined as

$$\mathcal{L} := \frac{1}{2} \sum_{i=1}^{d} \sum_{j=1}^{d} \sigma_{ij} S^{(i)} S^{(j)} \frac{\partial^2}{\partial S^{(i)} \partial S^{(j)}} + \sum_{i=1}^{d} (r - q_i) S^{(i)} \frac{\partial}{\partial S^{(i)}} - r.$$

After reformulation, we have the corresponding BSM Static Variational Inequality (SVI)

$$\begin{cases} \big(b(w - v, v) - \ell(w - v)\big) \geq (w - v, f), \\ v \geq g, \end{cases} \Leftrightarrow \begin{cases} b(w - v, v) \geq (w - v, f) + \ell(w - v) =: \tilde{\ell}_f(w - v), \\ v \geq g. \end{cases}$$

If only Dirichlet BCs are considered, then $\ell(\cdot) \equiv 0$ in the formulation. Compared with [27], $-\mathcal{L} = A$, $f \equiv 0$ and there is an extra linear form $\ell(\cdot)$ in our formulation. We will prove the existence and uniqueness to the BSM SVI by adapting the proof from [27]. Even though $f \equiv 0$ in our formulation, the following proof can applied to a more general case with $f \neq 0$. As a result, we will preserve the notation f in what follows.

A.1 Coercivity

Before moving to the detailed proof, we first recall the theorem of the unique solution to a general SVI with strong coercivity (or V-ellipticity).

Theorem A.1 *[44, Ch.1]*
Consider a Gelfand triple $H^1(\Omega) \hookrightarrow L^2(\Omega) \hookrightarrow H^{-1}(\Omega) = H^1(\Omega)$ with the induced norms $||\cdot||_H = ||\cdot||_{H^1(\Omega)}$ and $||\cdot||_L = ||\cdot||_{L^2(\Omega)}$ and a subspace $\mathbb{V}$ such that $H_0^1(\Omega) \subseteq \mathbb{V} \subset H^1(\Omega)$ where $H_0^1(\Omega)$ is the subspace with homogeneous/zero Dirichlet boundary conditions. Provided the linear form $\ell(\cdot) : \mathbb{V} \to \mathbb{R}$ and bilinear form $b(\cdot,\cdot) : \mathbb{V} \times \mathbb{V} \to \mathbb{R}$ in a steady variational inequality (BSM SVI) are bounded and the bilinear is strong coercive or V-elliptic, i.e., for all $v \in \mathbb{V}$

$$b(w,w) \geq c||w||_{\mathbb{V}}^2 \quad \textit{for some } c > 0,$$

where $||\cdot||_{\mathbb{V}}$ is a norm on $\mathbb{V}$, then there exists a unique solution to the SVI if f is $L^2(\Omega)-$integrable.

Recall our bilinear form (4.3) in the BSM SVI satisfies Garding's Inequality instead, i.e.

$$b(w,w) \geq c_H||w||_{H^\omega}^2 - c_L||w||_L^2 \quad \text{for some } c_H > 0, c_L \geq 0.$$

We now define a modified bilinear form

$$\tilde{b}(w,v) := b(w,v) + c_L(w,v)_{L^2(\Omega)} =: b(w,v) + c_L(w,v),$$

which satisfies the strong coercivity w.r.t. $||\cdot||_{H^\omega}^2$

$$\tilde{b}(w,w) = b(w,w) + c_L(w,w) \geq c_H||v||_{H^\omega}^2.$$

A.2 Existence

A.2.1 Envelope Functions

Provided $r > 0$ in the BSM operator

$$\mathcal{L} := \frac{1}{2}\sum_{i=1}^{d}\sum_{j=1}^{d}\sigma_{ij}S^{(i)}S^{(j)}\frac{\partial^2}{\partial S^{(i)}\partial S^{(j)}} + \sum_{i=1}^{d}(r-q_i)S^{(i)}\frac{\partial}{\partial S^{(i)}} - r,$$

we assume there exist two envelope functions u_m, u_M satisfying the following hypotheses.

Hypothesis A.2

H1: $v_m, v_M \in H^{1,\omega}(\Omega) \cap L^q(\Omega) \subset L^2(\Omega)$ *for some* $q > 2$.

H2: $v_M \geq v_m$ *and* $v_M \geq g \geq 0$.

H3: $-\mathcal{L}v_m \leq f \leq -\mathcal{L}v_M$.

A.2.2 Solution to Sequential Problems

Aim: $\exists (v_n)_{n\in\mathbb{N}} \subset H^{1,\omega}(\Omega) \cap L^q(\Omega) \subset L^2(\Omega)$ for $q > 2$ such that

[A] $\tilde{b}(w - v_n, v_n) \geq (w - v_n, f + c_L \cdot v_{n-1}) + \ell(w - v_n)$ for all $w \in \mathbb{K}$ and $n = 1, 2, \ldots$.

[B] $v_n \geq \psi \geq 0$where $\psi = g$ is the obstacle/payoff function defined to form the closed convex subset $\mathbb{K}$.

[C] $v_M \geq v_1 \geq v_2 \geq \ldots \geq v_{n-1} \geq v_n \geq v_{n+1} \geq \ldots v_m$.

It is known that there exists a unique solution $v_n \geq \psi \geq 0$ (i.e. $v_n \in \mathbb{K}$) to satisfy (A) and (B) if $f \in L^2(\Omega)$ and $v_{n-1} \in L^2(\Omega)$. To start with, we let $v_0 = v_M$. In this fashion, there exist unique solutions to [A] and [B] for $n \in \mathbb{N}$.

Recall the notation $x^- := \max\{-x, 0\}$. We choose $w - v_n = w - v_1 = -(v_0 - v_1)^-$ for $n = 1$ in [A] to obtain

$$[\text{A1}] \quad b((v_0 - v_1)^-, -v_1) + c_L \cdot ((v_0 - v_1)^-, +v_0 - v_1) \geq ((v_0 - v_1)^-, -f) \; - \; \ell((v_0 - v_1)^-).$$

The hypothesis $f \leq -\mathcal{L}v_M$ implies $(h^+, f) + \ell(h^+) \leq b(h^+, v_M)$ (see Hypothesis [**H3**]) for all $0 \leq h^+ \in H^{1,\omega}(\Omega)$. We take $v_0 = v_M$ and $h^+ = +(v_0 - v_1)^-$ to reach

$$[\text{D1}] \quad b((v_0 - v_1)^-, v_0) \geq ((v_0 - v_1)^-, f) \; + \; \ell((v_0 - v_1)^-).$$

Adding [A1] and [D1] up leads to

$$\begin{aligned} & -\Big(b((v_0 - v_1)^-, (v_0 - v_1)^-) + c_L \cdot ((v_0 - v_1)^-, (v_0 - v_1)^-)\Big) \geq 0 \\ \Rightarrow \quad & 0 \geq \tilde{b}((v_0 - v_1)^-, (v_0 - v_1)^-) \geq c_H ||(v_0 - v_1)^-||^2_{H^\omega} \geq 0 \\ \Rightarrow \quad & v_0 \geq v_1. \end{aligned}$$

Assume $v_{k-1} \geq v_k$. We now choose $-(v_k - v_{k+1})^-$ and $(v_k - v_{k+1})^-$ as the $w - v_n$ for $n = k+1$ and $n = k$ respectively in [A]. Summing the results up gives

$$\begin{aligned}
&-\Big(b((v_k - v_{k+1})^-, (v_k - v_{k+1})^-) + c_L \cdot ((v_k - v_{k+1})^-, (v_k - v_{k+1})^-)\Big) \\
&\geq c_L \cdot \big((v_k - v_{k+1})^-, (v_{k-1} - v_k)\big) \\
\Leftrightarrow \quad & 0 \leq c_H \cdot ||(v_k - v_{k+1})^-||^2_{H^\omega} \leq \tilde{b}((v_k - v_{k+1})^-, (v_k - v_{k+1})^-) \\
& \leq -c_L \cdot \big((v_k - v_{k+1})^-, (v_{k-1} - v_k)\big) = c_L \cdot \big((v_k - v_{k+1})^-, (v_k - v_{k-1})\big) \leq 0 \\
\Leftrightarrow \quad & ||(v_k - v_{k+1})^-||_{H^\omega} = 0 \Leftrightarrow (v_k - v_{k+1})^- = 0 \Leftrightarrow v_k \geq v_{k+1}.
\end{aligned}$$

Recall $v_0 := v_M \geq v_m$ and $v_0 \geq g$. We now assume $v_{k-1} \in \mathbb{K}$ and $v_{k-1} \geq v_m$ and set $w - v_n = (v_k - v_m)^-$ for $n = k$ in [A] to obtain

$$\begin{aligned}
&b((v_k - v_m)^-, v_k) + c_L \cdot ((v_k - v_m)^-, v_k) \\
&\geq ((v_k - v_m)^-, f + c_L \cdot v_{k-1}) + \ell((v_k - v_m)^-) \\
\Leftrightarrow \quad & b((v_k - v_m)^-, v_k - v_m) + c_L \cdot ((v_k - v_m)^-, v_k - v_m) + c_L \cdot ((v_k - v_m)^-, v_m) \\
& \geq ((v_k - v_m)^-, f + c_L \cdot v_{k-1}) - b((v_k - v_m)^-, v_m) + \ell((v_k - v_m)^-) \\
\Leftrightarrow \quad & -\Big(b((v_k - v_m)^-, (v_k - v_m)^-) + c_L \cdot ((v_k - v_m)^-, (v_k - v_m)^-)\Big) \\
& \geq ((v_k - v_m)^-, (f + \mathcal{L}v_m) + c_L \cdot (v_{k-1} - v_m)) \geq 0 \\
\Rightarrow \quad & -\tilde{b}((v_k - v_m)^-, (v_k - v_m)^-) \geq 0 \\
\Rightarrow \quad & 0 \leq c_H ||(v_k - v_m)^-||^2_{H^\omega} \leq \tilde{b}((v_k - v_m)^-, (v_k - v_m)^-) \leq 0 \\
\Rightarrow \quad & ||(v_k - v_m)^-||_{H^\omega} = 0 \Leftrightarrow (v_k - v_m)^- = 0 \Leftrightarrow v_k \geq v_m.
\end{aligned}$$

We hence complete the proof of [C].

A.2.3 Convergence

Strong Convergence

Recall $v_M =: v_0 \geq v_1 \geq v_2 \geq \ldots \geq v_m$ where $(v_n) \subset H^{1,\omega}(\Omega) \subset L^2(\Omega)$ and $u_M, u_m \in L^q(\Omega)$ for some $q > 2$. Consequently, $|v_k| \leq |v_M| + |v_m| + 1 \in L^q(\Omega)$. This implies there exists a subsequence (v_{n_k}) and a $v \in L^2(\Omega)$ such that $||v_{n_k} - v||_L \to 0 \Leftrightarrow v_{n_k} \to v$ in $L^2(\Omega)$ as $n_k \to \infty$. Since (v_n) is a decreasing sequence, the above result amounts to saying v is the limit of $(v_n)_{n\in\mathbb{N}}$ in $L^2(\Omega)$, i.e. $||v_n - v||_L \to 0 \Leftrightarrow v_n \to v$ in $L^2(\Omega)$ as $n \to \infty$.

Weak Convergence

$$\begin{aligned}
\text{Recall [A]} \quad & \Leftrightarrow \quad \tilde{b}(w, v_n) - (w - v_n, f + c_L v_{n-1}) - \ell(w - v_n) \geq \tilde{b}(v_n, v_n) \geq c_H ||v_n||^2_{H^\omega} \geq 0 \\
& \Rightarrow \quad b(w, v_n) + c_L(w, v_n) - (w - v_n, f + c_L v_{n-1}) - \ell(w - v_n) \geq c_H ||v_n||^2_{H^\omega} \geq 0.
\end{aligned}$$

We now take $w = v_0 := v_M$ in the inequality.

$$\begin{aligned} 0 &\leq c_H||v_n||^2_{H^\omega} \\ &\leq b(v_0, v_n) + c_L(v_0, v_n) - (v_0 - v_n, f + c_L \cdot v_{n-1}) - \ell(v_0 - v_n) \\ &\leq c_2||v_0||_{H^\omega}||v_n||_{H^\omega} + c_L||v_0||_L||v_n||_L + (||v_0||_L + ||v_n||_L)(||f||_L + c_L||v_{n-1}||_L) \\ &\quad + c_0(||v_0||_{H^\omega} + ||v_n||_{H^\omega}). \end{aligned}$$

Recall that $(v_n)_{n\in\mathbb{N}}$ is convergent in $L^2(\Omega)$ which implies $||v_n||_L$ is uniformly bounded by some positive constant; $(2)v_0 \in L^q(\Omega)$ with $q > 2$ also tells $||v_0||_L$ is uniformly bounded by another positive constant. In this manner, we can rewrite the inequality as

$$\begin{aligned} & 0 \leq c_H||v_n||^2_{H^\omega} \leq c||v_n||_{H^\omega} + \tilde{c} \qquad \text{(where } c \text{ and } \tilde{c} \text{ are some positive constants)} \\ \Leftrightarrow \quad & 0 \leq c_H||v_n||_{H^\omega} \leq c + \frac{\tilde{c}}{||v_n||_{H^\omega}}. \end{aligned}$$

The right hand side must be bounded and hence $||v_n||_{H^\omega}$ is bounded.

As $(v_n)_{n=1,2,\ldots}$ is a bounded sequence in $H^{1,\omega}(\Omega)$, there exist a subsequence $(v_{n_k}) \subset (v_n)$ and a limit $v \in H^{1,\omega}(\Omega)$ such that (v_{n_k}) converges to v weakly, i.e. $v_{n_k} \rightharpoonup v$. As (v_n) is a decreasing sequence and $H^{1,\omega}(\Omega) \subset L^2(\Omega)$, the result amounts to saying the (unique) strong limit v in $L^2(\Omega)$ of $(v_n)_{n=1,2,\ldots}$ is its weak limit in $H^{1,\omega}(\Omega)$, i.e. $v_n \rightharpoonup v$ in $H^{1,\omega}(\Omega)$ as $n \to \infty$.

A.2.4 Existence of Solution to Original Problem

The lemma below is also helpful to the following deduction.

Lemma A.3 [27, Lemma.B.3, p.110]
Consider a continuous/bounded bilinear form $b : H \times H \to \mathbb{R}$ where H is a Hilbert space. Provided $w_n \rightharpoonup w$ in $H$and $s_n \to s$ in H,

1. $\lim_{n\to\infty} b(w_n, h) = b(w, h)$ for all $h \in H$;
2. $\lim_{n\to\infty} b(w_n, s_n) = b(w, s)$;
3. if $b(\cdot, \cdot)$ is strongly coercive, then $\lim_{n\to\infty} \inf b(w_n, w_n) \geq b(w, w)$.

With [A], we have

$$\begin{aligned}
& \tilde{b}(w-v_n, v_n) \geq (w-v_n, f+c_L v_{n-1}) + \ell(w-v_n) \\
\Rightarrow \quad & \lim_{n\to\infty} b(w, v_n) + c_L \cdot \lim_{n\to\infty} (w, v_n) - \lim_{n\to\infty} (w-v_n, f) \\
& \geq \lim_{n\to\infty} \tilde{b}(v_n, v_n) + c_L \cdot \lim_{n\to\infty} (w, v_{n-1}) - c_L \cdot \lim_{n\to\infty} (v_n, v_{n-1}) + \ell(w) - \lim_{n\to\infty} \ell(v_n) \\
\Rightarrow \quad & b(w, v) + c_L \cdot (w, v) - (w-v, f) \geq \tilde{b}(v, v) + c_L \cdot (w, v) - c_L \cdot (v, v) + \ell(w-v) \\
\Leftrightarrow \quad & b(w-v, v) \geq (w-v, f) + \ell(w-v)
\end{aligned}$$

Since we consider continuous functions, $v_m \leq v_n \leq v_M$, $g \leq v_n$ for $n = 1, 2, \ldots$ and $v_n \to v$ (strongly) in $L^2(\Omega)$, we can conclude $\max\{v_m, g\} \leq v \leq v_M$.

A.3 Uniqueness

A.3.1 Comparison of Solutions

Lemma A.4
Assume $\mathbb{V}$ is a subspace of a Hilbert space $\mathbb{H}$. Suppose $\tilde{v}_1$ and $\tilde{v}_2$ are the solutions to the following variational inequality problems with $i = 1, 2$ respectively.

$$\begin{aligned}
& \text{For all } \tilde{w} \in \mathbb{K}_i := \{w \in \mathbb{V} : w \geq g_i\}, \text{ find } \tilde{v}_i \text{ such that} \\
& (\tilde{P}.1) \quad \tilde{b}(\tilde{w} - \tilde{v}_i, \tilde{v}_i) \geq (\tilde{w} - \tilde{v}_i, \tilde{f}_i) + \ell(\tilde{w} - \tilde{v}_i), \\
& (\tilde{P}.2) \quad \tilde{v}_i \in \mathbb{K}_i,
\end{aligned}$$

where $\ell(\cdot)$ and $\tilde{b}(\cdot, \cdot)$ are bounded. If $\tilde{b}(\cdot, \cdot)$ is strongly coercive, $\tilde{f}_1 \leq \tilde{f}_2$ and $g_1 \leq g_2$, then $\tilde{v}_1 \leq \tilde{v}_2$.

Proof.
Let $\tilde{w} - \tilde{v}_1 = -(\tilde{v}_2 - \tilde{v}_1)^-$ and $\tilde{w} - \tilde{v}_2 = +(\tilde{v}_2 - \tilde{v}_1)^-$ for $i = 1, 2$ in $(\tilde{P}.1)$ respectively. Summing the results gives

$$\begin{aligned}
& \tilde{b}((\tilde{v}_2 - \tilde{v}_1)^-, \tilde{v}_2 - \tilde{v}_1) \geq ((\tilde{v}_2 - \tilde{v}_1)^-, \tilde{f}_2 - \tilde{f}_1) \\
\Leftrightarrow \quad & 0 \leq c_H ||(\tilde{v}_2 - \tilde{v}_1)^-||^2_{H^\omega} \leq \tilde{b}((\tilde{v}_2 - \tilde{v}_1)^-, (\tilde{v}_2 - \tilde{v}_1)^-) \leq 0 \\
\Rightarrow \quad & \tilde{v}_2 \geq \tilde{v}_1.
\end{aligned}$$

■

Lemma A.5
Assume $\mathbb{V}$ is a subspace of a Hilbert space $\mathbb{H}$. Suppose $\tilde{v}_1$ and $\tilde{v}_2$ are the solutions to the

following variational inequality problems with $i = 1, 2$ respectively.

$$\begin{aligned}
&\text{For all } \tilde{w} \in \mathbb{K} := \{w \in \mathbb{V} : w \geq g\}, \text{ find } \tilde{v}_i \text{ such that} \\
&(\tilde{P}.3) \quad \tilde{b}(\tilde{w} - \tilde{v}_i, \tilde{v}_i) \geq (\tilde{w} - \tilde{v}_i, \tilde{f}) + \beta_i \cdot \ell(\tilde{w} - \tilde{v}_i), \\
&(\tilde{P}.4) \quad \tilde{v}_i \in \mathbb{K},
\end{aligned}$$

where $\ell(\cdot)$ and $\tilde{b}(\cdot, \cdot)$ are bounded and $\ell(\tilde{w}) \geq 0$ if $\tilde{w} \geq 0$. If $\tilde{b}(\cdot, \cdot)$ is strongly coercive, $0 < \beta_1 < \beta_2$, then $\tilde{v}_1 \leq \tilde{v}_2$.

Proof.
Similarly, let $\tilde{w} - \tilde{v}_1 = -(\tilde{v}_2 - \tilde{v}_1)^-$ and $\tilde{w} - \tilde{v}_2 = +(\tilde{v}_2 - \tilde{v}_1)^-$ for $i = 1, 2$ in $(\tilde{P}.3)$ respectively. Summing up the results gives

$$\begin{aligned}
& \tilde{b}((\tilde{v}_2 - \tilde{v}_1)^-, \tilde{v}_2 - \tilde{v}_1) \geq (\beta_2 - \beta_1) \cdot \ell((\tilde{v}_2 - \tilde{v}_1)^-) \geq 0 \\
\Leftrightarrow \quad & 0 \leq c_H ||(\tilde{v}_2 - \tilde{v}_1)^-||^2_{H^\omega} \leq \tilde{b}((\tilde{v}_2 - \tilde{v}_1)^-, (\tilde{v}_2 - \tilde{v}_1)^-) \leq 0 \\
\Rightarrow \quad & \tilde{v}_2 \geq \tilde{v}_1.
\end{aligned}$$

■

A.3.2 Solution to the Variational Equality Associated with a Distortion Function

In addition to the hypotheses of envelope functions, we further assume there exists a distortion function ϕ over the bounded domain Ω satisfying the following hypotheses.

Hypothesis A.6

H1': $0 \leq \phi \subset H^{1,\omega}(\Omega)$.

H2': $0 \leq -\mathcal{L}\phi$.

H3': $-\mathcal{L}(v_m + \phi) > 0$.

H4': $\sup_{\mathbf{s} \in \Omega} \dfrac{v_M + \phi}{-\mathcal{L}(v_m + \phi)} < \infty$.

We recall a classical elliptic PDE of the form

$$-\mathcal{L}v = f.$$

Assume it has no Neumann BCs, then its variational form is

$$b(w, v) = (w, f).$$

We now consider $\mathcal{L} : H^{1,\omega}(\Omega) \cap H^2(\Omega) \to L^2(\Omega)$. Assume there exists such function $v_\phi \in H^{1,\omega}(\Omega) \cap H^2(\Omega)$ such that, cf.[27, Lemma 3.21, p.35],

H5': $b(w, v_\phi) = (w, -\mathcal{L}\phi)$ *for all* $w \in H^{1,\omega}_0(\Omega)$.

H6': $\mathcal{L}v_\phi = \mathcal{L}\phi$.

Combining [H2] with [H6'], we have the following property.

$$0 < -\mathcal{L}(u_m + \phi) \leq f - \mathcal{L}v_\phi =: \tilde{f}_\phi \leq -\mathcal{L}(u_M + \phi) \tag{A.1}$$

A.3.3 Distorted Problem

We now consider the distorted variational inequality problem $(\hat{P})$ as below.

$$(\hat{P}) \begin{cases} \text{For all } \tilde{w}_\phi \in \tilde{\mathbb{K}}_\phi := \{w \in \mathbb{V} : w \geq \tilde{g}_\phi\}, \text{ find } \tilde{v}_\phi \text{ such that} \\ (\hat{P}.1) \quad b(\tilde{w}_\phi - \tilde{v}_\phi, \tilde{v}_\phi) \geq (\tilde{w}_\phi - \tilde{v}_\phi, \tilde{f}_\phi) + \ell(\tilde{w}_\phi - \tilde{v}_\phi), \\ (\hat{P}.2) \quad \tilde{v}_\phi \in \tilde{\mathbb{K}}_\phi, \end{cases}$$

where $\tilde{f}_\phi := f - \mathcal{L}v_\phi > 0$. We further assume there exists two envelope functions $\tilde{v}_m, \tilde{v}_M$ as previous discussion such that

- $\tilde{v}_m \leq \tilde{v}_\phi \leq \tilde{v}_M$.
- $-\mathcal{L}\tilde{v}_m \leq \tilde{f}_\phi \leq -\mathcal{L}\tilde{v}_M$.
- $\tilde{v}_M \leq v_M + \phi$.
- $-\mathcal{L}\tilde{v}_m \geq -\mathcal{L}(v_m + \phi)$.

Assume ${\tilde{v}_\phi}^1$ and ${\tilde{v}_\phi}^2$ are two distinct solutions to $\hat{P}$. Without loss of generality, we may assume $\exists D \subset \Omega$ such that

$$\text{[AA]} \ {\tilde{v}_\phi}^1(\mathbf{S}) \nleq {\tilde{v}_\phi}^2(\mathbf{S}), \forall \mathbf{S} \in D.$$

We define a function $\alpha(\mathbf{S}) := \min\{1, \frac{{\tilde{v}_\phi}^2(\mathbf{S})}{{\tilde{v}_\phi}^1(\mathbf{S})}\} \leq 1$ where we also define $\frac{0}{0} =: 0$ and $\frac{1}{0} =: \infty$. Note that

$$\alpha(\mathbf{S}) \cdot {\tilde{v}_\phi}^1(\mathbf{S}) = \min\{{\tilde{v}_\phi}^1(\mathbf{S}), {\tilde{v}_\phi}^2(\mathbf{S})\} \in \tilde{\mathbb{K}}_\phi,$$

because both solutions satisfy the obstacle condition $\tilde{v}_\phi \geq \tilde{g}_\phi$.

We further define the constant $\alpha_{\inf} := \inf_{\mathbf{S} \in \Omega} \alpha(\mathbf{S})$. If $\alpha_{\inf} = 1$, then it implies $\forall \mathbf{S} \in \Omega$, $\alpha(\mathbf{S}) = \min\{1, \frac{{\tilde{v}_\phi}^2(\mathbf{S})}{{\tilde{v}_\phi}^1(\mathbf{S})}\} \geq \alpha_{\inf} = 1$ and ${\tilde{v}_\phi}^2(\mathbf{S}) \geq {\tilde{v}_\phi}^1(\mathbf{S})$ over the whole Ω. This contradicts [AA]. As a result,

$$0 \leq \alpha_{\inf} < 1.$$

We now choose a constant β which is close enough to $\alpha_{\inf}$ such that

$$\begin{aligned}&\text{[BB]} \quad 0 \le \alpha_{\inf} < \beta < 1,\\ &\text{[CC]} \quad \tilde{f}^1 := \beta \cdot (\tilde{f}_\phi + c_L \tilde{v}_\phi{}^1) \le (\tilde{f}_\phi + c_L \tilde{v}_\phi{}^2) =: \tilde{f}^2.\end{aligned}$$

[CC] can be justified if the following holds.

$$\begin{aligned}&\beta \cdot (\tilde{f}_\phi + c_L \tilde{v}_\phi{}^1) \le \tilde{f}_\phi + c_L \cdot \alpha_{\inf} \cdot \tilde{v}_\phi{}^1\\ \Leftrightarrow \text{[CC']} \quad &\frac{\tilde{v}_\phi{}^1}{\tilde{f}_\phi} \le \frac{1-\beta}{c_L \cdot (\beta - \alpha_{\inf})}.\end{aligned}$$

On the one hand,

$$\frac{\tilde{v}_\phi{}^1}{\tilde{f}_\phi} \le \frac{\tilde{v}_M}{-\mathcal{L}\tilde{v}_m} \le \frac{v_M + \phi}{-\mathcal{L}(v_m + \phi)} \le \sup \frac{v_M + \phi}{-\mathcal{L}(v_m + \phi)} < \infty,$$

i.e. the LHS of [CC'] is bounded, say the LHS$< k$ for some $k > 0$. On the other hand, the RHS of [CC'] can be an arbitrarily large but finite number. As a result, we can select the β close enough to $\alpha_{\inf}$ (from its right) such that [CC'] holds.

Recall we assume $\tilde{v}_\phi{}^1$ and $\tilde{v}_\phi{}^2$ are two different solutions to $(\hat{P})$.
$\beta^2 \cdot \Big((\hat{P}.1) + c_L(\tilde{w}_\phi - \tilde{v}_\phi, \tilde{v}_\phi)\Big)$ with $\tilde{v}_\phi = \tilde{v}_\phi{}^1$ gives

$$\tilde{b}(\beta(\tilde{w}_\phi - \tilde{v}_\phi{}^1), \beta\tilde{v}_\phi{}^1) \ge (\beta(\tilde{w}_\phi - \tilde{v}_\phi{}^1), \beta(\tilde{f}_\phi + c_L\tilde{v}_\phi{}^1)) + \beta \cdot \ell(\beta(\tilde{w}_\phi - \tilde{v}_\phi{}^1)).$$

Let $\tilde{v}^1 := \beta\tilde{v}_\phi{}^1, \tilde{f}^1 := \beta(\tilde{f}_\phi + c_L\tilde{v}_\phi{}^1)$ and note $\tilde{v}^1 = \beta\tilde{v}_\phi{}^1 \ge \beta\tilde{g}_\phi =: \tilde{g}^1$. We find $\tilde{v}^1 = \beta\tilde{v}_\phi{}^1$ is the solution to the problem $(\hat{P}1)$.

$$(\hat{P}1)\begin{cases}\text{For all } \tilde{w} \in \tilde{\mathbb{K}}_\phi, \text{ find } \tilde{v}^1 \text{ such that}\\ (\hat{P}1.1) \quad \tilde{b}(\tilde{w} - \tilde{v}^1, \tilde{v}^1) \ge (\tilde{w} - \tilde{v}^1, \tilde{f}^1) + \beta \cdot \ell(\tilde{w} - \tilde{v}^1),\\ (\hat{P}1.2) \quad \tilde{v}^1 \in \tilde{\mathbb{K}}_\phi,\end{cases}$$

Similarly $(\hat{P}1) + c_L(\tilde{w}_\phi - \tilde{v}_\phi, \tilde{v}_\phi)$ with $\tilde{v}_\phi = \tilde{v}_\phi{}^2$ gives

$$\tilde{b}(\tilde{w}_\phi - \tilde{v}_\phi{}^2, \tilde{v}_\phi{}^2) \ge (\tilde{w}_\phi - \tilde{v}_\phi{}^2, \tilde{f}_\phi + c_L\tilde{v}_\phi{}^2) + \ell(\tilde{w}_\phi - \tilde{v}_\phi{}^2).$$

Let $\tilde{v}^2 := \tilde{v}_\phi{}^2, \tilde{f}^2 := \tilde{f}_\phi + c_L\tilde{v}_\phi{}^2$ and note $\tilde{v}^2 = \tilde{v}_\phi{}^1 \ge \tilde{g}_\phi =: \tilde{g}^2$. We find $\tilde{v}^2 := \tilde{v}_\phi{}^2$ is the solution to the problem $(\hat{P}2)$.

$$(\hat{P}2)\begin{cases}\text{For all } \tilde{w} \in \tilde{\mathbb{K}}_\phi, \text{ find } \tilde{v}^2 \text{ such that}\\ (\hat{P}2.1) \quad \tilde{b}(\tilde{w} - \tilde{v}^2, \tilde{v}^2) \ge (\tilde{w} - \tilde{v}^2, \tilde{f}^2) + 1 \cdot \ell(\tilde{w} - \tilde{v}^2),\\ (\hat{P}2.2) \quad \tilde{v}^2 \in \tilde{\mathbb{K}}_\phi,\end{cases}$$

Provided $\tilde{b}(\cdot,\cdot)$ is strongly coercive, $\tilde{f}^2 \geq \tilde{f}^1$ (by [CC]) and $\tilde{g}^2 = \tilde{g}_\phi \geq \tilde{g}^1$ (due to $0 < \beta < 1$), we conclude

$$\text{[DD]}\ \tilde{v}^2 := \tilde{v}_\phi{}^2 \geq \beta \tilde{v}_\phi{}^1 =: \tilde{v}^1,$$

with the help of Lemma A.4 and Lemma A.5 .

Recall $0 \leq \alpha_{\inf} < \beta < 1$. We can find $\epsilon > 0$ such that

$$0 < \epsilon < \beta - \alpha_{\inf} \ \Rightarrow\ \text{[EE]}\ 0 < \alpha_{\inf} + \epsilon < \beta.$$

Since $\alpha_{\inf} := \inf_{\mathbf{S}\in\Omega} \alpha(\mathbf{S})$, for the ϵ above, one can find a subset $D_\epsilon \subset \Omega$ such that for all $\mathbf{S} \in D_\epsilon$,

$$\begin{aligned} &\text{[FF]} \quad \alpha(\mathbf{S}) \leq \alpha_{\inf} + \epsilon < \beta, \\ &\text{[GG]} \quad 1 > \alpha(\mathbf{S}) := \min\{1, \frac{\tilde{v}_\phi{}^2(\mathbf{S})}{\tilde{v}_\phi{}^1(\mathbf{S})}\} = \frac{\tilde{v}_\phi{}^2(\mathbf{S})}{\tilde{v}_\phi{}^1(\mathbf{S})}. \end{aligned}$$

However, for all $\mathbf{S} \in D_\epsilon$, we have

$$\tilde{v}_\phi{}^2 = \min\{1, \frac{\tilde{v}_\phi{}^2(\mathbf{S})}{\tilde{v}_\phi{}^1(\mathbf{S})}\} \cdot \tilde{v}_\phi{}^1 = \alpha(\mathbf{S}) \cdot \tilde{v}_\phi{}^1 < \beta \cdot \tilde{v}_\phi{}^1 < \tilde{v}_\phi{}^2,$$

with the help of [DD],[FF] and [GG]. We reach the contradiction $\tilde{v}_\phi{}^2(\mathbf{S}) < \tilde{v}_\phi{}^2(\mathbf{S})$ for all $\mathbf{S} \in D_\epsilon$. We can now conclude that the solution to the distorted problem $\hat{P}$ is unique.

A.3.4 Original Problem

Suppose $\tilde{v}_\phi$ is the unique solution to the distorted variational problem $(\hat{P})$. Subtracting $(\tilde{w}_\phi - \tilde{v}_\phi, -\mathcal{L}\phi)$ from $(\hat{P}.1)$ and using $f - \mathcal{L}v_\phi =: \tilde{f}_\phi$ gives

$$b(\tilde{w}_\phi - \tilde{v}_\phi, \tilde{v}_\phi - \tilde{v}_\phi) \geq (\tilde{w}_\phi - \tilde{v}_\phi, f) + \ell(\tilde{w}_\phi - \tilde{v}_\phi).$$

Let $v := \tilde{v}_\phi - v_\phi$ and $w - v = \tilde{w}_\phi - \tilde{v}_\phi$. We find v is the solution to the original problem below.

$$\text{Original Problem (P)} \begin{cases} \text{For all } w \in \mathbb{K} := \{w \in \mathbb{V} : w \geq g\}, \text{ find } v \text{ such that} \\ (P.1) \quad \tilde{b}(w - v, v) \geq (w - v, f) + \ell(w - v), \\ (P.2) \quad v \in \mathbb{K}. \end{cases}$$

Suppose v^1 and v^2 are two solutions to the original problem (P). With identical ϕ and v_ϕ, we have $\tilde{v}_\phi{}^1 = v^1 + v_\phi$ and $\tilde{v}_\phi{}^2 = v^2 + v_\phi$ as two solutions to the corresponding distorted problem $(\hat{P})$. However, $(\hat{P})$ has a unique solution, which implies $v^1 + v_\phi = \tilde{v}_\phi{}^1 = \tilde{v}_\phi{}^2 = v^2 + v_\phi \Leftrightarrow v^1 = v^2$ over the whole domain Ω. Namely, the original problem (P) actually has a unique solution.

‘

Appendix B

Elemental Computation by Quadrature

Conventionally, numerical integration is adopted when treating integration for finite element techniques. To simplify the numerical procedure, a canonical approach is mapping a physical element to a reference oneand applying numerical quadrature over the reference domain.

B.1 Change of variable

A direct approach to map a hypercube to the reference one is to scale and shift it using

$$\mathbf{S}^* = \mathbf{J}^{-1}(\mathbf{S} - \mathbf{S}_1^{(e)}) \leftrightarrow \mathbf{S} = \mathbf{S}_1^{(e)} + \mathbf{J}\mathbf{S}^* =: \mathcal{T}_{\mathbf{e}}(\mathbf{S}^*)$$

where $\mathbf{J}^{-1}$ and $\mathbf{J}$ are Jacobian matrices. Take the two-dimensional square element as an example, we have

$$\mathbf{J} := \frac{d\mathbf{S}^T}{d\mathbf{S}^*} = \left[\frac{\partial S^{(j)}}{\partial S_*^{(i)}}\right]_{2\times 2} = \begin{pmatrix} h_1 & 0 \\ 0 & h_2 \end{pmatrix}, \tag{B.1}$$

and

$$\mathbf{J}^{-1} := \begin{pmatrix} \frac{1}{h_1} & 0 \\ 0 & \frac{1}{h_2} \end{pmatrix}. \tag{B.2}$$

Note both $\mathbf{J}$ and $\mathbf{J}^{-1}$ are symmetric diagonal in this case.

In this manner, integrals over a common element can be rewritten as follows. For the local indices $\ell_1, \ell_2 \in \{1, \ldots, 2^d\}$,

$$\begin{aligned}
\mathbf{M}^{(e)}_{\ell_1,\ell_2} &:= |\det(\mathbf{J})| \int_{\Omega^*} N^{(\ell_1)}_* N^{(\ell_2)}_* d\Omega^*, \\
\mathbf{K}^{(e)}_{\ell_1,\ell_2} &:= |\det(\mathbf{J})| \int_{\Omega^*} (\nabla_* N^{(\ell_1)}_*)^T (\mathbf{J}^{-1}\mathbf{T}_*\mathbf{J}^{-1})(\nabla_* N^{(\ell_2)}_*) d\Omega^*, \\
\mathbf{A}^{(e)}_{\ell_1,\ell_2} &:= |\det(\mathbf{J})| \int_{\Omega^*} N^{(\ell_1)}_* (\tilde{\mathbf{D}}_*{}^T \mathbf{J}^{-1})(\nabla_* N^{(\ell_2)}_*) d\Omega^*.
\end{aligned}$$

where

$$\begin{aligned}
\mathbf{T}_* &:= \frac{1}{2} \cdot \mathbf{\Sigma} \odot (\mathcal{T}_e(\mathbf{S}^*)\, \mathcal{T}_e(\mathbf{S})^T), \\
\tilde{\mathbf{D}}_* &:= \bar{\mathbf{D}} \odot (\mathcal{T}_e(\mathbf{S}^*)).
\end{aligned}$$

We now focus on $\mathbf{L}^{(B,b)}_\ell$ which is associated with the integral over a Neumann boundary element $\Gamma^{(b)}_{N^{(B)}} \subset \Gamma_{N^{(B)}} \subset \Gamma_N$ for some $B \in \{1, \ldots, d\}$. Analogously we define a boundary reference element $\Gamma^*_N := [0,1]^{d-1}$ and a domain transform function $\mathbf{S}_B = \mathcal{T}^B_b(\mathbf{S}^*)$ where $\mathbf{S}^* \in \Gamma^*_N$ and $\mathbf{S}_B = (S^{(1)}, \ldots, S^{(B)} = S_{\max}, \ldots, S^{(d)}) \in \Gamma^{(b)}_{N^{(B)}}$. Their *boundary Jacobian matrices* are denoted by $\mathbf{J_B}$ and $\mathbf{J_B}^{-1}$ of size $2^{d-1} \times 2^{d-1}$. A shape function over $\Gamma^{(b)}_{N^{(B)}}$ is denoted by N^ℓ_b. With the help of these notations, we can find the components of (Neumann boundary) load vector as follows. For all $\ell \in \{1, \ldots, 2^{d-1}\}$,

$$\mathbf{L}^{(B,b)}_\ell := |\det(\mathbf{J_B})| \int_{\Gamma^*_N} f^B_* N^{(\ell)}_* d\Gamma^*_N$$

where

$$\begin{aligned}
f^B_* &:= \mathbf{n} \cdot \mathbf{T}^B_* \nabla g \\
\mathbf{T}^B_* &:= \frac{1}{2} \cdot \mathbf{\Sigma} \odot (\mathcal{T}^B_b(\mathbf{S}^*)\, \mathcal{T}^B_b(\mathbf{S}^*)^T).
\end{aligned}$$

B.2 Comment

Conventionally, the integrals over each computational element are computed using quadrature techniques after a change of variable. The integrals of mass matrices are element-independent, so it is efficient to compute them once and for all on a reference element.

However, the integrals of other elemental matrices are still element-dependent which requests the numerical integration repeated element by element. As well, numerical integration can achieve satisfactory accuracy only when the number of Gaussian points (over the reference element) is large enough. This number generally increases as number of dimensions increases or order of needed accuracy increase.

If the numerical integration (up to satisfactory accuracy on the computational domain) is performed element by element in high-dimensional cases, then such process for our problems is time-consuming compared with using the exact closed-form formulas of the integrals. Due to this, we employ the closed-form formulas introduced in the chapter six for our computation.

Bibliography

[1] L. Angermann and S. Wang. Convergence of a Fitted Finite Volume Method for the Penalized Black-Scholes Equation Governing European and American Option Pricing. *Numerische Mathematik*, 106(1):1, 2007.

[2] S. Asmussen and P. W. Glynn. *Stochastic Simulation: Algorithms and Analysis*. Springer, 2007.

[3] K. Bahlali, M. Eddahbi, and E. Essaky. BSDE Associated with Levy Processes and Application to PDIE. *Journal of Applied Mathematics and Stochastic Analysis*, 16(1):1–17, 2003.

[4] Z. Bai. Modulus-based Matrix Splitting Iteration Methods for Linear Complementarity Problems. *Numerical Linear Algebra with Applications*, 17(6):917–933, 2010.

[5] C. Baiocchi and A. Capelo. *Variational and Quasivariational Inequalities: Applications to Free Boundary Problems*. Wiley, 1984.

[6] J. Barraquand and D. Martineau. Numerical Valuation of High Dimensional Multivariate American Securities. *Journal of Financial and Quantitative Analysis*, 30(3):383–405, 1995.

[7] E. Benhamou. Option Pricing with Levy Process. Finance 0212006, EconWPA, Dec 2002.

[8] F. Black and M. Scholes. The Pricing of Options and Corporate Liabilities. *The Journal of Political Economy*, 81(3):637–654, 1973.

[9] O. Bokanowski, S. Maroso, and H. Zidani. Some Convergence Results for Howard's Algorithm. *SIAM Journal on Numerical Analysis*, 47(4):3001–3026, preprint available in 2007 and published in 2009.

[10] T. Bokes. A Unified Approach to Determining the Early Exercise Boundary Position at Expiry for American Style of General Class of Derivatives. *Working paper*, 2011.

[11] S. C. Brenner and R. Scott. *The Mathematical Theory of Finite Element Methods*. Springer, 2007.

[12] M. Broadie and P. Glasserman. A Stochastic Mesh Method for Pricing High-dimensional American Options. *Journal of Computational Finance*, 7(4):35–72, 2004.

[13] M. Broadie, P. Glasserman, and Z. Ha. Pricing American Options by Simulation Using a Stochastic Mesh with Optimized Weights. *Probabilistic Constrained Optimization: Methodology and Applications.*, pages 32–50, 2000.

[14] Z. Brzezniak and T. Zastawniak. *Basic Stochastic Processes*. Springer, 2000.

[15] L. A. Caffarelli and N. M. Rivire. Smoothness and Analyticity of Free Boundaries in Variational Inequalities. *Annali della Scuola Normale Superiore di Pisa - Classe di Scienze, Sr. 4, 3 no. 2*, pages 289–310, 1976.

[16] L. A. Caffarelli, S. Salsa, and L. Silvestre. Regularity Estimates for the Solution and the Free Boundary of the Obstacle Problem for the Fractional Laplacian. *Inventiones Mathematicae*, 2008.

[17] L. Caramellino and A. Zanette. Monte Carlo Methods for Pricing and Hedging American Options in High Dimension. *Risk and Decision Analysis*, 2(4):207–220, 2011.

[18] N. Chegini and R. Stevenson. Adaptive Wavelet Schemes for Parabolic Problems: Sparse Matrices and Numerical Results. *Journal on Numerical Analysis*, 49(1):182, 2011.

[19] X. Chen and J. Chadam. A Mathematical Analysis for the Optimal Exercise Boundary of American Put Option. *SIAM Journal on Mathematical Analysis*, 2007.

[20] R. Chitlangi. *Hedging & Pricing of Options Using Least Squares Through Simulation: Application to the Black-Scholes and the Heston Models.* LAP Lambert Academic Publishing, 2011.

[21] C. Cho, S. Kang, T. Kim, and Y. Kwon. A New Approach for Numerical Identification of Optimal Exercise Curve. *Computational Science and Its Applications - ICCSA2004*, 2004.

[22] K. A. Cliffe, M. B. Giles, R. Scheichl, and A. L. Teckentrup. Multilevel Monte Carlo Methods and Applications to Elliptic PDEs with Random Coefficients. *Computing and Visualization in Science*, 14(1):3–15, 2011.

[23] R. Cont and E. Voltchkova. A Finite Difference Scheme for Option Pricing in Jump Diffusion and Exponential Levy Models. *Journal on Numerical Analysis*, 43(4):1596–1626, 2005.

[24] R. W. Cottle, J. S. Pang, and R. E. Stone. *The Linear Complementarity Problem.* 2009.

[25] C. W. Cryer. The Solution of a Quadratic Programming Problem Using Systematic Overrelaxation. *SIAM Journal on Control*, 9:385–392, 1971.

[26] D. M. Dang. *Modeling Multi-Factor Financial Derivatives by a Partial Differential Equation Approach with Efficient Implementation on Graphics Processing Units.* PhD thesis, Univ. of Toronto, 2011.

[27] P. Daskalopoulos and P. M. N. Feehan. Existence, Uniqueness, and Global Regularity for Degenerate Elliptic Obstacle Problems in Mathematical Finance. Working paper, 2011.

[28] J. L. Dong and M. Q. Jiang. A Modified Modulus Method for Symmetric Positive-definite Linear Complementarity problems. *Numerical Linear Algebra with Applications*, 16:129–143, 2009.

[29] I. S. Duff. A Survey of Sparse Matrix Research. *Proceedings of the IEEE*, 65(4):500, 1977.

[30] I. S. Duff, A. M. Erisman, and J. K. Reid. *Direct Methods for Sparse Matrices.* Oxford University Press, 1989.

[31] D. J. Duffy. *Finite Difference Methods in Financial Engineering: A Partial Differential Equation Approach.* John Wiley & Sons, 2006.

[32] E. Eberlein and S. Raible. Term Structure Models Driven by General Levy Processes. *Mathematical finance*, 9(1):31, 1999.

[33] L. Fenga, P. Kovalovb, V. Linetskyc, and M. Marcozzid. Variational Methods in Derivatives Pricing. *Handbooks in Operations Research and Management Science*, 15:301–342, 2007.

[34] N. P. Firth. *High Dimensional American Options.* PhD thesis, University of Oxford, 2005.

[35] P. A. Forsyth and G. Labahn. Numerical Methods for Controlled Hamilton-Jacobi-Bellman PDEs in Fnance. *The Journal of Computational Finance*, 11(2):1–44, 2007.

[36] S. Galluccio. Beyond Black-Scholes: Semimartingales and Levy Processes for Option Pricing. *The European Physical Journal B - Condensed Matter and Complex Systems*, 20(4):595–600, 2001.

[37] T. Gerstner and M. Griebel. Dimension-Adaptive Tensor-Product Quadrature. *Computing*, 71:2003, 2003.

[38] M. B. Giles. Improved Multilevel Monte Carlo Convergence Using the Milstein Scheme. *Monte Carlo and Quasi-Monte Carlo Methods 2006*, pages 343–358, 2007.

[39] M. B. Giles. Multilevel Monte Carlo Path Simulation. *Operations Research*, 56(3):607–617, 2008.

[40] M. B. Giles. Multilevel Monte Carlo for Basket Options. *Proceedings of the 2009 Winter Simulation Conference*, 2009.

[41] M. B. Giles and R. Carter. Convergence Analysis of Crank-Nicolson and Rannacher Time Marching. *Journal of Computational Finance*, 9:89–112, 2006.

[42] M. B. Giles, D. Higham, and X. Mao. Analysing Multi-level Monte Carlo for Options with Non-globally Lipschitz Payoff. *Finance and Stochastics*, 13(3):403–413, 2009.

[43] P. Glasserman. *Monte Carlo Methods in Financial Engineering.* Springer, 2004.

[44] R. Glowinski. *Numerical Methods for Nonlinear Variational Problems.* Springer, 2008.

[45] P. S. Hagan, D. Kumar, A. S. Lesniewski, and D. E. Woodward. Managing Smile Risk. *Wilmott Magazine*, pages 84–108, 2002.

[46] E. G. Haug. *The Complete Guide to Option Pricing Formulas.* McGraw-Hill Professional, 2 edition, 2007.

[47] S. L. Heston. *A Closed-form Solution for Options with Stochastic Volatility with Applications to Bond and Currency Options.* 1993.

[48] M. Hintermuller, K. Ito, and K. Kunish. The Primal-dual Active Set Strategy as a Semismooth Newton Method. *SIAM Journal on Optimization*, 13:865–888, 2002.

[49] J. Huang and J. S. Pang. Option Pricing and Linear Complementarity. *The Journal of Computational Finance*, 2(3), 1998.

[50] J. C. Hull. *Options, Futures and Other Derivatives (7th Edition).* Prentice Hall, 7 edition, 2008.

[51] S. Ikonen and J. Toivanen. Efficient Numerical Methods for Pricing American Options under Stochastic Volatility. *Numerical methods for partial differential equations.*, 24(1):104–126, 2008.

[52] I. Ipsen. *Numerical Matrix Analysis: Linear Systems and Least Squares.* Society for Industrial Mathematics, 2009.

[53] R. A. Jarrow and E. R. Rosenfeld. Jump Risks and the Intertemporal Capital Asset Pricing Model. *Journal of Business, University of Chicago Press*, 57(3):337–351, 1984.

[54] H. Johnson. Options on the Maximum or the Minimum of Several Assets. *Journal of Financail and Quantitative Analysis*, 22(3):277–283, 1987.

[55] D. Kinderlehrer. Variational Inequalities and Free Boundary Problems. *Bulletin, new series, of the American Mathematical Society*, 1978.

[56] D. Kinderlehrer and G. Stampacchia. *An Introduction to Variational Inequalities and their Applications.* SIAM, 2000.

[57] M. Kocvara and J. Zowe. An Iterative Two-step Algorithm for Linear Complementarity Problems. *Numerische Mathematik*, 68:95–106, 1994.

[58] S. G. Kou. Levy Processes in Asset Pricing. http://www.columbia.edu/ sk75/levy.pdf, 2006.

[59] Pavlo Kovalov, Vadim Linetsky, and Michael Marcozzi. Pricing Multi-asset American Options: a Finite Element Method-of-Lines with Smooth Penalty. *Journal Journal of Scientific Computing*, 33(3):209–237, 2007.

[60] R. A. Kuske and J. B. Keller. Optimal Exercise Boundary for an American Put Option. *Applied Mathematical Finance*, 5(2):107–116, 1998.

[61] P. Laurence and S. Salsa. Regularity of the Free Boundary of an American Option on Several Assets. *Communications on Pure and Applied Mathematics.*, 62(7):969, 2009.

[62] C. E. Lemke and J. T. Howson. Equilibrium Points of Bimatrix Games. *Journal of the Society for Industrial and Applied Mathematics*, pages 413–423, 1964.

[63] A. L. Lewis. *Option Valuation under Stochastic Volatility: with Mathematica Code.* Finance Pr, 2000.

[64] C. L. Chioma M. Briani and R. Natalini. Convergence of Numerical Schemes for Viscosity Solutions to Integro-differential Degenerate Parabolic Problems Arising in Financial Theory Numer. *Numerische Mathematik*, 98(4):607, 2004.

[65] O. L. Mangasarian. Solution of Symmetric Linear Complementarity Problems by Iterative Methods. *Journal Of Optimization Theory and Applications*, 22(4):465–485, 1977.

[66] W. Margrabe. The Value of an Option to Exchange One Asset for Another. *Journal of finance*, 33(1):177–186, 1978.

[67] A. Matache, P. Nitsche, and C. Schwab. Wavelet Galerkin Pricing of American Options on Levy Driven Assets. *Quantitative Finance*, 5(4):403–424, 2005.

[68] F. D. I. K. Mautner. *Numerical Treatment of the Black-Scholes Variational Inequality in Computational Finance.* PhD thesis, Humboldt-Universitt zu Berlin, 2006.

[69] R. C. Merton. Theory of Rational Option Pricing. *The Bell Journal of Economics and Management*, 4(1):141–183, 1973.

[70] K. G. Murty. *Linear Complementarity, Linear and Nonlinear Programming.* 1988.

[71] B. F. Nielsen, O. Skavhaug, and A. Tveito. Penalty and Front-fixing Methods for the Numerical Solution of American Option Problems., 2001.

[72] B. F. Nielsen, O. Skavhaug, and A. Tveito. Penalty Methods for the Numerical Solution of American Multi-asset Option Problems. *Journal of Computational and Applied Mathematics*, 222:3–16, 2008.

[73] D. P. O'Leary. A Generalized Conjugate Gradient Algorithm for Solving a Class of Quadratic Programming Problems. *Linear Algebra and its Applications*, 1980.

[74] C. W. Oosterlee, C. C. W. Leentvaary, and A. A. Vazquezy. Pricing Options with Discrete Dividends by High Order Finite Differences and Grid Stretching. *European Congress on Computational Methods in Applied Sciences and Engineering*, 2004.

[75] A. M. Quarteroni and A. Valli. *Numerical Approximation of Partial Differential Equations.* Springer, 2008.

[76] H. O. Rasmussen and P. Wilmott. Asymptotic Analysis of Stochastic Volatility Models. *New Directions in Mathematical Finance*, 2002.

[77] C. Reisinger and J. H. Witte. On the use of policy iteration as an easy way of pricing american options. *Working paper*, 2011.

[78] C. Reisinger and G. Wittum. Efficient Hierarchical Approximation of High-Dimensional Option Pricing Problems. *Journal on Scientific Computing*, 29(1):440, 2008.

[79] Y. Ren and M. E. Otmani. Generalized Reflected BSDEs Driven by a Levy Process and an Obstacle Problem for PDIEs with a Nonlinear Neumann Boundary Condition. *J. Comput. Appl. Math.*, 233(8):2027–2043, 2010.

[80] D. R. Rich and D. M. Chance. An Alternative Approach to the Pricing of Options on Multiple Assets. *Journal of Financial Engineering*, 2:271–285, 1993.

[81] M. Rubinstein and E. Reiner. Breaking Down the Barriers. *Risk*, 4(8):28, 1991.

[82] U. Schfer. On the Modulus Algorithm for the Linear Complementarity Problemp. *Operations Research Letters*, 32(4):350–354, 2004.

[83] D. Serre. *Matrices: Theory and Applications.* Springer, 2010.

[84] H. Shahgholian. Free Boundary Regularity Close to Iinitial State for Parabolic Obstacle Problem. *Transactions of the American Mathematical Society*, 360(4):20772087, 2008.

[85] S. E. Shreve. *Stochastic Calculus for Finance I.* Springer-Verlag, 2004.

[86] S. E. Shreve. *Stochastic Calculus for Finance II.* Springer-Verlag, 2004.

[87] L. Silvestre. Regularity of the Obstacle Problem for a Fractional Power of the Laplace Operator. *Communications on Pure and Applied Mathematics*, 2007.

[88] R. M. Stulz. Options on the Minimum or the Maximum of Two Risky Assets : Analysis and Applications. *Journal of Financial Economics*, 10(2):161–185, 1982.

[89] P. Tankov and R. Cont. *Financial Modelling with Jump Processes.* Chapman and Hall/CRC, 2008.

[90] J. Topper. *Financial Engineering with Finite Elements.* John Wiley & Sons, 2005.

[91] Ulji and G. Chen. New Multiplier Method for Solving Linear Complementarity Problems. *Frontiers of Mathematics in China*, 1(3):368, 2006.

[92] R. S. Varga. *Matrix Iterative Analysis.* Springer, 2009.

[93] A. M. Wang, Y. Liu, and Y. Hsiao. Barrier Option Pricing: a Hybrid Method Approach. *Quantitative Finance*, 9(3):341352, 2009.

[94] G. Wang and X. Yang. The Regularization Method for a Degenerate Parabolic Variational Inequality Arising from American Option Valuation. *International Journal of Numerical Analysis and Modeling*, 5(2):222–238, 2008.

[95] S. Wang. A Novel Fitted Finite Volume Method for the BlackScholes Equation Governing Option Pricing. *Journal of Numerical Analysis*, (24):699720, 2004.

[96] S. Wang, X. Q. Yang, and K. L. Teo. Power Penalty Method for a Linear Complementarity Problem Arising from American Option Valuation. *Journal Journal of Optimization Theory and Applications*, 129(2):227–254, 2006.

[97] A. E. Whalley and P. Wilmott. An Asymptotic Analysis of an Optimal Hedging Model for Option Pricing with Transaction Costs. *Mathematical Finance*, 7(3):307–324, 1997.

[98] P. Wilmott. *Paul Wilmott Introduces Quantitative Finance.*, volume 1. John Wiley & Sons, 1 edition, 2006.

[99] P. Wilmott. *Paul Wilmott on Quantitative Finance.* John Wiley & Sons, 2 edition, 2006.

[100] H. Windcliff, P. A . Forsyth, and K. R. Vetzal. Analysis of the Stability of the Linear Boundary Condition for the Black-Scholes Equation. *Journal of Computational Finance*, 8:65–92, 2004.

[101] W. L. Winston. *Financial Models Using Simulation and Optimization II: Investment Valuation, Options Pricing, Real Options, & Product Pricing Models.* Palisade Corp, 2008.

[102] X. Wu and J. E. Zhang. Options on the Minimum or the Maximum of Two Average Prices. *Review of Derivatives Research*, 3(2):183–204, 1999.

[103] Y. Xia. Multilevel Monte Carlo Method for Jump-diffusion SDEs. Quantitative Finance Papers 1106.4730, arXiv.org, 2011.

[104] M. Xua and C. Knessl. On a Free Boundary Problem for an American Put Option under the CEV process. *Applied Mathematics Letters*, 24(7):1191–1198, 2011.

[105] A. Yassine. Comparative Study Between Lemke's Method and the Interior Point Method for the Monotone Linear Complementary Problem. *Studia Universitatis Babes-Bolyai Mathematica*, LIII(3):119–132, 2008.

[106] T. Yeh. Trapezoidal Rule for Multiple Integrals over Hyperquadrilaterals. *Applied Mathematics and Computation*, 87(2-3):227, 1997.

[107] E. Zeidler. *Nonlinear Functional Analysis and its Applications, II/A.* Springer, 1990.

[108] C. Zhang. *Adaptive Finite Element Methods for Variational Inequalities: Theory and Applications in Finance.* PhD thesis, University of Maryland, 2007.

[109] K. Zhang. Pricing Options under Jump Diffusion Processes with Fitted Finite Volume Method. *Applied Mathematics and Computation*, 201(1-2):398, 2008.

[110] L. Zhang. Two-step Modulus-based Matrix Splitting Iteration Method for Linear Complementarity Problems. *Numerical Algorithms*, 57(1):83, 2011.

[111] R. Zvana, P. A. Forsytha, and K. R. Vetzalb. Penalty Methods for American Options with Stochastic Volatility. *Journal of Computational and Applied Mathematics*, 91(2):199–218, 1998.

[112] R. Zvana, K. R. Vetzalb, and P. A. Forsyth. PDE Methods for Pricing Barrier Options. *Journal of Economic Dynamics and Control*, 24(11-12):1563–1590, 2000.